CONVENTIONALLY PACKED POROUS POLYMER GAS CHROMATOGRAPHIC COLUMNS:- A STUDY OF THEIR PROPERTIES AND THEIR APPLICATION TO THE SEPARATION OF THE ISOTOPIC METHANES.

by

Joseph J. Czubryt

A thesis

submitted to

the Faculty of Graduate Studies and Research

of the University of Manitoba

in partial fulfillment

of the requirements for the degree of

Doctor of Philosophy

From the Parker Chemistry Laboratory of the

University of Manitoba

under the supervision of Professor H. D. Gesser

August, 1968

ACKNOWLEDGEMENTS

I wish to express my sincerest thanks to the following;

Dr. H.D. Gesser for the understanding, the advice, and the invaluable willing help he has given over the years.
Dr. Bock for the loan of some of the electronic equipment used in this study.
Dr. Wong for the lengthy loan of the 21 liter dewar.
Dr. N. Demchuk for the many enlightening discussions.
The Imperial Oil Analytical Section for the photomicrographs of the porous polymers.
Richard McKeag for his willingness to help.
The Chemistry Technical and Electronic staff for their co-operation in the time of need.
My wife for the typing of the thesis and above all for her understanding.
The National Reseach Council Of Canada for all the financial support received.

To My Wife Carolyn.

ABSTRACT

Out of the various porous polymers studied, it was found that Porapak S was best suited for the separation of the isotopic methanes. A CH_4-CD_4 mixture was separated on a 50 ft. 1/8" o.d. Porapak S (50-80 mesh) column at -32°C. in approximately 20 minutes. The gas chromatographic peaks were symmetrical with negligible tailing. Attempts to completely separate the five isotopic methanes (CH_4, CH_3D, CH_2D_2, CHD_3, and CD_4) on a 200 ft. 1/8" o.d. Porapak S (50-80 mesh) column were on the whole unsuccessful.

Experiments were carried out to determine the accuracy of the soap bubble flow meter. The results showed that the soap bubble flow meter was neither accurate nor reproducible in the low flow rate region. The error in the flow rate measurement was found to depend on the flow rate, the bubble thickness, the nature of the carrier gas, and the length of the flow meter used. Of necessity a new type of flow meter was devised. This simple and highly reproducible flow meter (reproducibility better than 0.05% on the average) which can be used in a pre or a post column arrangement and which can serve to measure flow rated more accurately than previously possible is described.

With the aid of this highly reproducible flow meter it was found that the flow of the carrier gas through the 200 ft. Porapak S column does not obey Darcy's Law nor can

it be described by the Ergun equation. The permeability of the column to gas flow was found to depend on the nature of the carrier gas, the mean column pressure, and the direction (increasing or decreasing) in which the column inlet pressure was changed. There is also evidence to indicate that the column possesses a permeability hysterisis. The anomalous results obtained for the helium carrier gas strongly suggest that helium can undergo flow through secondary 'channels' which under the present experimental conditions are impermeable or insignificantly permeable to argon, carbon dioxide, methane, and possibly most other gases.

The degree of interaction between the carrier gas and the column packing was measured by means of the net retention volume of methane. In this fashion adsorption isotherms at 273°K for helium, argon, and carbon dioxide were determined. It was also found that the choice of the carrier gas had an effect on the partition coefficient ratio $K(CH_4)/K(CD_4)$. In the case of argon and carbon dioxide, this ratio was found to decrease with increasing mean column pressure but not in the manner anticipated.

From the gas chromatographic temperature studies (above 273°K) the thermodynamic data for several gas samples was evaluated. Thermodynamic data for CH_4 and CO_2 was also obtained from a static system (below 273°K).

The two systems were found to give results which were in excellent agreement. The available data obtained from the two systems indicates that the porous polymer (Porapak S) undergoes a structural change at a temperature slightly above 273°K.

The relationship between the plate height and the carrier gas velocity was found to be described by the 'classical' plate height equation for helium, argon, and in the low carrier gas velocity region for carbon dioxide. Considerable levelling-off, of the type associated with coupling and turbulence, was observed for carbon dioxide and under certain conditions for argon in the high carrier gas velocity region. The complexity of the system is further illustrated by the presence of the plate height hysterisis.

TABLE OF CONTENTS

LIST OF FIGURES

LIST OF TABLES

INTRODUCTION

Although chromatography can be traced as far back as 1906 (1), elution gas chromatography has only been in existence for approximately fifteen years. After the appearance of the initial paper by James and Martin (2), the potentialities of this method were recognized almost immediately and an intensive investigation began in this field. The rapid growth of gas chromatography is reflected in the increase in the yearly publications. In 1955 there were approximately 50 publications, in 1958 approximately 400 (3, 4) and in 1967 the figure is close to 2,000 (5). Up to date there are a total of 13,000 to 14,000 publications dealing with theoretical and practical aspects of this field not to mention the large number of books. To quote Ettre and Zlatkis (6), "It is often said that gas chromatography is the most widely used analytical technique and that its rapid growth is unparalleled in the history of analytical chemistry". The versatility of the technique can only be demonstrated by specifying its applications but such would be an almost impossible task. To state that gas chromatography (G C) has been used in the detection and identification of bacteria (7), in the evaluation of the sex attractants of the black carpet beetle (8), in the separation of isotopic molecules (9, 10), in the study of complexing reactions (11), and in

the separation of diastereoisomeric compounds (12), is not sufficient to illustrate the vast potential and versatility of gas chromatography as an analytical tool.

Gas chromatography is divided into two main branches. The difference between the two lies in the choice of the partitioning phases. While in each case one phase is gaseous the other can be a liquid or a solid and the terms gas-liquid and gas-solid chromatography respectively describe the two systems. The various relationships and theories, aside for minor differences, are applicable to both systems since the underlying gas chromatographic principles are essentially the same.

In order to obtain meaningful information from the raw experimental data, whether the system is gas-solid or gas-liquid, certain basic relationships between the gas chromatographic processes, the gas chromatographic design, the operating conditions and the raw experimental data must be established. Since a detailed discussion is forbidding, the various relationships will be presented in their simplest and most general form. In the subsequent chapters reference will be made to these general expressions as starting points in their development to the point where they can be applied to the experimental data.

The following development of the basic concepts of gas chromatography will in most parts be applicable to

either a gas-liquid or a gas-solid system. Where distinctions must be made the gas-solid system will receive most of the emphasis since the system in the present study is of this nature.

THERMODYNAMIC ASPECTS

In a system of two immiscible phases, A and B, in direct contact with one another, any substance (the solute) miscible in both of these phases, will distribute itself between them. In terms of Gibbs free energy (G), equilibrium will be reached when

$$(dG)_{T,P} = 0 \qquad (1.1)$$

for the system (13). It can be shown (14), that for an isolated system under the conditions of constant temperature and pressure,

$$(dG)_{T,P} = \Sigma G_i dn_i = 0 \qquad (1.2)$$

where

$$G_i = (\partial G/\partial n_i)_{T,P,n_{j\neq i}} \qquad (1.3)$$

and n_i is the number of moles of the respective participants in the process. Since μ_i (the chemical potential) is an alternative notation to G_i (the partial molar free energy) then eqn. (1.2) can be written as

$$(dG)_{T,P} = \Sigma \mu_i dn_i = 0 \qquad (1.4)$$

For n number of moles of a single solute distributed between two phases (A and B) eqn. (1.4) becomes;

$$\mu_A dn_A + \mu_B dn_B = 0 \qquad (1.5)$$

where n_A and n_B represent the number of moles of the solute in phase A and B respectively. Since;

$$n_A + n_B = n = \text{constant} \qquad (1.6)$$

then

$$dn_A + dn_B = 0 \qquad (1.7)$$

or

$$dn_A = -dn_B \qquad (1.8)$$

Substituting the results of eqn. (1.8) into eqn. (1.5), it can be shown that at equilibrium;

$$\mu_A = \mu_B \qquad (1.9)$$

or

$$G_A = G_B \qquad (1.10)$$

The chemical potential, or the partial molar free energy can be related to the activity of the solute by the

following relationship (15);

$$G_i - G_i^\circ = RT\ln a_i \qquad (1.11)$$

where a_i is the activity and G_i° is the partial molar free energy of the solute (i) in its standard state where $a_i = 1$. Expressing eqn. (1.10) in terms of eqn. (1.11) and re-arranging, the following result is obtained;

$$G_B^\circ - G_A^\circ = \Delta G^\circ = -RT\ln(a_B/a_A) \qquad (1.12)$$

Since (a_B/a_A) is the partition coefficient (K), eqn. (1.12) can be written as;

$$\Delta G^\circ = -RT\ln K \qquad (1.13)$$

As it was pointed out by James et. al. (16), the partition coefficient (K) as well as the value of the standard thermodynamic properties will depend upon the choice of the standard states chosen for the solute in the participating phases. The value of K, as well as the standard thermodynamic properties derived from it must be accompanied by the definition of the standard states chosen for their evaluation.

In the case where several components are distributed between the two phases (A and B), and if the distribution process of each component is unaffected by the presence of the others, then eqn. (1.13) is applicable to the

individual components each, however, having in general a different value of K and consequently different values of ΔG^{o}.

GAS CHROMATOGRAPHY

Gas chromatography in the analytical sense is a method of separation. The principle of this method is the partitioning process just described which takes place in the gas chromatographic column. The column is a length of tubing containing the stationary phase which may be either liquid or solid over which the gas phase is made to flow.

The choice of the stationary phase is dictated by the nature of components to be separated in that it, combined with the gas phase, must result in a different K value for each component present in the mixture. Since there are no true criteria in predetermining whether a particular stationary phase will give rise to different K values, the choice of it is brought to the level of trial and error.

Even though a stationary phase can be found which does give rise to different K values of each component, the final separation may not be successful since there exist various effects in both of the phases that tend to destroy the separation. As it will be seen later that although these undesirable effects cannot be completely eliminated, they can be minimised by the column design.

The manner in which the stationary phase is contained in the column is known to affect the magnitude of the various effects and consequently the separation. In view of this a variety of column designs have been introduced over the years. In order to establish the terminology a brief description of the various columns that may be encountered in gas-solid chromatography will now be given. Aside for a few passing comments, no attempt will be made to give a critical comparison of the various columns.

Gas-Solid Chromatographic Columns

There are two main classes of gas chromatographic columns, the open tubular and the packed. The former was originally introduced into the gas-liquid system by Golay and columns of this class are often referred to as the Golay columns (for a detailed discussion of the Golay columns in terms of theory, preparation and uses, one can refer to the following sources (17-30)). These are prepared by coating the inner wall of a capillary tubing with a thin layer of the stationary phase. Due to their small content of the stationary phase these columns have a very small capacity, that is, only very small sample sizes can be used for analysis. The consequence of this is that they are limited to analytical purposes only.

The packed columns are prepared by filling a length of tubing with a granular stationary phase (in the gas-liquid system this is achieved by first coating the granules with the liquid phase pior to packing). Since these have a much larger capacity, they can be used for analytical purposes or for preparative work.

Open Tubular Columns

It was first pointed out by Golay (18) and Purnell (31) that open tubular columns could be made by replacing the liquid phase of the capillary columns with a layer of porous material. Since the suggestion in 1958, many such columns have been prepared. One method of producing such an active layer is by direct chemical reaction on the tube wall. In this fashion a layer of alumina may be produced on an aluminum wall (32), or a layer of porous silica may be made to replace the smooth inner wall of a glass capillary column by etching the glass by various processes (33, 34). An alternative method of putting a porous layer on the wall of the capillary tube is by direct attachment of the porous material to the inner wall. Two different methods of achieving this have been described. One method which is relatively new gives rise to a thick layer open tubular glass column and requires the glass-tube drawing apparatus described by Desty (35). The glass-tube

containing the packing material and a tungsten wire which is anchored to the apparatus, is drawn out into a capillary. The purpose of the wire is to insure an opening of a constant diameter in the final column. In this manner capillary columns coated with carbon (36) and Celite (37) have been prepared. Since the process required the presence of the solid support during the capillary formation, it is restricted to solids which do not decompose at the softening point of glass. These columns once formed can be liquid coated and can be used as gas-liquid chromatographic columns.

The second method of producing a porous layer on the inner wall of the capillary by direct attachment of the support to the capillary tube was first described by Halász and Horváth (38, 39). This method requires first the formation of a colloidal suspension of the solid support. After the capillary tube is filled with this suspension, the liquid is carefully evaporated by a heating process (see (38)). This method has been used to line capillary tubes with graphatized carbon black (38), fibrilar Boehmite (40), colloidal silica (41, 42) and molecular sieve (43). It should be pointed out that this process is not restricted to the gas-solid system, but as in the previous method the porous layer can be coated with the liquid phase (39, 44) to give liquid coated

capillaries with larger capacity and as good or better separation than the conventional gas-liquid capillary columns. This is attributed to the fact that more liqiud phase can be accommodated with a thinner distribution.

Packed Columns

The packed gas-solid chromatographic columns may fall into one of several classes (this could equally well apply to gas-liquid systems in most cases), and will be discussed under class headings.

Regularly Packed Columns

Conventional Columns

These columns are most common and are used for routine analytical work. With some exceptions, the inside diameter of the tubing is in the range between 2 and 4 mms. The particle size most generally used lies between 0.1 and 0.2 mm. in diameter therefore giving the particle-to-column diameter ratio of approximately 0.2. For a particular choice of particle diameter it is important to insure that the deviation of particle sizes from this value are as small as possible. A large spread of particle sizes results in a tighter packing and consequently lower permeability. This also has an effect on the column performance and will be discussed later. The particles

themselves may be of porous nature or they may only have a porous layer with an impenetrable core. The latter is more probably the better choice since the particles have a considerably large surface area, but since the gas as well as the solute cannot penetrate into the inner region of the particle, certain mass transfer effects are minimised. This, again, will be discussed later. Textured particles have been used in both gas-solid and gas-liquid systems (45-48).

Micro Packed Columns

These columns are very much similar to the conventional packed columns. They differ in that the inside diameter of the tube is less than 1 mm. however, the particle-to-column diameter ratio is roughly the same. These columns are superior to the conventional type in their speed and performance (49-51).

High Inlet Pressure Micro Column System (H.I.P.M.C.)

This system was first described by Myers and Giddings (52). The columns employed in this system were made from 0.47 mm. i.d. stainless steel capillary tubing and particles of diameter as small as 0.5 microns. These columns are similar to the micro packed columns but have a different particle-to-column diameter ratio. Due to the

size of particles very high (~2,500 p.s.i.) operating inlet pressures are required. This system is fairly high in speed of operation in comparison to all other columns, but undoubtedly it is the fastest of the regularly packed column class.

Irregularly Packed Columns

If for one reason or another the particles cannot achieve dense packing then the entire column will be packed irregularly and will have a high inter-particle porosity (as high as 0.9).

Aerogel Columns

This type of column was first described by Halasz and Gerlach (53). These columns are produced by drawing out a glass tube containing loosely packed highly dispersed silica into a capillary of 0.4 mm. inside diameter by means of the glass drawing apparatus already mentioned. The packing material of approximately 1 micron diameter is composed of spherical and pore free primary particles (30-150A° diameter) which tend to aggregate into straight and branched chains giving an overall irregular three dimensional network. Since the packing is highly dispersed, only 2 to 4 percent of the total column volume is occupied by the packing despite the fact that the particles appear to be closely packed. The high surface area

(approximately 380 sq. meters per gram) and the minimum packing volume affords extremely fast analysis time.

Packed Capillary Columns

The use of this type of column was first reported by Halasz and Heine (54). The capillary packed columns differ from the micro packed columns in that they are irregularly and loosely packed having the particle-to-column diameter ratio greater than 0.2. As it was pointed out by these workers (55-57) the capillary tube should have an inside diameter of 1 mm. or less but preferably in the range of 0.25 to 0.5 mm. The loose and irregular packing comprises less than two thirds of the column volume. Since the packed capillary columns are made by drawing out a larger bore glass tubing already containing the packing, the depressions made in the inner walls by the packing during the process help to prevent particle shifting. These columns are very efficient, that is they are capable of good separations in a relatively short time.

Despite the fact that the column characteristics vary from class to class in either gas-solid or gas-liquid systems, the fundamental gas chromatographic relationships are the same for all cases. The slight difference between a gas-solid and a gas-liquid system stems from terminology in that in the former case one speaks of the partitioning process in terms of adsorption on the surface where as in

the latter case one speaks of solubility in the liquid. Although the forthcoming discussion is in terms of gas-solid chromatography, it can equally apply to the gas-liquid system by making certain obvious substitutions. It should be noted that nowhere in the discussion is the class of column specified.

Fundamental Relationships In GC

The gas chromatographic apparatus consists of the injection port, the column, and the detector, arranged in that order. The mobile phase is made to flow continuously through these components. If a solute in a gaseous or vapor form is introduced by means of the injection port at the inflow end of the column in a form of a sharp concentration pulse, it will distribute itself between the two phases according to its partition coefficient. If the solute is nonsorbing, it will be carried down stream by the carrier gas at the carrier gas velocity, and will eventually reach the end of the column after time t_m (the detector will indicate this event). For a sorbing solute distributed between the two phases, each molecule will spend some time t_g in the mobile phase and some time t_s adsorbed on the surface. Since the molecular processes are statistical, t_s, t_g, and any other value pertaining to a molecular process must be considered as the average

value. While in the mobile phase the molecule will be carried by the carrier gas at the same velocity as the nonsorbing molecule. The duration of this flight will last for a time t_g before it is terminated by adsorption. While adsorbed the molecule is immobilised and its effective velocity is reduced to a value less than that of the carrier gas or the nonsorbing molecule. Since this is true for every solute molecule, the solute band will migrate down the column with a velocity less than that of the nonsorbing solute and will eventually reach the end of the column in time t_R. In order to reach the end of the column each molecule must spend time t_m in the mobile phase. Considering this, t_R can be expressed as;

$$t_R = t_R' + t_m \qquad (1.14)$$

where t_R' is the total time that each molecule was adsorbed in the column.

The fraction of solute in the mobile phase, R, can be expressed as;

$$R = n_m/(n_m + n_s) \qquad (1.15)$$

where n_m and n_s are the number of moles of the solute in the mobile and the stationary phases respectively. $1-R$ is then the fraction of solute adsorbed on the surface. The ratio $R/(1-R)$ can then be expressed as;

$$R/(1-R) = n_m/n_s \qquad (1.16)$$

If one considers a small section of column containing the solute, then the weight of the solid contained in this section will be ΔW_s and the gas volume will be ΔV_m. The concentration in the mobile phase (C_m) can be expressed as

$$C_m = n_m/\Delta V_m \qquad (1.17)$$

and the concentration in the stationary phase (C_s) is

$$C_s = n_s/\Delta W_s . \qquad (1.18)$$

Substituting eqn. (1.17) and eqn. (1.18) into eqn. (1.16) the following relationship can be obtained.

$$R/(1-R) = C_m \Delta V_m / C_s \Delta W_s \qquad (1.19)$$

Since the ratio $\Delta V_m/\Delta W_s$ is the same for any section of the column, it is also the same for the entire column and eqn. (1.19) can be rewritten as

$$R/(1-R) = C_m V_m / C_s W_s \qquad (1.20)$$

where W_s and V_m are the total weight of the packing in the column and the total gas volume of the column respectively.

The partition coefficient (K) was previously expressed as the ratio of the activities. If the amount of solute present is very small approaching the conditions where

Henry's Law is obeyed, then the partition coefficient can be expressed in terms of concentrations rather than in activities (58), or;

$$K = C_s/C_m \qquad (1.21)$$

Substituting this into eqn. (1.20) and rearranging, the following expression is obtained.

$$(1-R)/R = KW_s/V_m \qquad (1.22)$$

Since R represents the fraction of time a molecule spends in the mobile phase (59), and 1-R is the fraction of time a molecule spends on the solid phase, then

$$(1-R)/R = t_s/t_g = t_R'/t_m. \qquad (1.23)$$

Substituting this into eqn. (1.22) the desired result is obtained.

$$t_R'/t_m = KW_s/V_m \qquad (1.24)$$

Rewriting eqn. (1.14) in terms of eqn. (1.24) a relationship between t_R and K is obtained

$$t_R = t_m(1 + KW_s/V_m) \qquad (1.25)$$

As can be seen from eqn. (1.25) that the time required for each component of the mixture to traverse the column will depend on its K value. If each component has a con-

siderably different K value separation could be possible.

The retention times (the t_R values) are flow rate dependent and are not suitable quantities to work with. The most often used quantity is the retention volume. The retention volume is described as the volume of the carrier gas which flows through the column during the retention time. Each component in the sample will therefore be characterised by its retention volume.

The retention volume can be calculated from the retention time and the flow rate since;

$$V = Ft \qquad (1.26)$$

where V, F, and t are the volume, the flow rate, and the time respectively. Due to the pressure drop across the column and carrier gas compressibility, the flow rate in the column will vary from point to point along the length of the column. The flow rate which is suitable in the calculation of retention volume is the mean value of flow rate in the column. Since this value corresponds to a particular point within the column, its measurement is not possible. It is possible however, to calculate this value if the flow rate at the outlet of the column is known. The relating equation is as follows;

$$\overline{F} = F_o P_o / \overline{P} \qquad (1.27)$$

where $\bar{F}$, F_o, P_o, and $\bar{P}$ are the mean flow rate, flow rate at the column outlet, the column outlet pressure, and the mean column pressure respectively. The ratio $P_o/\bar{P}$ is better known as the Martin-James compressibility factor j (60), which has the form;

$$j = \frac{3\{(P_i/P_o)^2 - 1\}}{2\{(P_i/P_o)^3 - 1\}} \qquad (1.28)$$

where P_i and P_o are the inlet and outlet pressures respectively. The corrected retention volume of the solute V_R^o is then;

$$V_R^o = t_R F_o j \qquad (1.29)$$

The corrected retention volume of a nonsorbed solute is;

$$V_m = t_m F_o j \qquad (1.30)$$

which is identical to the gas space volume of the column (V_m of eqn. (1.25)). Upon rearranging eqns. (1.29) and (1.30) and substituting them into eqn. (1.25) the following expression is obtained;

$$V_R^o = V_m(1 + KW_s/V_m) \qquad (1.31)$$

or

$$V_R^o - V_m = KW_s = V_N \qquad (1.32)$$

V_N is termed the net retention volume for a particular solute and as can be seen is directly related to the partition coefficient.

Since the total surface area (S) of the packing is directly proportional to the weight of the packing (W_s), that is,

$$W_s = kS \qquad (1.33)$$

where k is the proportionality constant then eqn. (1.32) can be written as;

$$V_N = Kk S = KS \qquad (1.34)$$

This result could have been obtained directly if C_s was originally expressed in terms of moles per square meter or some other suitable surface area unit. As can be seen the value of the partition coefficient will depend on the choice of the concentration units. Since, the standard thermodynamic quantities are related to the partition coefficient, they become meaningful only when standard states in the two phases and the concentration units are clearly defined.

Zone Broadening

As the solute migrates from one end of the column to the other, there are three basic effects operating which

cause the initially sharp solute pulse to broaden. While in the mobile phase the solute band undergoes gaseous diffusion. Since diffusion is a time dependent process, the diffusional contribution to band broadening will depend on the carrier gas velocity and the magnitude of the diffusion coefficient.

The presence of the solute in the mobile phase is soley responsible for the solute band (zone) migration. Since a finite time is required to attain true equilibrium, the front of the moving solute zone will have excess concentration in the mobile phase while the opposite will be true for the rear (61). Considering the fact that the solute velocity is directly proportional to the fraction of solute in the mobile phase, the front of the zone will migrate at a higher velocity than the main body of the zone while the rear of the zone will continuously fall back. This source of zone broadening is directly proportional to the carrier gas velocity.

In packed columns there exists a third source of zone broadening. As the gas flows around and in between the packing granules, there will exist point-to-point velocity differences. A solute molecule caught in a fast stream will be displaced further down the column then the one caught in a slow one or in some stagnant region. This contribution to band broadening is independent of gas

velocity, but depends on the column choice since, as it will be seen later, its magnitude is proportional to the particle diameter. Due to these three basic effects, the initially very narrow solute band (sometimes referred to as the δ function if the solute band is infinitely thin (62)), upon elution will be much broader and will have a Gaussian concentration profile. A detector, attached to the end of the column, coupled to a recorder will reveal this. The degree of broadening, or spreading, will of course, depend on the magnitude of the various contributions.

Resolution

Band broadening plays an important role in achievement of separation, and in many cases is the deciding factor. To illustrate this, three hypothetical chromatograms (concentration-time plots) of a two component mixture are shown in Figure (1.1). Although the band centers are equally separated, the degree of separation varies from (a) to (c). The degree or extent of separation of two components is usually expressed in terms of resolution (R). R can only be expressed in terms of various values obtained from a chromatogram. Fig. (1.2) shows a hypothetical two component chromatogram including all the values required for the calculation of R. The relationship

FIGURE (1.1)

EFFECT OF BAND BROADENING ON SEPARATION.

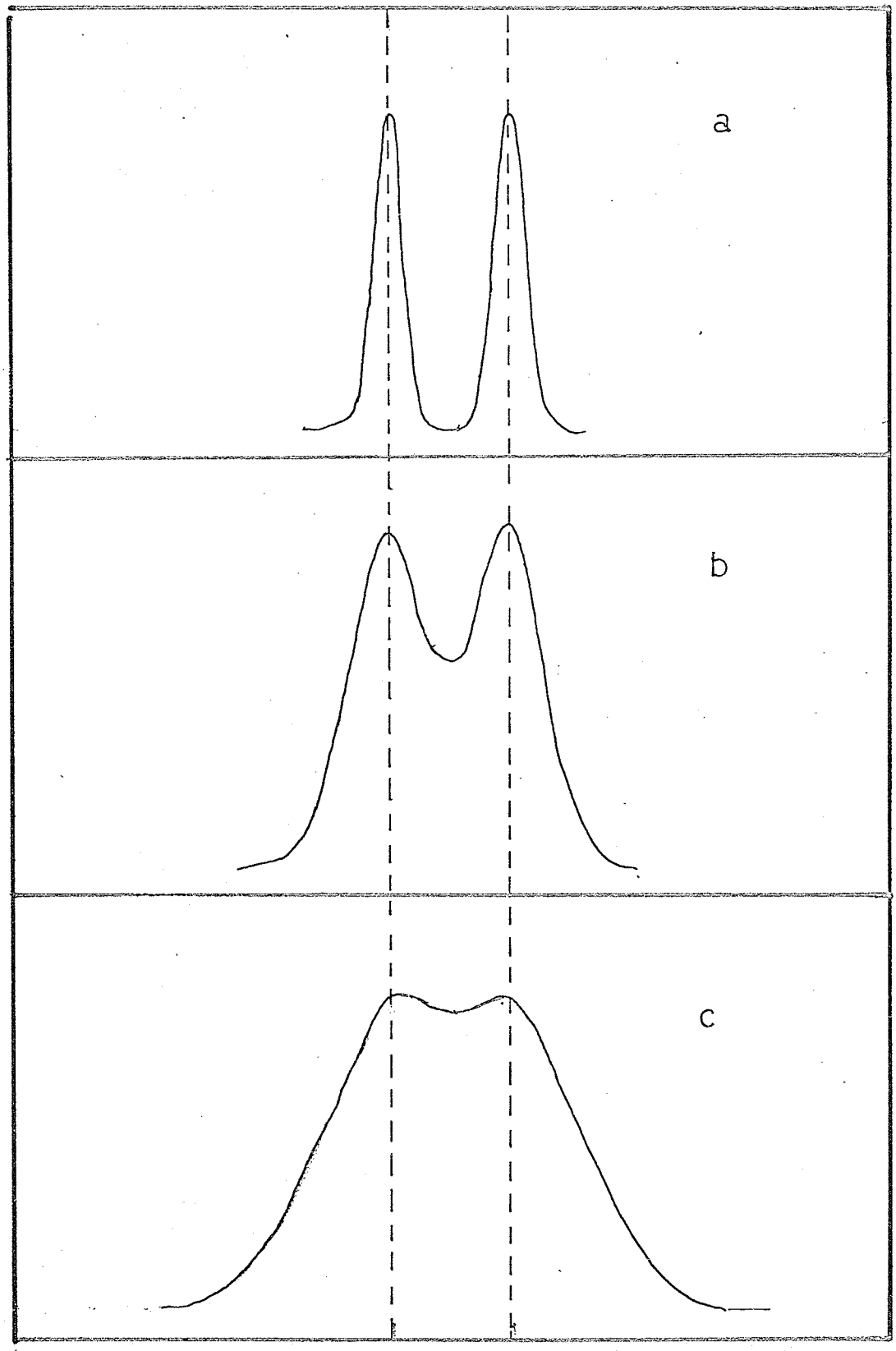
a
b
c

FIGURE (1.2)

PICTORIAL DEFINITION OF t_R, Δt_R, AND W.

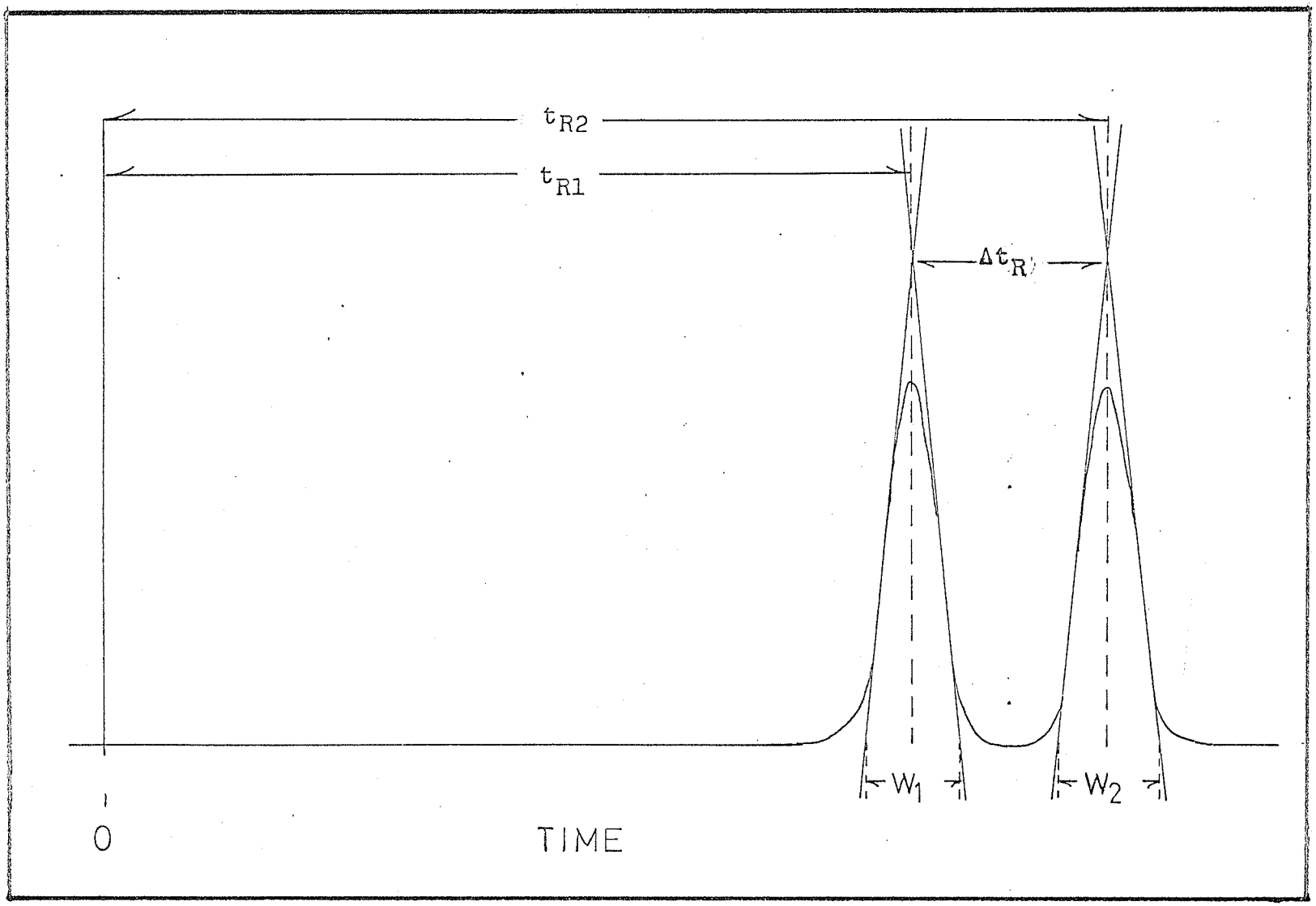
t_{R2}
t_{R1}
$\Delta t_{R'}$
W_1
W_2
0
TIME

between R and the measurable quantities is (63)

$$R = 2\Delta t_R/(W_1 + W_2) \qquad (1.35)$$

Two components are considered to be fully resolved (their separation being 99.7% complete) when $R = 1.5$. The speed of separation may be expressed as the ratio (R/t_{R2}), which is resolution per unit time (63).

H.E.T.P.

A measure of zone broadening or spreading is the standard deviation σ which is approximately quarter-width of the zone. As the zone migrates through the column there will be a continuous contribution to zone broadening. The rate (H) of zone broadening per unit length of column can be expressed in terms of the variance (σ^2);

$$d\sigma^2/dx = H \qquad (1.36)$$

where x is the column length (64). For a uniform column of length L the variance of the solute zone upon elution can be expressed as;

$$\sigma^2 = HL \qquad (1.37)$$

σ can also be expressed in time units (65) that is;

$$\sigma = L\tau/t \qquad (1.38)$$

where τ and t are the time for σ to elute and the total

time of zone travel respectively. Since σ can be equated to the quarter-width of the zone and t is the retention time, then in terms of experimental results obtained from a chromatogram (see Fig (1.2)), the ratio τ/t can be expressed as;

$$\tau/t = W/4t_R \qquad (1.39)$$

In view of eqns. (1.38) and (1.39), eqn. (1.37) can be expressed as;

$$H = L/(4t_R/W)^2 \qquad (1.40)$$

H is described as the plate height or the 'height equivalent to a theoretical plate' (H.E.T.P.). This name has originated from the old distillation plate theory. Although the theory has been discarded, the name still remains.

The W of eqn. (1.40) refers to the extrapolated base width of the elution curve (see Fig. (1.2)). H can also, and most often is, expressed in terms of the elution curve width at half its height ($W_{\frac{1}{2}}$). This is generally preferable since considerable error can be introduced by extrapolation. In terms of $W_{\frac{1}{2}}$, H can be expressed as (63);

$$H = \frac{L}{5.545(t_R/W_{\frac{1}{2}})^2} \qquad (1.41)$$

The quantities $5.545(t_R/W_{\frac{1}{2}})^2$ and $(4t_R/W)^2$ are known

as the plate number (N). In the plate theory, the length of the column was assumed to be divided into discrete segments (plates) in which the solute was completely equilibrated between the two phases. Although the chromatographic process is known to be continuous rather than discrete, the efficiency of the column is still characterized by the number of plates.

It has already been pointed out that there are three basic contributions to zone broadening two of which are carrier gas velocity dependent. Since the diffusion is time dependent, the diffusional contribution to the variance upon elution (σ_D^2) is inversely proportional to the carrier gas velocity and directly proportional to the column length L, or

$$\sigma_D^2 = BL/u \qquad (1.42)$$

where B and u are the proportionality constant and the average carrier gas velocity respectively.

The second velocity dependent contribution to zone broadening stems from the presence of various resistance to mass transfer effects and consequently the zone broadens by virtue of motion. In this case the contribution to the variance upon elution (σ_M^2) will depend directly on the carrier gas velocity and the column length. This can be expressed as;

$$\sigma_M^2 = CLu \qquad (1.43)$$

where C as before is a constant.

The velocity independent contribution (σ_L^2) depends only on the column length and can be written as;

$$\sigma_L^2 = AL \qquad (1.44)$$

where A is a constant.

If the various contributions are independent of each other, then the variance upon elution will be the sum of all contributions (66), or;

$$\sigma^2 = \sigma_D^2 + \sigma_M^2 + \sigma_L^2 \qquad (1.45)$$

In view of equations (1.37), (1.42), (1.43), (1.44), and (1.45) the following relationship can be established;

$$H = A + B/u + Cu \qquad (1.46)$$

Equation (1.46) is generally referred to as the general form of the van Deemter equation (67). Its hyperbolic nature necessitates the presence of a minimum value of H at some value of carrier gas velocity. Since H is related to zone broadening (eqn. (1.37)), then the minimum value of H establishes the carrier gas velocity at which maximum resolution can be obtained.

Tailing

One other effect which destroys the resolution is tailing. Tailing is said to occur when the rear of the Gaussian concentration profile of the zone is badly distorted. Since frontal distortion occurs much less frequently, it will not be discussed here.

Tailing can very often be attributed to nonlinearity of the adsorption isotherms (68, 69). If this is the situation a decrease of sample size will generally result in a symmetric concentration profile. There are many instances where a decrease in sample size causes tailing to be more severe (70) and this cannot be explained by nonlinearity of the adsorption isotherm. Giddings (71) has shown how tailing can occur in the linear region of adsorption isotherm if sorption sites exist which hold the solute molecules for a time equal to that necessary for one quarter of the zone to pass by. Symmetrical elution curves can be obtained only when these secondary sites are deactivated. Deactivation can be achieved by chemically treating the column packing (72, 73) or by charging the carrier gas with a polar material (74, 75) which will be preferentially adsorbed on these active sites.

Tailing can also originate from dead volumes which may be present in the gas chromatograph. Solute molecules

that find themselves in these stagnant regions, slowly diffuse out into the moving stream. For a detailed discussion of the extracolumn contribution to band broadening, one should refer to the article by Sternberg (76).

In order to illustrate the effect of tailing on separation, a hypothetical chromatogram is shown in Fig. (1.3).

PHYSICAL MEASUREMENTS BY GAS CHROMATOGRAPHY

Gas-Solid Chromatography

Thermodynamic Data

It can be seen from eqn. (1.32) or eqn. (1.34) that the net retention volume is directly related to the partition coefficient. In terms of eqn. (1.32), eqn. (1.13) can be written as;

$$\Delta G^\circ = -RT\ln V_N + RT\ln W_s \qquad (1.47)$$

But since (16),

$$\Delta G^\circ = \Delta H^\circ - T\Delta S^\circ \qquad (1.48)$$

where ΔG°, ΔH°, and ΔS° are the partial molar standard free energy, standard heat, and the standard entropy of adsorption respectively, then;

$$\ln V_N = -\Delta H^\circ/RT + q \qquad (1.49)$$

FIGURE (1.3)

EFFECT OF TAILING ON SEPARATION.

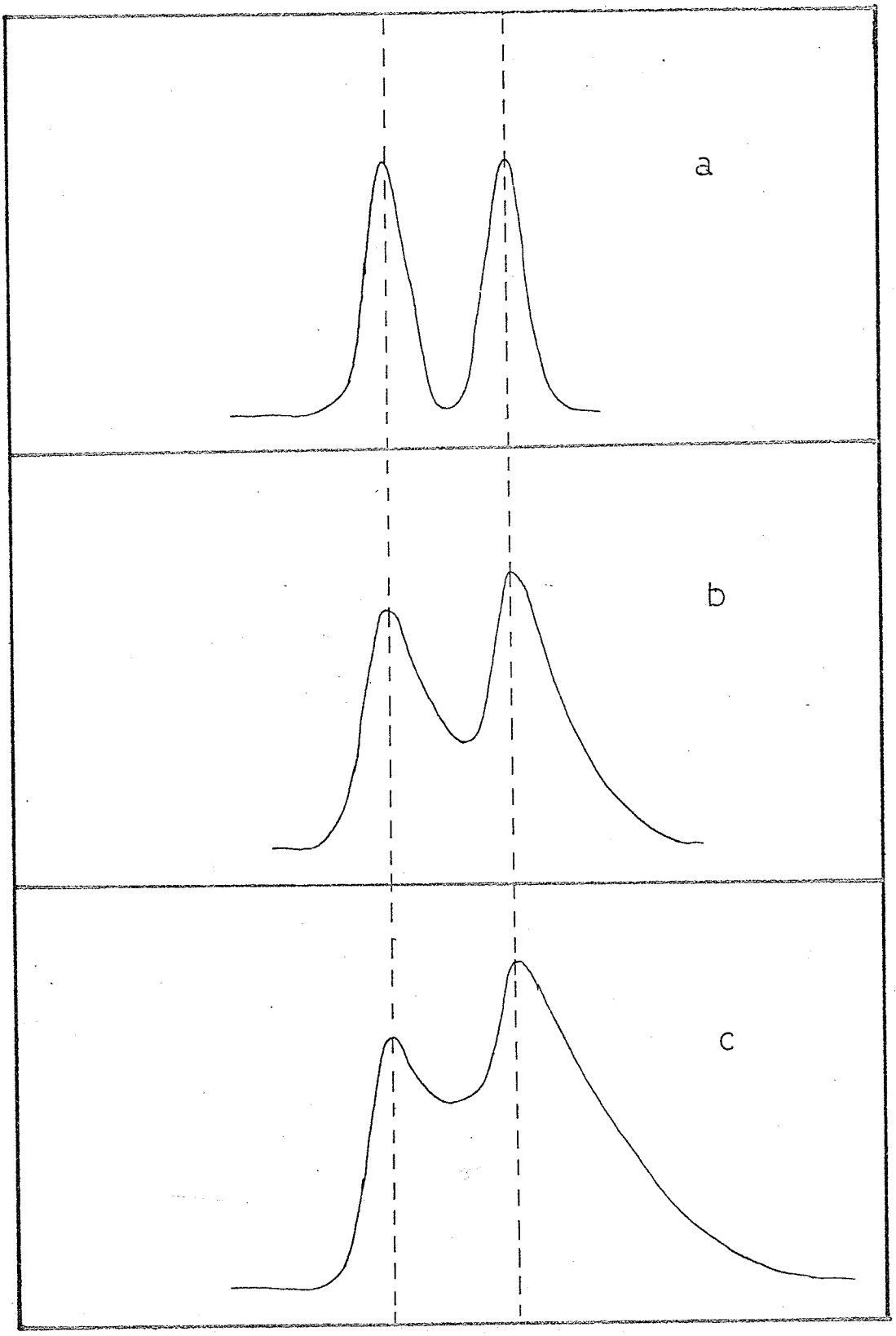
a
b
c

where;

$$q = \Delta S^{\circ}/R + \ln W_s . \qquad (1.50)$$

A plot of $\log V_N$ (or under suitable conditions $\log t_R$) against 1/T gives a straight line with a slope of $-\Delta H^{\circ}/2.303R$ from which ΔH° can be calculated (77-82).

The thermodynamic quantities ΔS° and ΔG° can be calculated if the value of K is known (see eqn. (1.13) and eqn. (1.48)).

Adsorption Isotherms

It was already mentioned that tailing can occur under conditions of adsorption isotherm nonlinearity. If the isotherm is concave to the pressure axis the chromatogram will have a sharp front and a diffuse (tailing) rear where as if the isotherm is convex to the pressure axis the chromatogram will have a diffuse front and a sharp rear (83). In the case of linear adsorption isotherm the chromatogram will have a Gaussian profile.

Since the first derivative of the adsorption isotherm is related to a so called specific retention volume (retention volume per gram of the stationary phase) of the corresponding points on the diffuse edge of the chromatogram, then the adsorption isotherm can be reconstructed by graphical integration of a single peak (chromatogram) (84) with appropriate corrections for diffusional broadening

(80, 85, 86). This method has been used to obtain adsorption isotherms of various solute-solid systems (80, 84, 85, 87).

Frontal analysis serves as an alternative method for determining adsorption isotherms. The method as described by Gregg and Stock (83) is as follows. The carrier gas is first passed through a saturator containing the solute at a known temperature and then through the column. When a constant signal is obtained from the detector for fifteen minutes or so, the column is considered to be saturated with respect to the solute. The carrier gas is then quickly rerouted so as to bypass the saturator. By switching from pure carrier gas to solute charged carrier gas, a set of chromatograms can be obtained which are rectangular in nature. The individual points of the isotherm can be calculated from the diffuse regions, either tailing or leading (depending whether the adsorption isotherm is concave or convex) of the chromatogram by the graphical integration method. This method and its modifications have been used in several studies (83, 88, 89, 90).

Kipping and Winter (91) have obtained adsorption isotherms from sample size-retention volume data.

Surface Area Measurements

A gas chromatographic method for surface area measurement was developed by Nelson and Eggertsen (92). A blend

of He and N_2 of known N_2 to He ratio is used as a carrier gas. A small tube containing the solid sample is placed in a liquid nitrogen bath so that adsorption of N_2 on the sample can take place. The amount of nitrogen adsorbed at the corresponding relative pressure is determined by the recorder response after the liquid nitrogen bath is removed. From three such determinations each at a different N_2 partial pressure and a B.E.T. plot the surface area can be calculated. Stock (93) has proposed a method of surface area measurement where only a single experiment is required. The method resembles that of Gregg and Stock (83) used for the adsorption isotherm study.

Gas-Liquid Chromatography

Although gas-liquid chromatography is of no immediate importance to the present study, there is one aspect of it which is very interesting and should be mentioned.

A relationship between the net retention volume and the partition coefficient can be established for gas-liquid chromatography by substituting the total volume of the liquid phase (V_L) for the total weight of the solid (W_s) of eqn. (1.32). Since V_L is a constant for a particular column any change in V_N will solely be caused by a change in the partition coefficient. This however, cannot be extended to the gas-solid system since although W_s itself

does not change there may be a change in the effective W_s due to pressure. Referring back to eqn. (1.33)

$$W_s = \hat{k}S \qquad (1.33)$$

it can be seen that any carrier gas-surface interaction will change the value of S with pressure and as the result of this will decrease the effective W_s. A change in S will also cause a change in the V_N value. For this reason it is difficult to determine whether a change in V_N is due to a change in S, in the partition coefficient, or in both.

Gas-liquid chromatography serves as a means of directly observing the partitioning process with changing experimental conditions. Aside from its applicability to thermodynamic studies (94-99) gas-liquid chromatography has become a simple and fast method of evaluating the "mixed" second virial coefficients (B_{12}) of the solute-carrier gas pairs. It has been shown that the partition coefficient can be related to the B_{12} term by the following or a related expression (100A, 100B, 100C);

$$\log K = A + \bar{P}/2.303RT\{2B_{12} - v_2^o\} \qquad (1.51)$$

where A, $\bar{P}$, and v_2^o are a constant, the average column pressure, and the molar volume of the solute (at T°K) respectively. A plot of ln K against the mean column pressure gives a straight line with a slope $(2B_{12} - v_2^o)/RT$

from which the B_{12} term can be evaluated since the value of v_2^o often available.

Since the B_{12} term is specific for a solute-carrier gas pair, a change in carrier gas at appreciable mean column pressures should affect the relative retention times of the various solutes. Goldup et. al. (101) have observed a change in separation as they changed the carrier gases. Several experiments were carried out in which the B_{12} values were actually obtained (100A, 100B, 100D-100G, 102, 103). Giddings (104) has pointed out that pressure induced equilibrium shifts may lead by virtue of carrier gas-solute interaction to the mobility of heavy molecular weight species which generally do not migrate. This in fact has become a reality since he and his co-workers were able under high pressures (2,000 atmospheres) to elute substances of molecular weight as high as 400,000 (105). This, of course, has a tremendous potential in biological systems.

The role of gas chromatography for physical measurements appears to be unlimited. Its use in determining the thermodynamic properties of silver ion-olefine complexes (106), the measurement of gas diffusion coefficients (107, 108), the deduction of relative configuration of substituents in cyclopentane skeleton (109), and the determination of energy of hydrogen bonds in the adsorbed layer of alcohols on graphitized carbon black (110), can only

serve as a few examples of the versatility of the method. For a more detailed discussion on the use of gas chromatography for physical measurements, one may refer to the following sources (111-113).

SEPARATION OF ISOTOPIC METHANES

INTRODUCTION

Gas chromatography has been used with considerable success in separating isotopic molecules (9, 33, 114-126) but it appears that the separation of the five isotopic methanes (CH_4, CH_3D, CH_2D_2, CHD_3, and CD_4) still remains a problem. The efforts of Gant and Yang (127) on a conventionally packed high activity charcoal column were on the whole unsuccessful, although they did manage to obtain a chromatogram in which it was possible to see the presence of five components. In comparison, Bruner and Cartoni (128), obtained excellent results on an etched glass capillary column of the type already mentioned (34). They were able to achieve a base line separation between CH_4-CH_3D-CH_2D_2 but after which the resolution decreased very rapidly. Although this was an excellent achievement it could not be used for analytical purpose where, CHD_3 or CD_4 may be present only in very small concentrations.

A gas chromatographic column which allows a complete separation of all such components would be an invaluable tool for following reactions in which the deuterated methanes are either reactants or products.

The purpose of this study was to find such a column preferably a conventionally packed type so that its use

could be extended to preparative work. Since there are no guide lines as to what type of packing is specific for the separation of the deuterated methanes, the problem was brought to the level of trial and error. Rather than preparing a multitude of columns (and these would have to be of considerable length) of prospective solid support, trying them and finally rejecting them completely, it was decided that it would be more economical both in cost and time to do desorption studies of the two extreme molecular weight methanes from the various solids. The material which would lead to the largest pressure difference of the two methanes at a particular temperature would be the most likely choice for the column packing.

DESORPTION STUDIES

Experimental

CH_4 (C.P. grade) was obtained from Matheson and Co. and was purified by degassing on a vacuum apparatus at solid nitrogen temperature.

The deuterated methanes were obtained from Merck, Sharp, and Dohme Co. Ltd., Montreal, and were not purified any further. CD_4 was introduced into the apparatus with utmost care so as not to contaminate it.

The block diagram of the desorption apparatus is shown in Fig. (2.1). A and B were 1 liter storage bulbs.

FIGURE (2.1)

BLOCK DIAGRAM OF THE ADSORPTION APPARATUS.

A, B 1 liter storage bulbs.

C Desorption cell.

D Thermocouple pressure gauge.

E McLeod gauge.

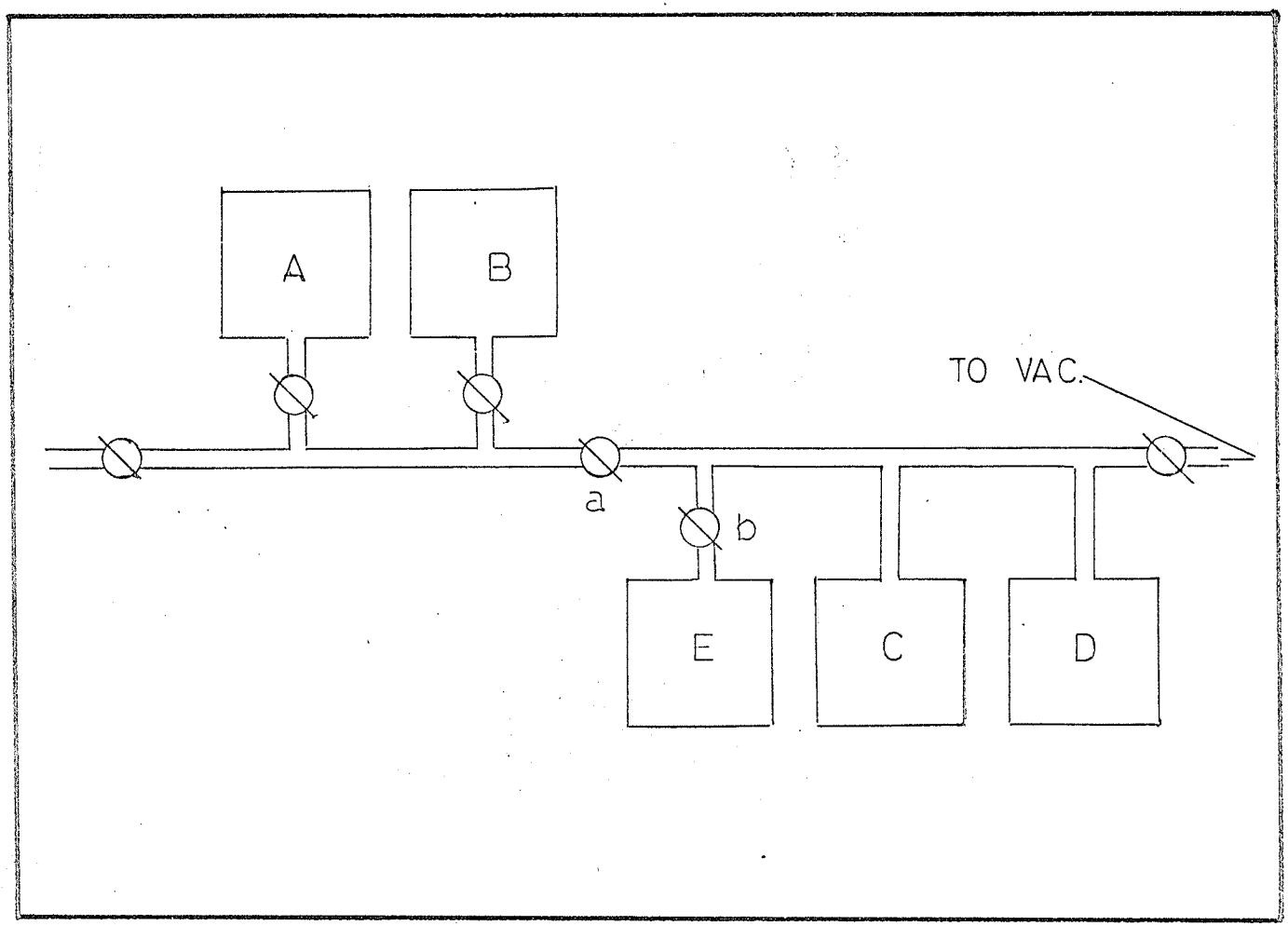
A
B
TO VAC.
a
b
E
C
D

C is a modified Leroy still which allowed for sample introduction, and the removal of the heater coils and the thermocouple wires prior to sample degassing. This is shown in Fig. (2.2). The brass tube closed off at one end in which the heating coil and the thermocouples were mounted, had an inside diameter very close to the outside diameter of the sample containing tube. While in use a tight contact between it and the sample containing tube was assured by a piece of styrofoam (S, Fig. (2.2)) placed in the outer jacket.

D is a thermocouple pressure gauge (R.C.A. - model 1946) and is shown in Fig. (2.3). During operation the pressure gauge was maintained at 0°C. with ice and water. A 6 volt battery served as a constant current source. Since the gauge produced an output of approximately 12 mv. at stick vacuum, it was necessary to use a bucking e.m.f. in order that a 5 mv. recorder could be used. This was accomplished by two thermocouple junctions one kept at 0°C. and the other at -196°C. placed in series (but opposite in polarity) with one of the leads going to the recorder. The correspondence between stick vacuum and zero e.m.f. output was achieved by adjusting the current through the pressure gauge.

The temperature of the sample was varied by means of a motor driven Powerstat. The range of scan was determined

FIGURE (2.2)

MODIFIED LEROY STILL.

A Brass tube on which the sample heating coil and the thermocouples are mounted.

B Outer jacket.

C Heating and thermocouple wires.

T_1, T_2, T_3, T_4, T_5, Thermocouples.

S Styrofoam.

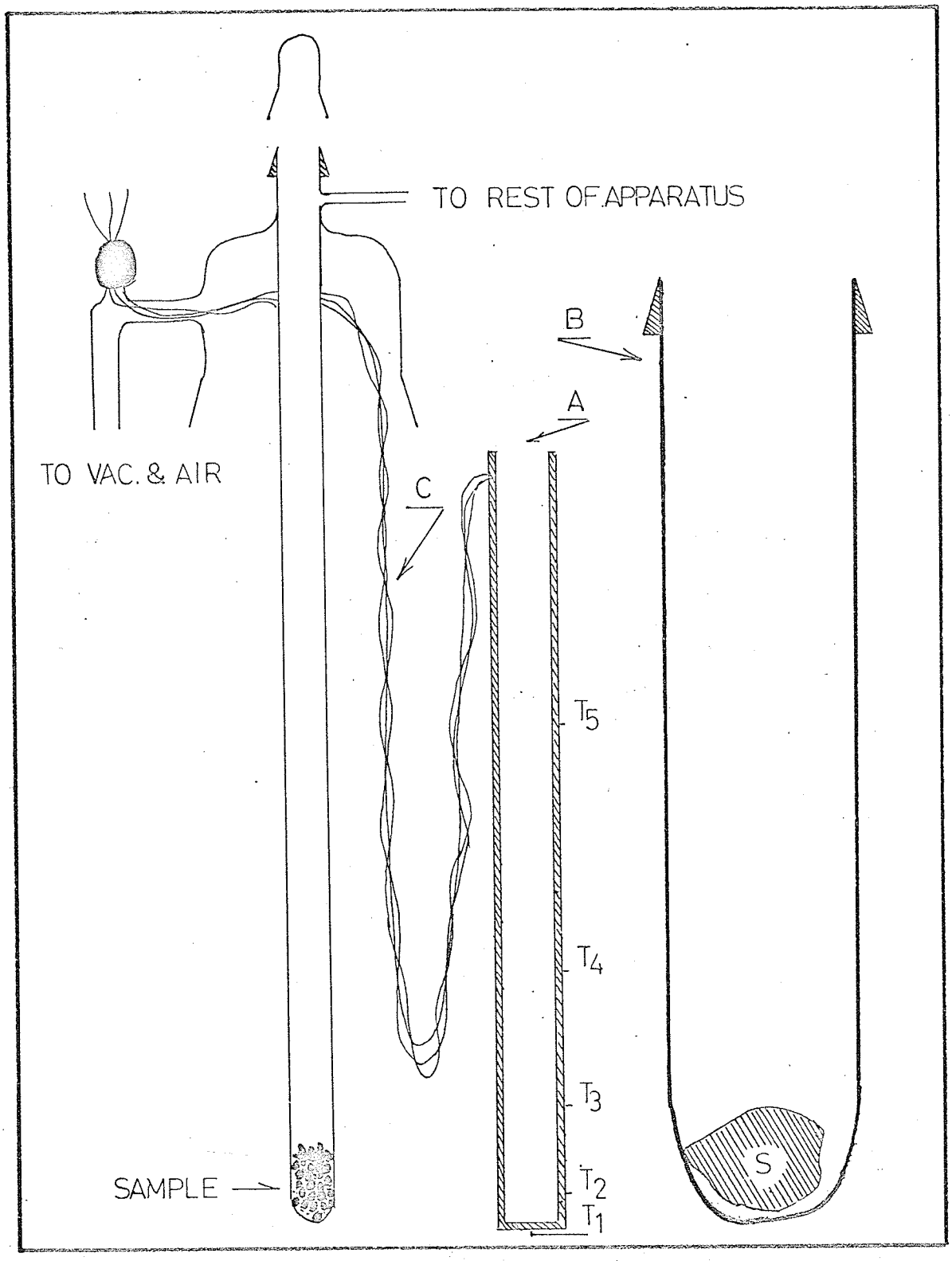
TO REST OF APPARATUS
B
A
TO VAC. & AIR
C
T5
T4
T3
T2
T1
S
SAMPLE

FIGURE (2.3)

THERMOCOUPLE PRESSURE GAUGE.

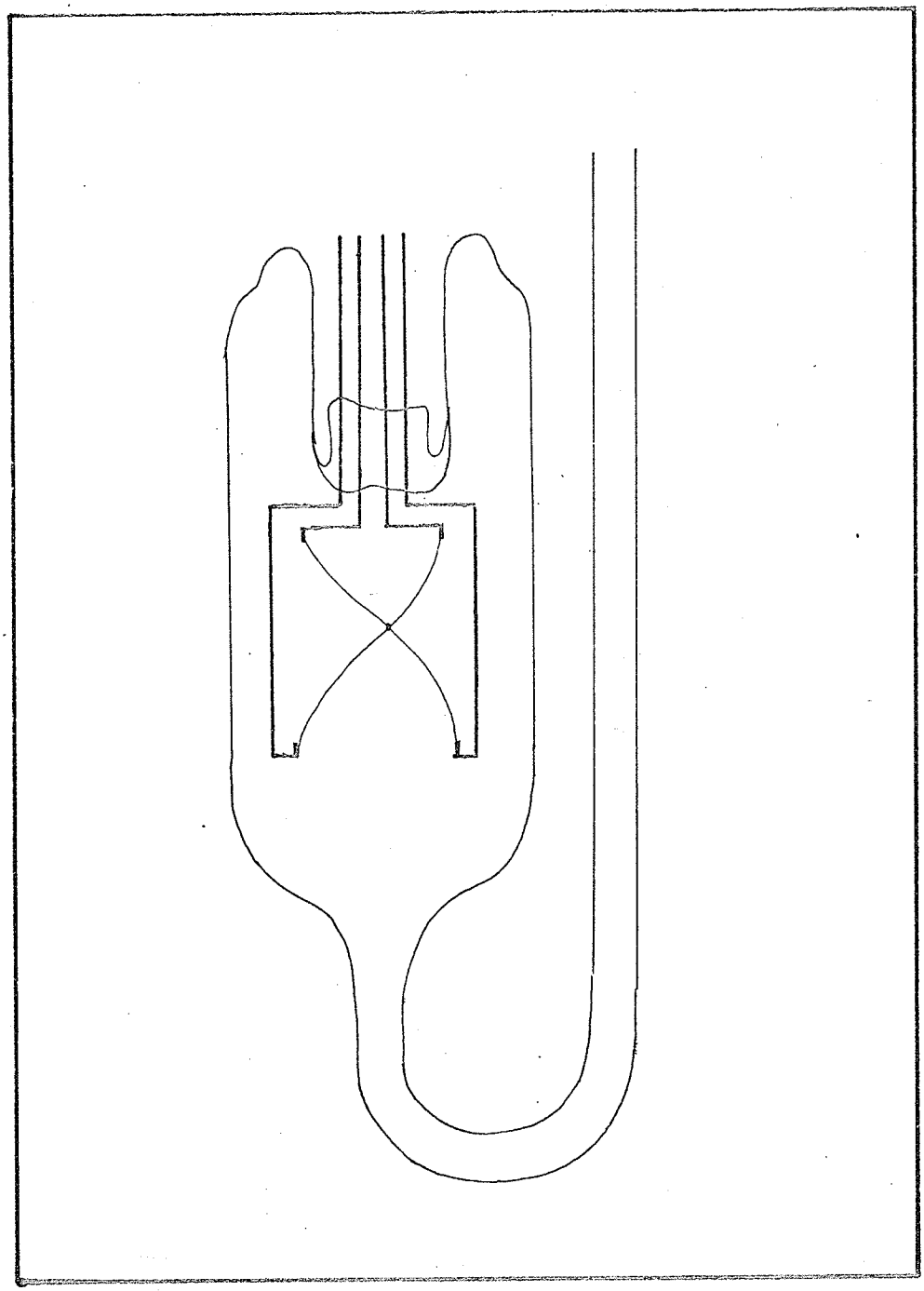

by a setting of another Powerstat whose output served as the imput of the scanning Powerstat. On the average the temperature was increased at the rate of ½° per minute.

Since the interest was in the lower temperature range, (-196 to -60) the temperature of the sample was measured with a thermocouple(s) whose reference was at -196°C. By doing this both the pressure and temperature could be represented on the same chart by sampling the e.m.f. of the pressure gauge and the thermocouple respectively. A record of recorder fluctuation (zero base line) was kept by sampling a zero e.m.f. of a thermocouple pair maintained at -196°C.

Frequent checks on the recorder response were made by switching the e.m.f. source from the recorder to a potentiometer by means of a double pole double throw switch. Where e.m.f. switching was necessary great care was taken in switch choice and connecting so as not to introduce spurious e.m.fs..

The electrical wiring of the apparatus is shown in Fig. (2.4).

Experimental Procedure

After the sample was degassed under vacuum (most often overnight degassing was sufficient to reach the desired vacuum (∿0.1 micron)) and allowed to cool down, a

FIGURE (2.4)

WIRING DIAGRAM OF THE DESORPTION APPARATUS.

Rec.	Recorder.
Pot.	Potentiometer.
SS	Cycling sampling switch.
SSM	Sampling switch drive motor.
PM	Powerstat motor.
TR	Transmission.
SHC	Sample heating coil.
TPG	Thermocouple pressure gauge.
R_1	Fine current adjust.
R_2	Coarse current adjust.
ST	Sample temperature thermocouple.
S_1, S_2,	Switches.
D_1	Recorder-Potentiometer switch.
D_2	Polarity switch.
D_3	Thermocouple reference temperature switch.

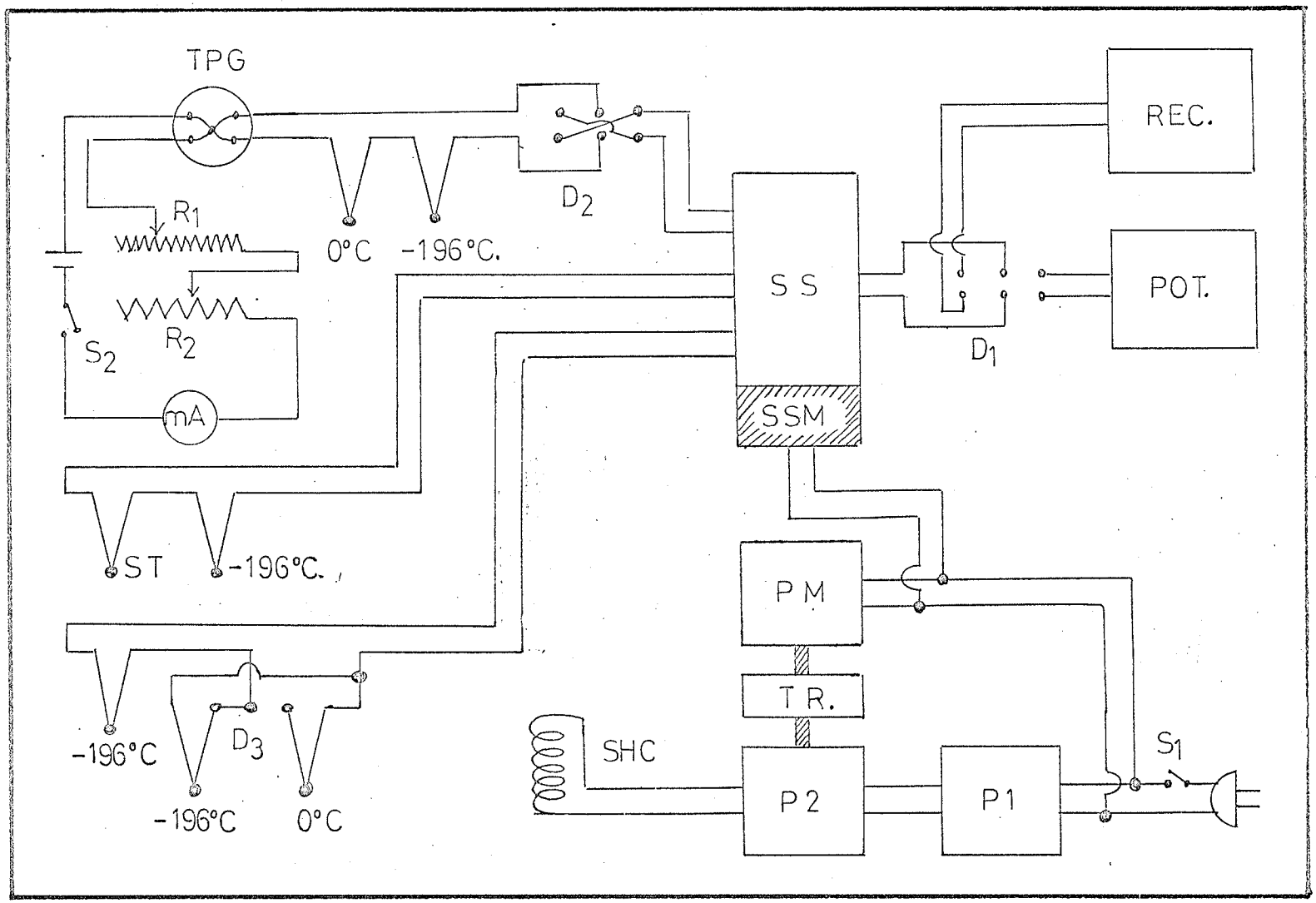
TPG
R1
R2
S2
mA
0°C
-196°C.
D2
S S
SSM
REC.
POT.
D1
ST
-196°C.
P M
T R.
SHC
P 2
P 1
S1
-196°C
D3
-196°C
0°C

small sample of gas (CH_4 or CD_4) was introduced into the system. The pressure of the gas was measured with the McLeod gauge. After the modified LeRoy still was re-assembled it was immersed in a liquid nitrogen bath. The temperature of the liquid nitrogen was measured with the potentiometer by means of switches D_1 and D_3. It was important to use only pure liquid nitrogen for this work since the e.m.f. of the pressure gauge and its relationship to the sample temperature was liquid nitrogen temperature dependent. In order to obtain quick cooling of the sample air was admitted into the jacket of the modified LeRoy still. When the sample temperature had reached approximately -190° C., the jacket was evacuated after which switch S_1 (Fig. (2.4)) and the chart drive of the recorder were turned on. It can be seen from Fig. (2.4) that the switch S_1 can simultaneously activate the two Powerstats, the Powerstat driving motor and the cyclic stepper switch.

This procedure was followed for each of the gases and each solid sample. The experimental data (a plot of recorder stability, temperature change, and pressure change as a function of time) for each run was contained on a single chart paper. A direct comparison of CH_4 and CD_4 pressures above a solid could be made by superposition of the temperature curves.

Results and Discussion

For illustrative purposes only a typical time against temperature, pressure, and recorder stability plot is shown in Fig. (2.5).

The results of a series of experiments are summarised in Table (2.1). The designations of 0 or + refer to unobserved or observed pressure differences respectively.

As can be seen from Table (2.1) only the saran charcoal gave a positive result. On these findings a saran charcoal column was prepared and tried.

GAS CHROMATOGRAPHY

Introduction

While the desorption studies were going on, attention was being focused on the porous polymer beads used by Hollis and others (129-132). Desorption studies, as can be seen from Table (2.1), indicated that Poropak Q was not suitable for isotopic methane separation. Despite this a 20 foot 1/8" o.d. column of ((50-80) mesh) Porapak Q was prepared and tried. At room temperature and at comparatively low flow rates, the chromatogram showed a shoulder. By successively reducing the column temperature the separation became more and more pronounced. It became apparent that the desorption apparatus although quite

FIGURE (2.5)

PLOT OF TIME AGAINST TEMPERATURE,

PRESSURE, AND RECORDER STABILITY.

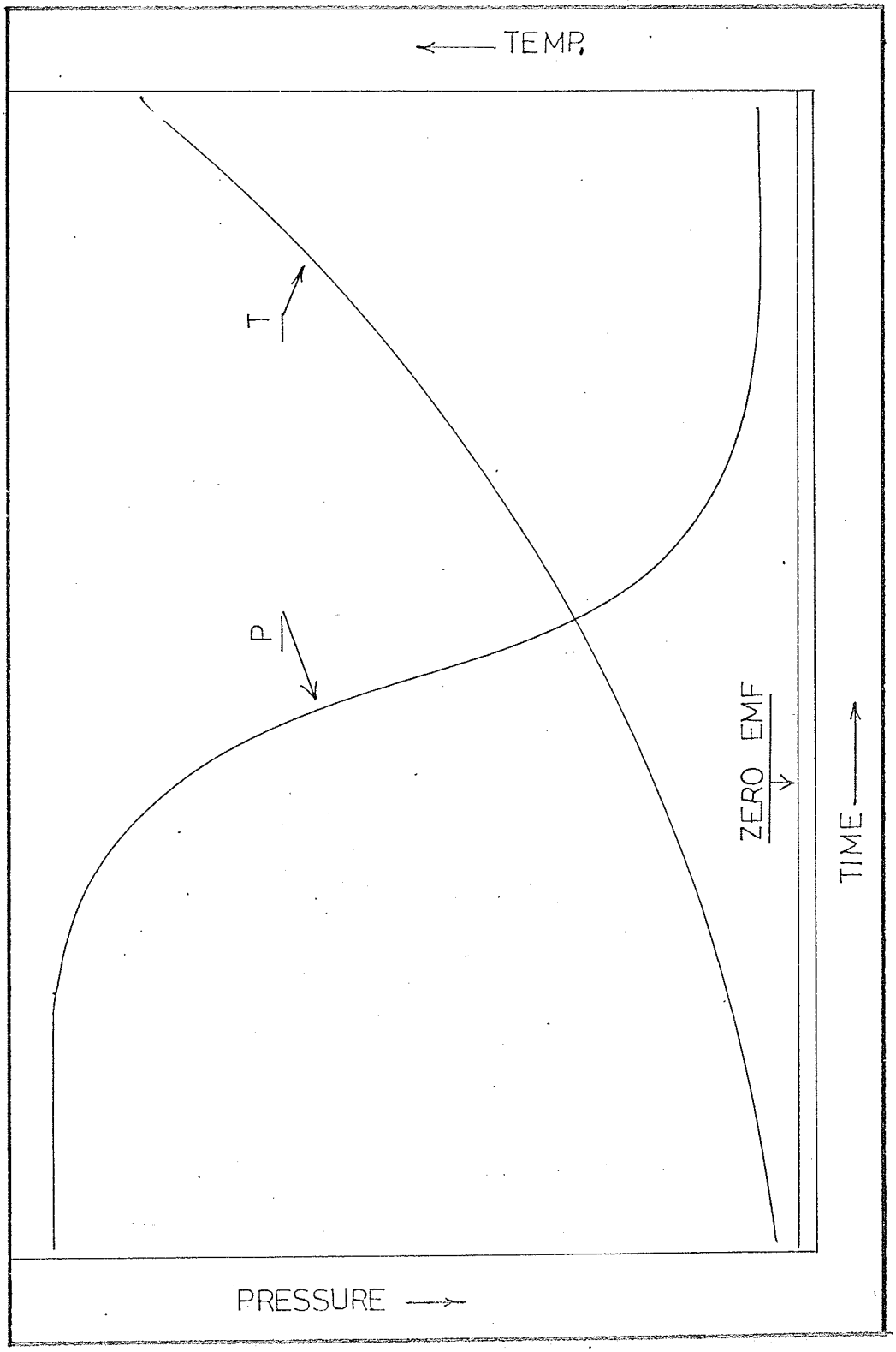
TEMP.
T
P
ZERO EMF
TIME
PRESSURE

TABLE (2.1) RESULTS FROM DESORPTION STUDIES

Solid Sample	Weight (gms.)	Degas. Temp. (°C.)	Initial Press. (μ) CH_4	CD_4	Result
Silica Gel (28-40 mesh)	0.189	98	5	5	0
Silica Gel (28-40 mesh)	0.189	200	21	21	0
Silica Gel (28-40 mesh)	0.189	495	21	20	0
Porous Glass (60-80 mesh)	0.210	495	21	20	0
Saran Charcoal (∿30-60 mesh)	0.205	495	21	21	+
Dowex A-1 Resin (25-50 mesh)	0.213	80	20	20	0
Firebrick (60-80 mesh)	0.197	347	23	21	0
Cobalt Powder (∿30-60 mesh)	0.185	200	21	22	0
Porapak Q (50-80 mesh)	0.185	200	20	20	0

sensitive to pressure differences, was actually quite crude in comparison to the gas chromatographic method. These findings led to the preparation of a number of columns most of which were packed with a variety of available porous polymers.

Experimental

Columns

The columns were made from 1/8" o.d. (0.03" wall thickness) copper tubing. They were hung in a stairwell and filled through both ends by means of a two stem funnel. During the packing process a rotating hexagonal brass nut driven by an electric motor was used to promote a tighter packing. The vibrational process was always started at the bottom and was slowly worked up. When no further particle settling was noticed, the columns were considered to be packed. The ends of the column in most cases were terminated with a thin (approximately 1/16") plug of G.E. Foametal. In order to prevent the Foametal from falling out, the ends of the copper tube were filed in such a manner so as to form a lip over the porous metal. This is shown in Fig. (2.6). In cases where the column was longer than 50 ft., the sections were connected with a Swagelok unions which were filled with the packing material so as to minimise dead space.

FIGURE (2.6)

COLUMN TERMINATION.

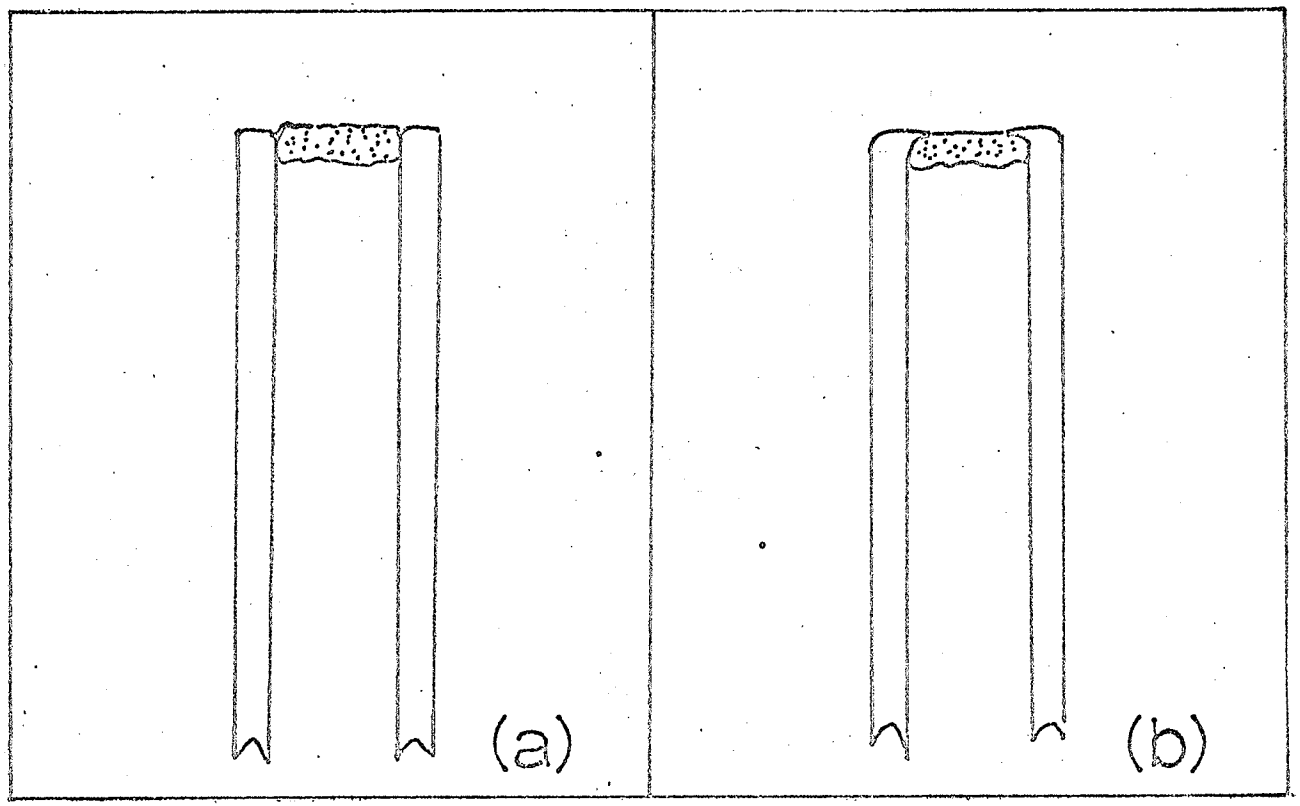
(a)
(b)

Columns which were investigated in this phase of work were as follows;

a) Saran Charcoal (~25-50 mesh) 20 ft.

b) Solid Carbon (~25-50 mesh) 20 ft.

c) Porapak Q (50-80 mesh) 20 ft.

d) Porapak Q (50-80 mesh) 100 ft.

e) Porapak Q (80-100 mesh) 100 ft.

f) Porapak P (50-80 mesh) 20 ft.

g) Porapak R (50-80 mesh) 20 ft.

h) Porapak S (50-80 mesh) 30 ft.

i) Porapak S (50-80 mesh) 50 ft.

j) Porapak S (100-120 mesh) 50 ft.

k) Porapak T (50-80 mesh) 20 ft.

l) Porapak N (50-80 mesh) 50 ft.

m) Chromosorb 102 (50-80 mesh) 50 ft.

n) Porous Glass (2,500A° pores) (50-80 mesh) 20 ft.

o) Dowex A-1 resin (~25-50 mesh) 20 ft.

p) Polystyrene (3%) - a 3% polystyrene column was prepared by first dissolving the polystyrene in methyl ethyl ketone and then adding to the solution with constant stirring an appropriate amount of (60-80 mesh) firebrick. The solvent was then dried off at 100°C. and the 20 ft. column was packed in the usual manner. All columns were purged at 190°C. with nitrogen before use.

Packing material for columns (c)-(l) inclusive was obtained from Waters Associates.

Packing for column (a) was kindly donated by Dr. S. Barton at Royal Military College, Kingston, Ontario.

The granular solid carbon used in column (b) was obtained from Shawinigan Chemicals.

Chromosorb 102 which is basically similar to the Porapaks, is a product of Johns Mansville.

The 2,500A° pore porous glass was obtained from Bio-Rad Laboratories.

The ion exchange resin, Dowex A-1 was obtained from Baker Chemicals.

In many cases the porous polymers as obtained from the manufacturer tended to aggregate and stick to the walls of the tubing. Under such conditions proper column packing was not possible. It was found that this could be remedied by first subjecting the packing material to T.H.F. (tetra-hydrofurane) and then drying them at 100° C..

Low Temperature Bath

In this phase of work most experiments were carried out at subambient column temperatures. Low temperatures were attained by an arrangement which is shown in Fig. (2.7). The liquid nitrogen contained in a 25 liter dewar is boiled by means of an electric heater whose power output is determined by the Powerstat setting. The nitrogen gas

FIGURE (2.7)

EXPERIMENTAL ARRANGEMENT FOR SUBAMBIENT STUDIES.

a 25 liter dewar.

b Nitrogen gas precooler coil.

c Heating coil.

d Insulation.

e 5 liter dewar.

f Heat exchange coil.

g Column.

1
2
3
4
5
6
7
8
9
10

which is forced to travel down a coiled 3/16" o.d. copper tube, is precooled before it leaves the dewar and serves as the coolant. Heat exchange between the column and the cold nitrogen gas was accomplished by means of a heat exchange coil and ethanol (see Fig. (2.7)).

The temperature bath can be brought down from ambient temperature to the desired temperature relatively quickly by direct addition of liquid nitrogen to the ethanol. With little care it is possible to reach the working temperature to within ±½° by this method. Once this has been done, the heater in the large dewar can be turned on. The actual setting of the Powerstat for a particular working temperature requires some initial trial and error. Once this setting is found the temperature of the bath can be maintained to within less than ±½° for many hours.

Sampling

A model CSV-1 X (Chromatronix Incorporated) sampling valve having a 1.4 μ.l. sample volume was used in this phase of work. The sampling valve could be filled or evacuated by means of a three way stopcock as is shown in Fig. (2.8). The bulk of the sample was stored in a gas buret which served as a means of controlling the sample size. A 3/4" length of capillary teflon tubing (1/16" o.d.) was used to

FIGURE (2.8)

SAMPLING ARRANGEMENT.

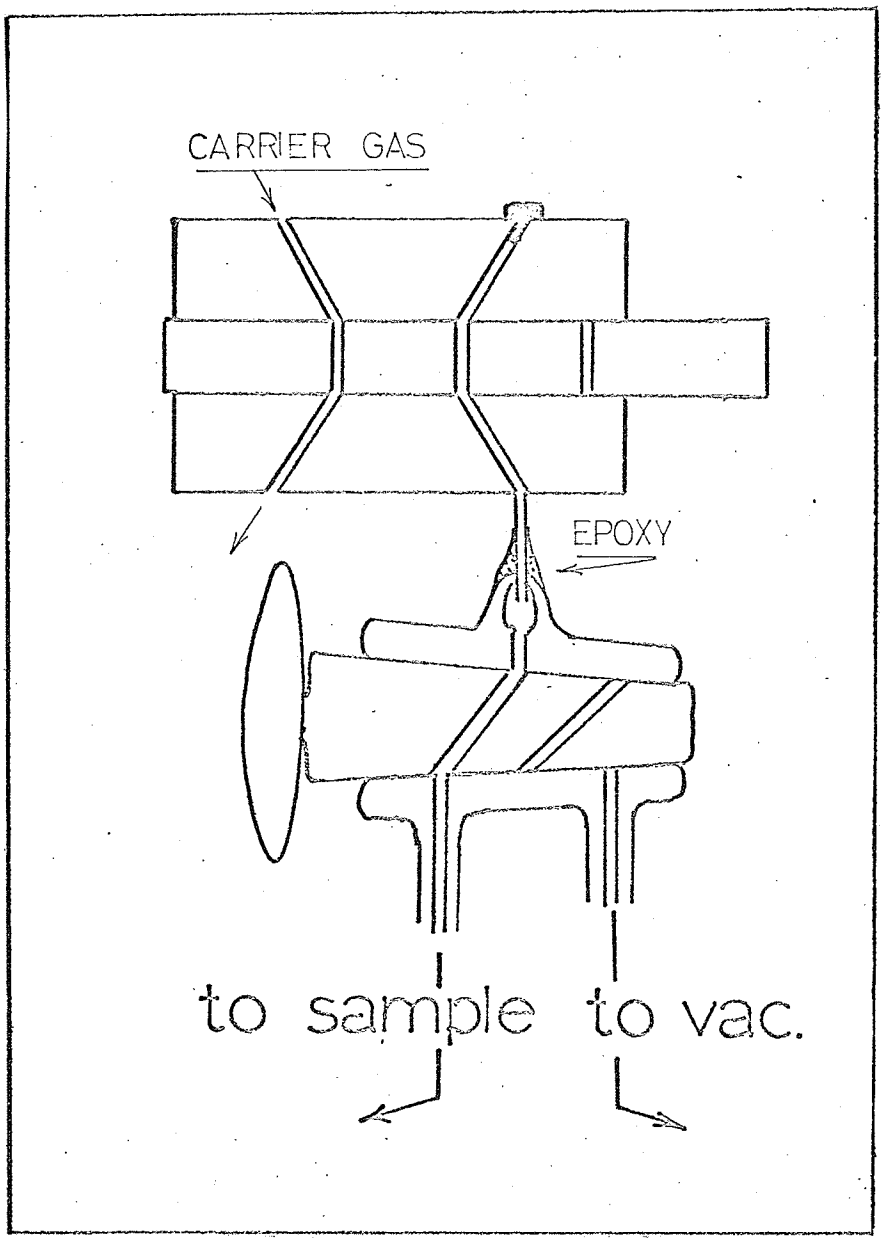
CARRIER GAS
EPOXY
to sample
to vac.

connect the valve and the column. The dead volume contribution from this was considered to be negligible.

The sample sizes of CH_4-CD_4 mixture were generally 0.2 μl. (at S.T.P.) or less.

Detector

A Beckman GC-4 hydrogen flame detector was used most often but on occasions use was made of the Aerograph electron capture (250 m.c. tritium source) in a "helium detector" mode. A Keithley 240 power supply and a Keithley 410 electrometer were used with the above detectors. The columns were attached to the detectors with a length of stainless steel capillary tubing of negligible volume.

Air Supply

During experiments the air for the hydrogen flame detector was supplied by a compressed air cylinder. Between experiments the system was switched to a small aquarium pump. In either case the air was passed through a molecular sieve (5A) trap at ambient temperature before it was allowed to enter the detector.

Helium

The helium gas was purified by an activated charcoal trap in series with a molecular sieve (5A) trap both of

which were held at liquid nitrogen temperature.

Hydrogen

The hydrogen gas was purified by a molecular sieve (5A) trap at liquid nitrogen temperature.

Results And Discussion

The results obtained on a 20 ft. Porapak Q column led to the preparation of a 50 ft. column. A series of experiments at various temperatures (as low as -100°C.) and flow rates showed conclusively that a complete separation of the CH_4-CD_4 mixture was not possible on this length of column. In view of this a 100 ft. Porapak Q column was prepared and tried.

As can be seen from Fig. (2.9) the separation of CH_4-CD_4 mixture can be achieved on a 100 ft. column. The chromatographic peaks are symmetrical and have relatively short retention times. It was found that a somewhat better separation could be achieved at lower temperatures and/or slower flow rates, but the retention times became of considerable length.

From Fig. (2.10) it can be seen that at 0°C. there is a considerable degree of separation. The separation can be increased, as is shown in Fig. (2.11), by a sample freezing technique. This can be achieved by forming a

FIGURE (2.9)

SEPARATION OF CH_4-CD_4 MIXTURE.

Column 100 ft. Porapak Q (50-80 mesh).

Column temperature -45 ± 1° C.

CH_4/CD_4 1.9

Inlet pressure 70 psi.

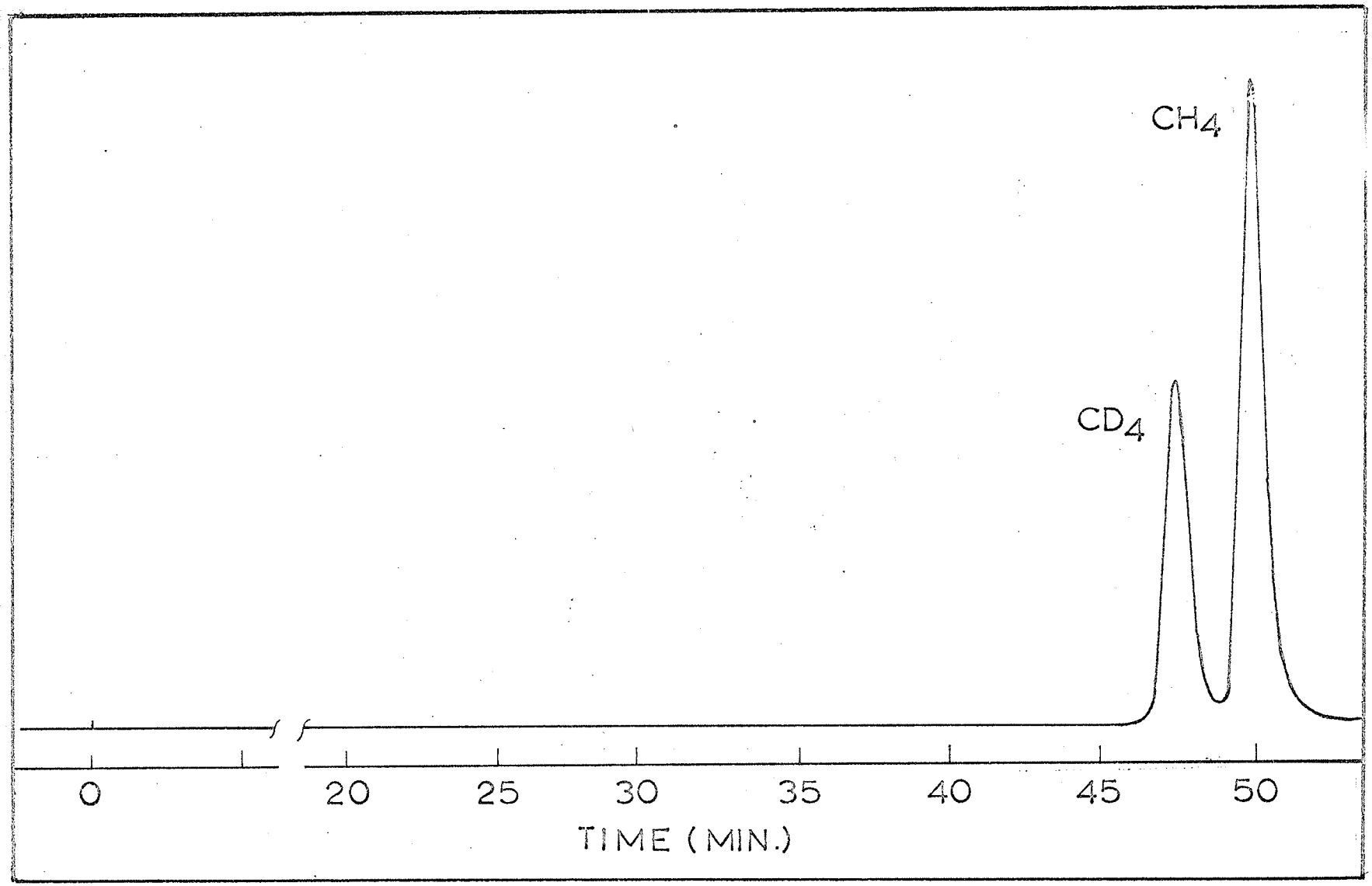
CH4
CD4
0
20
25
30
35
40
45
50
TIME (MIN.)

FIGURE (2.10)

SEPARATION OF CH_4-CD_4 MIXTURE.

Column 100 ft. Porapak Q (50-80 mesh).

Column temperature 0° C.

CH_4/CD_4 1.5

Inlet pressure 70 psi.

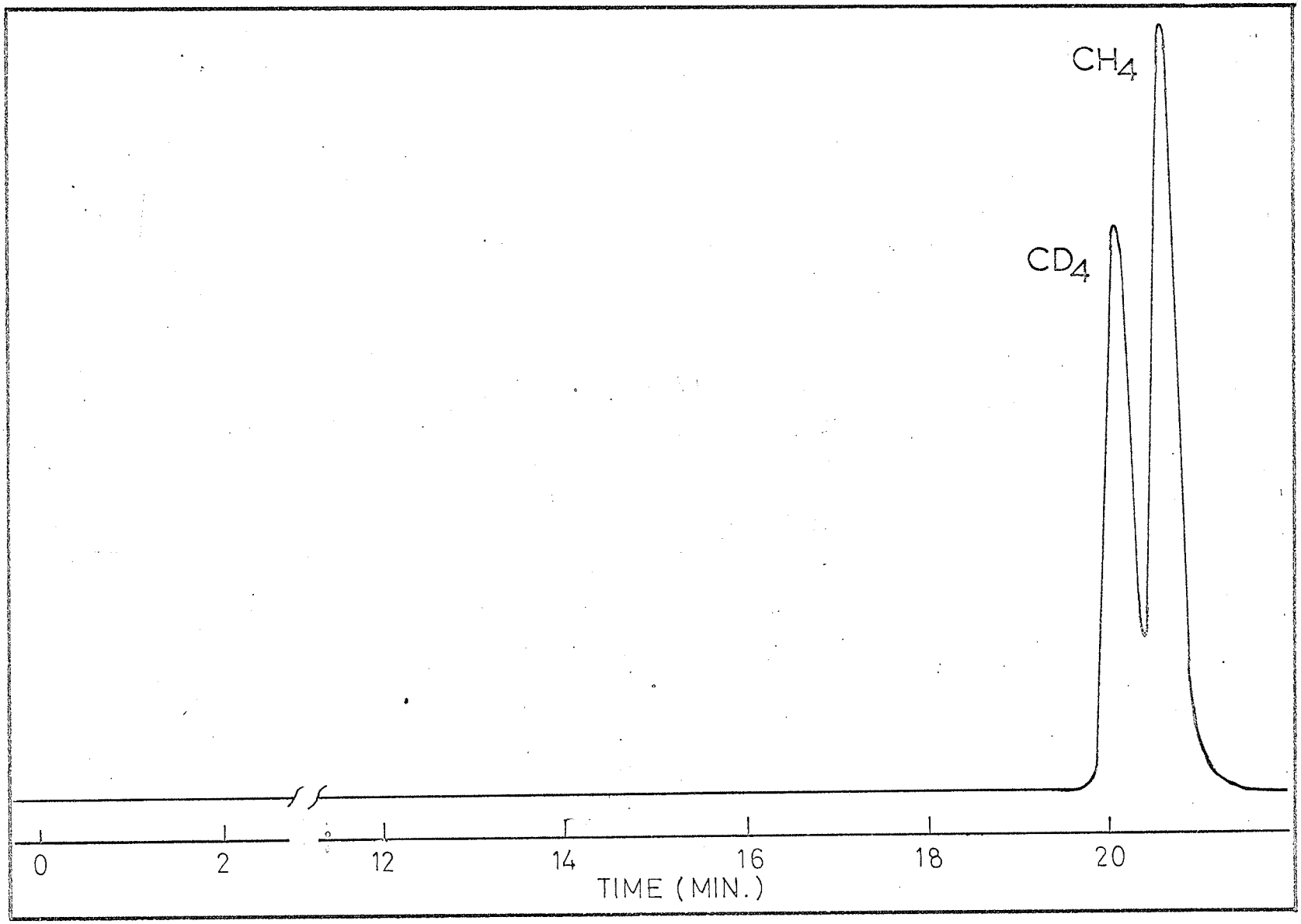
CH4
CD4
0
2
12
14
16
18
20
TIME (MIN.)

FIGURE (2.11)

SEPARATION OF CH_4-CD_4 MIXTURE.

Column 100 ft. Porapak Q (50-80 mesh).

Column temperature 0° C.

CH_4/CD_4 1.5

Inlet pressure 70 psi.

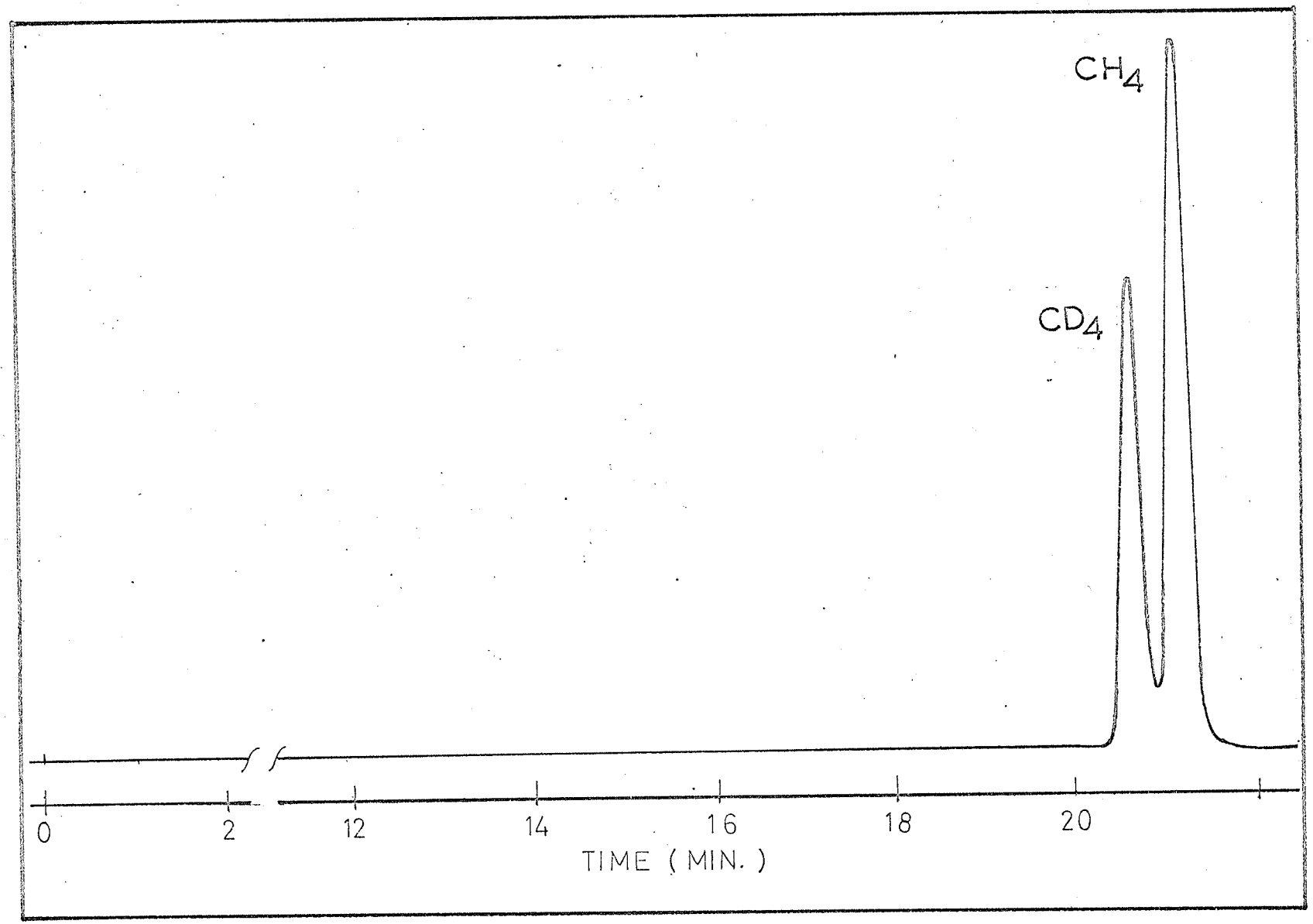
CH_4
CD_4
0
2
12
14
16
18
20
TIME (MIN.)

small narrow U just past the injection port out of approximately 6 inches of the column. The U is then cooled to liquid nitrogen temperature. The sample is then injected and allowed to freeze out in the U after which the liquid nitrogen is quickly removed. The removal of liquid nitrogen is referred to as t = 0 in Fig. (2.11). This technique appears to be most effective at higher column temperatures. When applied to conditions in Fig. (2.9), only slight improvement in separation was noted.

This effect can be explained in the following manner. The sample which is under reduced pressure (approximately 0.25 atmosphere) is suddenly exposed to a carrier gas at 70 p.s.i.. The onrush of the carrier gas into the sample volume causes mixing and as a result the initial mixed solute band is broadened. As the mixture travels from the point of injection to the column entrance further band broadening takes place. One source is the gas diffusion and another is the presence of stagnant regions introduced by mechanical connections (133). As can be seen considerable band broadening can take place before the sample reaches the column. By applying liquid nitrogen to a small part of the column the advancing sample is frozen out on a relatively narrow region. On warm up the sample starts off as a narrower band than that which it was when it entered the column. The quicker release of the more volatile

component upon warm up most probably contributes insignificantly in improving the separation since the rate at which the U warms up is quite fast. A comparison between Fig. (2.10) and Fig. (2.11) shows that the difference in resolution is due to peak width rather than an increased difference of retention times. This of course substantiates the above argument.

It can be seen from either figure that the heavy methane is eluted before the light. This isotope effect has been observed in other cases (126, 127, 134). Cartoni et. al. (126) have shown that at very low temperatures the elution order is reversed, and that the resolution below the inversion temperature (T where $t_{R2}/t_{R1} = 1$) increases rapidly with decreasing temperature (136).

The calculated number of theoretical plates (with respect to CD_4) was 140 per foot for conditions of Fig. (2.10).

The resolution for Fig. (2.9) and Fig. (2.10) were 1.7 and 0.95 respectively.

The preliminary experiment with a saran charcoal column was started at ambient column temperature. When no elution occurred after approximately half an hour, heat ($\sim 50^{\circ}$C.) was applied to the column and the flow rate was increased to approximately 40 cc./min..

Failure to obtain elution after an additional fifteen

minutes warranted the column temperature to be raised to approximately 200°C.. After about 5 minutes of this prolonged heating, elution was obtained. The chromatogram showed two broad peaks which were reasonably well separated. The acquisition of a number of different porous polymers terminated the work on this column with full intentions of resuming it after preliminary studies were carried out with the various polymers. Unfortunately this work was never resumed but more will be said about it later.

The preliminary results of various polymer columns were as follows. Porapak P had no separating ability. Very slight separation could be obtained with Porapak T. Porapak R and Chromosorb 102 gave some separation but not as good as Porapak Q. Porapak S was found to be superior to all the others. Fig. (2.12) shows a separation which was obtained on a 50 ft. (50-80 mesh) Porapak S column. The resolution is approximately the same as that obtained on a 100 ft. Porapak Q column, but the retention time is approximately one-half. Porapak N was found to be very good giving t_2/t_1 ratios similar to Porapak S, but the peaks were somewhat broader. Perhaps with some surface modification the material may be made as useful as Porapak S.

Porapak S (100-120 mesh) column showed to be somewhat superior to Porapak S (50-80 mesh) but involved much longer retention times for the same column pressure drop. Since the components of the apparatus put a restriction on

FIGURE (2.12)

SEPARATION OF CH_4-CD_4 MIXTURE.

1 CD_4

2 CH_4

Column 50 ft., Porapak S (50-80 mesh).

Column temperature -32 ± ½° C.

CH_4/CD_4 ~ 1.

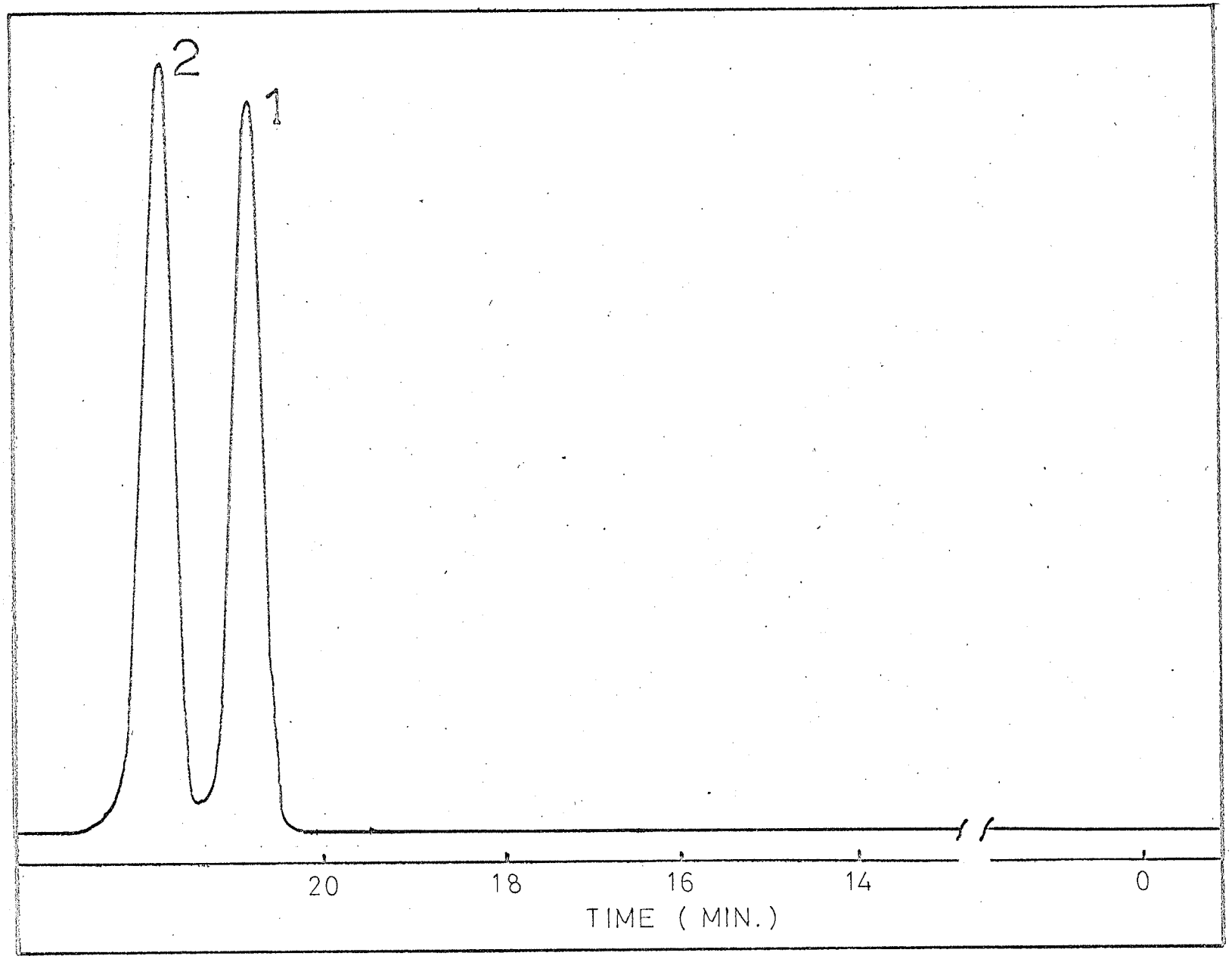
2
1
20
18
16
14
0
TIME (MIN.)

the working pressure, the 50-80 mesh column was used.

Columns b, n, o, and p showed absolutely no separating ability at any temperature.

As it was found that Porapak S was most suitable for the present problem, longer columns were constructed. Experiments showed that it was not possible to separate CH_4 and CD_4 to the point where sufficient room was made for the other three methanes on a 100 ft. column at any temperature. A 200 ft. column (the preparation of this column and the experimental arrangement will be discussed in the following chapter) gave only a partial success. The separation of the five methanes was somewhat better then that obtained by Gant and Yang, but it was not comparable to the separation obtained by Bruner and Cartoni. Calculations showed that in order to achieve complete separation with this packing, unrealistic column lengths and retention times were required. With this in mind this phase of work was terminated.

It now remains to evaluate the usefulness of this phase of study. Several workers (127, 134, 135) have succeeded in separating the CH_4-CD_4 mixture. A comparison of retention times (for a comparable resolution) is given in Table (2.2). Although the retention times listed in Table (2.2) are only approximate, they do illustrate the superiority of the porous polymer bead column over other packed

TABLE (2.2) COMPARISON OF COLUMNS USED TO SEPARATE CH_4-CD_4 MIXTURES

Column	Length (ft.)	Approx. ret. time (min.)
Modified glass capillary (136)	114	20
Porous polymer beads	50	20
High activity charcoal (127)	50	180
Molecular sieve (134)	350	840

columns. It is also a strong competitor to the capillary column. As was mentioned earlier, the use of packed columns can be extended to preparative work whereas capillary columns are restricted to analytical work only. In this sense the Porapak S column is superior to the capillary column. Besides having associated with it a relatively short retention time, the porous polymer bead column has the following desirable features which set it apart from the others;

a) the column can be packed very easily and quickly without any previous treatment of the packing;

b) the column is mechanically stable involving no danger of crushing the packing upon coiling;

c) the column requires neither special treatment aside from the initial degassing nor regeneration; and

d) the column is unaffected by water or by impurities in the carrier gas.

PHYSICAL MEASUREMENTS

INTRODUCTION

The one factor which defeated the separation of the five methanes was the band width of the individual components. In order to improve the separation, carrier gases such as CO_2, Ar and N_2 were tried since diffusion in these gases is less than in He (136, 137). Preliminary experiments were carried out on an 80 ft. 1/8" o.d. Porapak S (50 - 80 mesh) column at 0°C. and a constant flow rate of 20 cc. per min.. The results of these experiments showed that there was a large difference in both the retention times and resolution with the various carrier gases. A superimposed plot for all the carrier gases is shown in Fig. (3.1). The effect of carrier gas on retention times has been reported in other instances (138, 139) (the differences in these reports were much larger than where gas nonideality was considered). Hoffman and Evans (139) interpreted their results in terms of carrier gas-solute competition for the active sites and desorption hinderance mechanism involving the carrier gas atomic cross section. Brookman et. al. (140) rightfully criticised this by pointing out that in order to get meaningful interpretation, the data must be converted into retention volumes where viscosity and gas compressibility is taken into consideration. They repro-

FIGURE (3.1)

ELUTION OF CH_4-CD_4 MIXTURE WITH VARIOUS CARRIER GASES.

Column 80 ft. Porapak S (50-80 mesh).

Flow rate 20 cc./min..

Temperature 0 ± ½° C.

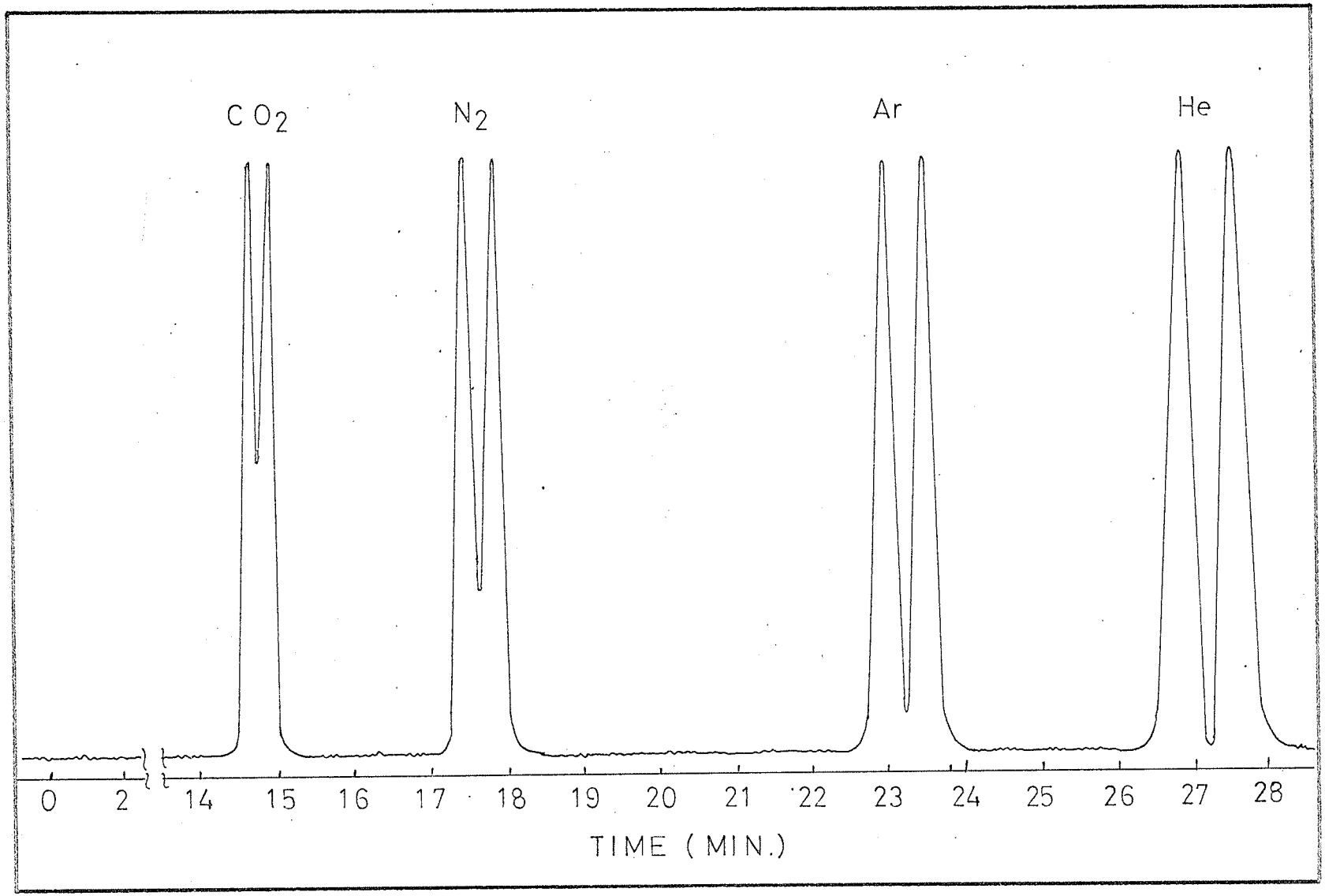
C O2
N2
Ar
He
0
2
14
15
16
17
18
19
20
21
22
23
24
25
26
27
28
TIME (MIN.)

duced experiments analogous to Hoffman and Evans and showed that although the retention times varied in the order of carrier gas viscosities (Ar > He > N_2 > H_2), the specific retention volumes for n-butane (thus K) remained constant for all gases within 1-3%. They concluded that for the series studied, the carrier gas has no influence on the partition process.

These findings were very interesting since in our experiments the retention times of the methanes varies as t(He) > t(Ar) > t(N_2) > t(CO_2) (see Fig. (3.1)) where as the viscosities vary as Ar > He > N_2 > CO_2 (141). Furthermore, by the use of the electron capture detector (in the "helium detector" mode) it was found that nitrogen, argon, and carbon dioxide can be separated on an 80 ft. Porapak S column. This in itself is evident that there is a differential interaction between these gases and the solid.

A study was begun to determine the extent to which the carrier gas affects the net retention volume. As the study progressed other aspects were considered and side studies developed. The results of these studies will be presented in this chapter.

In order that the results can have full significance, the experimental apparatus and experimental procedure must be described in detail.

EXPERIMENTAL APPARATUS AND PROCEDURE

The Column

Four 50 ft. 1/8" o.d. Porapak S (50-80 mesh) columns were joined together in a manner which was already described to form a 200 ft. column. Each 50 ft. section was prepared in the following way.

The inside of the copper tubing was washed with acetone, T.H.F., and analytical grade methyl alcohol in this order. After the washing the copper tubing was dried at room temperature for two hours by passing nitrogen gas through it.

Porapak S (50-80 mesh) (batch #457) was first washed in T.H.F., dried at 100°C., and degassed under vacuum at room temperature. While still under vacuum the temperature of the packing was raised slowly to 200°C. and sustained at that temperature for approximately 5 minutes after which the heat was switched off. Once the packing had reached room temperature it was removed from the vacuum line and was transferred immediately into a 10% trimethylchlorosilane in benzene solution. After 20 minutes the packing was filtered out and washed in an analytical grade methyl alcohol. After drying at 100°C. it was degassed under vacuum at 100°C. for three days. The final packing of the column was carried out in the same manner as that already described.

The resulting 200 ft. column was coiled on a 4 inch diameter copper pipe.

The packing material was examined under a 40 power microscope and it was found that the granules were shiny, smooth, and spherical. A photomicrograph taken at Imperial Oil Research Department confirmed this finding. A reproduction of the photomicrograph along with a scale is shown in Fig. (3.2). Out of 100 random particles the average particle diameter was measured to be 0.20 ± 0.02 mm. by means of Unitron (U-11) microscope with a micrometer scale in the eyepiece.

Sampling

A Seiscor model VIII high pressure and helium purge modified valve, having a sample volume of 0.5 µl. was used throughout the study. This pneumatically actuated diaphragm valve with a total switching time of about 10 milliseconds is capable of introducing accurately and repeatedly samples into a fast flowing gas stream. Due to its low dead volume and high speed of operation, it is ideal for band broadening studies. A schematic diagram of the valve along with the manufacturer's description of its operation is given in Fig. (3.3). The internal construction of the valve is shown in Fig. (3.4). This figure is included in order to illustrate the significance of the three chambers

FIGURE (3.2)

REPRODUCTION OF THE PHOTOMICROGRAPH SHOWING THE POROUS POLYMER PACKING.

Magnification ~ x50

1 major div. = 0.1 mm.

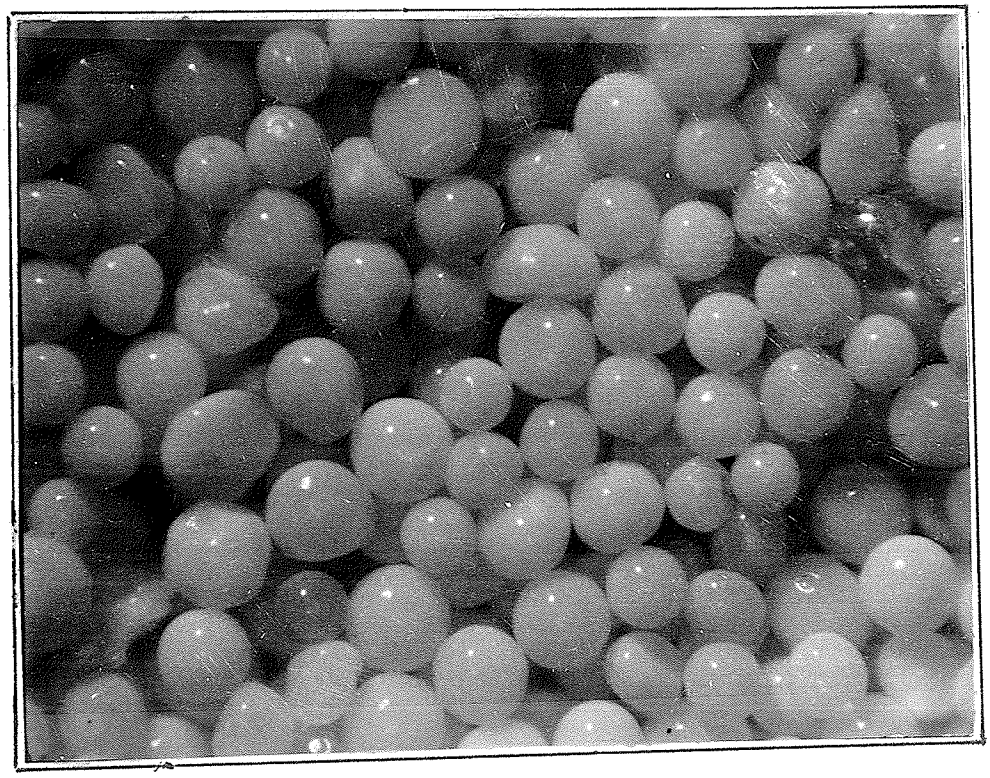

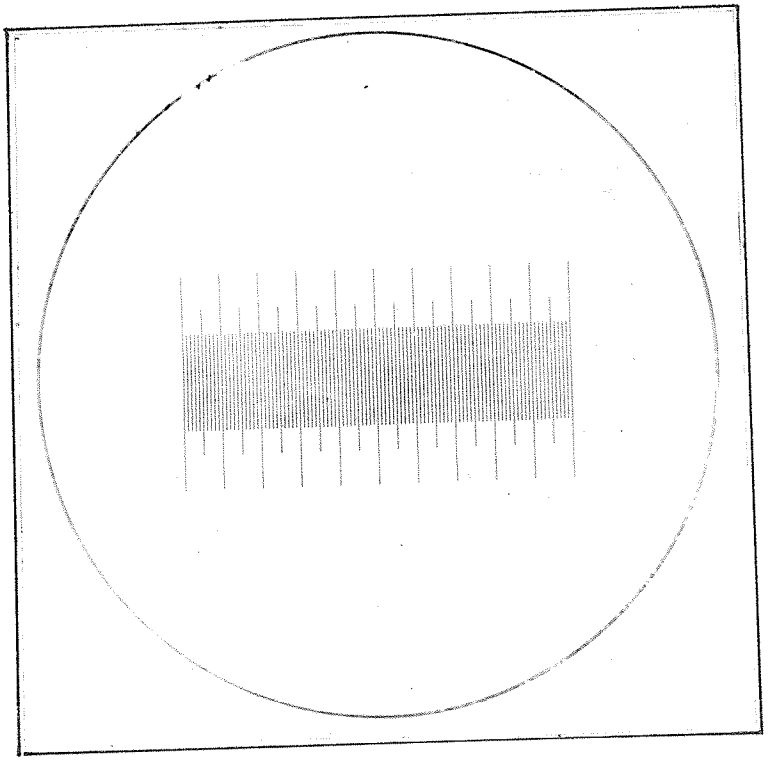

FIGURE (3.3)

SCHEMATIC DIAGRAM OF THE SAMPLING VALVE.

MODE 1

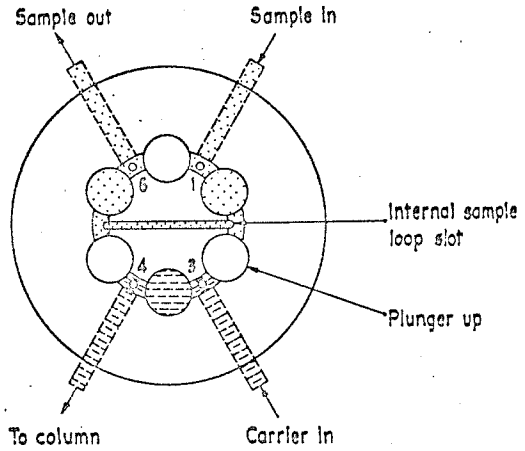
Sample out
Sample in
6
1
Internal sample loop slot
4
3
Plunger up
To column
Carrier in

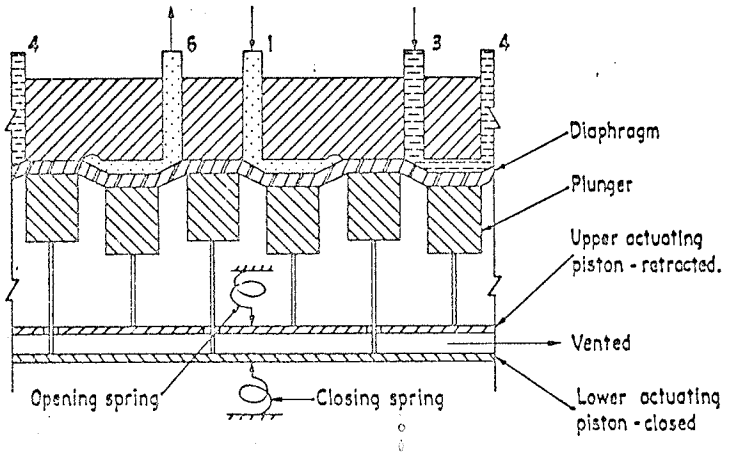
4
6
1
3
4
Diaphragm
Plunger
Upper actuating piston - retracted.
Vented
Opening spring
Closing spring
Lower actuating piston - closed

MODE 2

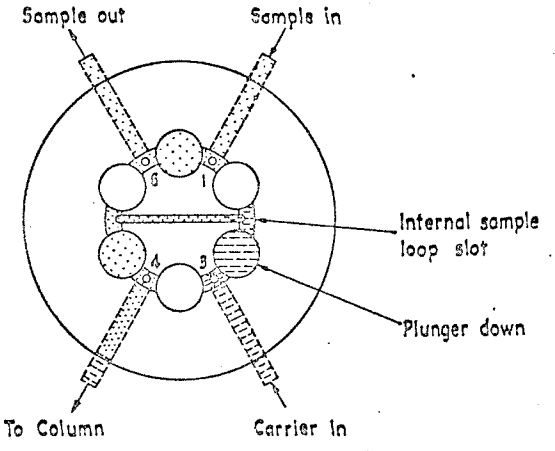
Sample out
Sample in
6
1
Internal sample loop slot
4
3
Plunger down
To Column
Carrier In

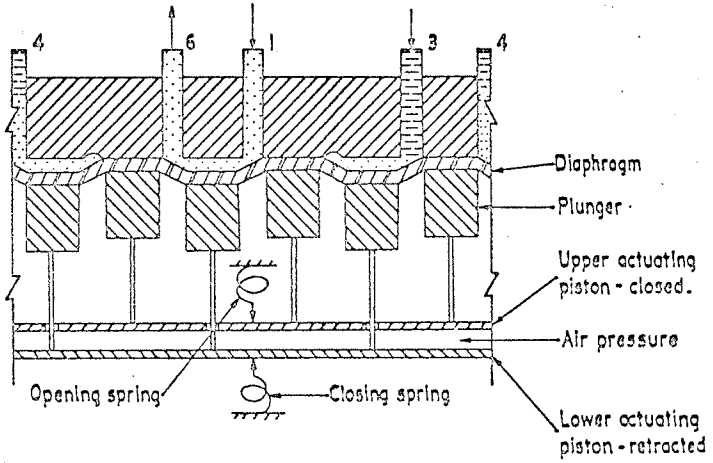
4
6
1
3
4
Diaphragm
Plunger
Upper actuating piston - closed.
Air pressure
Opening spring
Closing spring
Lower actuating piston - retracted

FIGURE (3.4)

INTERNAL CONSTRUCTION OF THE SAMPLING VALVE.

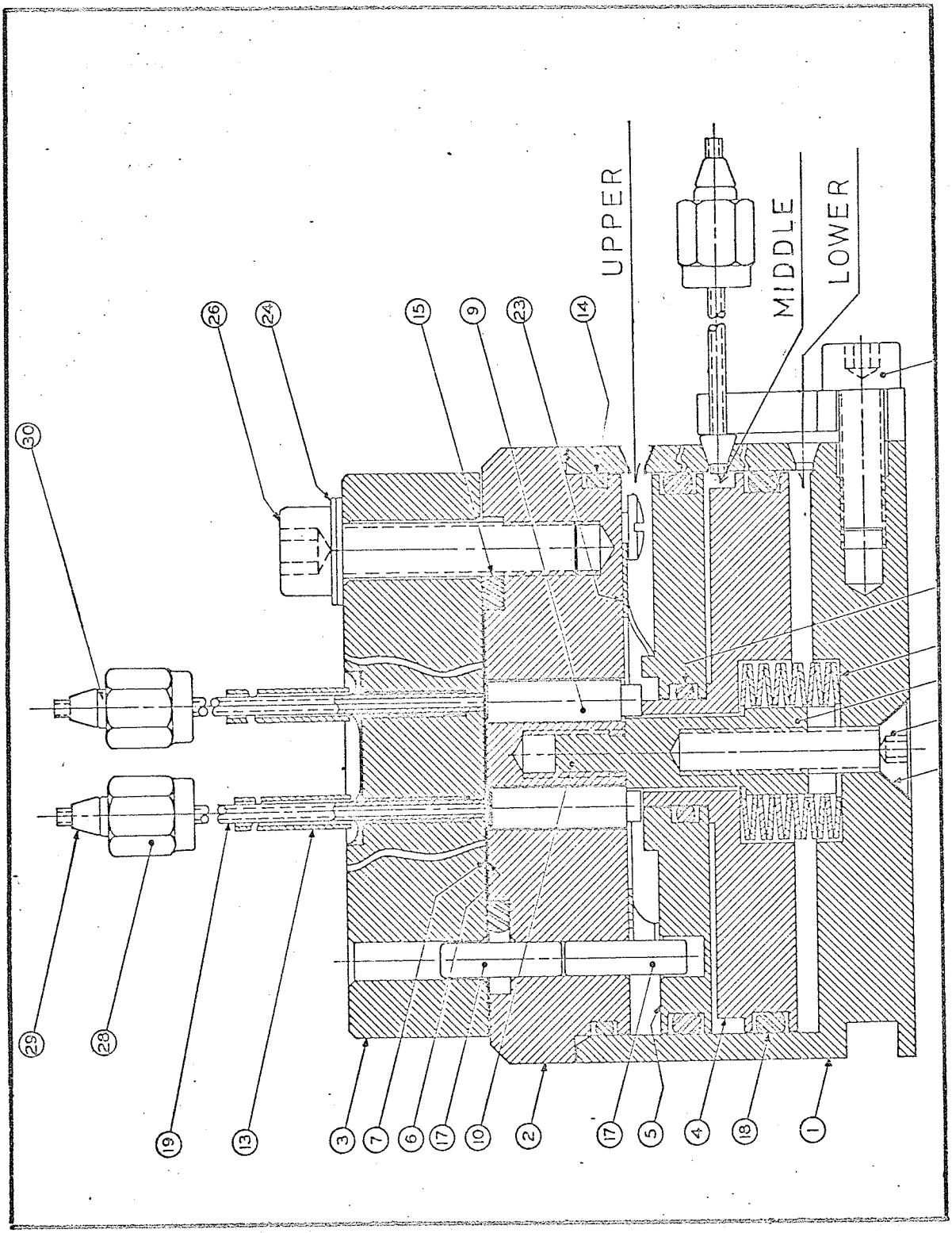
UPPER
MIDDLE
LOWER
26
24
15
9
23
14
30
29
28
19
13
3
7
6
17
10
2
17
5
4
18
1

of the valve. Under conditions of low sample pressure and relatively high carrier gas pressures, reliable and reproducible sampling can be obtained if the two outer chambers are kept under vacuum. Between sampling the middle chamber (the chamber between the actuating pistons) is also held under vacuum. To activate the valve, a gas at 36 psi. is admitted into the middle chamber. After the sampling operation is completed the middle chamber is returned to vacuum conditions. The pressure-vacuum switching can be easily accomplished by means of a three way solenoid valve. This arrangement is shown in Fig. (3.5) (a and b). Helium filtered through a 5 micron Swagelok snubber was used as the actuating gas in all experiments.

Due to the delicate nature of the valve the incoming carrier gas was also filtered through a 5 micron stainless steel 1/16" snubber. The output from the valve (1/16" stainless steel tubing) was cut to approximately 1.5 inch in length and was joined to the column by means of 1/8" to 1/16" Swagelok reducing union.

One of the tubes leading to the 0.5 µl. sample volume was cut to approximately 0.5 inch and was sealed off. The other tube was joined to the vacuum line and consequently to the gas buret by means of a three way stopcock in a manner similar to that already described.

FIGURE (3.5)

APPLICATION OF THE THREE WAY SOLENOID VALVE

FOR VACUUM-PRESSURE SWITCHING.

U	Upper chamber of the sampling valve.
M	Middle chamber of the sampling valve.
L	Lower chamber of the sampling valve.

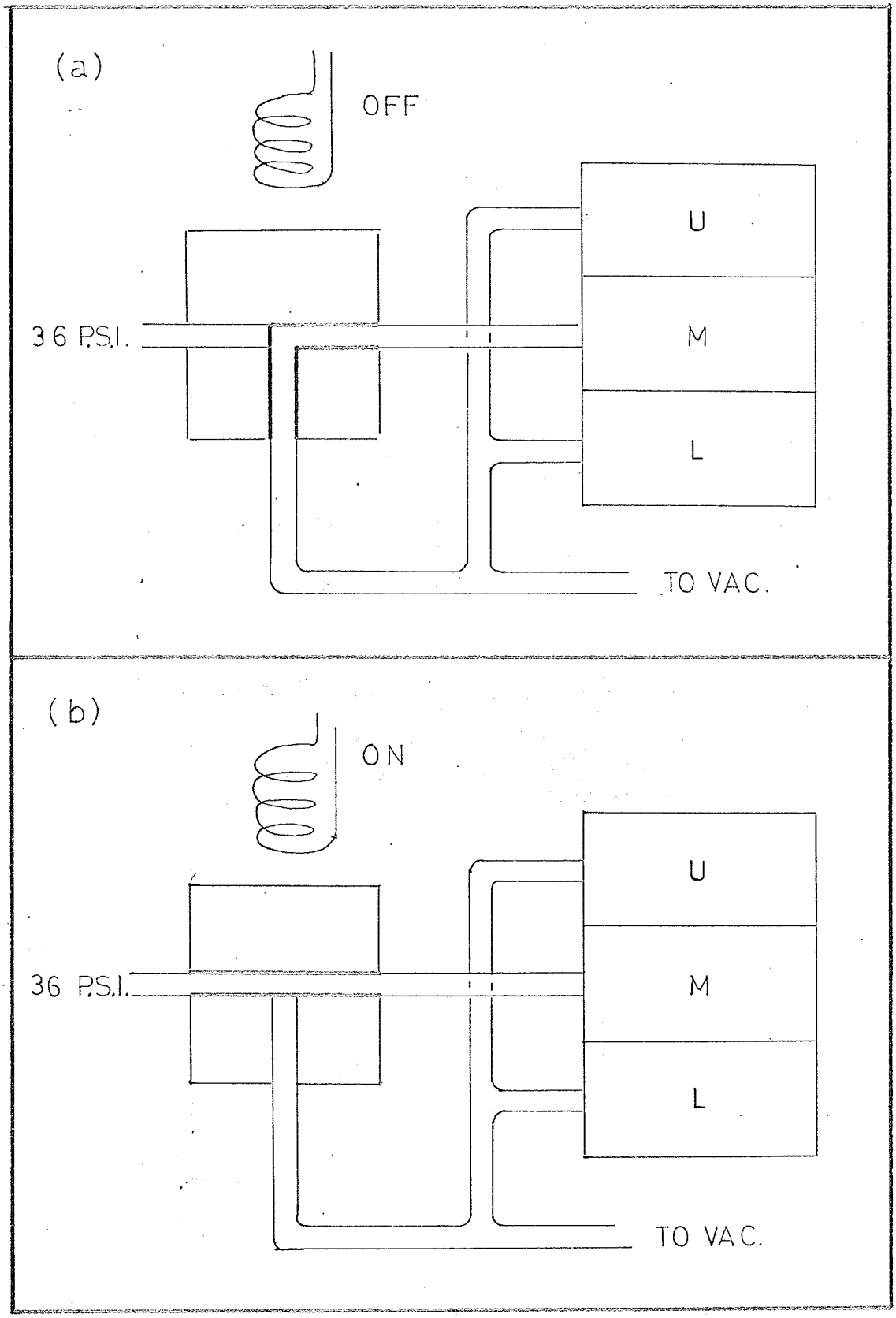
(a)
OFF
U
M
L
36 P.S.I.
TO VAC.
(b)
ON
U
M
L
36 P.S.I.
TO VAC.

Recorder

A 1 millivolt, 11" chart, 0.5 sec. response Bristol's recorder was used. The chart drive motor was connected in parallel to Lab-Chron timer which served as a check on the accuracy of the chart advance. Too much faith is generally put on the performance of the Cabot-Holtzer motor with the author as no exception. Due to an erratic performance of a previous motor approximately six months of concentrated work had to be discarded, much of which could not be repeated.

Sampling-Chartdrive Synchronization

The instance of sampling and its designation on chart paper by manual method can lead to the introduction of error which can contribute considerably to the scatter of experimental results. To eliminate this source of human error the coincidence of sampling and $t = 0$ with respect to the chart paper was obtained in the following way.

The synchronizing network involved a three unit cycling switch and a single function solenoid operated stepper switch. The sequence in which the individual microswitches of the cycling switch were activated was predetermined by the cam settings, and the duration of the off or on position was determined by the size of the cut on the cam. The cams were mounted on a common shaft which was driven by a small

d.c. motor. The single function stepper switch refers to a solenoid operated switch which can advance only one position regardless of the solenoid activation time. The interconnection between the recorder, the timer, and the solenoid three way valve which activates the sampling valve is shown in Fig. (3.6). The switches as shown in this figure are in a presampling position.

Sampling Procedure

Once the sampling valve was evacuated and then filled with the sample, the stepper switch S_3 was manually switched to the (b) position. This as can be seen from Fig. (3.6) only activates the chart drive motor and the timer. When the chart paper had advanced to the position where the recorder pen was on a major division, the stepper switch S_3 was immediately reverted to the (a) position and the timer returned to zero. The sampling cycle can be initiated by means of a push button switch S_1. Once this switch is pushed in, the d.c. motor begins to rotate the cams. The first switch to be activated is $S_2(a)$, which does no more than to cut in the d.c. motor internally and allows one to release the switch S_1. From this point on the process is automatic. The second switch to cut in is $S_2(b)$, but as can be seen from Fig. (3.6) it by itself cannot perform any function. Once the switch $S_2(c)$ cuts in, the three way

FIGURE (3.6)

ELECTRICAL CIRCUIT USED TO ACHIEVE COINCIDENCE BETWEEN SAMPLING AND t = 0.

S_1	Push button switch.
S_2	Three unit cycling switch.
S_3	Stepper switch.
T_1	117 V. to 12 V. step down transformer.
REC.	Rectifier.
SV	Three way solenoid valve.
CDM	Chart drive motor.

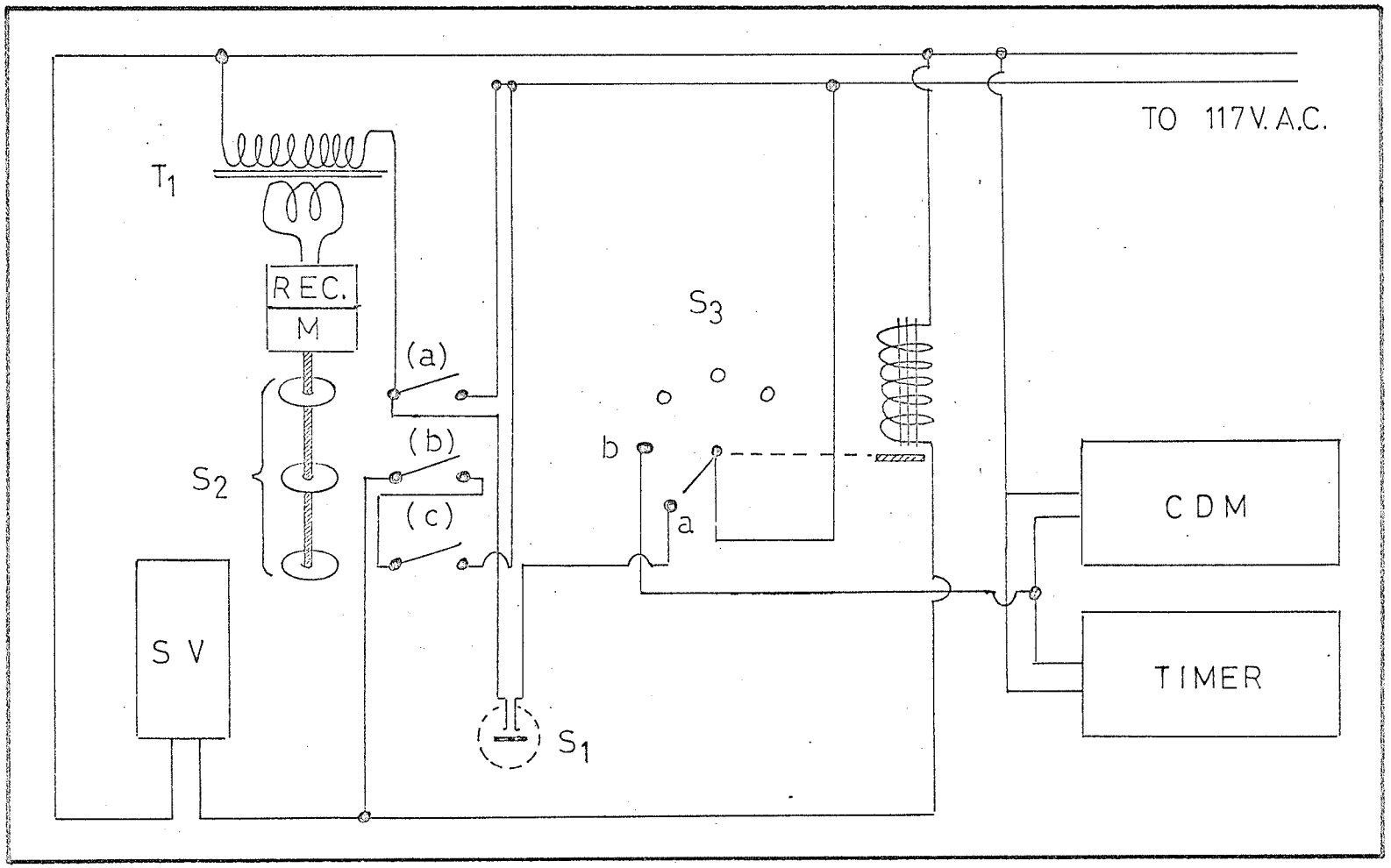
TO 117V. A.C.
T1
REC.
M
S2
(a)
(b)
(c)
S3
b
a
S V
S1
C D M
TIMER

solenoid valve and the solenoid of the stepper switch are activated. These in time activate the sampling valve and the chart drive plus the timer respectively. By using two switches (S_2(b) and S_2(c)) the duration of the "on" position of the sampling valve can be preset by cam adjustment. When the switch S_2(b) goes into an off position the sampling valve also returns to its initial "off" position. The return of the switch S_2(a) to the off position completes the sampling cycle by shutting off the d.c. motor. At the end of the cycle the stepper switch is left in the (b) position while the sampling valve, the three way solenoid valve, and the cycling switch have all been returned to their initial state. As can be seen from Fig. (3.6) it is not possible to restart the sampling cycle while the stepper switch is in the (b) position. This feature served as a protection against accidental secondary sampling during an experiment.

Column Temperature

Most experiments were carried out at a column temperature of 0°C.. For these experiments a 21 liter cylindrical dewar containing ice-water mixture served as a temperature bath. The cold water was circulated by means of a motor driven stirrer (see Fig. (3.7)).

In cases where the experiments were carried out at temperatures above the ambient, a large glass vessel

FIGURE (3.7)

273°K CONSTANT TEMPERATURE BATH.

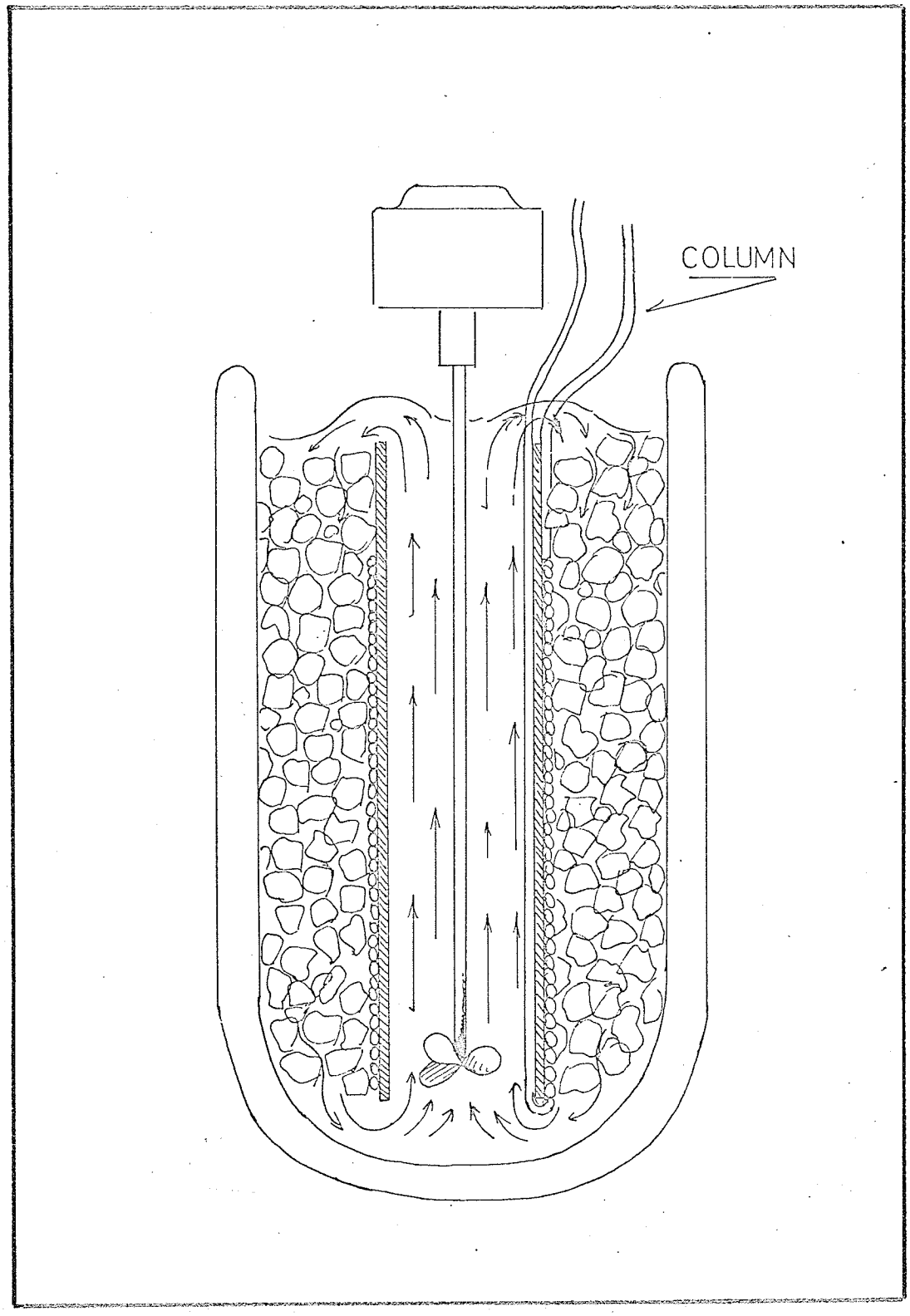
COLUMN

(approximately 12 liter capacity) filled with paraffin oil served as a temperature bath. The bath was heated by means of a Powerstat and a helixical heater constructed from a length of 1/4" copper tubing containing two strands of asbestos covered chromel wire. It was found that once the temperature had stabilized, the temperature drift during an experiment was no more than ±½°. Since this drift had a negligible effect on these experiments, better temperature control was not necessary.

Pressure Measurements

The pressure at the column inlet was measured by a Marsh 4½" diameter, 0-200p.s.i. range Mastergauge placed as close to the sampling valve as possible. The gauge was subdivided at an interval of 2 p.s.i. and had an accuracy of better than 0.5% of the pressure reading. With care it was possible to estimate the pressure to within 0.25p.s.i..

The pressure of the column outlet (the local pressure) was measured with a mercury manometer to within ±0.1cm. It was found that there was a slight difference between the readings obtained with this manometer and the one in the Physical Chemistry Laboratory. This difference could be possibly explained in terms of local building pressures since the laboratory in which the experiments were carried out was in the basement and the accurate manometer was two floors up. Since the difference was very small (+0.2cm.)

its origin was not investigated.

Detector

The detector, the constant voltage supply, and the electrometer, were the same as in the previous study.

Gas Purification

Air Supply For The Detector

During the experiments air was supplied from four compressed air cylinders joined together by a manifold. The air was first passed through a molecular sieve (5A) trap at room temperature and then through a Cu-CuO furnace maintained at approximately 850°C.. The Cu-CuO furnace was constructed from a 1/4"o.d. stainless steel tube which contained a length of 1/8"o.d. copper tubing. The copper tubing was oxidized by passing oxygen through the furnace while it was at the elevated temperature.

Carrier Gases

The use of CO_2 and Ar in these experiments prevented the use of gas purification method described in the previous study. The carrier gases were purified by passing them through a Cu-CuO furnace of the type already described and a molecular sieve (5A) trap at room temperature. The molecular sieve trap served only to remove any water which

may have been formed in the Cu-CuO furnace. No experiments were performed for three days after changing carrier gases. This time was considered to be sufficient for a fast flowing new carrier gas to displace all of the previous gas.

Hydrogen Gas

Hydrogen for the detector was initially purified by passing it through an activated charcoal trap at -196°C.. It was found that by doing so there was some decrease in the noise level of the detector. It was also found that the refilling of liquid nitrogen introduced considerable base line fluctuations. Since the hydrogen was in no way associated with the gas chromatographic process, the liquid nitrogen was not used in the present experiments since base line stability was of more importance than a small decrease in the noise level.

Flow Rate Measurements

One of the principal parameters in gas chromatography is the flow rate of carrier gas. The degree of accuracy with which the flow rates are measured are generally governed by the problem. In many cases where the flow rate serves only as a guide to the working conditions, accuracy of flow rate measurement is not important. It does become important however, in the calculation of retention volumes particularly in cases where the retention volume is a variable of some

other parameter.

Flow rates are generally measured with the familiar moving bubble or soap bubble flow meter. The popularity of this flow meter stems from its simplicity and its potential high accuracy. The bubble flow meter is assumed to have a one percent or better accuracy (142, 143) and this assumption appears to be accepted generally as it is sufficient to state in publications that this type of flow meter was used for flow rate measurements. It is the intent of the author to show that this implication of accuracy is not valid and to describe a method for measuring flow rates to a higher degree of accuracy.

Inaccuracy Of The Moving Bubble Flow Meter In The Low Flow Rate Region

In the present study of carrier gas-surface interaction where the retention volume of methane was used as a measure of this interaction, the initial results for argon and carbon dioxide were found to be quite unrealistic. Fig. (3.8) given for illustrative purposes only, shows the general shape of both the experimental and the expected curves for these two gases. Although the unexpected drop-off in the low pressure region was persistent, it was not reproducible. Failure to reproduce this region cast suspicion on the reliability of the bubble meter. When the

FIGURE (3.8)

ANOMOLOUS EFFECTS AT LOW CARRIER GAS FLOW RATES.

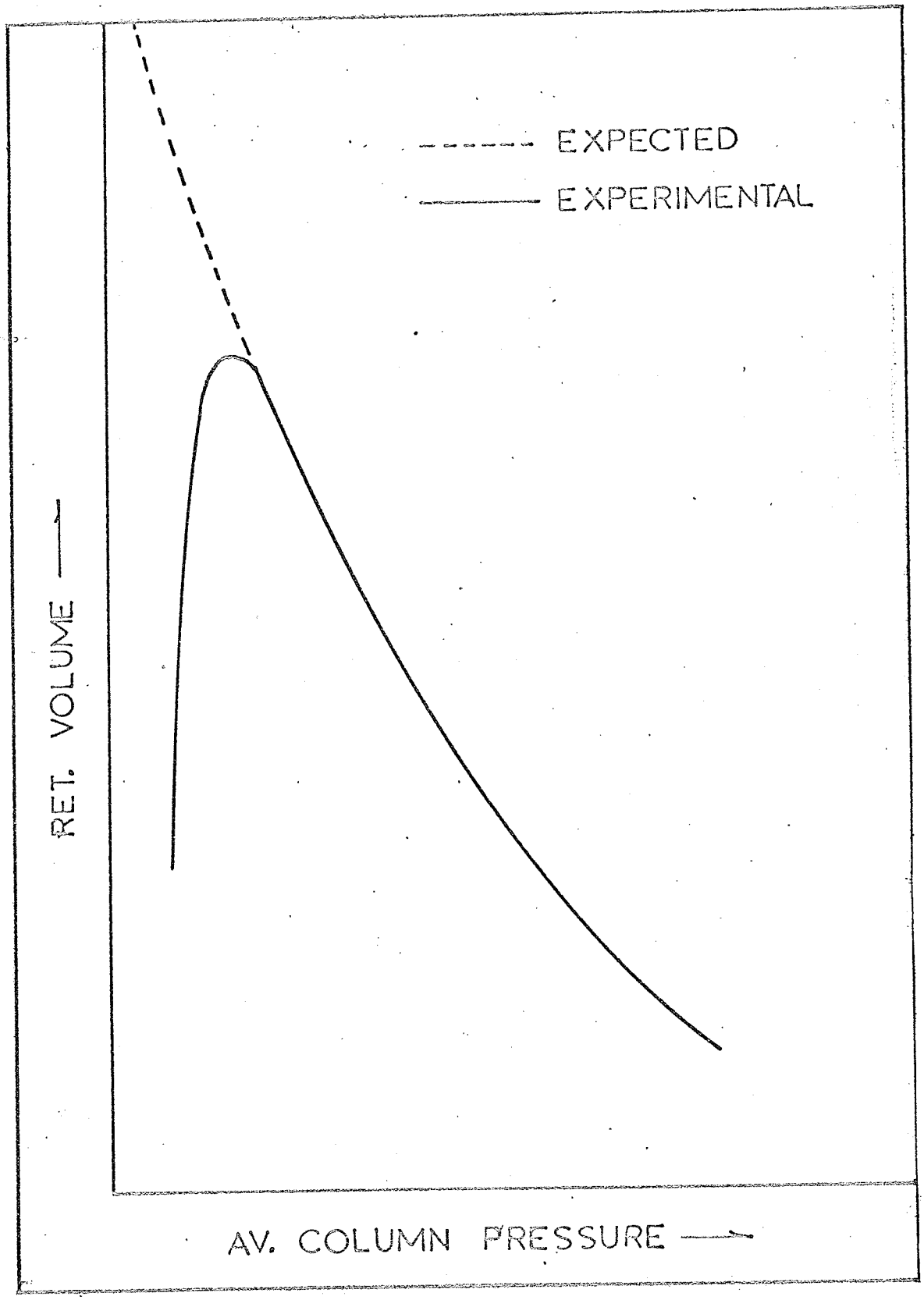
EXPECTED
EXPERIMENTAL
RET. VOLUME
AV. COLUMN PRESSURE

flow rates were measured by the method to be described, expected results were obtained.

In order to substantiate the fact that the low pressure drop-off was caused soley by the flow meter, the following simple experiment was carried out.

Experimental

The apparatus was arranged as is shown in Fig. (3.9).

A fast chart speed recorder was used as an event marker by shorting out the input terminals with a microswitch. With the aid of this event marker it was possible to follow the soap film as it travelled through the flow meter. Since each event corresponded to the arrival of the soap film at a major division of the flow meter, (the flow meter was made from a precision bore buret and had a useful volume of 40 mls.), it was possible to calculate both the flow rate and the time interval between the events. For comparison the flow rate was also determined by the accurate flow meter.

This experiment was carried out for argon and carbon dioxide.

Results And Discussion

Since all of the experiments were not carried out with the same chart speeds, it was found that the results of these experiments could be best fitted into one figure by

)0

FIGURE (3.9)

BLOCK DIAGRAM OF THE APPARATUS USED TO DETERMINE THE ACCURACY OF THE SOAP BUBBLE FLOW METER.

A Compressed gas cylinder.

B Pressure regulator assembly.

C Constriction.

D Accurate thermal conductivity flow meter.

E Soap bubble flow meter.

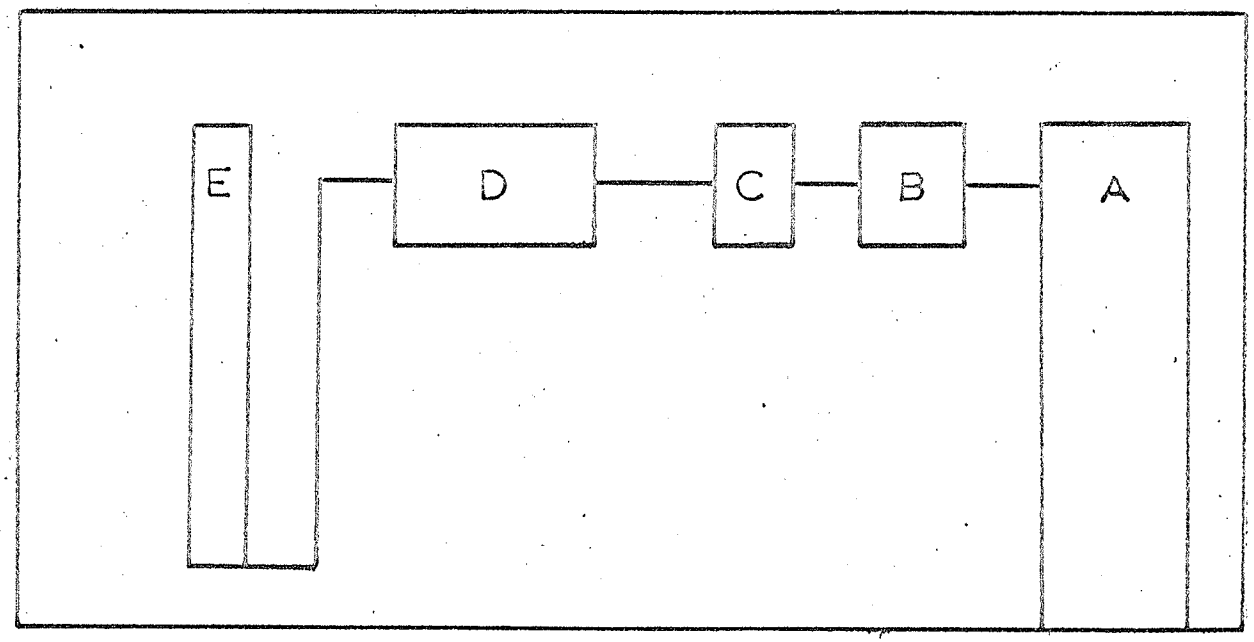
E
D
C
B
A

plotting the actual chart paper distances between events rather than time as a function of the total distance travelled by the soap film.

The results for the two gases are given in Fig. (3.10). The flow rates associated with the three curves are as follows:

CO_2 (A)	2.74 mls/min.
CO_2 (B)	1.63 mls/min.
Argon	1.22 mls/min.

The region 0 - 15 was found to be linear for all three curves and was not included for clarity.

The most obvious feature of Fig. (3.10) is that the soap film velocity is not constant for the full length of the flow meter. It should be mentioned that in the case of carbon dioxide, the soap film appeared motionless at the extreme end of the flow meter while the gas maintained a constant flow rate. Repeat of experiment (A) showed that the results were highly reproducible. The slight difference between the two sets of results was attributed to the difference of soap film thickness.

In another experiment where the flow rate of carbon dioxide was about 6.2 mls/min., the soap film velocity was found to be constant for the entire length of the flow meter. Considering this and Fig. (3.10), it is obvious that the

FIGURE (3.10)

SOAP BUBBLE FLOW METER INACCURACY

FOR ARGON AND CARBON DIOXIDE.

CO_2 (A)	2.74 mls./min.
CO_2 (B)	1.63 mls./min.
Argon	1.22 mls./min.

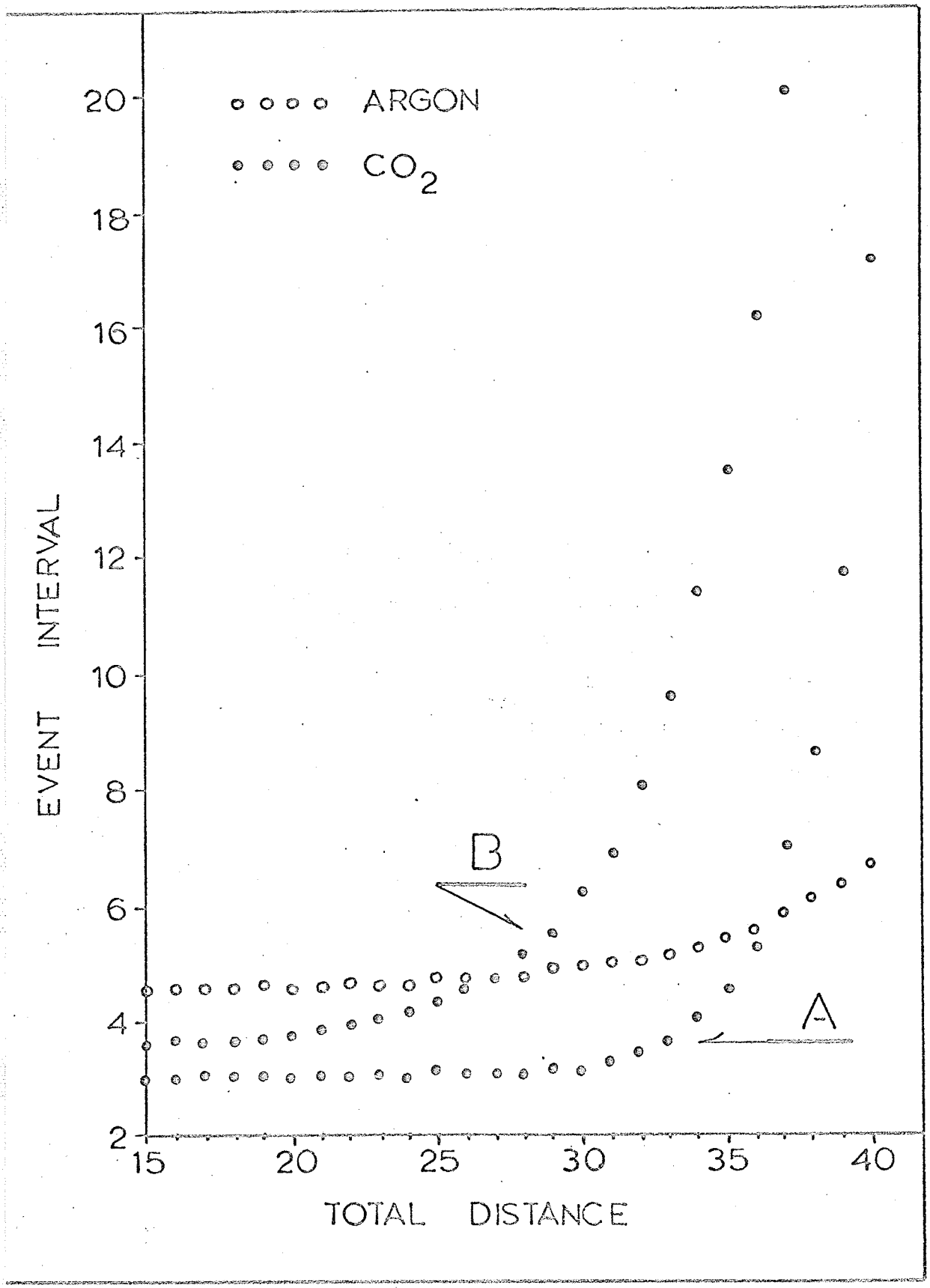
ARGON
CO_2
EVENT INTERVAL
TOTAL DISTANCE
B
A
2
4
6
8
10
12
14
16
18
20
15
20
25
30
35
40

point of deviation of the soap film velocity from a constant value is flow rate dependent. One can conclude from this that a certain time is required before the soap film becomes permeable to the gas. The time and the rate at which the soap film becomes permeable seems to depend on the nature of the gas.

Flow rate measurements in the linear soap film velocity region of the flow meter are not without error as can be seen from Table (3.1).

It is most probable that variables such as the temperature, the type of detergent, its concentration and the film thickness would lead to some interesting results, but it is not the intent of these experiments to represent a detailed study of the observed phenomena. These experiments demonstrate the inaccuracy at the bubble flow meter in the lower flow rate region and show that there is a need for a more reliable and accurate method of flow rate measurement.

A Simple But Accurate Method Of Flow Rate Measurement

Aside from the placement of the injection port, the flow meter is basically an empty column chromatograph which can be easily constructed from spare parts. The component arrangement of the unit is shown in Fig. (3.11).

The entire unit except for the gas inlet, the injection port and the gas outlet are kept in a constant temperature enclosure (see Fig. (3.11)).

TABLE (3.1) ERROR IN THE SOAP BUBBLE FLOW METER

Gas	Actual Flow Rates* (mls./min.) (a)	% Error of Bubble Meter**
CO_2	6.201	-2.7
CO_2 (A)	2.740	-4.2
CO_2 (repeat of A)	2.740	-7.0 (b)
CO_2 (B)	1.6348	-6.1
Argon	1.2175	-3.0

* Average deviations of these values are 0.05%.

** Flow rates were water vapour pressure corrected.

(a) The accuracy of these values was calculated to be approximately 0.3%.

(b) The deviation of this value from -4.2 is attributed to the soap film thickness.

FIGURE (3.11)

ACCURATE THERMAL CONDUCTIVITY FLOW METER.

I	Injection port.
T_1, T_2	Elements of a microthermal conductivity detector.
V_m	Total volume between T_1 and T_2.

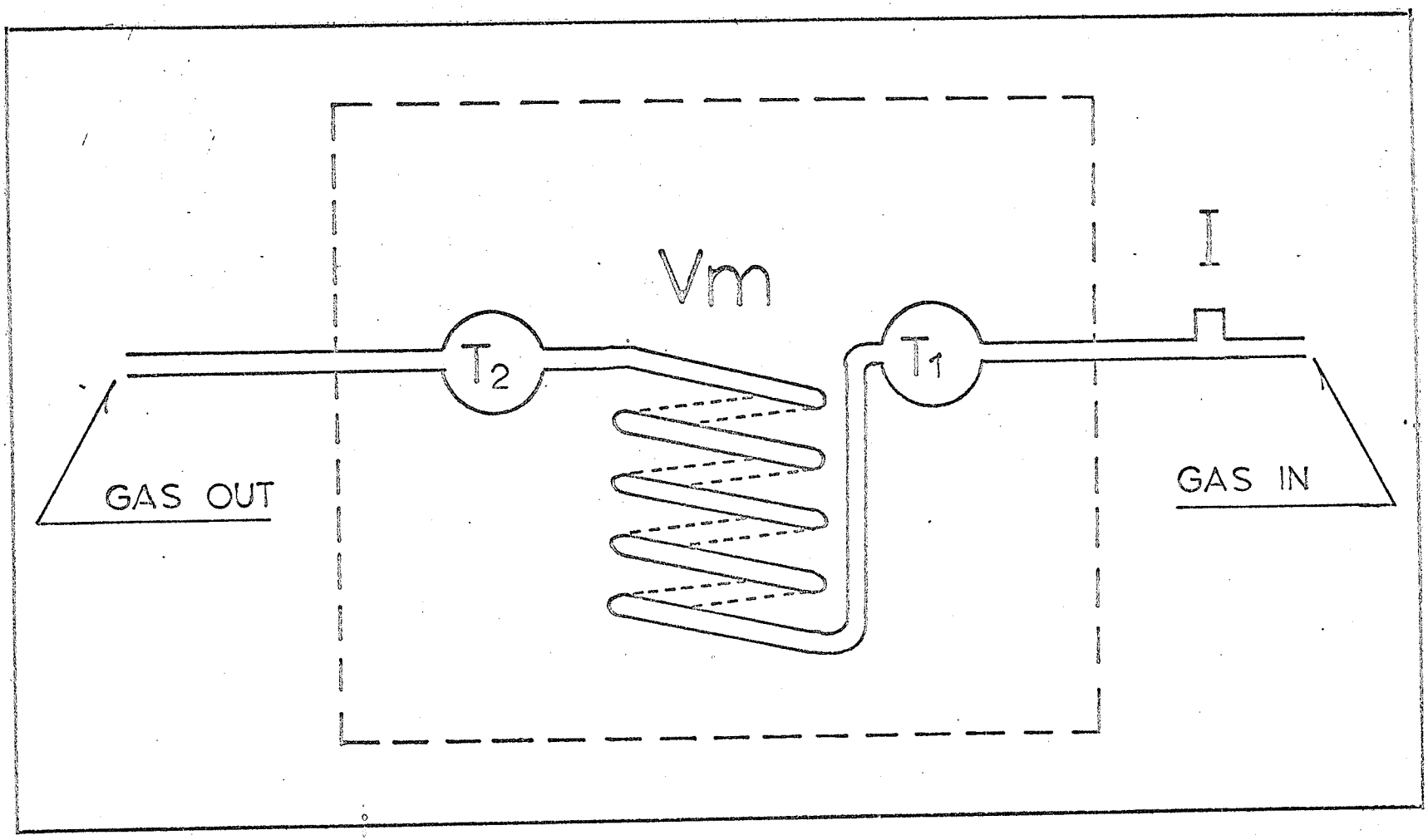
Vm
I
T2
T1
GAS OUT
GAS IN

The dimensions of the flow meter are not critical, but the value of Vm should be chosen to suit the range of flow rates to be measured (this will become self evident later). It is important, however, to construct the unit so that there is a minimum pressure drop across it.

Flow rates are measured by injecting into the unit a small sample of a foreign gas whose thermal conductivity is much different than that of the gas whose flow rate is being measured. The passage of the gas plug past the first thermal conductivity cell T_1 is indicated by the recorder response. When the plug passes the second thermal conductivity cell T_2 the recorder responds in the opposite direction. From the time interval between the maxima of the two deflections the flow rate can be calculated.

Before calculations can be made it is necessary to determine the total volume (Vm) between T_1 and T_2 very accurately since the absolute accuracy of the flow rate measurement will depend on this. It is also necessary to determine the pressure drop (ΔP) across the unit as a function of the time (t) required for the foreign gas to pass from T_1 to T_2.

The flow rate out of the flow meter can be calculated by:

$$F = \frac{Vm}{t} \frac{\overline{P}}{P_o} \qquad (3.1)$$

where $\bar{P}$ is the average pressure in the meter and P_o is the outlet pressure. In a post column arrangement where the flow meter is at a temperature T_F and the column is at a temperature T_C , the flow out of the column is:

$$F = Vm\bar{P}T_C/t(P_o + \Delta P)T_F \qquad (3.2)$$

This method of flow rate measurement has been used successfully in this laboratory and it was found that the unit is dependable for helium, argon and carbon dioxide and has an average deviation in reproducibility of ± 0.05% in the range used (1 ml./min. to 60 mls./min.). It should be possible to get higher reproducibility by eliminating some of the peak broadening sources.

With the exception of Vm, all the variables in eqn. (3.2) can be measured quite accurately (143) and their contribution to the inaccuracy of F will be small. Considering the definition of Vm, direct measurement of this value will generally not be possible. Vm can be obtained indirectly by calibrating the flow meter against some other unit. The accuracy of Vm, therefore of the flow rate measurements, will be approximately that of the calibrating flow meter. In view of this it should be possible to obtain Vm values with accuracies of better than ± o.1% if the calibration is done with instruments such as that described by Noble, Abel, and Cook (144). Except for very unusual circumstances where the absolute values are required, this high degree of

accuracy is unnecessary. For most critical work Vm can be calibrated with helium and an accurate bubble flow meter. To qualify this, attention must be drawn to the fact that the magnitude and direction of the error introduced into Vm is also introduced into every flow rate calculation. Although each flow rate may deviate as much as 1% from the absolute value, its accuracy with respect to Vm will be of the same order as the resproducibility.

Considering that the unit can be built to withstand pressures it can serve as a pre or post column flow meter. Aside from its function as a flow meter, the unit can be used for measuring gaseous diffusion coefficients.

A meter constructed out of glass or some other inert material using glass coated thermisters as sensing units can be used to accurately measure flow rates of unusual and corrosive carrier gases (104).

Flow Meter Specifications

The empty column was made from approximately 19.5 ft. length of 3/16"o.d. (0.03" wall thickness) copper tubing. A Gow - Mac micro-cell (Model 470) thermistor served as a sensing device. Since the detector's lead-in wires were enclosed in approximately 6 inches of stainless steel tubing, the entire flow meter could be immersed in an ice-water mixture which was made to serve as a constant temperature bath.

The volume, Vm, was calibrated against the bubble flow meter using He. as the calibrating gas. The calibration was carried out at four different flow rates. The results are summarised in Table (3.2).

The flow rates in this study were always measured with this type of flow meter at 0°C. using the value of 49.24cc. as Vm.

Experimental Procedure

Pior to an experiment, the 21 liter dewar was first filled with ice and a sufficient quantity of distilled water was added to bring the level to within ± 1/4" of a specified mark. Since the column was suspended some 6" below a platform on which the sampling valve and the detector were mounted there was 6 inches of column leading to each unit which was exposed to the ambient temperature. In order to make experimental conditions as reproducible as possible an ice-water level mark was chosen. In preliminary experiments it was noticed that if this procedure was not followed, particularly in the case of He carrier gas, the expermental results had some scatter. Once the temperature bath was filled, the inlet pressure was adjusted to a desirable value by means of a two stage regulator. After the completion of these two steps, the system was allowed to stabilize for an average of 16 hours. This of course meant that only one

TABLE (3.2) V_m VALUES AS A FUNCTION OF BUBBLE METER FLOW RATE

Bubble meter flow rate (cc./min.)* (6 readings)	V_m (calc.)
3.67 ± 0.01	49.23
7.72 ± 0.02	49.24
24.68 ± 0.03	49.21
39.77 ± 0.05	49.28

$\overline{V}_m = 49.24 \pm 0.02$ cc.

* Water vapour pressure corrected.

experiment could be performed a day.

The sample pressure in the gas buret was checked and adjusted if necessary prior to each experiment. A sample size of 0.12µl. (at S.T.P.) was maintained in all experiments involving a single component, and 0.24µl. sample sizes were used in experiments where two components (CH_4-CD_4) were present. The inlet and the outlet pressures were noted before and after each experiment. After the sample injection (this procedure has already been described) the flow meter was refilled with ice and distilled water and the d.c. filament power supply was turned on in order that the unit may stabilize before its use.

Immediately after elution the chart paper was allowed to advance till the recorder pen corresponded with a major division, at which instant both the chart drive motor and the timer were shut off by manually placing the stepper switch into the (a) position. At this point the chart distance was compared with the timer reading. It was found that in most cases the difference was approximately ± 1 sec. In some cases corrections had to be made since the difference was as high as 8 seconds, (in experimental times of ½ to 6 hours). It was found out later that the discrepancy was in the chart paper divisions. After the flow rate was measured, the experiment was complete. The 21 liter dewar was emptied and recharged with fresh ice and distilled water for the next experiment.

An experiment was conducted to determine the reproducibility of the measured retention times. It was found that if two experiments were carried out one immediately after another there was a slight difference in the retention times. The difference depended on the duration of the first experiment and shortest experiments the difference was as high as 10 seconds. If 2 to 3 hours were allowed between the two experiments the retention times of the two experiments were reproducible to within the experimental error. This has been observed on several other occasions. The fact that it is the second experiment which gives the longer retention time and also that the peak areas of the two experiments are the same disallows this to be explained on any adsorption phenomenon. It is the author's belief that this is somehow related to flow interruption during sampling.

POROSITY, PERMEABILITY, AND GAS FLOW

Up to this point porosity, permeability, gas flow, the inlet and the outlet column pressures have only been mentioned in passing. In this section more meaning will be given to these quantities and a relationship between them will be developed. The experimental data pertaining to gas flow, will be interpreted in terms of these relationships.

Porosity

A packed gas chromatographic column consists of the granular solid and the intergranular voids which are occupied by the carrier gas. The relative amount of either phase present in the column will depend upon the way the granules are packed. There are two ways (the rhombohedral and the face-centered cubic) in which spheres of equal diameter can be packed so as to give densest packing (having only 26% of the interparticle space)(145). In gas chromatographic columns this dense packing is never realized. During the packing process the gravity works in the direction so as to achieve dense packing while the filling process due to its very random nature opposes this effect. The final column will have a packing which is a compromise of the two effects, in that, regions of low and high packing density will be randomly distributed throughout the column. The particle size and shape will have a further effect on the magnitude of the interparticle voids and the packing density. Considering the effect of gravity on the packing process, one can expect a denser normal packing from columns which contain a high density material than from columns whose material has low density.

Porosity by definition is the fraction of a total volume element occupied by all free space. That is, for a

total volume V_T which contains a volume V_S of the packing material, the porosity (ϵ) is;

$$\epsilon = (V_T - V_S)/V_T = 1 - V_S/V_T \qquad (3.3)$$

A particular point within a column will have a porosity of one or zero depending whether the point finds itself in the interparticle void or within the solid packing. As the total volume is increased so as to contain a number of particles (5-10), the porosity will be greater than zero but will be less than one and will vary from point to point in the column. As the volume is increased so as to incorporate more and more particles, the porosity of the various regions in the column will be found to approach a constant value. It is this limiting value which will characterise the column porosity.

Since $(V_T - V_S)$ of eqn. (3.3) is equal to V_m, the porosity can be rewritten as;

$$\epsilon = V_m/V_T \qquad (3.4)$$

where in this case V_T will be defined as the volume of the empty column having the value $\pi r^2 L$. L and r are the column length and the inside radius of the tubing respectively. V_m, as it has already been defined, is the total gas volume of the column. This value however, may contain in it the interparticle void volume plus the volume which may be present in the particles themselves if they are porous. If

this is the case, the porosity defined by eqn. (3.4) is referred to as the total porosity and can be written as;

$$\varepsilon_T = V_m/V_T \qquad (3.5)$$

where ε_T (the total porosity) is a specific designation of δ.

The free space which allows the gas to flow is the interparticle void. It is for this reason a quantity, the interparticle porosity (ε), must be defined. Interparticle porosity is the fraction of the column occupied by the interstitial channels and gaps between the particles. It is smaller than or at best equal to the total porosity, that is;

$$\varepsilon_T = \varepsilon + \Delta \qquad (3.6)$$

where Δ is the porosity due to the porous nature of the particles. For nonporous materials such as glass beads, Δ vanishes and the interparticle porosity becomes equal to the total porosity.

The interparticle porosity can vary from 0.35 to 0.9, but for a fairly well packed column the value is very close to 0.4 (146). The value of 0.9 is encountered only in very unusual cases such as in the aerogel columns.

The quantity which is most easily accessible to measurement is the total porosity since both the V_m and the V_T values are readily available. The measurement of the

interparticle porosity in the case where the particles are porous, is more difficult. A method which is often used (147, 148) is described by Bohemen and Purnell (147). ε can be measured by the use of the following equation;

$$\varepsilon = 1 - m\rho_b/V_T \qquad (3.7)$$

where ρ_b is the particle density measured under mercury (bulk density), and m is the mass of the packing. Mottlau and Fisher (149) describe a method where pore volumes can be obtained by titration (it should be mentioned that the orginal work was done by Innes (150)). Once the pore volume for the entire column is determined, it can be subtracted from V_m to give the interparticle volume with which the value of ε can be calculated.

Equation Of Flow

Due to compressibility, the carrier gas as it passes from the inlet of the column to the outlet where the pressures are P_i and P_o respectively, will experience an acceleration and its velocity will vary from point to point along the length of the column. Texts treating fluid motion often describe the velocity profile in terms of the Navier-Stokes equation (151, 152). The one dimensional form of the equation for a viscous fluid can be written as (153);

$$\rho(dv/dt) = -\partial P/\partial z + F + \eta\nabla^2 v + (\eta/3)(\partial^2 v/\partial z^2) \quad (3.8)$$

where ρ, η, v, ∇^2, and F are the fluid density, the viscosity, the z component of local flow velocity, the Laplacian operator and the z component of the external force which may be acting on the fluid respectively. As it has been pointed out by Giddings (153), this equation has been found extremely intractable even for moderately simple geometries, and that the complex geometry of the flow space in the gas chromatographic column is beyond exact treatment.

An empirical law which is generally used to describe flow in a porous media is Darcy's Law. For a volume of gas Q (using Carman's notation (154)) flowing in time t across a cross-sectional area A, the apparent linear rate of flow (u_a) is;

$$u_a = Q/At \quad (3.9)$$

Darcy's Law states that for a flow in the x direction;

$$u_a = -(B_o/\eta)(dP/dx) \quad (3.10)$$

where B_o is the specific permeability coefficient. It has been pointed out on several occasions (153, 155, 156) that u_a is not the true velocity of the gas since the actual cross-sectional area of a packed column through which gas

can flow is $A\varepsilon$. In terms of true gas velocity (u) eqn. (3.10) becomes;

$$u = -(B_o/\varepsilon\eta)(dP/dx) \qquad (3.11)$$

Since the volume flow rate (F) is related to the gas velocity, that is;

$$F = uA\varepsilon \qquad (3.12)$$

then eqn. (3.11) can be expressed in terms of flow rate.

$$F = -(B_oA/\eta)(dP/dx) \qquad (3.13)$$

When a gas flow in a column has reached a steady state, then the following relationship must be satisfied at every point in the column;

$$\text{rate of mass inflow} = \text{rate of mass outflow} \qquad (3.14)$$

From this relationship it can be stated that the number of moles of gas leaving the column (n_o) in time t, must be equal to the number of moles (n) passing any cross-section in the column in the same time, or;

$$n_o/t = n/t \qquad (3.15)$$

For an ideal gas whose equation of state is;

$$n = PV/RT \qquad (3.16)$$

eqn. (3.15) becomes;

$$P_o V_o/t = PV/t \qquad (3.17)$$

With the relationship of eqn. (3.17) and remembering that V_o/t and V/t are the flow rates at the appropriate points of the column, eqn. (3.13) can be written to give;

$$F_o P_o dx = -(B_o A/\eta) P dP \qquad (3.18)$$

Upon integration between the limits of $x = 0$ and $x = L$ where the column pressures are P_i and P_o respectively, and rearrangement, a relationship between the flow rate at the outlet of the column, the inlet pressure and the outlet pressure is obtained.

$$F_o = B_o A(P_i^2 - P_o^2)/2\eta L P_o \qquad (3.19)$$

A plot of F_o as a function of $(P_i^2 - P_o^2)/P_o$ should give a straight line from whose slope the B_o value can be calculated since all the other values are readily available.

To be more correct the author has considered the non-ideality of the carrier gas and has obtained a modified form of eqn. (3.19). The derivation is as follows.

To a very good approximation the equation of state for a real gas can be written as (157);

$$n = PV/(RT + B_{11}P) \qquad (3.20)$$

where B_{11} is the second virial coefficient of the gas at temperature T. Substituting this into eqn. (3.15) and going through the steps which lead to eqn. (3.18), the following expression is obtained;

$$P_o F_o dx/(RT + B_{11}P_o) = -B_o A P dP/\eta(RT + B_{11}P) \quad (3.21)$$

Integration between the limits of x = 0 and x = L, where the column pressures are P_i and P_o respectively leads to;

$$P_o F_o L/(1 + bP_o) = \{(B_o A)/\eta b^2\}\cdot\{b(P_i - P_o) + \ln(1 + bP_o) - \ln(1 + bP_i)\} \quad (3.22a)$$

where

$$b = B_{11}/RT \quad (3.22b)$$

Since the ln terms are small, they can be expanded to the first term in the series as an approximation without introducing significant error. After expansion and algebraic rearrangement, the final expression is;

$$F_o = \{B_o A/\eta L P_o\}\cdot\{(1 + bP_o)(P_i^2/(2 + bP_i) - P_o^2/(2 + bP_o))\} \quad (3.23)$$

Equation (3.23) has the desirable feature in that for an ideal gas where $B_{11} = 0$, it reduces to eqn. (3.19). In this study eqn. (3.23) will be used unless otherwise stated.

Permeability

The specific permeability (B_o) has the units of cm^2. It is also often expressed in Darcy units where 1 Darcy = $9.87 \times 10^{-9} cm^2$. It has a function of resistance (as in Ohm's Law), and is related to the column construction. An equation which relates this quantity to the column properties is the Kozeny-Carmen equation (154) which may be written as;

$$B_o = d_p^2 \varepsilon^3 / 36k(1 - \varepsilon)^2 \qquad (3.24)$$

where d_p is the diameter of a sphere with the same specific surface as the particle. For a spherical nonporous particles, d_p will be that of the particle diameter. For nonspherical porous particles the definition of d_p is as above.

Equation (3.24) is an approximate equation derived from a capillaric model using a variable k. It appears that for a normal granular packed columns there are two distinct values of k that are in use. In some publications (147, 153, 154, 155, 158), the accepted value of k is 5.0. Using this value, eqn. (3.24) becomes;

$$B_o = d_p^2 \varepsilon^3 / 180(1 - \varepsilon)^2 \qquad (3.25)$$

In other publications (156, 159-163), the accepted value of k is very close to 4.17, thus making eqn. (3.24) become;

$$B_o = d_p^2 \varepsilon^3 / 150(1 - \varepsilon)^2 \qquad (3.26)$$

Eqn. (3.26) is referred to as the Blake-Kozeny equation (156, 159, 160), whereas eqn. (3.25) is the Kozeny-Carman equation (153, 154, 155, 158). On occasions eqn. (3.26) has been called the Kozeny-Carman equation (162) and the Ergun equation (158). Furthermore, there exists sufficient experimental data to support both equations (154, 159, 162).

Flow Pattern In Gas Chromatography

Since slip flow and molecular (Knudsen) flow occur only at very low pressures (164), they are of no importance to the present study and will not be discussed.

At higher pressures the flow is laminar (it is also known as viscous or streamline flow). Giddings describes the flow in the following way (153). "The zig-zag pattern is unvarying, however, in the sense that any subsequent fluid element, started in the same position, will follow its predecessor's path exactly, neglecting diffusion. This is a consequence of the fact that the two fluid elements are subject to the same relative forces at each point, and thus move off on identical trajectories despite the time interval between them.. Thus the liminar flow of

chromatographic interest is spatially erratic but temporally constant - the flow pattern, although complex, remains fixed with the passage of time". Guiochon (156) speaks of the flow in a packed column as corrugated laminar, "with the flow lines of the gas moving away from the surface of the particles on entering and leaving the constrictions, to form local stable eddies." Whatever physical picture is accepted, the fact remains that under laminar flow conditions equations (3.19 and (3.23) are valid in that they allow for the calculation of F_o from P_i and P_o if the various constants are known. Hargrove and Sawyer (148) have observed a linear relationship between F_o and $(P_i^2-P_o^2)$ up to $F_o \simeq 800$ cc./min..

As the gas velocity is increased the laminar flow becomes unstable and gives way to a flow of an erratic pattern which is generally known as turbulant flow. With the onset of turbulance it is found that there is an apparent decrease in permeability with increasing flow rate in that higher pressure differentials must be applied then that required by eqn. (3.19) or eqn. (3.23). The deviations are too large to be accounted for by the nonideality of the gas, and can be explained by the loss of the gas kinetic energy through heat dissipation in the numerous eddies and cross-currents of turbulent flow. To account for this a quadratic velocity term is added to Darcy's relationship, (153, 165), that is;

$$- dP/dx = au + bu^2 \qquad (3.27)$$

The degree of turbulance can be estimated by a velocity dependent dimensionless term known as Reynolds number R_e, which has the form (153, 156);

$$R_e = \rho u d_p/\eta \qquad (3.28)$$

where ρ is the specific gravity (density) of the gas. It should be pointed out that the value ρu will be constant throughout the entire column if the relationship (3.14) is to be satisfied.

According to Giddings (153), turbulance develops gradually from a minor to a dominant role as R_e increases from 1 to 100. He further states that the departure from Darcy's Law when $R_e > 1$ constitutes evidence that turbulance is occuring, and at $R_e \sim 1$ turbulance can be expected in only a few of the largest channels. On the other hand Guiochon (156), contends that the flow must be laminar at $R_e \sim 1$ and that Darcy's Law can be extended to $R_e = 10\text{-}15$. Bird et. al. (159) mention that for $\varepsilon < 0.5$ the Blake - Kozeny equation (which by their notation contains the integrated form of Darcy's Law) is valid up to $R_e/(1 - \varepsilon) < 10$, or (if $\varepsilon \approx 0.4$) $R_e < 6$.

Guiochon points out that use can be made of the Ergun's equation for calculating the permeability coefficient in the turbulant region. Using the present notation the re-

lationship is as follows;

$$1/k = 150(1 - \varepsilon)^2/d_p^2\varepsilon^2 + 1.75\rho u_o(1 - \varepsilon)/d_p\eta\varepsilon \quad (3.29a)$$

where k and u_o are the permeability coefficient in terms of gas velocity and the gas velocity at the column outlet respectively. As can be seen his choice of $36k$ is 150. To express this in terms of volume flow rates, eqn. (3.29) can be modified by multiplying both sides by $1/\varepsilon$ to give;

$$1/k\varepsilon = 1/B = 150(1 - \varepsilon)^2/d_p^2\varepsilon^3 + 1.75\rho u_o(1 - \varepsilon)/d_p\eta\varepsilon^2 \quad (3.29b)$$

where B is the permeability coefficient in terms of flow rates. Regardless of the constant chosen (150 or 180), the first term on the right hand side is $1/B_o$ (see equations (3.25) and (3.26)). Keeping in mind that;

$$\rho = P_oM/RTx10^3 \quad (3.30)$$

where M is the molecular weight of the gas, and that;

$$F = uA\varepsilon \quad (3.12)$$

eqn. (3.29) can be written as;

$$1/B = 1/B_o + 1.75P_oMF_o'(1 - \varepsilon)/RTAd_p\varepsilon^3\eta x10^3 \quad (3.31)$$

where F_o' is expressed in cc./sec.. To express F_o in cc./min., eqn. (3.31) must be rewritten to incorporate the

factor $F_o/60$ instead of F_o'. The final expression can be reduced to;

$$1/B = 1/B_o + Y(M/n)F_o \qquad (3.32)$$

where Y is a column constant independent of the carrier gas. The assumption that $P_o = 1$ for columns operating at ambient outlet pressures, negligibly affects the final results.

Results And Discussion.

The experiments from which the data is extracted will be designated by the carrier gas used. For example ArI, ArII, and ArIII refer to three distinct experiments using argon as the carrier gas. Since the data presented in this section deals only with the gas flow of the various experiments, this designation will be used in the subsequent sections where other aspects of the present study are discussed.

For simplicity of notation eqn. (3.23) can be rewritten as;

$$F_o = \chi\phi \qquad (3.33)$$

where

$$\chi = BA/\eta L = F_o/\phi \qquad (3.34)$$

and

$$\phi = \{1/P_o\}\cdot\{(1 + bP_o)(P_i^2/(2 + bP_i) - P_o^2/(2 + bP_o))\} \qquad (3.35)$$

The values of $B_{11}(273^\circ K)$ for He and Ar were calculated from an empirical equation referred to by Guggenheim and McGlashan (166) as a Beattie-Bridgeman type which has the form;

$$B_{11}/V^* = 0.461 - 1.158(T^*/T) - 0.503(T^*/T)^3 \qquad (3.36)$$

where T^* and V^* are the characteristic temperature and volume respectively. The values of V^* and T^* were obtained from the same source as eqn. (3.36)(166).

The value of B_{11} for CO_2 at $273^\circ K$ was calculated from eqn. (3.37) and available tables (167).

$$B_{11}(T) = b_o B^*_{11}(T^*) \qquad (3.37)$$

where B^*_{11}, (T^*), and b_o are the reduced second virial coefficient, the reduced temperature (as defined in (167)), and the steric parameter respectively. The calculated value of He and Ar were found to be 14.4 and -19.7 cm^3/mole respectively. The calculated value of CO_2 was found to be $-145.8 cm^3$/mole, which is in excellent agreement with the experimental value of $-147.4 cm^3$/mole as was determined by Dadson, Evans, and King (168).

Table (3.3) contains the F_o, the ϕ, the χ, and the $\bar{P}$

TABLE (3.3) F_o, ϕ, χ, AND $\bar{P}$ VALUES FOR EXPERIMENTS HeI, Ar(II and III), AND CO_2I.

F_o (cc./min.)	ϕ (atm.)	χ*	$\bar{P}$
		HELIUM	
54.62	98.6	0.554	9.302
41.98	76.0	0.552	8.215
32.96	59.5	0.554	7.293
26.34	47.2	0.558	6.518
19.98	35.4	0.565	5.665
13.729	24.1	0.570	4.731
9.459	16.4	0.576	3.951
5.575	9.6	0.582	3.089
3.077	5.3	0.586	2.394
		ARGON	
41.64**	90.3**	0.461**	8.889**
36.67	78.3	0.468	8.277
34.15**	72.8**	0.469**	8.009**
29.27	62.1	0.472	7.426
27.72**	58.5**	0.474**	7.197**
23.48	49.2	0.478	6.625
19.96**	41.3**	0.483**	6.069**
18.063	37.2	0.485	5.747
16.077**	32.8**	0.490**	5.411**

TABLE (3.3) (CONTINUED)

12.256	24.9	0.492	4.768
8.184	16.4	0.499	3.938
4.711	9.3	0.508	3.026
1.538	3.0	0.517	1.892

** Ar(III)

CARBON DIOXIDE

61.37	106.6	0.576	9.615
48.17	79.8	0.604	8.330
37.87	60.9	0.622	7.316
30.52	47.2	0.647	6.491
20.72	30.4	0.683	5.273
13.893	19.8	0.703	4.286
8.453	12.7	0.722	3.373
4.597	6.2	0.743	2.562
2.291	3.0	0.766	1.930

---

* The units of χ are cc./min. atm.

values for experiments HeI, Ar(II and III), and CO_2I. The raw experimental data may be found in Appendix A. Plots of F_o against ϕ for the three carrier gases are shown in Figures (3.12), (3.13), and (3.14) respectively. As can be seen from Fig. (3.12), a straight line relationship exists between the variables for the helium gas. If for the present it can be assumed that $\varepsilon \simeq 0.4$, then it can be concluded from this observation that the helium flow through the column obeys Darcy's Law in the outlet gas velocity range of 0 to ~120 cm./sec.. Hargrove and Sawyer (148) have observed a linear relationship between F_o and ϕ on a glass bead column using helium as a carrier gas up to F_o values of approximately 500 cc./min.. If one considers that the tubing they used had an inside diameter of 0.325 cm. and if one allows ε to be 0.4, then this F_o value corresponds to an outlet gas velocity of approximately 250 cm./sec.. This finding should be sufficient to serve as a support to the above conclusion.

In the case of Ar and CO_2 it was found that a straight line could be drawn through only four or five points at the lowest F_o values. This line, extended to the higher F_o region, can serve as an indication of the deviation from Darcy's Law. Since the line has been extrapolated from the region where Darcy's Law is obeyed, its slope can serve to evaluate χ_o and consequently B_o. From the slope of the various lines the following χ_o values were obtained;

FIGURE (3.12)

F_o AS A FUNCTION OF ϕ FOR HeI.

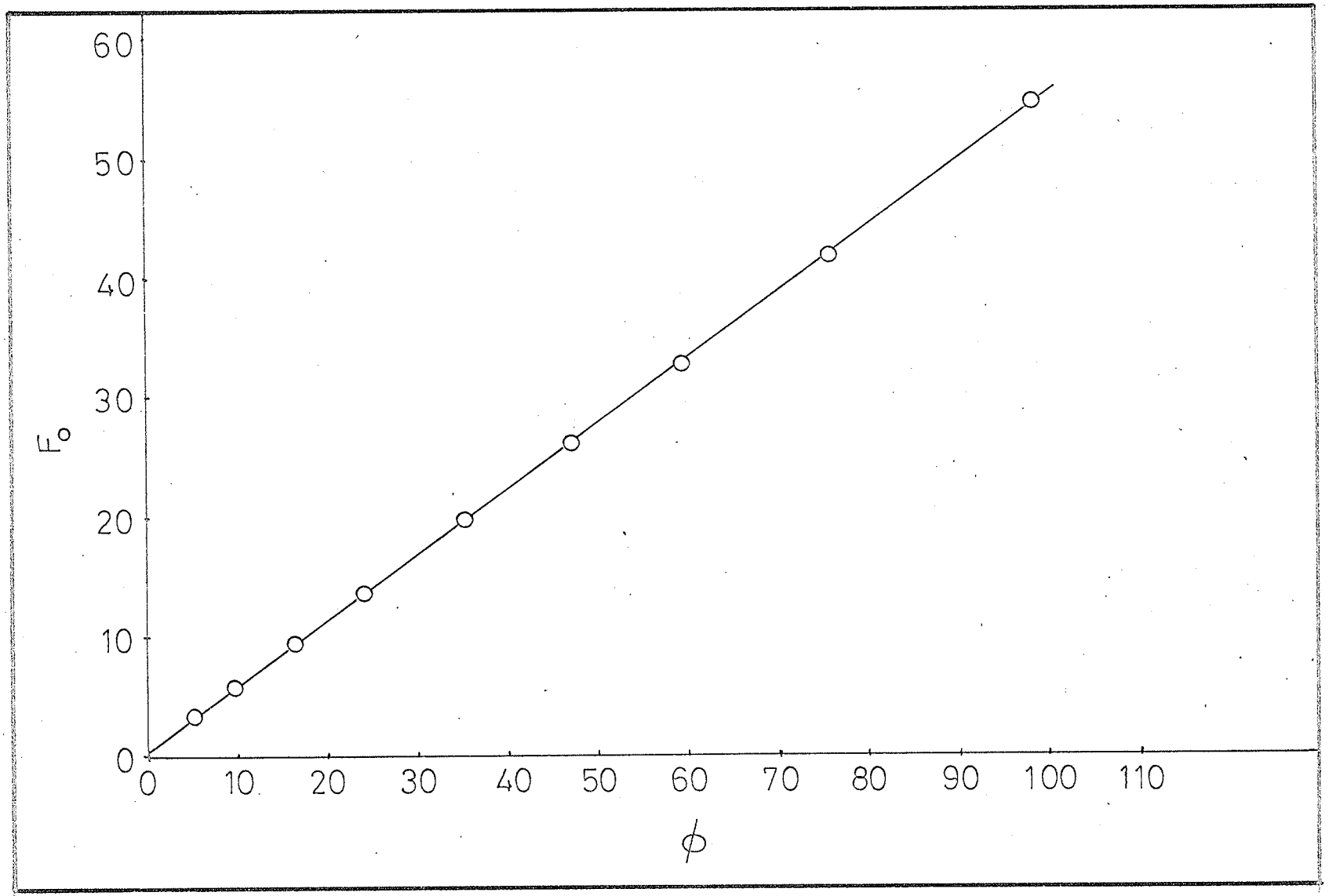
60
50
40
30
20
10
0
E^o
0
10
20
30
40
50
60
70
80
90
100
110
ϕ

FIGURE (3.13)

F_o AS A FUNCTION OF ϕ FOR Ar(II AND III).

○ ArII

◎ ArIII

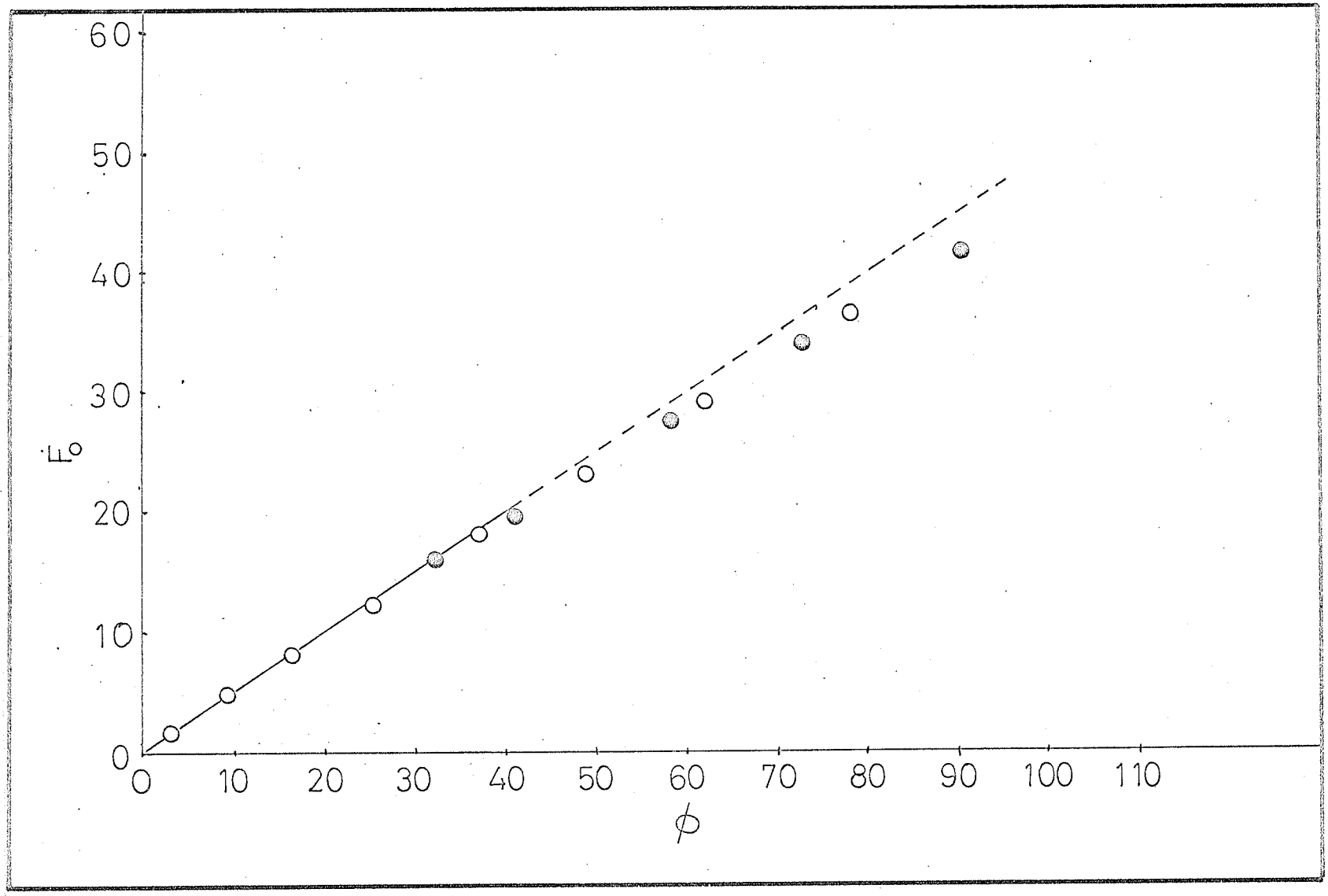
60
50
40
30
20
10
0
E°
0
10
20
30
40
50
60
70
80
90
100
110
φ

FIGURE (3.14)

F_o AS A FUNCTION OF ϕ FOR CO_2I.

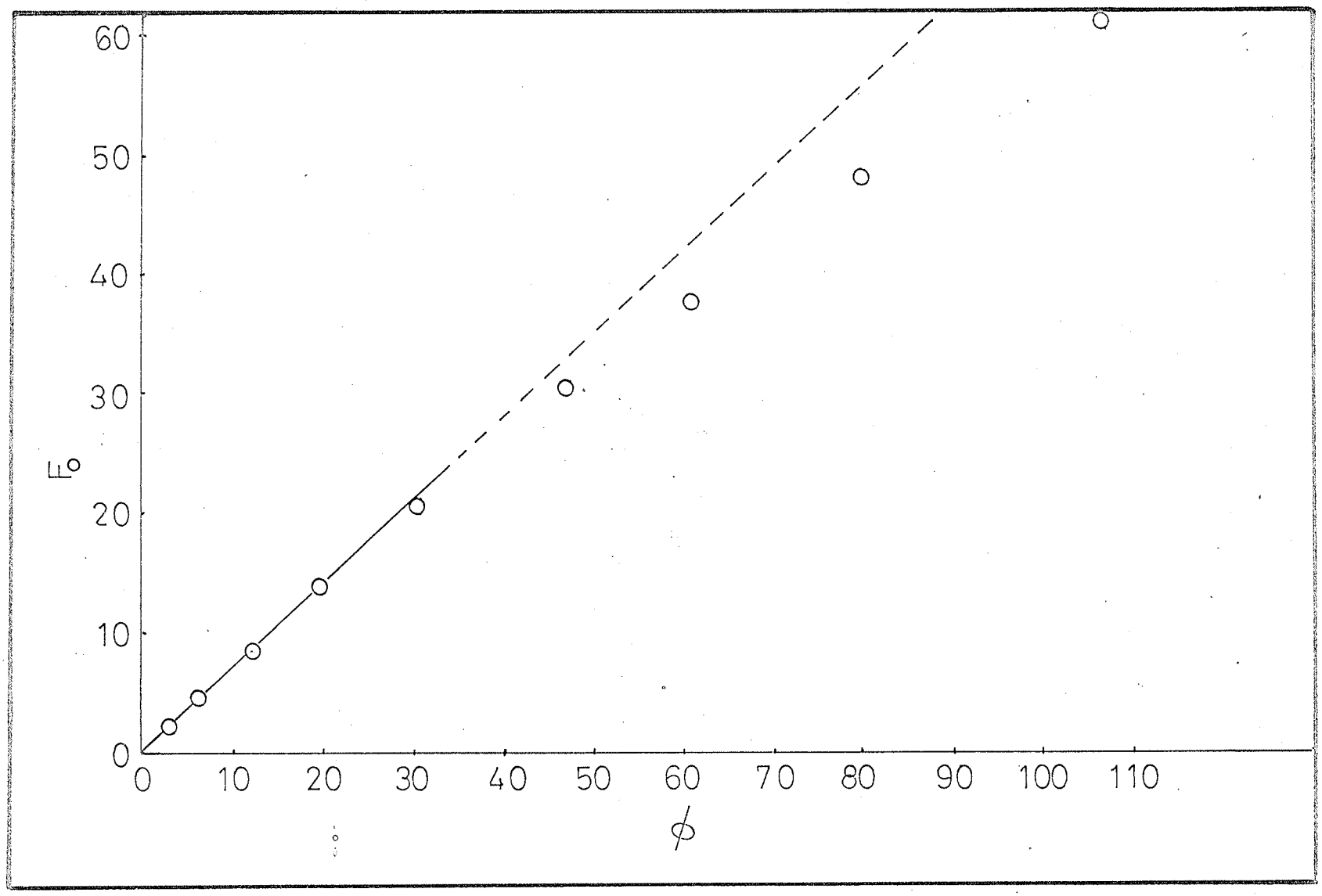
60
50
40
30
20
10
0
Eo
0
10
20
30
40
50
60
70
80
90
100
110
ϕ

$\chi_o(He)$ = 0.55 cc./min. atm.

$\chi_o(Ar)$ = 0.51 cc./min. atm.

$\chi_o(CO_2)$ = 0.68 cc./min. atm.

In order to convert these values to B_o, the following constants were used;

latm. = 1.0133×10^6 dynes/cm^2.

L = 6096 cm.

A = 2.14×10^{-2} cm^2.

$\eta(He)$ = 1.887×10^{-4} gm./cm.sec. (141)

$\eta(Ar)$ = 2.104×10^{-4} gm./cm.sec. (141)

$\eta(CO_2)$ = 1.380×10^{-4} gm./cm.sec. (141)

The corresponding B_o values were calculated to be;

$B_o(He)$ = 4.88×10^{-7} cm^2.

$B_o(Ar)$ = 5.05×10^{-7} cm^2.

$B_o(CO_2)$ = 4.40×10^{-7} cm^2.

The average value of B_o was calculated to be;

$\bar{B}_o$ = $(4.78 \pm 0.25) \times 10^{-7}$ cm^2.

The deviation from Darcy's Law is reflected in the variation of the B value which in turn is directly related to χ (see eqn. (3.34)). Although no present theory warrants it, it was found that χ can be plotted against $\bar{P}$

to give a straight line relationship. $\bar{P}$ was calculated from the equation derived by Martire and Locke (60), which takes into account the carrier gas nonideality. Its form is;

$$\bar{P} = \{(a^3 - 1)/3 - b(a^3P_i - P_o)/4\}/\{(a^2 - 1)/2P_o - b(a^3 - 1)/3\} \qquad (3.38)$$

where

$$a = P_i/P_o \qquad (3.39)$$

A plot of χ against $\bar{P}$ for HeI, Ar(II and III), and CO_2I is shown in Figures (3.15), (3.16), and (3.17) respectively.

The first interesting feature of the helium plot is that χ is not a constant as the plot of F_o against ϕ had implied. This then means that the helium flow does not obey Darcy's Law for if it did χ would remain constant. The second point of interest is the sudden increase in χ (thus in permeability) in the high pressure region. It should be noted that this effect is not noted for the other two gases in this pressure range. It is unfortunate that the present apparatus did not allow to explore the higher $\bar{P}$ region. By doubling or tripling the $\bar{P}$ range it should be possible to determine whether there is a limit to which χ will increase, and to see whether there exists this "breakthrough" for the other gases.

It was found that in the linear region the relationship

FIGURE (3.15)

χ AS A FUNCTION OF $\bar{P}$ FOR HELIUM CARRIER GAS.

○ HeI

● HeII

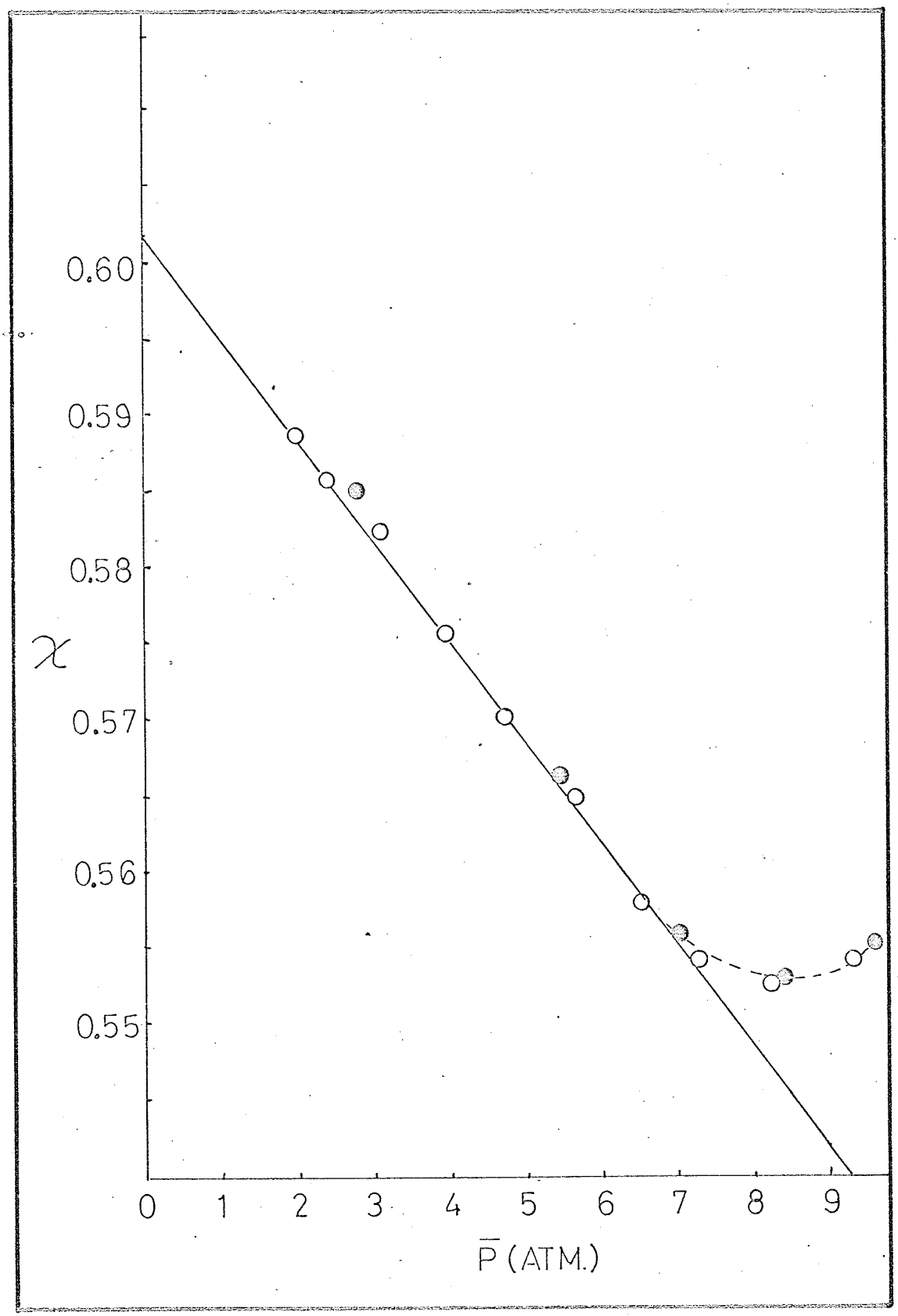
0.60
0.59
0.58
χ
0.57
0.56
0.55
0
1
2
3
4
5
6
7
8
9
P̄ (ATM.)

FIGURE (3.16)

χ AS A FUNCTION OF $\bar{P}$ FOR Ar(II AND III).

○ ArII

● ArIII

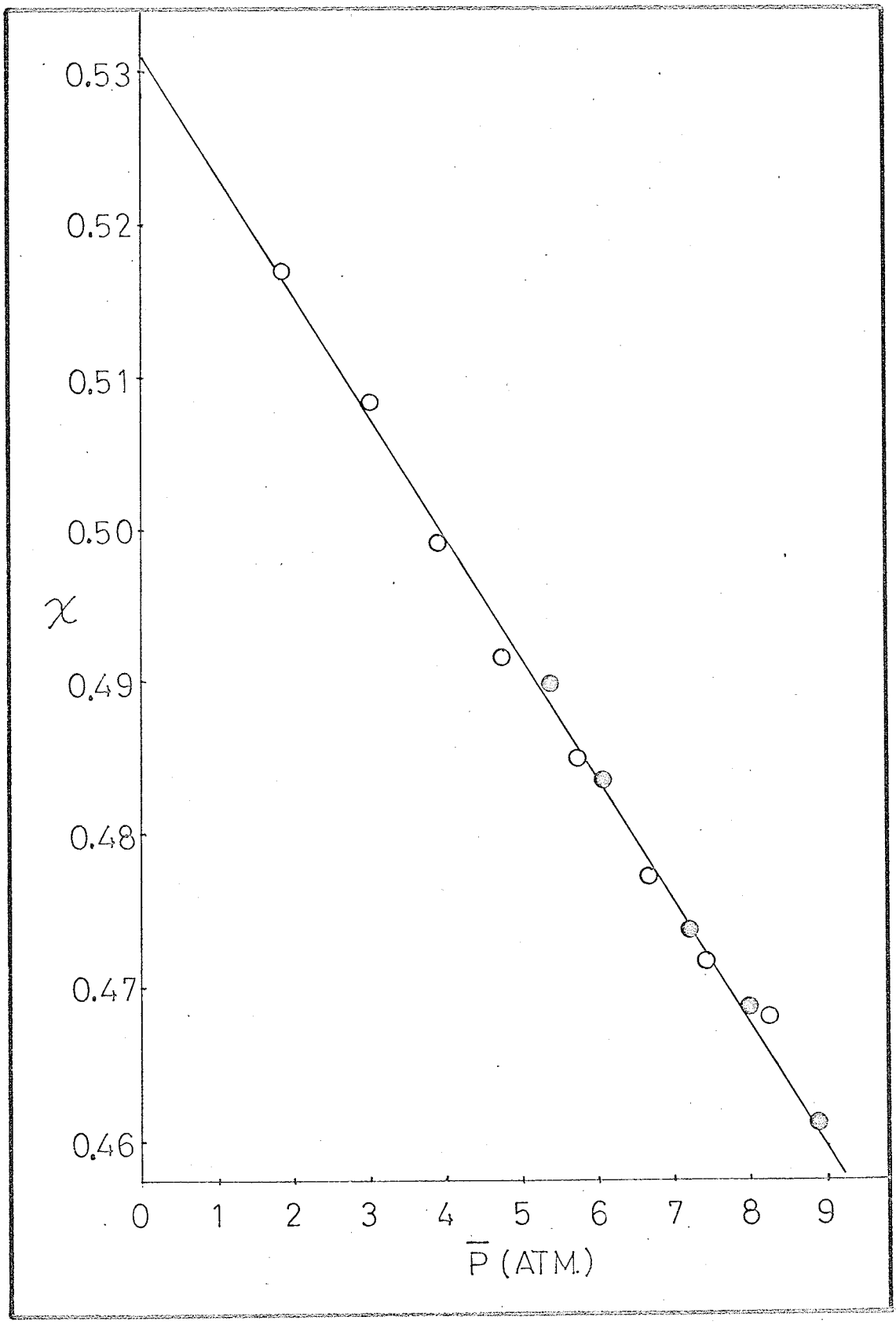
0.53
0.52
0.51
0.50
χ
0.49
0.48
0.47
0.46
0
1
2
3
4
5
6
7
8
9
P̄ (ATM.)

FIGURE (3.17)

χ AS A FUNCTION OF $\bar{P}$ FOR CO_2I.

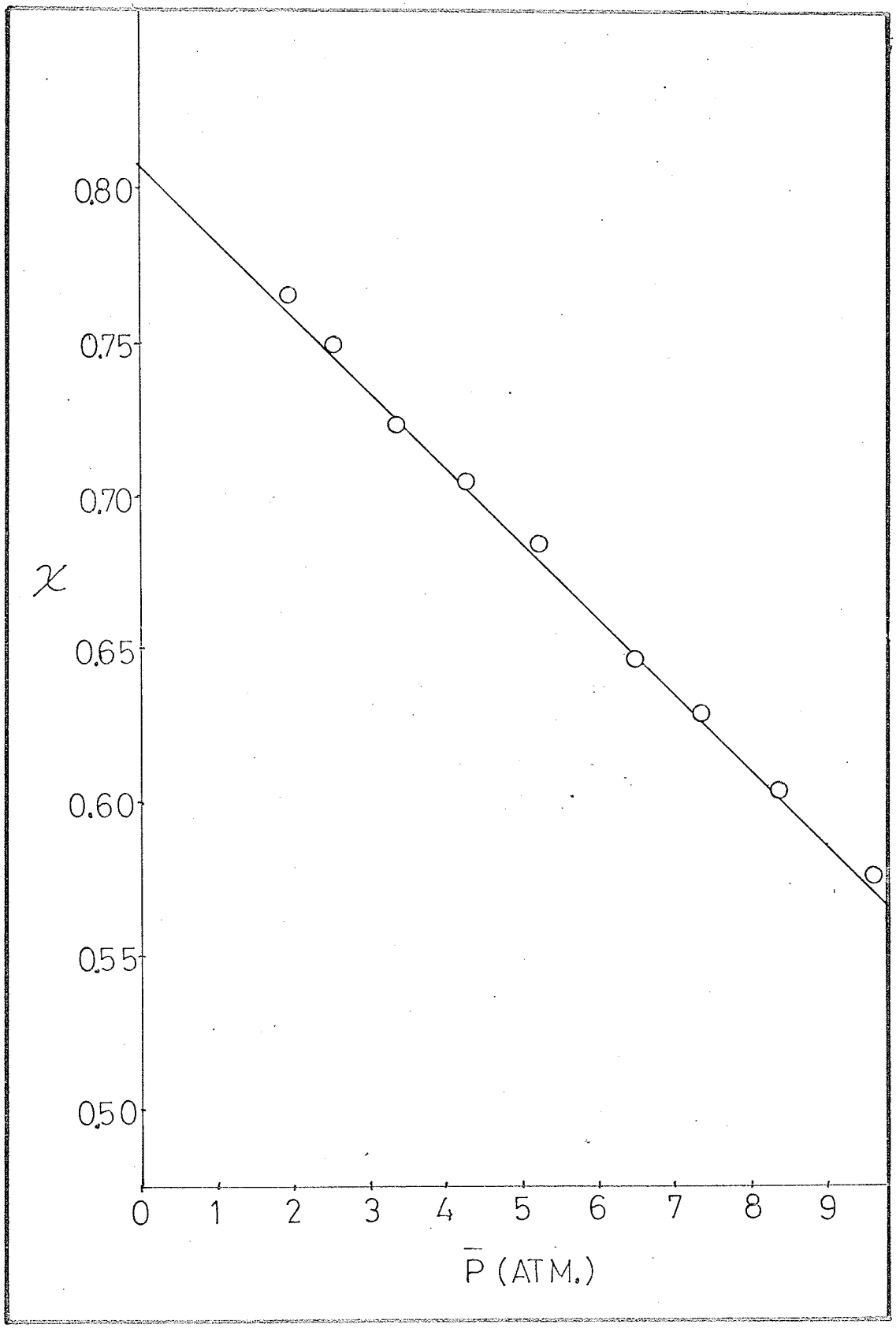
0.80
0.75
0.70
χ
0.65
0.60
0.55
0.50
0
1
2
3
4
5
6
7
8
9
P̄ (ATM.)

between χ and $\bar{P}$ can be expressed as;

$$\chi = \chi_o - m\bar{P} \qquad (3.40)$$

for all the gases. By a method of least squares, the experimental data was fitted to straight lines having the following equations;

$$\chi(He) = 0.602 - 0.00666\bar{P} \qquad (3.41)$$

$$\chi(Ar) = 0.531 - 0.00794\bar{P} \qquad (3.42)$$

$$\chi(CO_2) = 0.809 - 0.0247\bar{P} \qquad (3.43)$$

From the various χ_o values, the following B_o values were calculated;

$B_o(He) = 5.32 \times 10^{-7}$ cm.^{2}

$B_o(Ar) = 5.24 \times 10^{-7}$ cm.^{2}

$B_o(CO_2) = 5.23 \times 10^{-7}$ cm.^{2}

The average value of B_o was found to be;

$$\bar{B}_o = (5.26 \pm 0.04) \times 10^{-7} \text{ cm.}^2$$

This $\bar{B}_o$ value is somewhat higher than the former and has a much smaller deviation. It is most probable that this value is more correct.

By using the Kozeny-Carman equation (constant factor 1/180) and the Blake-Kozeny equation (constant factor

1/150), the interparticle porosity of the column was found to be 0.427 and 0.410 respectively. The ε values by either equation are close to what is expected, Giddings (146) states that for a well packed granular columns the ε value will only occasionally vary by more than $\pm$ 0.03 from a normal value of 0.40.

The χ values when ploted against F_o give a quadratic relationship. This can be seen in Figures (3.18), (3.19), and (3.20) for HeI, Ar(II and III), and CO_2I respectively. The helium plot is of particular interest since unlike the χ v.s. $\bar{P}$ it is continuous. These plots can be expressed as;

$$\chi = AF_o^2 + BF_o + C \qquad (3.45)$$

where A, B, and C are constants. The reason for this relationship is not clear. Aside for C, the interpretation of the constants was found to be fruitless.

In order to test whether the deviation of B from B_o is described by Ergun's relationship, 1/B was ploted against F_o for the three gases. These plots for HeI, Ar(IIandIII), and CO_2I are shown in Figures (3.21), (3.22), and (3.23) respectively. Included in each figure is also the plot of eqn. (3.32), that is;

$$1/B = 1/B_o + \gamma(M/\eta)F_o \qquad (3.32)$$

FIGURE (3.18)

χ AS A FUNCTION OF F_o FOR HeI.

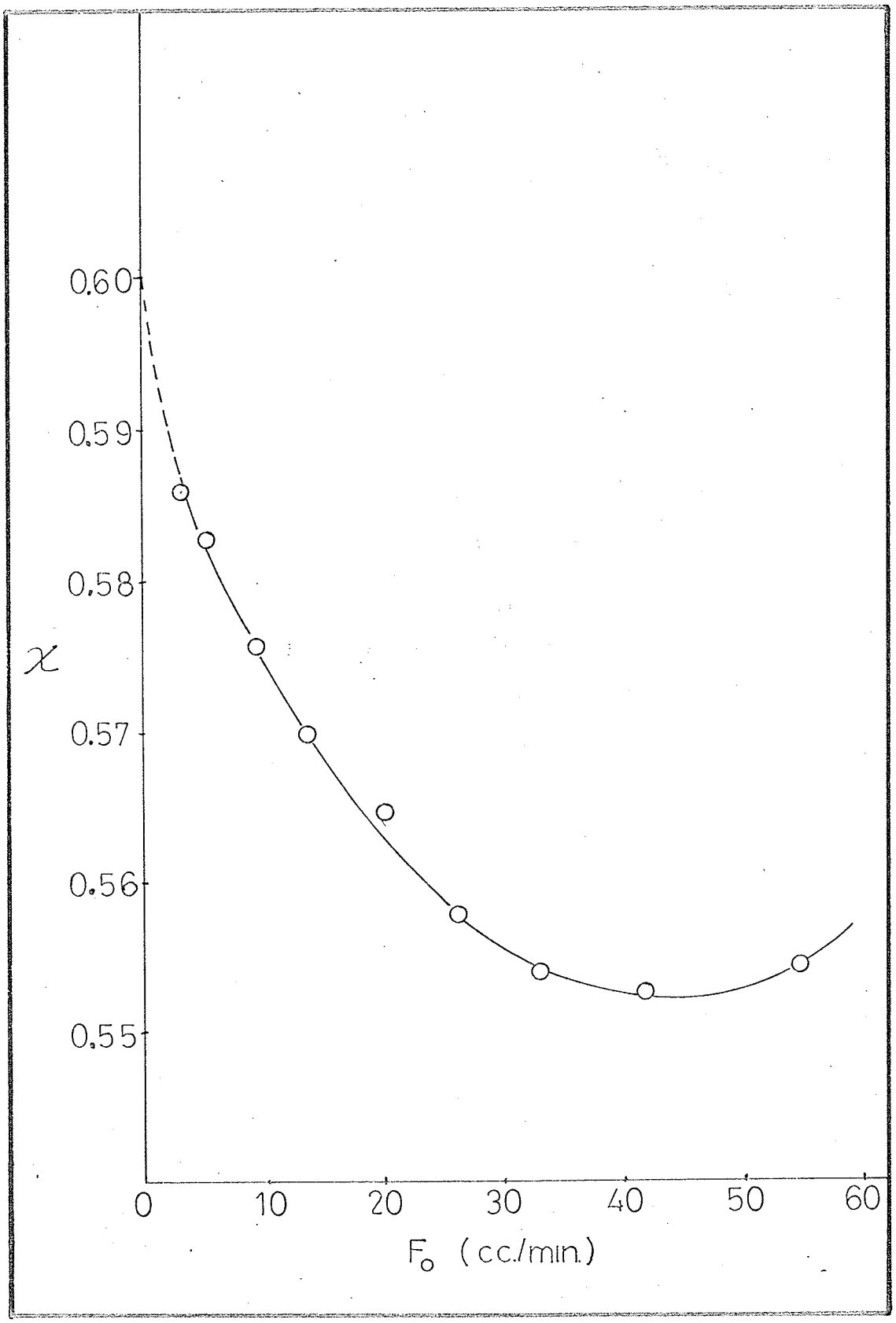
0.60
0.59
0.58
x
0.57
0.56
0.55
0
10
20
30
40
50
60
F₀ (cc./min.)

FIGURE (3.19)

χ AS A FUNCTION OF F_o FOR Ar(II AND III).

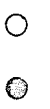

○ ArII

● ArIII

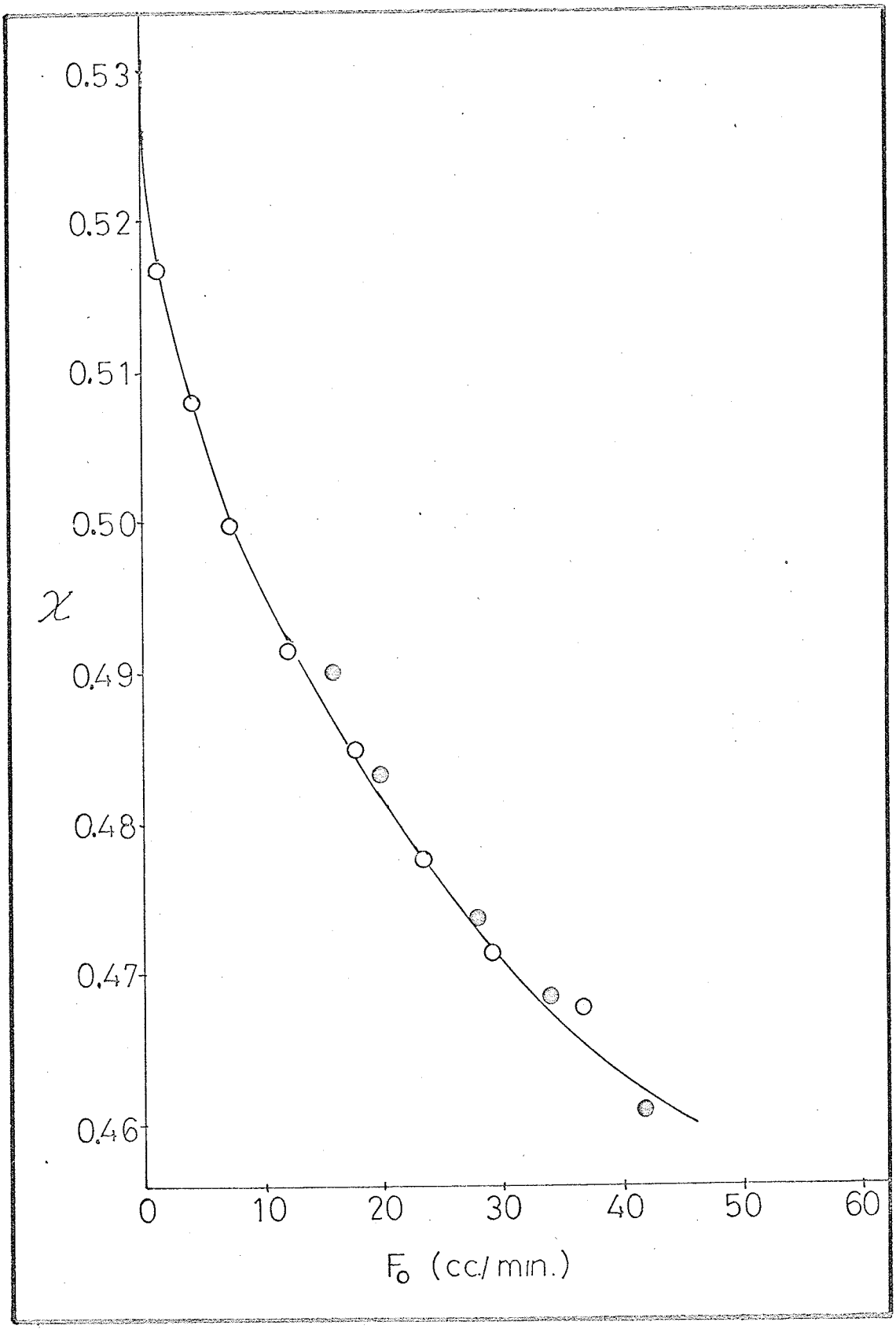
0.53
0.52
0.51
0.50
χ
0.49
0.48
0.47
0.46
0
10
20
30
40
50
60
F₀ (cc/min.)

FIGURE (3.20)

χ AS A FUNCTION OF F_o FOR CO_2I.

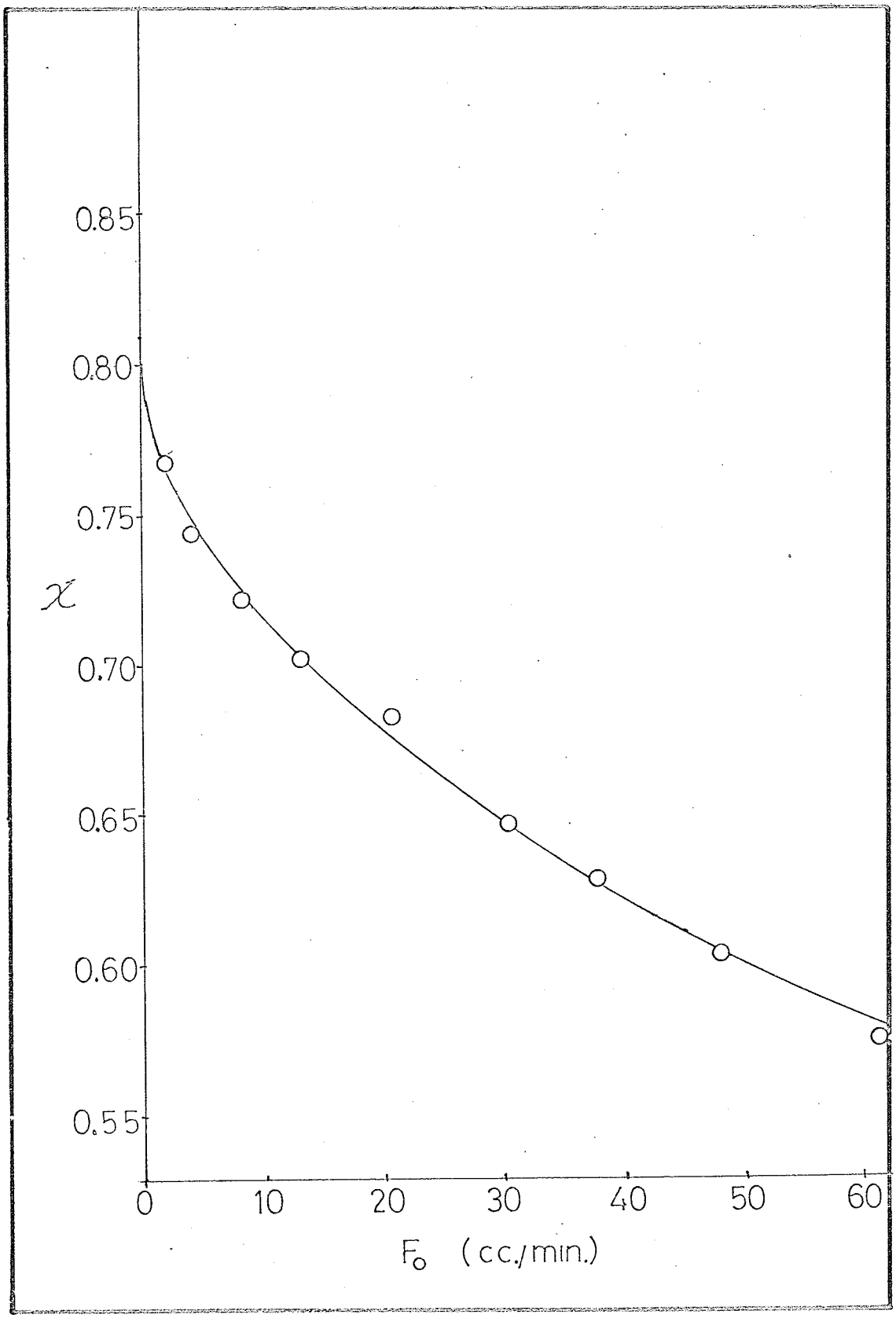
0.85
0.80
0.75
0.70
0.65
0.60
0.55
x
0
10
20
30
40
50
60
F₀ (cc./min.)

FIGURE (3.21)

1/B AS A FUNCTION OF F_o FOR HeI.

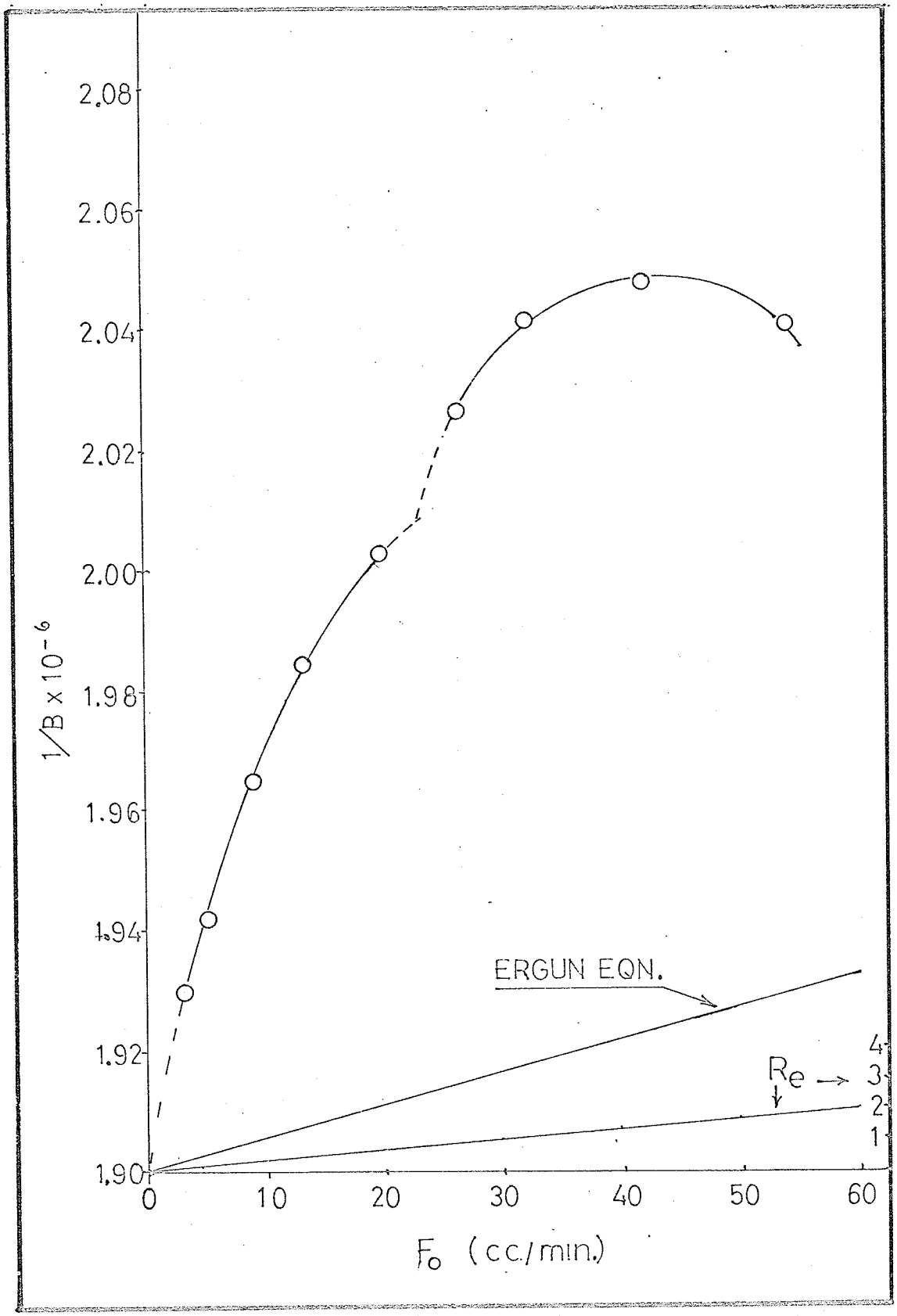
2.08
2.06
2.04
2.02
2.00
1.98
1.96
1.94
1.92
1.90
1/B x 10⁻⁶
ERGUN EQN.
Re
4
3
2
1
0
10
20
30
40
50
60
Fo (cc./min.)

FIGURE (3.22)

1/B AS A FUNCTION OF F_o FOR Ar(II AND III).

○ ArII

◎ ArIII

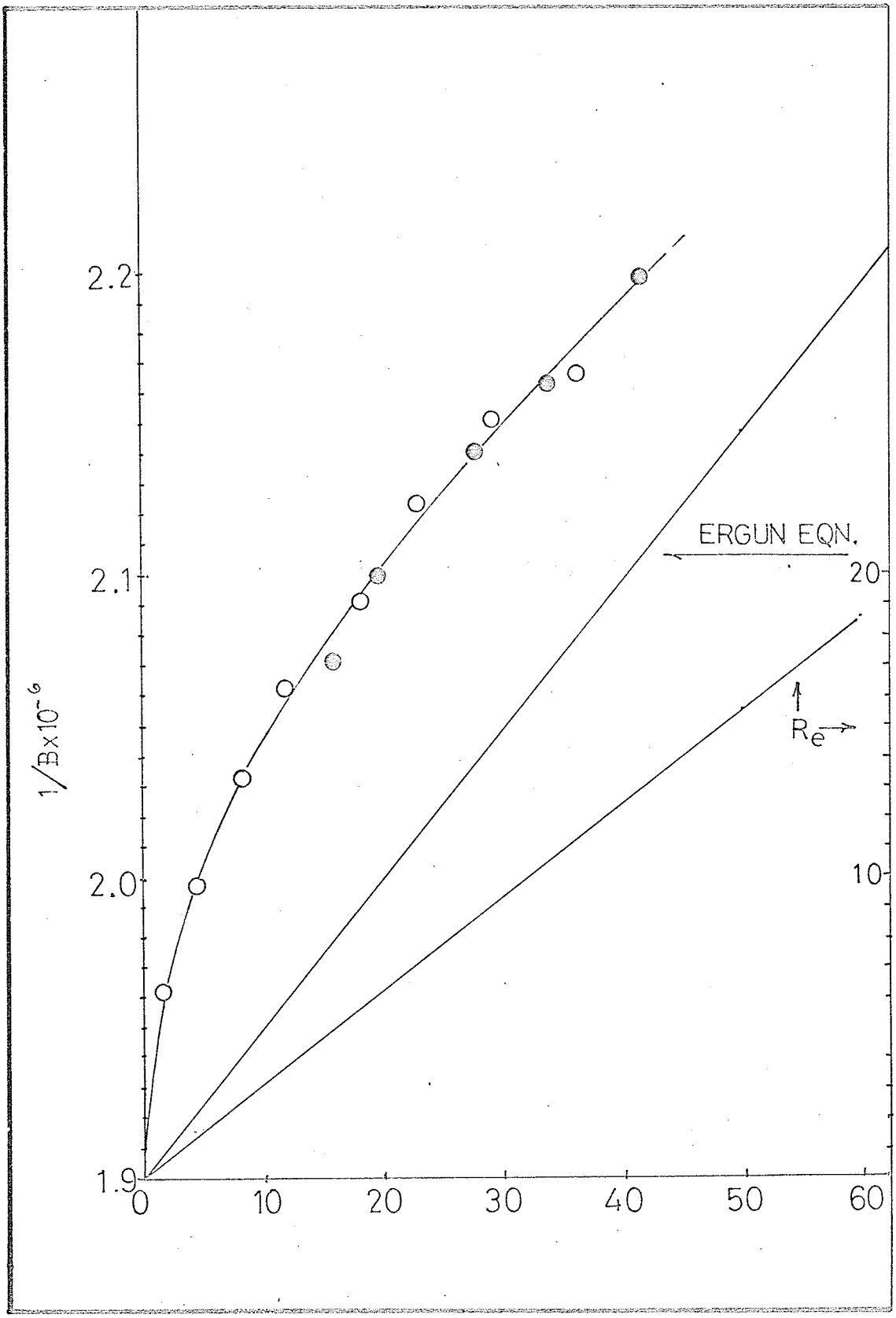
2.2
2.1
2.0
1.9
1/B x 10⁻⁶
0
10
20
30
40
50
60
ERGUN EQN.
20
10
Re

FIGURE (3.23)

1/B AS A FUNCTION OF F_o FOR CO_2I.

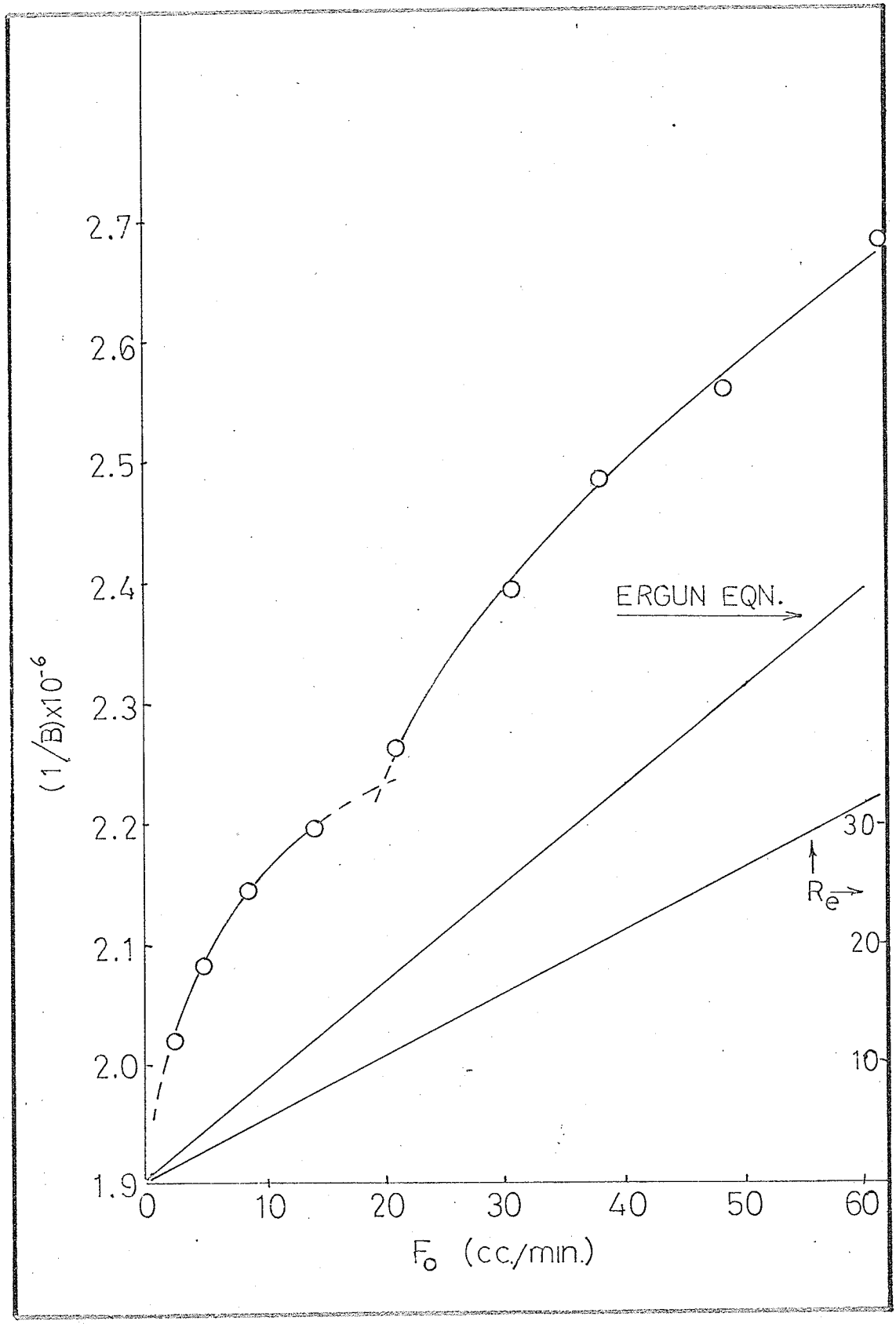
2.7
2.6
2.5
2.4
2.3
2.2
2.1
2.0
1.9
(1/B)x10^-6
ERGUN EQN.
30
20
10
Re
0
10
20
30
40
50
60
Fo (cc./min.)

and the approximate Reynolds number (R_e) as a function of F_o for each gas. In the calculation of γ and R_e, the value of 0.410 was used as ε. It was found that if use was made of $\varepsilon = 0.427$, the overall picture did not change to any extent. The B_o values which were used in plotting eqn. (3.32) were those obtained from eqns. (3.41), (3.42), and (3.43).

The most obvious feature of Figures (3.21), (3.22), and (3.23), is that the experimental variations in B are not described by the Ergun equation. All these figures show that the permeability coefficient decreases at a much faster rate than that predicted by the Ergun equation. This is particularly true for the low F_o region. In the case of Ar and CO_2, it can be seen that as the flow rate is increased the slope of the experimental curve decreases and begins to approach that of the Ergun equation. This however, cannot be said about the helium case since the "breakthrough" effect tends to mask this trend. Since the rate of permeability decrease is the highest in the low F_o (therefore low $\bar{P}$) region, it cannot be explained through pressure induced viscosity change.

Another interesting feature of these figures is the presence of a break in the curve at about $F_o = 20$ cm.^{3}/min.. It is difficult to visualize a mechanism by which the permeability can decrease in a cascading manner. One possibility is that this effect maybe somehow related to particle

shifting in the individual sections of the column by means of a viscous drag mechanism. Since the ratio $\varepsilon^3/(1-\varepsilon)^2$ is very sensitive to changes in ε, a slight change in packing density of either section of the column could produce a considerable decrease in the permeability. A discussion relating the variation of the inlet pressure to the gas velocity profile in each section of the column, and the gas velocity affect on the particles in terms of enhancement of packing density is beyond the scope of this study.

The above mechanism should not be dismissed completely since there is sufficient evidence to indicate that the column possesses a permeability hysterisis effect. This can be best illustrated by directly comparing the experimental results of HeI, Ar(II and III), and CO_2I to those of ArI, CO_2II, CO_2III, and CO_2IV. The basic difference between the two groups is the manner in which the working inlet pressures were approached. In the first group, each experiment was carried out by starting at the highest operating inlet pressure. After the completion of the highest inlet pressure experiment, the gas pressure regulating valve was turned down by a suitable amount. Due to the column resistance and the presence of a volume ($\sim$ 200 cc.) between the regulator valve and the column, the inlet pressure fell relatively slowly to the next value. Under these circumstances the experimental working conditions

were approached gradually. The inlet pressures of all the subsequent experiments were approached in the same way.

Experiments ArI and CO_2IV were carried out by starting at the lowest inlet pressure and incrementally increasing it to the highest value. In this case the alteration of the pressure regulating valve resulted in a sudden inrush of gas into the column. Under these circumstances the entire column experienced a pressure pulse before it reached a steady state.

In experiment CO_2II, the inlet pressure was first allowed to fall to approximately 4 p.s.i. above atmospheric (4 p.s.i. + P_o), after which it was raised to the first operating pressure (19.25 p.s.i. + P_o). After sufficient time was allowed for equilibration ($\sim$16 hrs.), the first experiment was performed. The subsequent inlet pressures were approached in the normal manner.

The only difference between experiments CO_2II and CO_2III is that in experiment CO_2III the inlet pressure was first allowed to fall to approximately 16 p.s.i. + P_o after which it was raised to the first operating pressure (20.25 p.s.i. + P_o).

Table (3.4) contains the F_o, the χ, the 1/B, and the $\bar{P}$ values for experiments CO_2II, CO_2III, CO_2IV, and ArI.

A plot of χ against $\bar{P}$ for experiments CO_2I, CO_2II, CO_2III, and CO_2IV is shown in Fig. (3.24). CO_2I is included

TABLE (3.4) F_o, χ, 1/B, AND $\bar{P}$ VALUES FOR EXPERIMENTS ArI, CO_2II, CO_2III, AND CO_2IV.

F_o cc./min.	χ^*	$1/B \times 10^{-6}$ ($cm.^{-2}$)	$\bar{P}$ (atm.)
		ARGON I	
2.297	0.534	1.899	2.186
3.984	0.515	1.970	2.797
6.664	0.509	1.992	3.553
9.825	0.505	2.009	4.283
14.32	0.500	2.030	5.139
19.97	0.491	2.065	6.036
26.14	0.478	2.123	6.944
32.55	0.471	2.155	7.778
40.65	0.461	2.198	8.748
		CARBON DIOXIDE II	
1.654	0.754	2.050	1.720
4.701	0.743	2.080	2.556
9.117	0.730	2.119	3.452
14.38	0.710	2.177	4.330
20.87	0.687	2.253	5.240
27.90	0.666	2.321	6.098
35.98	0.632	2.448	7.061

TABLE (3.4) (CONTINUED)

44.75	0.609	2.541	7.969
53.43	0.586	2.639	8.877
		CARBON DIOXIDE III	
1.889	0.802	1.929	1.760
5.267	0.741	2.088	2.688
9.679	0.726	2.130	3.530
14.91	0.710	2.179	4.376
22.08	0.683	2.264	5.368
28.63	0.663	2.334	6.203
36.51	0.636	2.430	7.098
45.13	0.612	2.526	7.981
57.59	0.585	2.642	9.167
		CARBON DIOXIDE IV	
3.118	0.790	1.959	2.146
6.549	0.746	2.073	2.958
10.881	0.731	2.116	3.761
17.13	0.712	2.171	4.703
24.02	0.688	2.247	5.572
33.29	0.646	2.394	6.703
41.24	0.619	2.499	7.619
49.22	0.590	2.623	8.512
61.28	0.567	2.728	9.658

* The units of x are cc./min. atm.

FIGURE (3.24)

χ AS A FUNCTION OF $\bar{P}$ FOR

CO_2I, CO_2II, CO_2III, AND CO_2IV.

CO_2I

CO_2II

CO_2III

CO_2IV

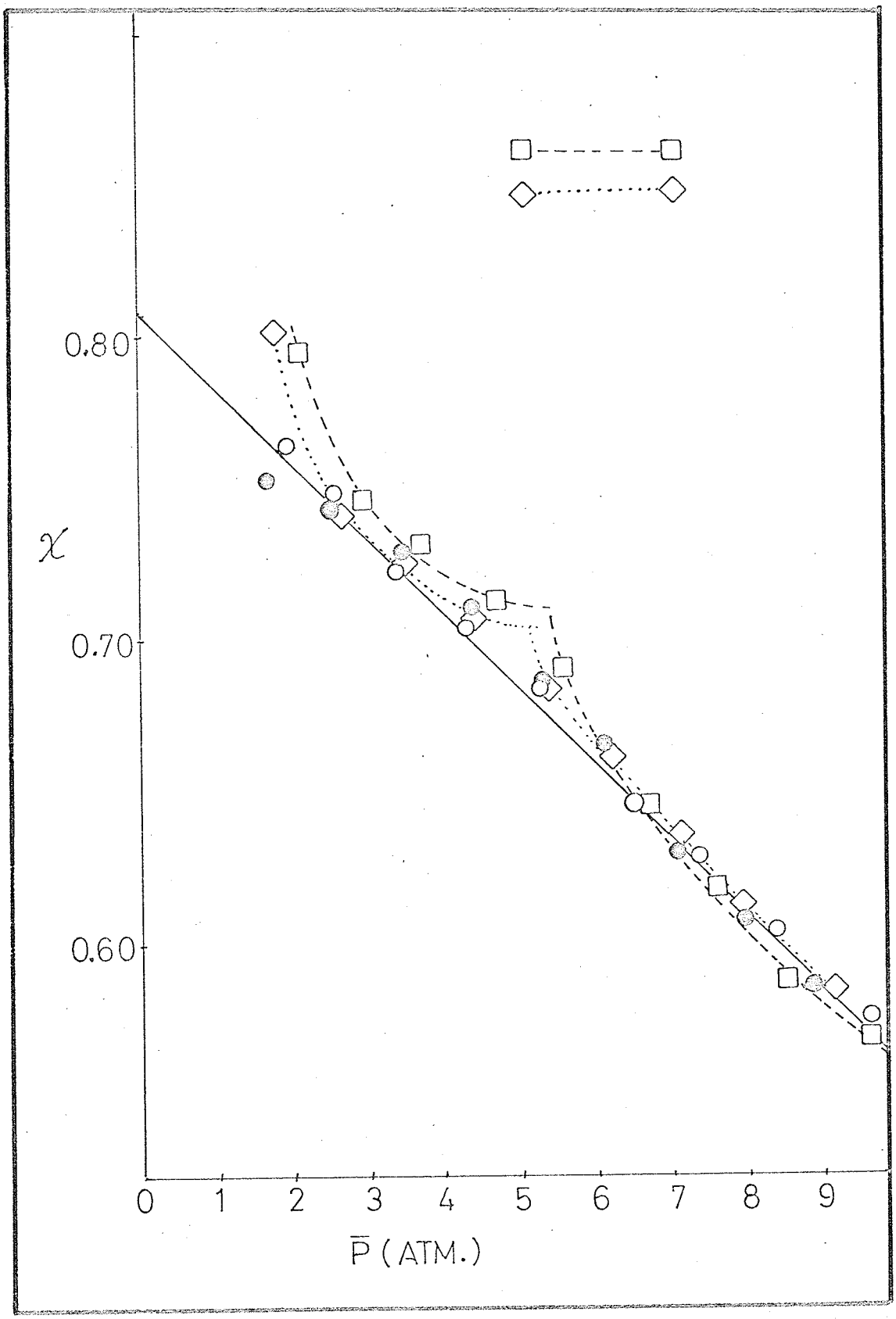
0.80
0.70
0.60
χ
0
1
2
3
4
5
6
7
8
9
P̄ (ATM.)

for comparison. The same plot for ArI, and Ar(II and III) is shown in Fig. (3.25).

One obvious feature of Figures (3.24) and (3.25) is that the relationship between χ and $\bar{P}$ depends on whether the inlet pressure is progressively increased or decreased. It was found in other experiments that a large scatter in the χ against $\bar{P}$ plot is obtained if the operating inlet pressures were chosen randomly.

From the plots for CO_2II, CO_2III, and CO_2IV, it can be seen that the relationship between χ and $\bar{P}$ also depends on the magnitude of the lowest inlet pressure attained.

In both the Ar and the CO_2 case, the break in the curve is unmistakable. The similarity between the curves for Ar(II and III) and CO_2I, and between curves for ArI and CO_2II is worthy of notice. For both gases this break occurs at a $\bar{P}$ value close to 6 atm. which corresponds to an F_o value of approximately 20cc./min.. This and the cascading shape of the curve is in accordance with the previous observations.

The experiments ArI, ArII, CO_2II, CO_2III, CO_2IV and ArIII were performed in the order written. Considering this and the fact that experiments ArII and ArIII are reproducible, it can be concluded that there exists a permeability hysterisis. The term hysterisis serves here only to describe the fact that a different set of results are obtained if one changes the inlet pressure in the increas-

FIGURE (3.25)

χ AS A FUNCTION OF $\overline{P}$ FOR ArI, AND Ar(II AND III).

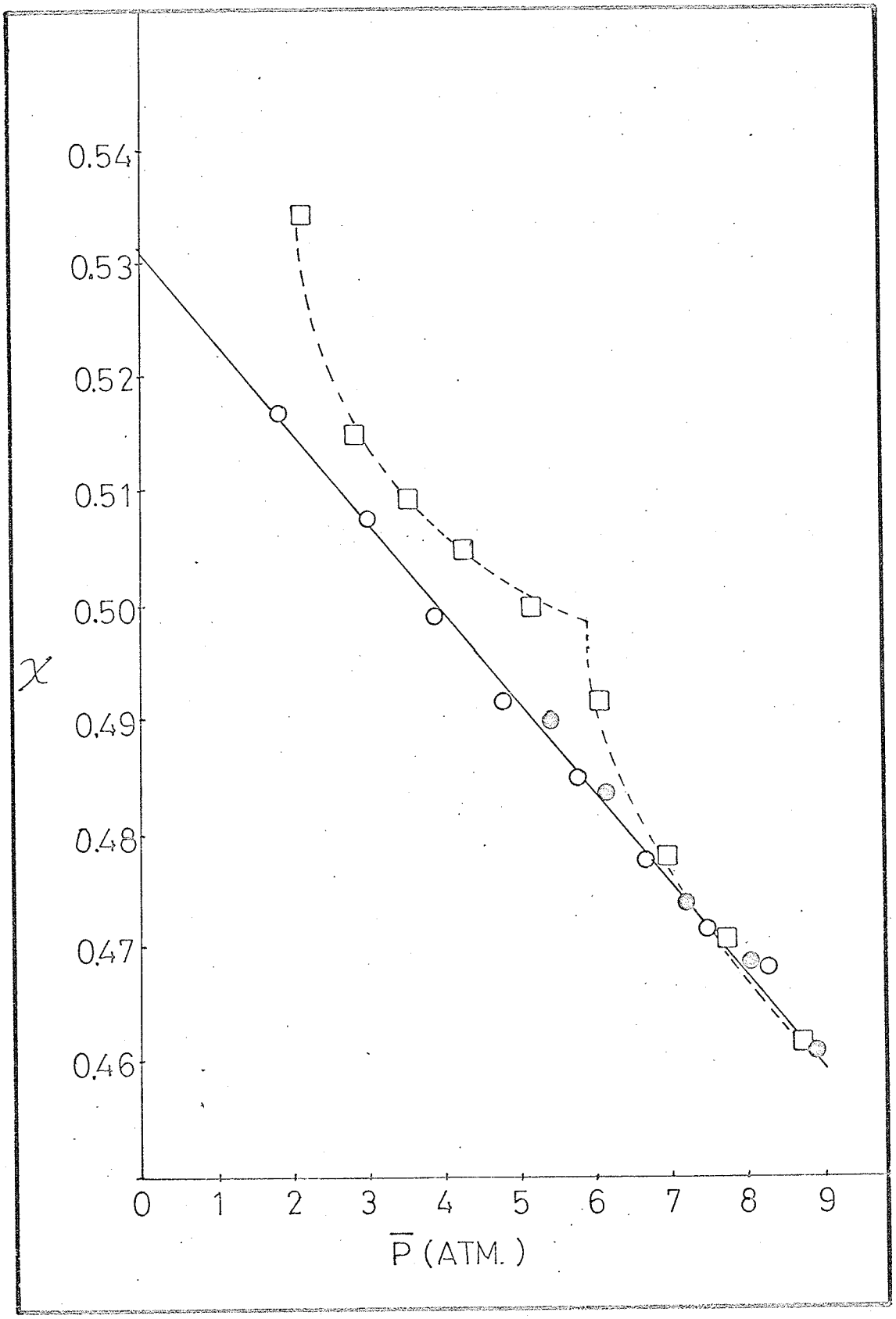
0.54
0.53
0.52
0.51
0.50
0.49
0.48
0.47
0.46
χ
0
1
2
3
4
5
6
7
8
9
P̄ (ATM.)

ing or decreasing direction.

To further illustrate the fact that the direction in which the inlet pressure is changed has an effect on the column permeability, plots of 1/B against F_o are shown for CO_2II, CO_2III, and CO_2IV in Figures (3.26), (3.27), and (3.28) respectively. This plot for ArI along with Ar(II and III) is shown in Fig. (3.29). A common 1/B against F_o plot for all CO_2 experiments is shown in Fig. (3.30). It can be seen from this figure that although the individual CO_2 plots are nonlinear, they tend to hug a common straight line. This line has a slope somewhat similar to that of the Ergun equation plot. The same effect, although not as obvious, can be seen in the Ar case. By a vertical displacement of the Ergun plot (this can be done by the use of a larger $1/B_o$ value), some coincidence between the Ergun plot and the common experimental plot can be obtained. If the deviation from the Ergun equation can be attributed to particle shifting, then the common experimental line when extrapolated to $F_o = 0$ would give a B_o value which would correspond to a more tightly packed column.

The undue decrease in the column permeability can in part be qualitatively explained through a particle shift mechanism. If this is actually the case, then it is difficult to explain the permeability increase in the helium case.

FIGURE (3.26)

1/B AS A FUNCTION OF F_o FOR CO_2II.

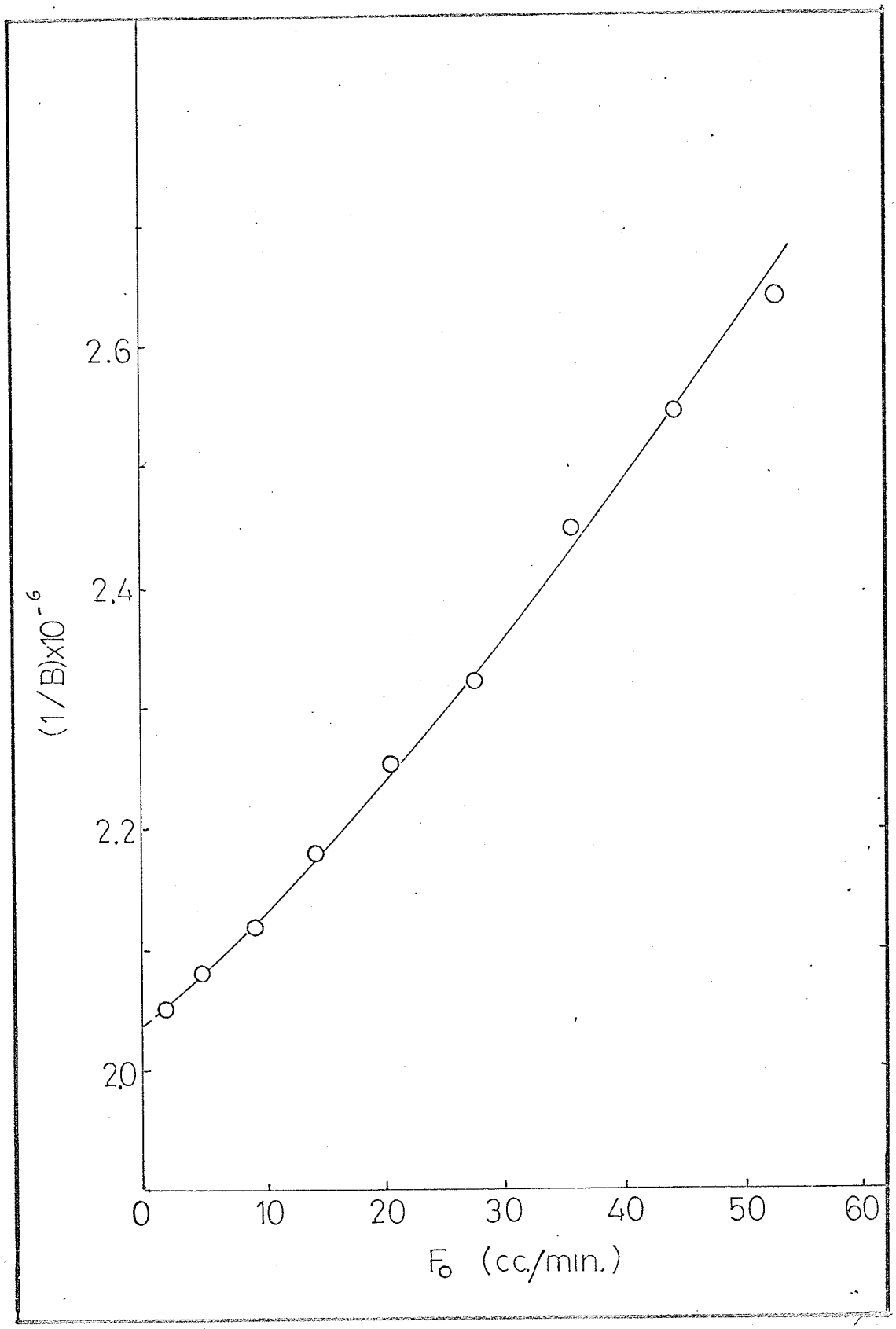
2.6
2.4
2.2
2.0
(1/B)x10⁻⁶
0
10
20
30
40
50
60
F₀ (cc/min.)

FIGURE (3.27)

1/B AS A FUNCTION OF F_o FOR CO_2III.

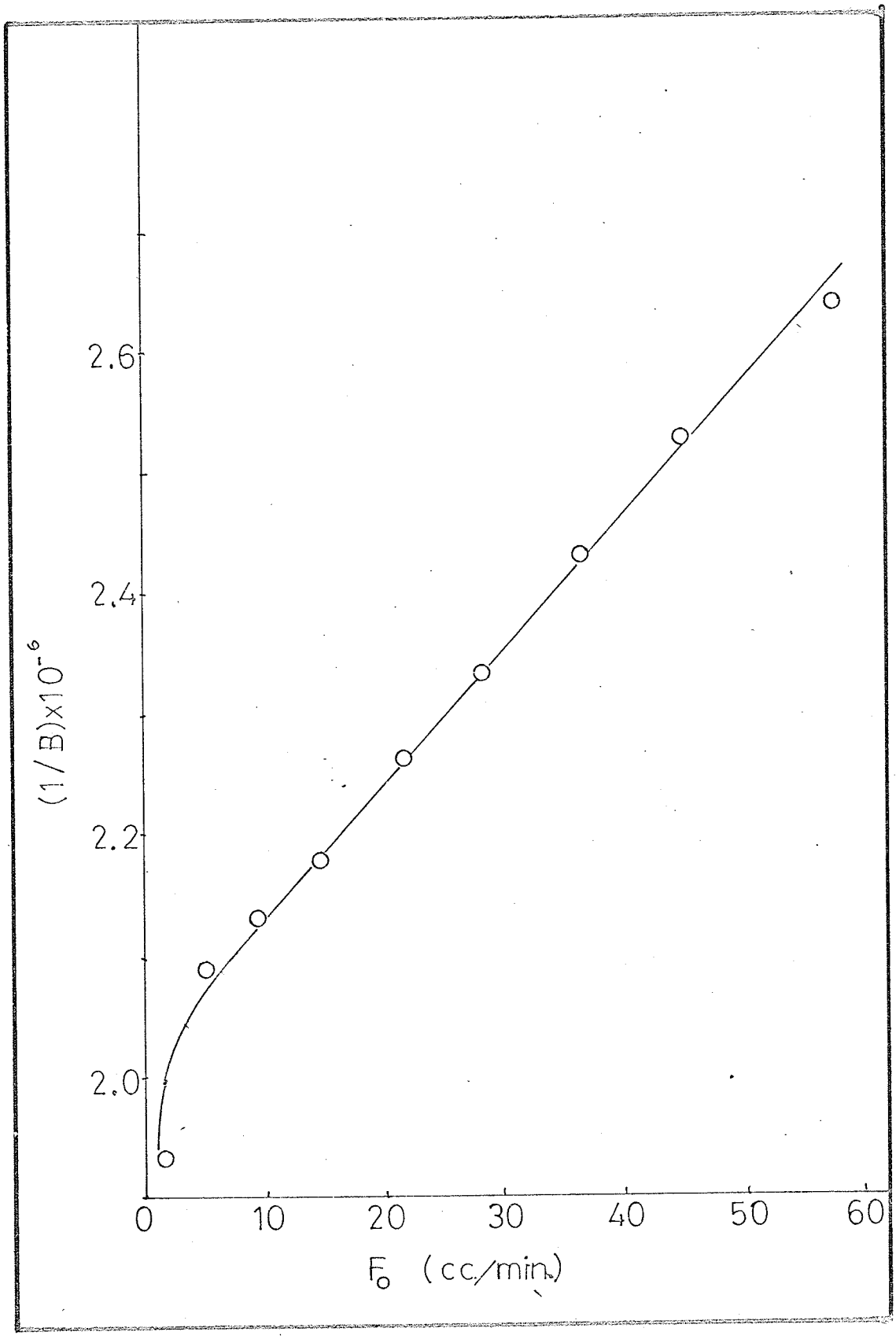
2.6
2.4
2.2
2.0
(1/B)x10^-6
0
10
20
30
40
50
60
Fo (cc./min.)

FIGURE (3.28)

1/B AS A FUNCTION OF F_o FOR CO_2IV.

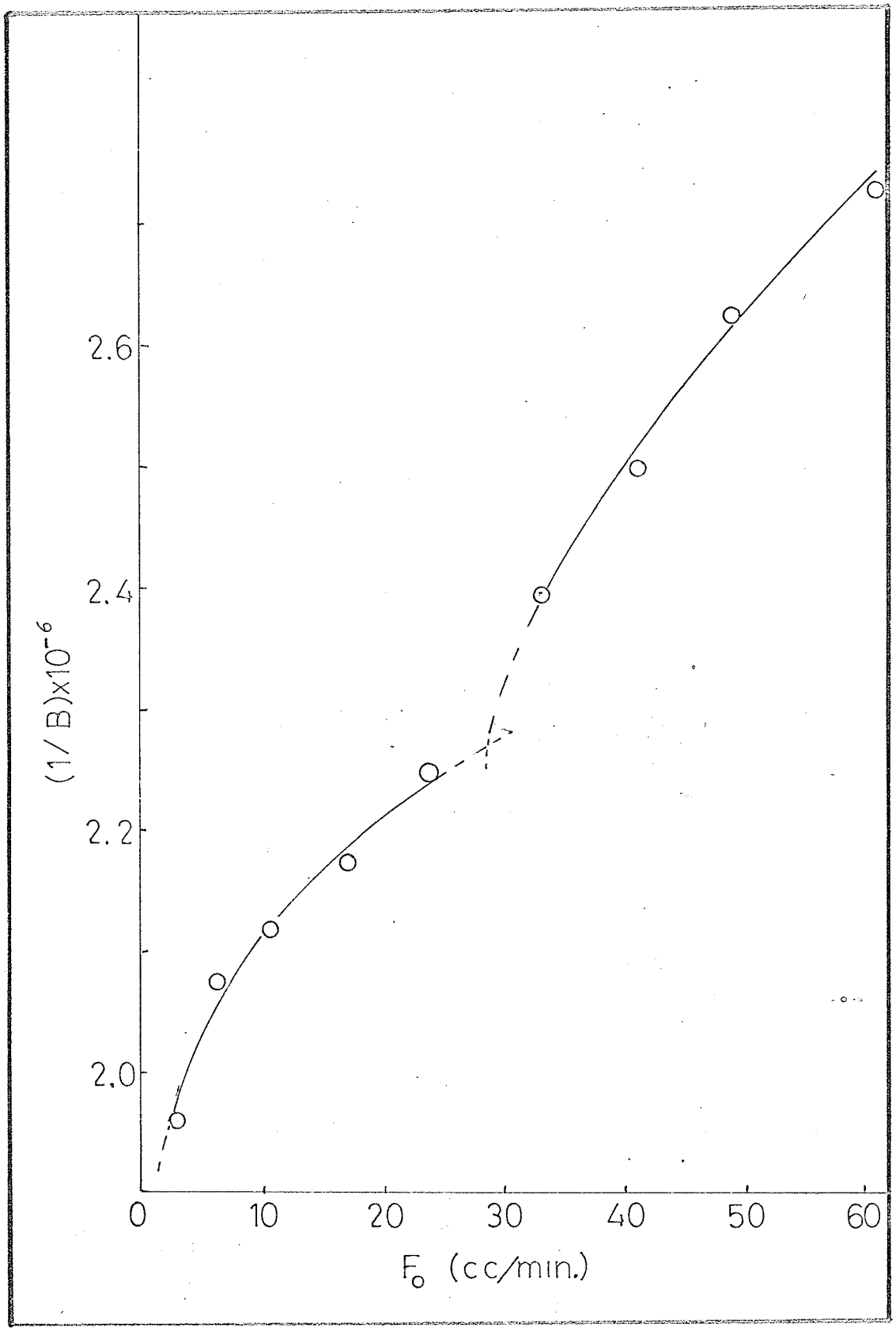
2.6
2.4
2.2
2.0
(1/B)x10^-6
0
10
20
30
40
50
60
F0 (cc/min.)

FIGURE (3.29)

A COMMON 1/B AGAINST F_o PLOT FOR ArI AND Ar(II AND III).

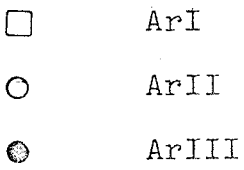

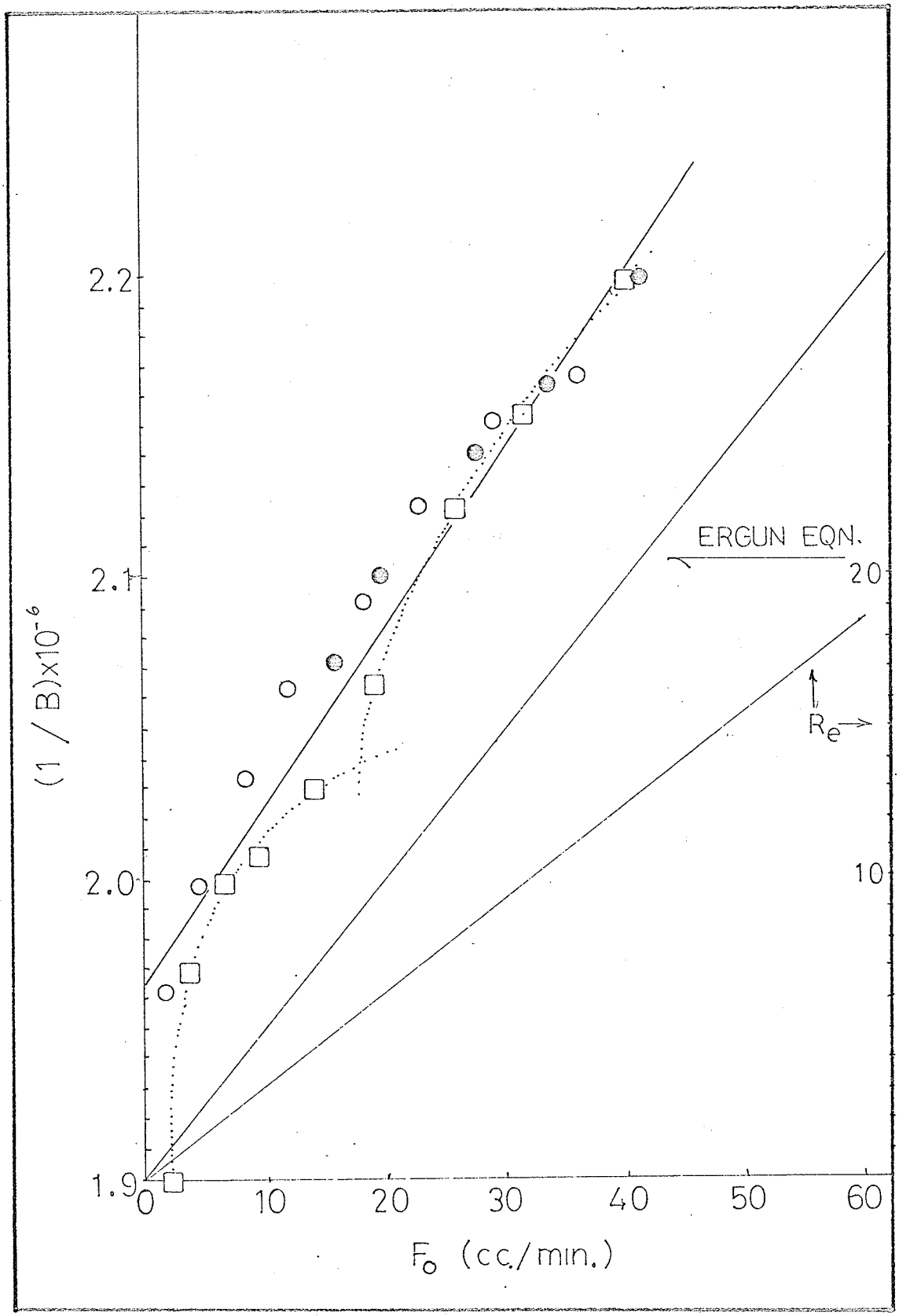
2.2
2.1
2.0
1.9
(1 / B)x10⁻⁶
0
10
20
30
40
50
60
F₀ (cc./min.)
ERGUN EQN.
20
10
Re

FIGURE (3.30)

A COMMON 1/B AGAINST F_o

FOR CO_2I, CO_2II, CO_2III, AND CO_2IV.

◇ CO_2I

○ CO_2II

◎ CO_2III

□ CO_2IV

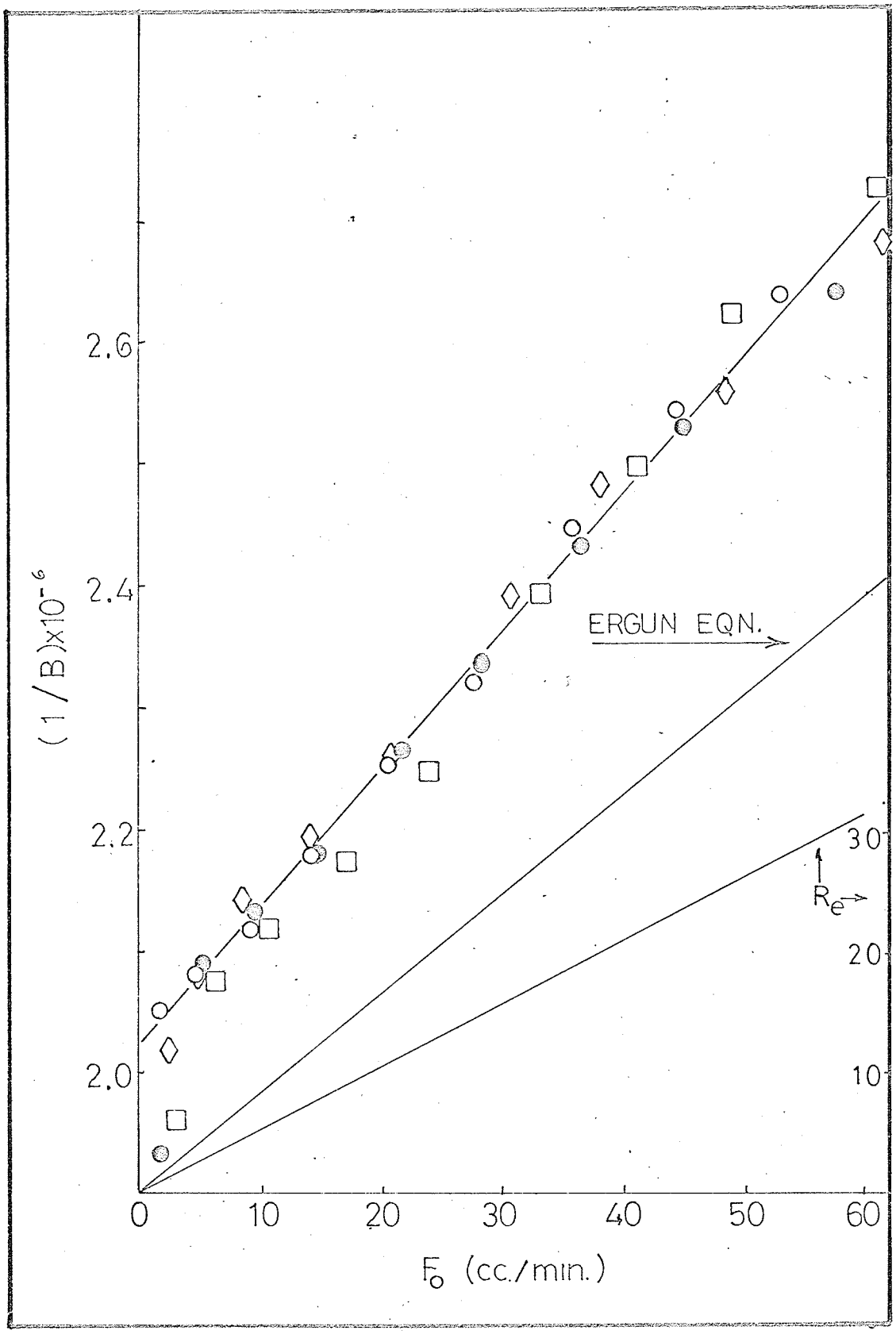
(1/B)x10⁻⁶
2.6
2.4
2.2
2.0
ERGUN EQN.
Re
30
20
10
0
10
20
30
40
50
60
Fo (cc./min.)

THE NET RETENTION VOLUME AS A FUNCTION OF TEMPERATURE AND PRESSURE

Martire and Locke (60) have pointed out that for most accurate calculations of the mean column pressures and the corrected retention volumes, the nonideality of the carrier gas should be considered. They have shown that to a good approximation the expression for the mean column pressure is given by eqn. (3.38).

Having shown that only a very small error (0.16% for CO_2 at a = 5) is introduced into the $\bar{P}$ value if the carrier gases (He, H_2, N_2, Ar, CO_2) are treated as ideal, the authors have concluded that this correction need not be applied except in the unusual circumstances or where the highest accuracy is desired.

The author wishes to point out that the assumption of the carrier gas ideality introduces a much more serious error to the calculation of the net retention volumes than to the mean column pressure.

For an ideal carrier gas the equation of state can be expressed as;

$$n = PV/RT \qquad (3.16)$$

If the mass balance is to be maintained within the chromatographic column, then the number of moles of the carrier gas passing any point in the column per unit time must be con-

stant. Considering this and equation (3.16), the following relationship can be established;

$$P_o V_o = \overline{P}_i \overline{V} = P_o F_o t \qquad (3.46)$$

where:

$\overline{P}_i$ is the mean column pressure of the ideal carrier gas

V_o is the volume of the carrier gas exciting the column in time (t) at pressure P_o

$\overline{V}$ is the volume of the carrier gas which is swept past a point (in time t) where $P = \overline{P}_i$

F_o is the flow rate of the carrier gas at the column outlet.

Rearrangement of equation (3.46) gives;

$$\overline{V} = F_o t P_o / P_i = F_o t j \qquad (3.47)$$

where as before j is the Martin-James compressibility factor. If t of equation (3.47) is replaced by t_R, the residence time of the solute in the column, then $\overline{V}$ is defined as the corrected retention volume (V_R^o) for that solute, and eqn. (3.47) becomes;

$$V_R^o = F_o t_R P_o / \overline{P}_i = F_o t_R j \qquad (1.29)$$

The true or the net retention volume (V_N) is most often the desirable quantity and can be obtained from V_R^o from various forms of eqn. (3.48)

$$V_N = V_R^o - V_m = F_o t_R P_o / \bar{P}_i - V_m = F_o t_R j - V_m \qquad (3.48)$$

For ideal chromatographic systems V_m is the volume of the column occupied by the carrier gas. In realistic chromatographic systems where one may have instrument dead volumes, V_m is to be considered as the sum of the two types of volumes.

Substitution of $\bar{P}_i$ of eqn. (3.48) by $\bar{P}$ eqn. (3.38) gives;

$$V_N = F_o t_R P_o / \bar{P} - V_m = F_o t_R J - V_m \qquad (3.49)$$

J has the form of j and reduces to j where $B_{11} = 0$, but the V_N calculated by eqn. (3.49) is only partially corrected for the carrier gas nonideality and will also be in error. The proper expression for V_N should be obtained by starting with the equation of state of a nonideal gas. To a good approximation it can be expressed as;

$$n = PV/(RT + B_{11}P) \qquad (3.20)$$

Analogous to the ideal gas case the following relationships exist;

$$P_o V_o/(RT + B_{11}P_o) = \bar{P}\bar{V}/(RT + B_{11}\bar{P}) \qquad (3.50)$$

where $\bar{P}$ is given by eqn. (3.38) and;

$$V_N = F_o t_R P_o (1 + b\bar{P})/\bar{P}(1 + bP_o) - V_m$$

$$= F_o t_R J(1 + b\bar{P})/(1 + bP_o) - V_m \qquad (3.51)$$

Equation (3.51) has the desirable feature that when $B_{11} = 0$, the expression reduces to the ideal gas expression (eqn. (3.48)).

As can be seen from eqn. (3.51) the error introduced into V_N value by assuming ideal gas behaviour of the carrier gas will depend on the magnitude of the following;

a) B_{11}/RT

b) P_i/P_o

c) $V_R^o - V_m$

In order to show the magnitude of error that can be introduced into the V_N value by assuming ideal behaviour of the carrier gases, Table (3.5) has been prepared. The contents of Table (3.5) are based on actual experimental results which are still to be presented. It should be pointed out that the contents of Table (3.5) represent a gas-solid chromatography system where V_N (the net retention volume of methane) is itself a function of both the nature of the carrier gas and the mean column pressure, so that a comparison of data within the table may lead to wrong conclusions.

As can be seen from Table (3.5) that the assumption of carrier gas ideality may lead to a more serious error in the calculation of the net retention volumes than has been previously anticipated.

TABLE (3.5) PERCENT ERROR (%E) INTRODUCED IN THE V_N VALUES OF METHANE IF CARRIER GAS IDEALITY IS ASSUMED (T = 273°K)

He		Ar		CO_2	
$\bar{P}$ (atm.)*	(%E)	$\bar{P}$ (atm.)*	(%E)	$\bar{P}$ (atm.)*	(%E)
* Calculated from eqn. (3.38)					
9.303	0.86			9.615	-17.77
8.215	0.75	8.277	-1.17	8.329	-14.55
7.293	0.66	7.426	-1.03	7.316	-12.10
6.518	0.58	6.625	-0.89	6.491	-10.06
5.664	0.49	5.747	-0.75	5.273	- 7.32
4.731	0.39	4.768	-0.58	4.286	- 5.34
3.951	0.31	3.938	-0.45	3.373	- 3.65
3.089	0.21	3.026	-0.31	2.562	- 2.26
2.393	0.14	1.892	-0.16	1.930	- 1.27

In this study eqn. (3.51) will be used to calculate the net retention volume.

Evaluation Of V_m

The V_m value is normally determined from the retention time of a nonsorbing gas. The normal calibrating gases (air or methane) are known to interact with the packing and for this reason could not serve as inert gases in the present study. The use of helium as an inert gas presented a problem. The problem was to choose a suitable carrier gas and a detector so that a very small sample of helium could be detected. A thermal conductivity cell could be of use as a detector but its relative insensitivity would require much larger samples than that which can be delivered by the sampling valve. The sampling valve could not be replaced by another sampling unit since this would alter the system. This problem was overcome by using helium as a carrier gas, the electron capture detector (in the 'helium detector' mode) and hydrogen as the sample. It was not known at that time whether hydrogen was sorbing or not. To determine this the net retention volumes of hydrogen were measured at several column temperatures. If the hydrogen gas is nonsorbing, its corrected retention volume should remain constant with increasing temperature but if it is sorbing, then a decrease in the corrected retention volume

should be observed as the temperature is increased. An experiment was carried out to determine this.

The results of this experiment are tabulated in Table (3.6). The $B_{11}(T)$ values were calculated by the method already described.

It can be seen from Table (3.6) that there is a decrease of the corrected retention volume with increasing temperature. Since;

$$V_R^o = V_m(1 + KW_s/V_m) \qquad (1.31)$$

then an extrapolation of V_R^o to infinitely high temperature where K = 0 should give $V_R^o = V_m$. As can be seen from Fig. (3.31)(a and b) that due to the curvature of the V_R^o against T or V_R^o against 1/T plots such extrapolation is not possible without introducing a large error.

The problem was solved by utilizing eqn. (1.49), that is;

$$\ln V_N = - \Delta H^o/RT + q \qquad (1.49)$$

or

$$\log(V_R^o - V_m) = - C'/T + q' \qquad (3.52)$$

Various values of V_m at 0.5 cc. interval were substituted into eqn. (3.52) and ploted against 1/T. It was noted that if the choice of V_m was too low the resulting plot was

TABLE (3.6) CORRECTED RETENTION VOLUME OF HYDROGEN AT VARIOUS TEMPERATURES.

Temp. (°K)	$1/Tx10^3$	B_{11}/RT	V_R^o (cc.)
351 ± ½	2.849	0.00051	97.9
335 ± ½	2.985	0.00053	98.5
320 ± ½	3.125	0.00056	99.1
306 ± ½	3.268	0.00058	99.8
273	3.663	0.00064	101.9

FIGURE (3.31)

$V_R^{\circ}(H_2)$ AS A FUNCTION OF T.

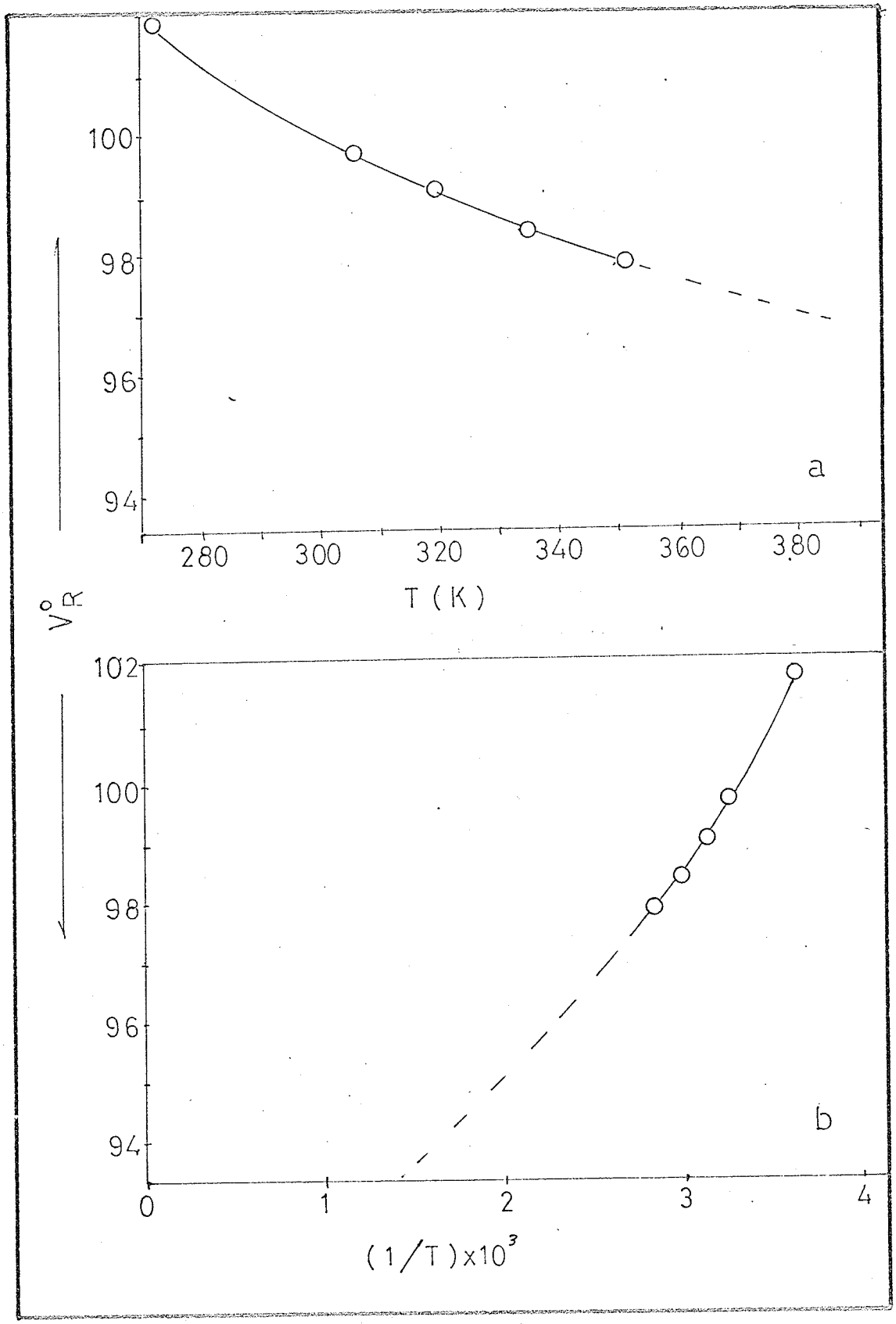
100
98
96
94
280
300
320
340
360
380
T (K)
a
V° (V)
102
100
98
96
94
0
1
2
3
4
(1/T) x 10³
b

concave to the 1/T axis, and when the choice of V_m was too high the plot was convex to the 1/T axis. It was found that a best straight line fit could be obtained if the value of V_m = 89.5 cc. was used. This value of V_m has been accepted and was used in all other calculations.

V_N As A Function Of $\bar{P}$

Equation (1.34) relates the net retention volume to the total surface area of the packing and the partition coefficient, that is;

$$V_N = KS \qquad (1.34)$$

It has already been pointed out that any change in V_N can be attributed to a change in K in S or in both. If there is considerable interaction between the carrier gas and the surface, then S can be expected to decrease with an increasing pressure. The fraction of the surface covered (θ) can be expressed as;

$$\theta = (S_o - S)/S_o \qquad (3.53)$$

where S_o is the value of S when the surface is completely bare. The value $S_o - S$ is then the amount of surface covered. In static systems the coverage is more or less homogeneous over the entire surface. In gas chromatographic columns, due to the pressure gradient, the surface coverage

will decrease from P_i to P_o. In either case, θ, as defined in eqn. (3.53), refers to the mean value of the fraction of the surface area covered (θ).

The amount of gas adsorbed on the surface maybe represented as a function of the gas pressure (169). For a gas chromatographic column this can be expressed as;

$$\theta = g(\bar{P}) \qquad (3.54)$$

where $\bar{P}$ is the mean column pressure. In terms of eqns. (3.53) and (3.54), eqn. (1.34) can be written as;

$$V_N = KS_o(1 - g(\bar{P})) \qquad (3.55)$$

Locke (170) has shown that for a nonideal carrier gas and a nonideal solute, having a Langmuir and a linear adsorption isotherm respectively, the distribution coefficient (K_a) can be expressed as;

$$\ln K_a = \ln(K_a^o/(1 + b\bar{P})) + \bar{P}(2B_{12} - B_{11})/RT \qquad (3.56)$$

where K_a^o is K_a at $\bar{P} = 0$, and b is a constant. The other terms have already been defined. The quantity $1/(1 + b\bar{P})$ is a specific expression of $(1 - g(\bar{P}))$. In terms of the present notation, maintaining the general expression for the gas-solid interaction, eqn. (3.55) can be rewritten in terms of eqn. (3.56) as;

$$V_N = K_o S_o (1 - g(\bar{P}))\exp\{\bar{P}(2B_{12} - B_{11})/RT\} \qquad (3.57)$$

where K_o is K at $\bar{P} = 0$. When $\bar{P} = 0$, then;

$$V_N = K_o S_o = V_N^o \qquad (3.58)$$

where V_N^o is the limiting value of V_N at $\bar{P} = 0$. In view of this eqn. (3.57) can be rewritten as;

$$V_N = V_N^o (1 - g(\bar{P}))\exp\{\bar{P}(2B_{12} - B_{11})/RT\} \qquad (3.59)$$

If the B_{11} and B_{12} values can be obtained, or calculated, then the $\exp\{\bar{P}(2B_{12} - B_{11})/RT\}$ contribution to the variation in V_N can be extracted out of the experimental data, that is;

$$V_N/\exp\{\bar{P}(2B_{12} - B_{11})/RT\} = V_N^o(1 - g(\bar{P})) = V_N^* \qquad (3.60)$$

V_N^* is now a function of the surface coverage only, and can be used to determine the expression for $g(\bar{P})$. Since $\theta = g(\bar{P})$, then;

$$\theta = 1 - V_N^*/V_N^o \qquad (3.61)$$

and the fraction of the surface available (θ_a) is;

$$\theta_a = V_N^*/V_N^o \qquad (3.62)$$

There are a few points which must be first discussed before the experimental data is presented. In the intro-

ductory section it was stated that for a gas-liquid system, the partition coefficient was related to the "mixed" second virial coefficient through eqn. (1.51), that is;

$$\log K = A + \bar{P}(2B_{12} - v_2^o)/2.303RT \qquad (1.51)$$

The A term which was then termed a constant is infact $\log K_o$.

This equation or its equivalent with $\bar{P} = P_o/j$ (see page 19), have been used by several workers (96, 100A, 170) to either calculate the B_{12} term or to make allowances for the carrier gas nonideality in the calculation of other thermodynamic data. Martire and Locke (60) have criticised the use of $\bar{P}$ as defined above in the study of carrier gas nonideality since this form of $\bar{P}$ was deduced for an ideal gas. They have shown that a more correct form of $\bar{P}$ is that of eqn. (3.38) which allows for carrier gas nonideality.

Everett on the other hand questioned the insertion of the mean values of K and P into eqn. (1.51). Starting from the basic principles, he deduced the expression for V_N as a function of pressure having the following form;

$$V_N = K_o V_L (1 + \kappa P_o J_3^4) \qquad (3.63)$$

where

$$\kappa = (2B_{12} - v_2^o)/RT \qquad (3.64)$$

$$V_N = V_R'/J_2^3 \qquad (3.65)$$

$$J_n^m = (n/m)\{[(P_i/P_o)^m - 1]/[(P_i/P_o)^n - 1]\} \qquad (3.66)$$

$$V_R' = t_R' F_o \qquad (3.67)$$

By letting m and n of eqn. (3.66) equal to 3 and 2 respectively, it can be seen that J_2^3 is the reciprocal of the Martin and James compressibility factor j. t_R' has already been defined in eqn. (1.41).

Remembering that V_N and K are directly related, it can be seen that there are two basic differences between eqn. (1.51) and eqn. (3.63). It first may be noted that in the former equation, the K or V_N are exponentially related to the pressure where as in the latter equation, the relationship is direct. This difference stems from the fact that one of the steps in deriving eqn. (3.63) was to perform a linear expansion of $\exp\kappa P$ to the first term. By applying this to eqn. (1.51) a similar result can be obtained. Although expanded, eqn. (1.51) will still differ from eqn. (3.63) in that the former will contain a $P_o J_2^3$ term where as the latter contains a $P_o J_3^4$ term. Everett points out that over a small pressure range the experimental data will not distinguish between the choice of J_3^4 or J_2^3 but the value of κ will be lower some 12% for the former case since the ratio J_3^4/J_2^3 rises from about 1.03 to 1.25 as P_i/P_o goes from 2 to 10. Since κ is related to the B_{12} term, the value of B_{12} obtained from experimental data will obviously depend on

the choice of J_n^m. The lack of available data at that time prevented the above author to test out his equation.

Cruickshank et. al. (100C) starting from basic relationships, were able to derive an exact expression for the retention volume in terms of P_i, P_o, and the various constants pertaining to the gas and the liquid phase. Their equation is exact in the sense that the approximations it contains are much smaller than the observational uncertainty on any experimental values of V_R currently available. With further approximations they were able to show the following relationship for an ideal gas;

$$\ln V_N = \ln V_N^o + \beta P_o J_3^4 + \zeta (P_o J_3^4)^2 \qquad (3.68)$$

and for a real gas;

$$\ln V_N^{'} = \ln V_N^o + \beta P_o J_3^4 + \zeta (P_o J_3^4)^2 \qquad (3.69)$$

where

$$V_N^{'} = V_N(1 + b\bar{P})/(1 + bP_o) \qquad (3.70)$$

$$\bar{P} = P_o/j \qquad (3.71)$$

$$b = B_{11}/RT \qquad (3.22b)$$

$$\beta = \kappa(\text{eqn.}(3.64)) \qquad (3.72)$$

and ζ is a very small constant containing the second and third virial coefficients. These authors, by using the

exact expression for the retention volume and by specifying b and β, were able to obtain for every value of P_i and P_o a value of V_R/V_N^c for a hypothetical column (for a more detailed discussion of this, the reader can refer to the original article (100C)). The experimental data thus obtained served as a means of testing equations (1.51), (3.63), (3.68), and (3.69). The retrieved β values as obtained by the various equations, when compared to the originally assumed β value, served to estimate the correctness of the above equations. For simplicity they let $\zeta = 0$.

For an ideal gas ($b = 0$) their findings were as follows. Equation (3.63) deviated badly in comparison to equations (1.51) and (3.68). Equation (3.68) was slightly superior to eqn. (1.51), but as the authors pointed out, it is doubtful if the difference between these two equations under higher pressure conditions could ever be significant experimentally. The case of eqn. (3.69) is covered by eqn. (3.68) since under ideal gas conditions eqn. (3.69) reduces to eqn. (3.68).

The above findings are of value since they indicate that it is permissible to use the mean value of K and P in eqn. (1.51) without introducing too much error.

In an nonideal gas case the above workers used two different values of B_{11} (20 and -100cm^3/mole). Equation (3.63), as before, gave the worst results. The other three

equations gave good results at $(P_i - P_o) = 1$ atm. and $P_o =$ 1 to 14 atm.. At $(P_i - P_o)$ values 1 to 5 atm. and $P_o = 1$ atm., both eqns. (1.51) and (1.68) failed. Equation (3.69) on the other hand gave results very much more closer to the expected. Again these findings are of significance since the only difference between eqn. (3.68) and eqn. (3.69) is that the former does not correct for the volumetric imperfections of the carrier gas. Since it has already been shown that eqn. (1.51) and eqn.(3.68) show good agreement in the ideal gas case, it is quite probable that if this volumetric correction was applied to eqn. (1.51), the results would have been quite accordant to those expected.

The above discussion was intended to serve a dual purpose. In the first place it accounts for the existence of the various equations in the literature. Secondly, it justifies the use of eqns. (3.59) and (3.60). One point which cannot be overemphasised is that the V_N value as given in eqns. (3.59) and (3.60) is identical to that of eqn. (3.51) and represents a net retention volume which has been corrected for volumetric imperfections of the carrier gas.

The remaining point which must be brought to attention deals with the choice of the B_{12} term. To the best of the author's knowledge, no data on the B_{12} term for mixtures;- $He-CH_4$, $Ar-CH_4$, and CO_2-CH_4 is in existence. From necessity these values must be calculated from the available equations.

The equation chosen for these calculations is in form the same as eqn. (3.36) (166), that is;

$$B_{12}(T)/V^{*}_{12} = 0.461 - 1.158(T^{*}_{12}/T) - 0.503(T^{*}_{12}/T)^{3} \qquad (3.73)$$

where;

$$T^{*}_{12} = (T^{*}_{1} \cdot T^{*}_{2})^{\frac{1}{2}} \qquad (3.74)$$

and

$$(V^{*}_{12})^{1/3} = \{(V^{*}_{1})^{1/3} + (V^{*}_{2})^{1/3}\}/2 \qquad (3.75)$$

The subscripts 1 and 2 refer to the carrier gas and the solute respectively.

By comparing the calculated B_{12} values to those obtained experimentally, Guggenheim (166) was able to show that the above relationship holds very well for many gas mixtures. Desty et. al. (100A) have shown that for mixtures of He, H_2, and Ar with various hydrocarbons, there is some disagreement between the calculated B_{12} values and those obtained from gas-liquid chromatography. Both Sie et. al. (100E) and Desty et. al. (100A) have shown a drastic difference (~50%) between the calculated and experimentally obtained values for systems using CO_2 as a carrier gas. Locke et. al. (102) have shown that a fair agreement between the calculated and the experimental B_{12} values can be ob-

tained for systems using CO_2. On the whole the use of eqn. (3.73) appears to be controversial. Since the $(2B_{12} - B_{11})$ values were anticipated to be small in the present study, any error introduced from eqn. (3.73) will only have a very small effect on the final results.

Results And Discussion

Table (3.7) contains the $V_N^{\ddagger}$ and the $\bar{P}$ values for experiments HeI, ArII, and CO_2I. Included are also the B_{12} values and the $(2B_{12} - B_{11})/2.3RT$ factor for each carrier gas. A plot of $V_N^{\ddagger}(CH_4)$ against $\bar{P}$ for HeI, ArII, and CO_2I is shown in Figures (3.32), (3.33), and (3.34) respectively. The three features of the helium plot are as follows;

a) There is a measurable interaction between the helium gas and column packing.

b) As $\bar{P}$ tends towards zero, the curve begins to approach a limiting value. Extrapolation of this curve to $\bar{P} = 0$, allows for the determination of the $V_N^{\circ}(CH_4)$ value, which in this case it was found to be 214.7 cc..

c) It can be noted that $V_N^{\ddagger}(CH_4)$ first decreases with the increasing $\bar{P}$, reaches a minimum, and then begins to increase. Although the decrease of $V_N^{\ddagger}(CH_4)$ can be explained in terms of increasing θ, the increase of $V_N^{\ddagger}(CH_4)$ cannot be related to θ since this would require that the surface be uncovered as $\bar{P}$ is increased. The author believes that this

TABLE (3.7) THE V_N^{**} AND THE $\bar{P}$ VALUES FOR EXPERIMENTS HeI, ArII, AND CO_2I.

He (a,b)		Ar (c,d)		CO_2 (e,f)	
$\bar{P}$	V_N^{**}	$\bar{P}$	V_N^{**}	$\bar{P}$	V_N^{**}
9.303	208.5			9.615	55.3
8.215	207.6	8.277	152.4	8.330	58.2
7.293	208.4	7.426	155.0	7.316	61.1
6.518	209.7	6.625	159.4	6.491	65.2
5.665	211.4	5.747	164.4	5.273	72.4
4.731	212.2	4.768	169.1	4.286	79.1
3.951	213.1	3.938	175.4	3.373	86.9
3.089	213.5	3.026	182.5	2.562	97.2
2.394	214.1	1.892	192.4	1.930	107.3

a $B_{12} = 18.0$ cc./mole.

b $(2B_{12} - B_{11})/2.3RT = 0.00042$ atm.$^{-1}$.

c $B_{12} = -32.7$ cc./mole.

d $(2B_{12} - B_{11})/2.3RT = -0.00088$ atm.$^{-1}$

e $B_{12} = -87.2$ cc./mole.

f $(2B_{12} - B_{11})/2.3RT = -0.00055$ atm.$^{-1}$

FIGURE (3.32)

$V_N^*(CH_4)$ AS A FUNCTION OF $\bar{P}$ FOR HeI.

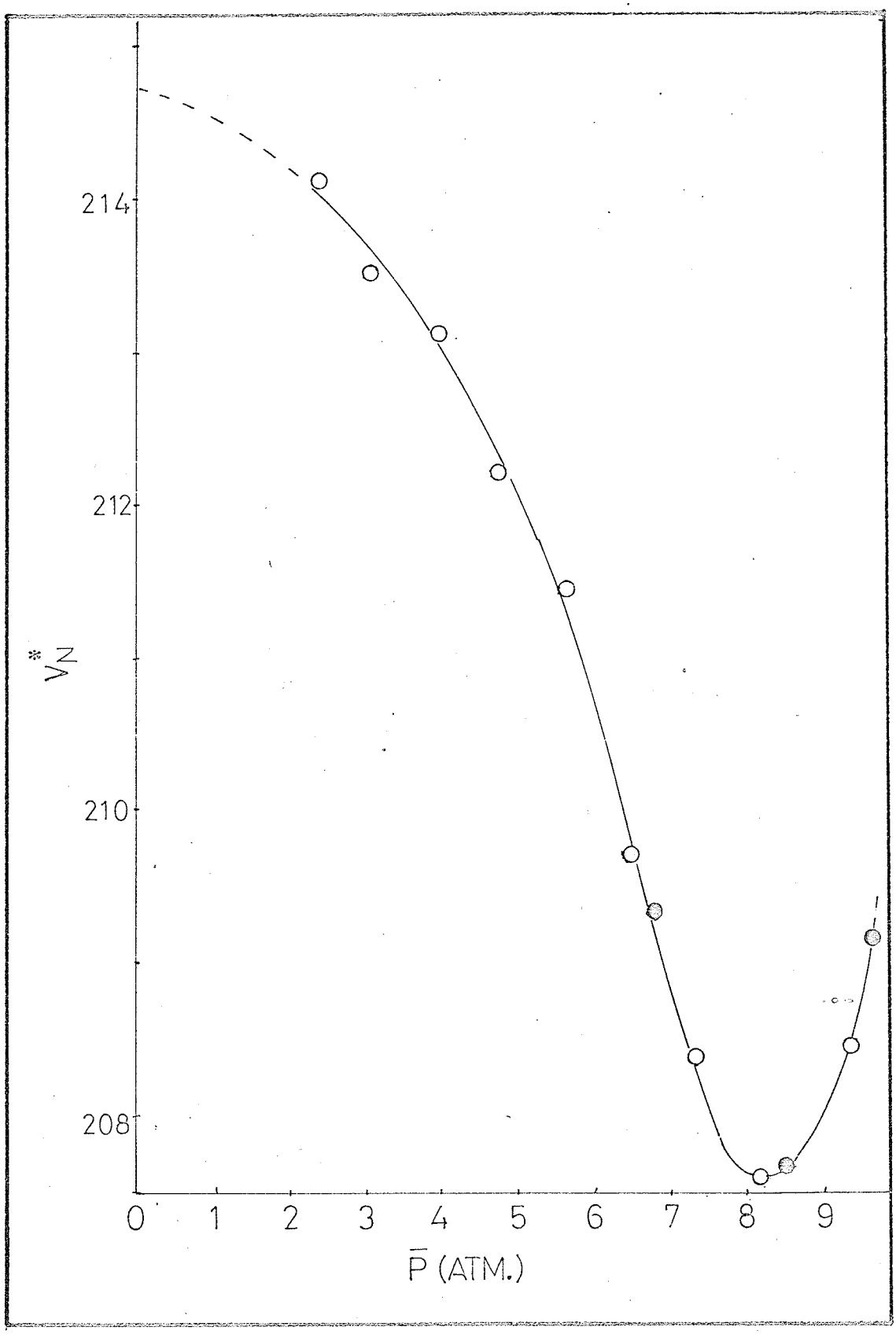
214
212
210
208
V_N^*
0
1
2
3
4
5
6
7
8
9
$\bar{P}$ (ATM.)

FIGURE (3.33)

$V_N^{*}(CH_4)$ AS A FUNCTION OF $\overline{P}$ FOR ArII.

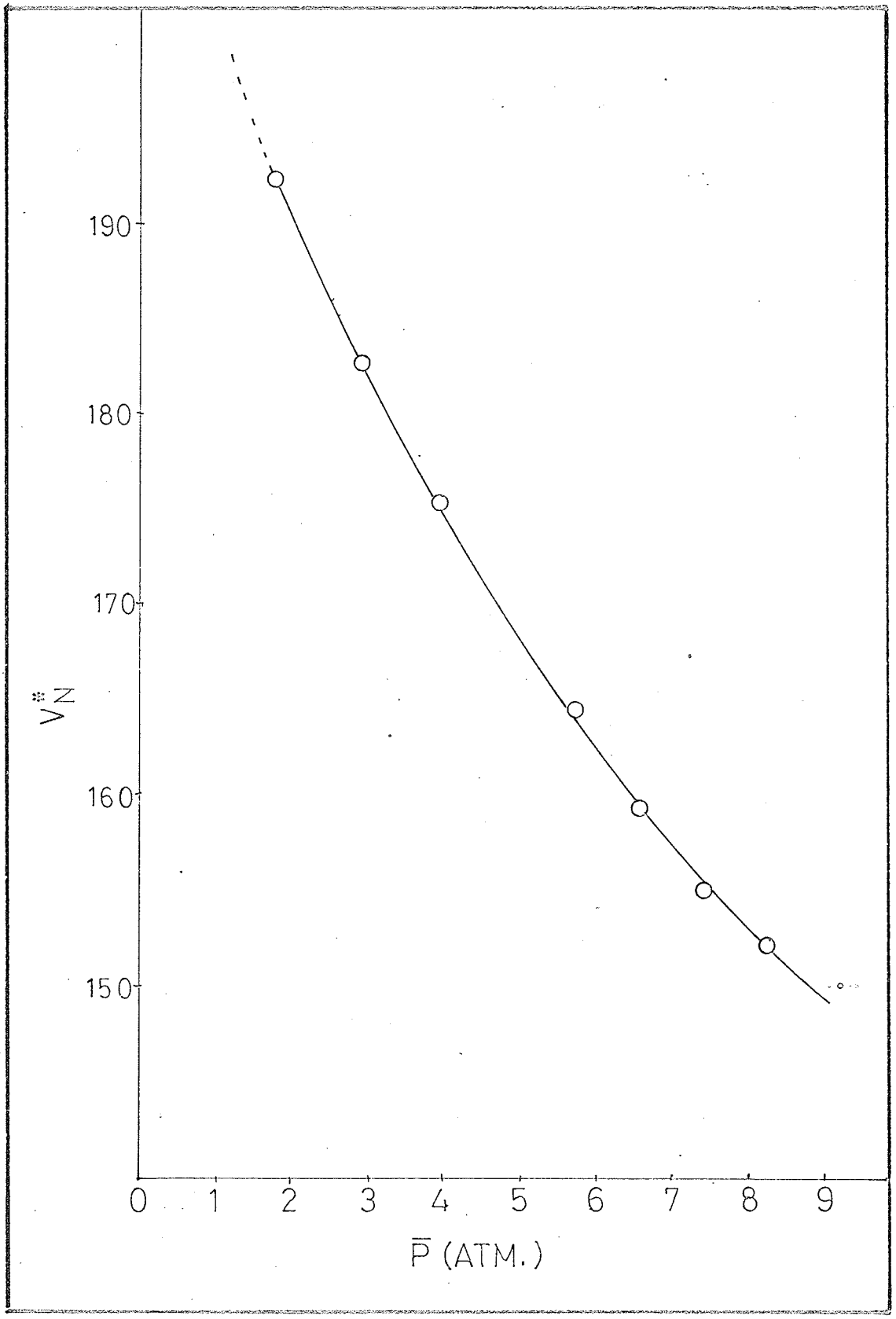
190
180
170
160
150
V_N^{**}
0
1
2
3
4
5
6
7
8
9
$\bar{P}$ (ATM.)

FIGURE (3.34)

$V_N^*(CH_4)$ AS A FUNCTION OF $\bar{P}$ FOR CO_2I.

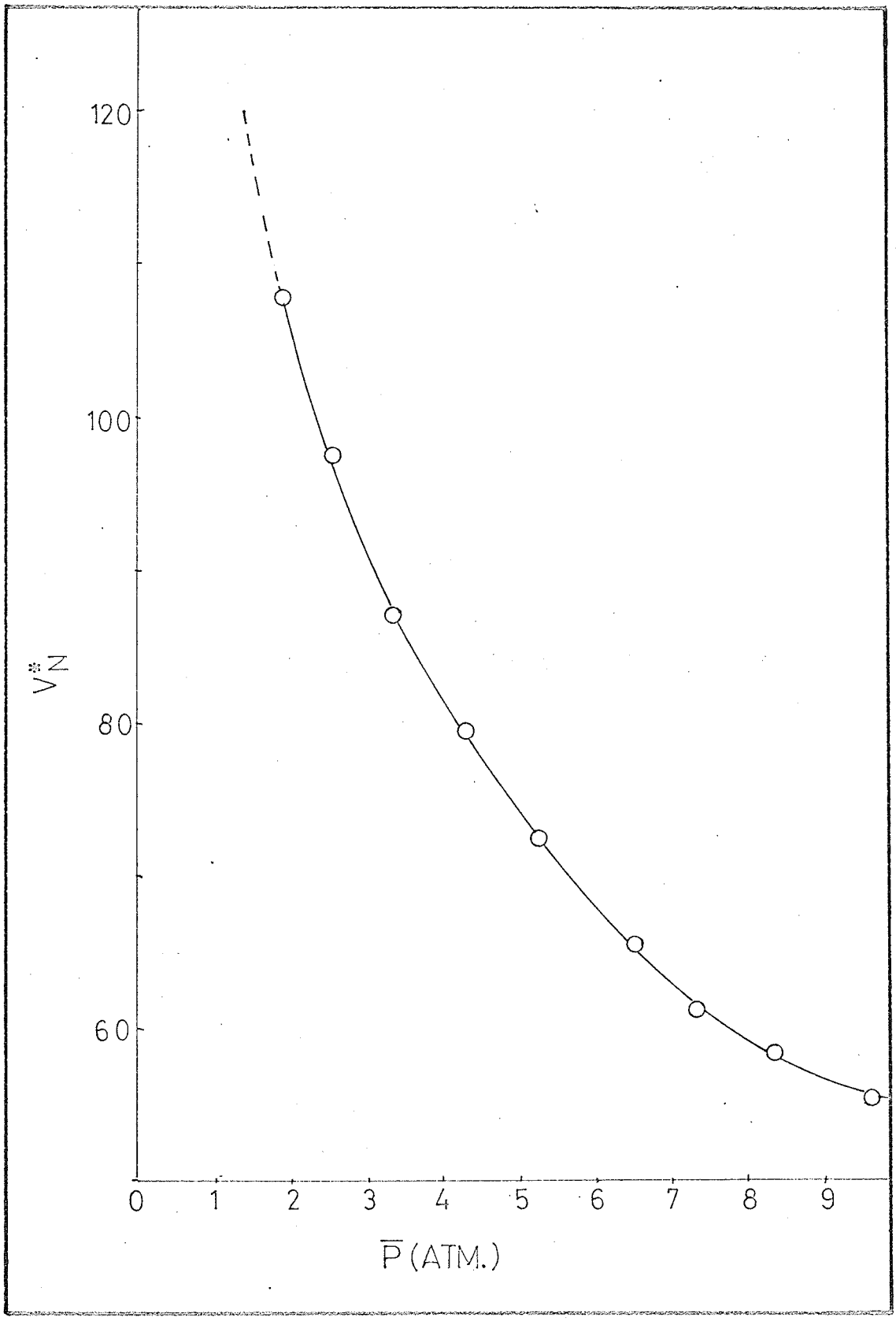
120
100
80
60
V_N^*
0
1
2
3
4
5
6
7
8
9
$\overline{P}$ (ATM.)

effect is related to the undue increase in permeability which was noted in the previous section. Before an attempt is made to account for this effect, few other facts must be considered.

In the previous section it was found that the inter-particle porosity (ε) was very close to 0.4. The total porosity is defined as;

$$\varepsilon_T = V_m/V_T \qquad (3.5)$$

V_m was found to be 89.5 cc. where as V_T was calculated to be 130.5 cc.. The ratio V_m/V_T is then 0.685. Since

$$\varepsilon_T = \varepsilon + \Delta \qquad (3.6)$$

then $\Delta \simeq 0.28$ (the value of ε used was $(0.427 + 0.410)/2$). The finite value of Δ shows that the particles are porous, in fact approximately 40% of the column void can be attributed to the voids within the particles. Since the difference between V_T and V_m is V_S (the total particle volume excluding the void space within the particle) then the total volume of the solid is 41 cc.. From the definition of Δ, it can be shown that the total volume within the particles is approximately 36.5 cc.. This then means that the particle porosity is $36.5/77.5 = 0.47$. Considering the nature of the particles, it is most probable that the voids within the particles are uniformly distributed and inter-

connected. Each particle can then be thought of as containing a very large number of interconnecting channels.

In the previous section it was noted that in the case of helium, there was an undue increase in the column permeability. There are only two alternatives which can cause this;

a) As the column pressure drop is increased, the particles shift apart so as to give a lower interparticle porosity.

b) As the column pressure drop is increased, a secondary flow, parallel to the main flow comes in to existance.

Since an increase in flow rate causes a larger viscous drag on the particles, the resultant force will be in the direction so as to compact the particles and give a smaller interparticle porosity. Considering this, alternative (a) is then unlikely. This then leaves alternative (b) to explain the observed effect. The existence of such a secondary flow is not completely inconceivable since the particle channels can serve to transport the gas.

From the previous results it can be seen that out of the three gases studied, only helium has the desired physical properties so as to undergo this secondary flow. The other two gases, due to their larger interaction with the surface, or molecular diameter, or some other physical property, are restricted to flow in the normal interparticle

channels. This situation may change however, if the $\bar{P}$ range is extended considerably.

Under the conditions of secondary flow, the helium flow rate out of the column may be written as;

$$F_o = F_n + F_s \qquad (3.76)$$

where F_o is the measured flow rate, F_n is the flow rate contribution from the normal interparticle channels, and F_s is the flow rate contribution from the secondary flow mechanism. If the methane sample, like argon and carbon dioxide, is restricted to flow through the interparticle channels, then its velocity in any part of the column will be related to F_n and not to F_o.

For simplicity, the net retention volume can be expressed in terms of the measurable quantities as;

$$V_N = F_o t_R{}^j - V_m \qquad (3.48)$$

In terms of eqn. (3.76), eqn. (3.48) can be rewritten to give;

$$V_N = (F_n + F_s) t_R{}^j - V_m \qquad (3.77)$$

or

$$V_N = V_N' + F_s t_R{}^j \qquad (3.78)$$

where V_N' is the net retention volume in the absence of the

secondary flow. As far as the methane sample is concerned, the secondary flow does not exist and it should be characterised by V_N' only. If the above holds, then in the present study the methane sample was characterised by V_N rather than V_N' since F_o was used in all the calculations.

From eqn. (3.78) it can be seen that if F_s depends on the magnitude of $(P_i - P_o)$ and it should, then the difference between V_N and V_N' can be expected to increase with increasing $(P_i - P_o)$ value, and consequently with increasing $\bar{P}$. This is exactly what is observed in the helium $V_N^*(CH_4)$ against $\bar{P}$ plot (Fig. (3.32)). The rate at which $F_s t_R j$ increases with $\bar{P}$ has not been investigated and no comment can be made on it.

As one goes from Fig. (3.32) to Fig. (3.33) to Fig. (3.34), one can observe the increasing interaction of the carrier gas with the packing. The degree of interaction can be best illustrated by a θ v.s. $\bar{P}$ plot. Fig. (3.35) shows this plot for HeI. This plot for ArII and CO_2I can be seen in Fig. (3.36). It may be mentioned again that in the helium plot of θ v.s. $\bar{P}$, the results at the highest $\bar{P}$ values are meaningless if they are taken at their face value. The only way to give continuity to the trend is to reduce the appropriate $V_N^*(CH_4)$ (thus F_o) values.

Figure (3.36) shows that in the case of argon almost 30% of the surface is covered at $\bar{P} \simeq 8.5$ atm.. The inter-

FIGURE (3.35)

θ AS A FUNCTION OF $\bar{P}$ FOR HeI.

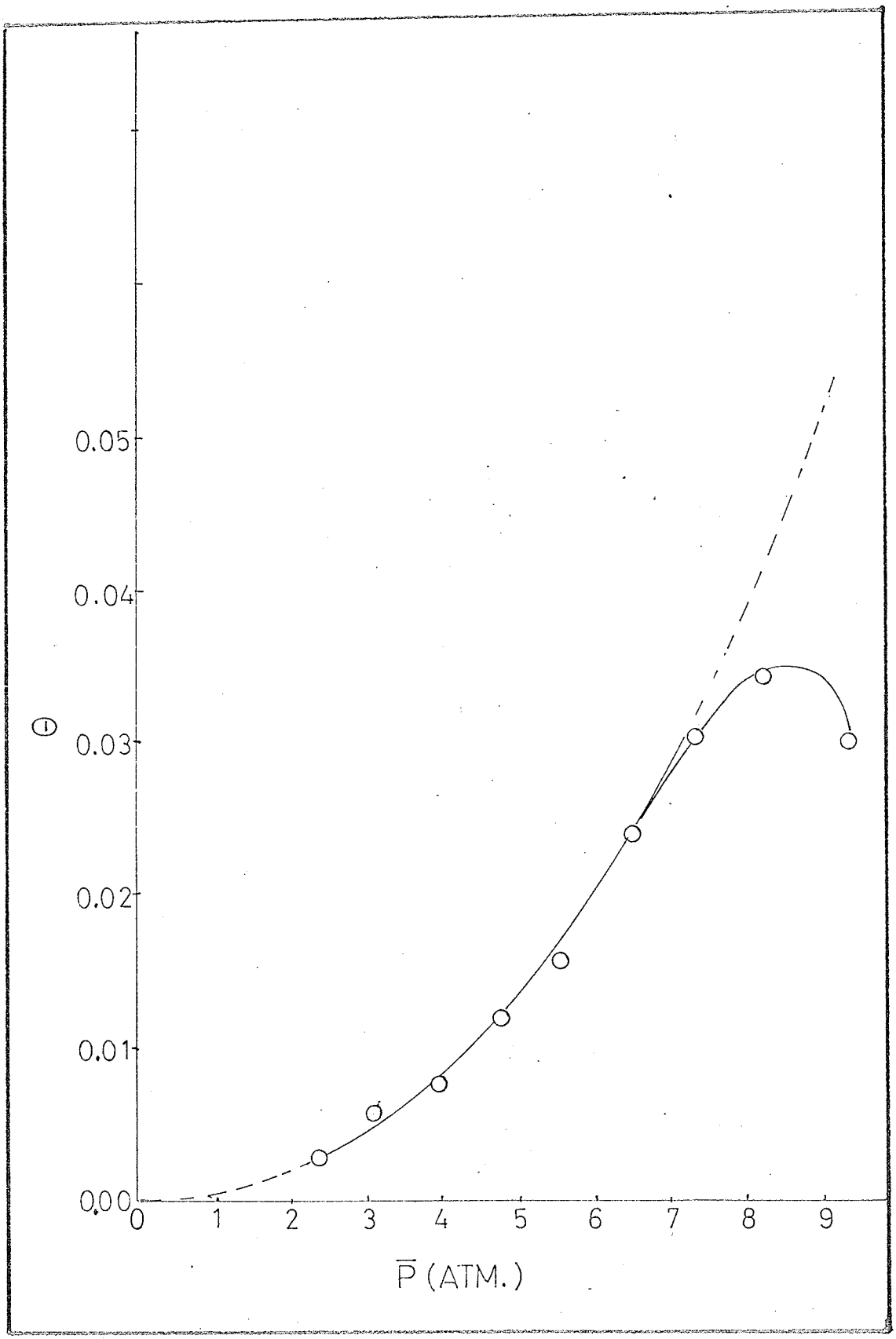
0.05
0.04
0.03
0.02
0.01
0.00
I
0
1
2
3
4
5
6
7
8
9
P̄ (ATM.)

FIGURE (3.36)

Θ AS A FUNCTION OF $\bar{P}$ FOR ArII AND CO_2I.

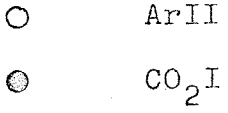

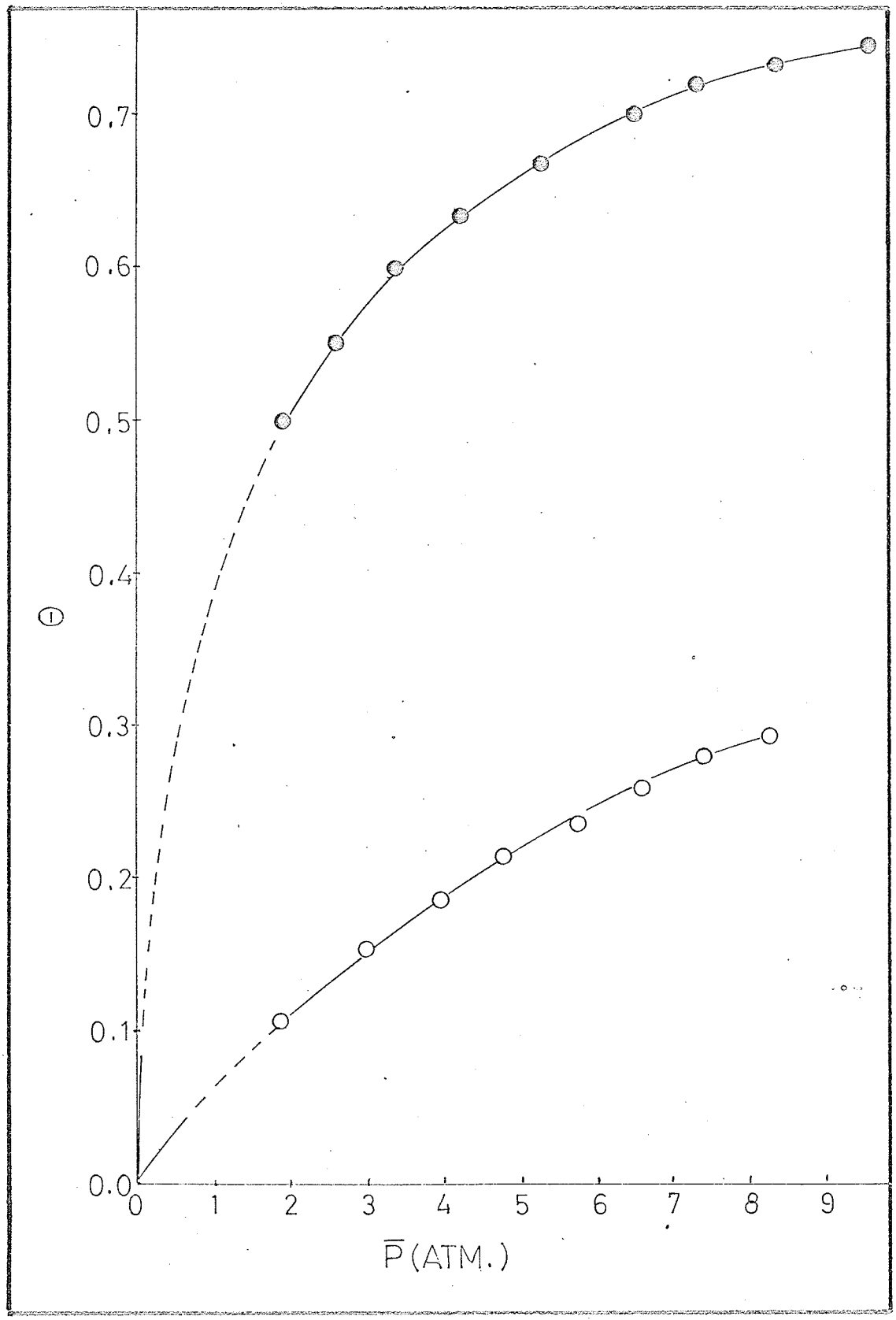
0.7
0.6
0.5
0.4
0.3
0.2
0.1
0.0
0
1
2
3
4
5
6
7
8
9
P̄ (ATM.)

action between carbon dioxide and the surface is more severe since at $\bar{P} \simeq 8.5$ atm. almost 75% of the surface is covered. This of course is expected since carbon dioxide when treated as a sample, has a much longer retention time than argon. It should be noticed that unlike the argon and the carbon dioxide case, the plot of θ v.s. $\bar{P}$ for helium is concave to the pressure axis.

Aside for the slightly noticeable break in the curve, the other Ar and CO_2 experiments gave the same results.

The experimental data was tested out in terms of the following equations;

The Langmuir Equation (171, 172, 173)

$$\theta = K'\bar{P}/(1 + K'\bar{P}) \qquad (3.79)$$

The Freundlich Equation (174, 175)

$$\theta = K''\bar{P}^{n} \qquad (3.80)$$

The Hill-de Boer Equation (174, 176)

$$\bar{P} = K'''\{\theta/(1 - \theta)\}\exp\{\theta/(1 - \theta) - \hat{a}\theta/\hat{b}RT\} \qquad (3.81)$$

where K', K'', and K''' are constants, and $\hat{a}$ and $\hat{b}$ are the van der Walls constants. It was found that all three gases did not obey any of the above equations. A straight line relationship may be obtained if $\log\{\theta/(1 - \theta)\}$ is plotted against $\log\bar{P}$. This can be seen in Figures (3.37), (3.38),

FIGURE (3.37)

PLOT OF $\log(\theta/(1-\theta))$ AGAINST $\log\bar{P}$ FOR HeI.

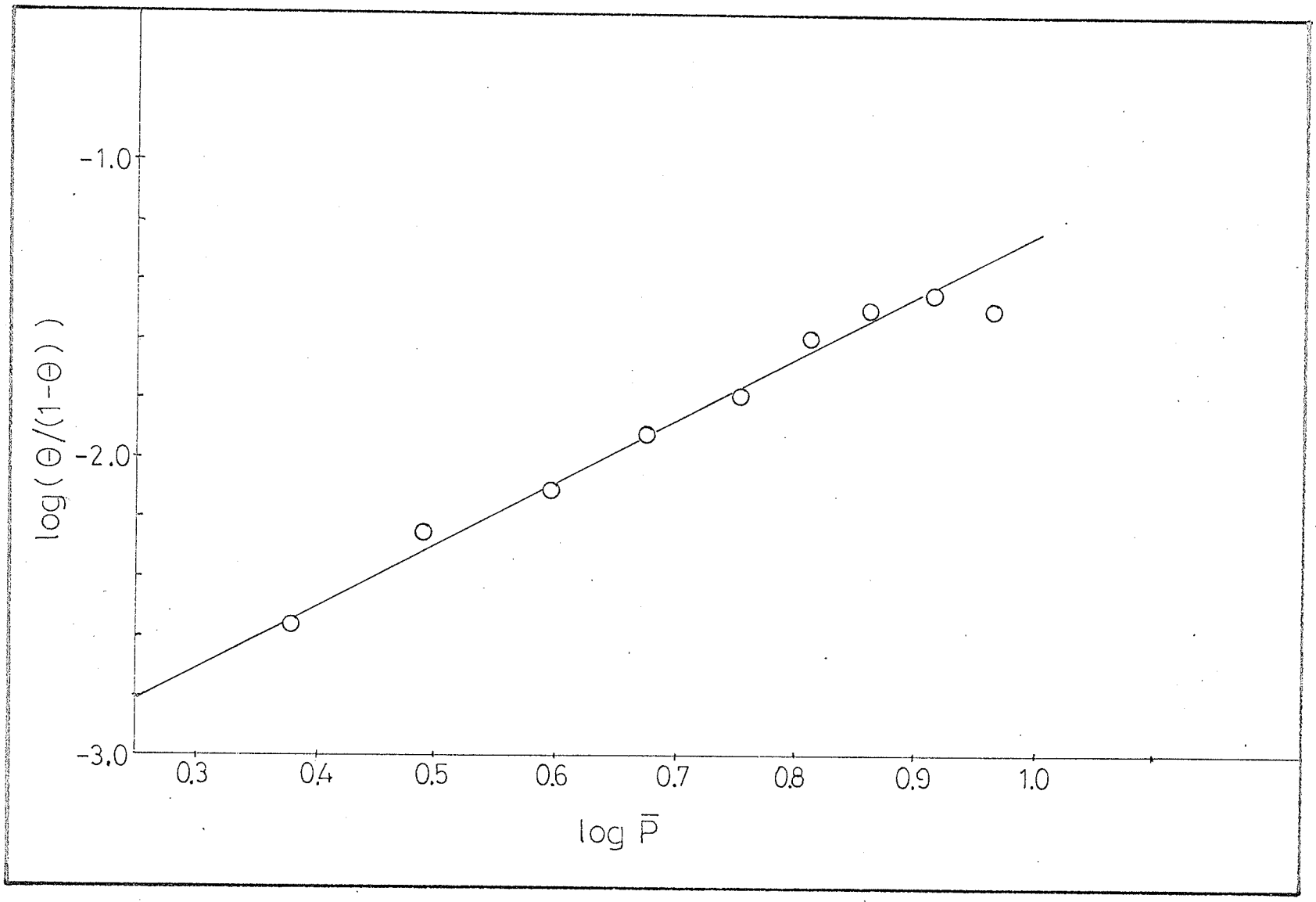
-1.0
-2.0
-3.0
log (Θ/(1-Θ))
0.3
0.4
0.5
0.6
0.7
0.8
0.9
1.0
log P̄

FIGURE (3.38)

PLOT OF $\log(\theta/(1-\theta))$ AGAINST $\log\bar{P}$ FOR ArII.

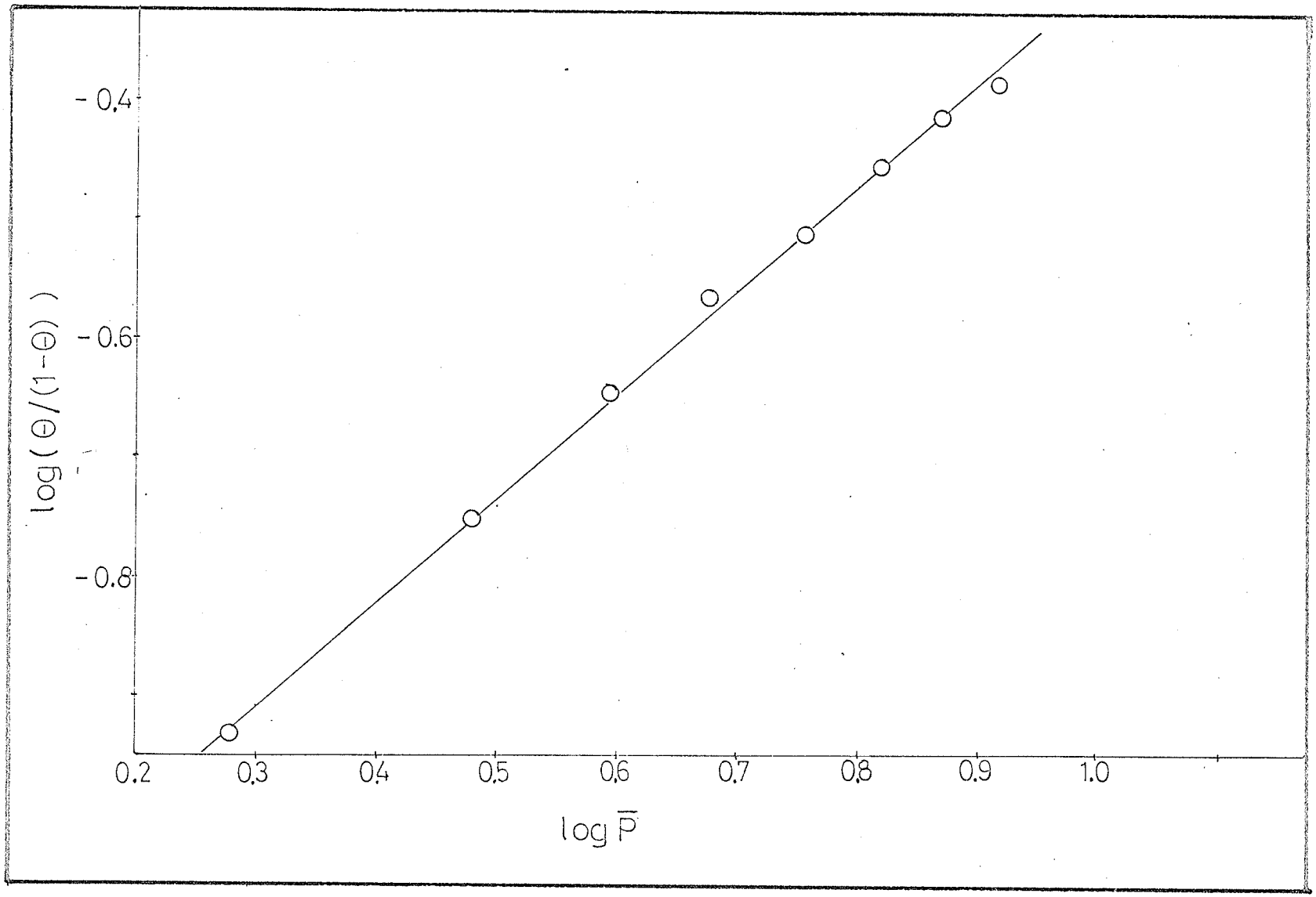
- 0.4
- 0.6
- 0.8
log (Θ/(1-Θ))
0.2
0.3
0.4
0.5
0.6
0.7
0.8
0.9
1.0
log P̄

FIGURE (3.39)

PLOT OF $\log(\theta/(1-\theta))$ AGAINST $\log\bar{P}$ FOR CO_2I.

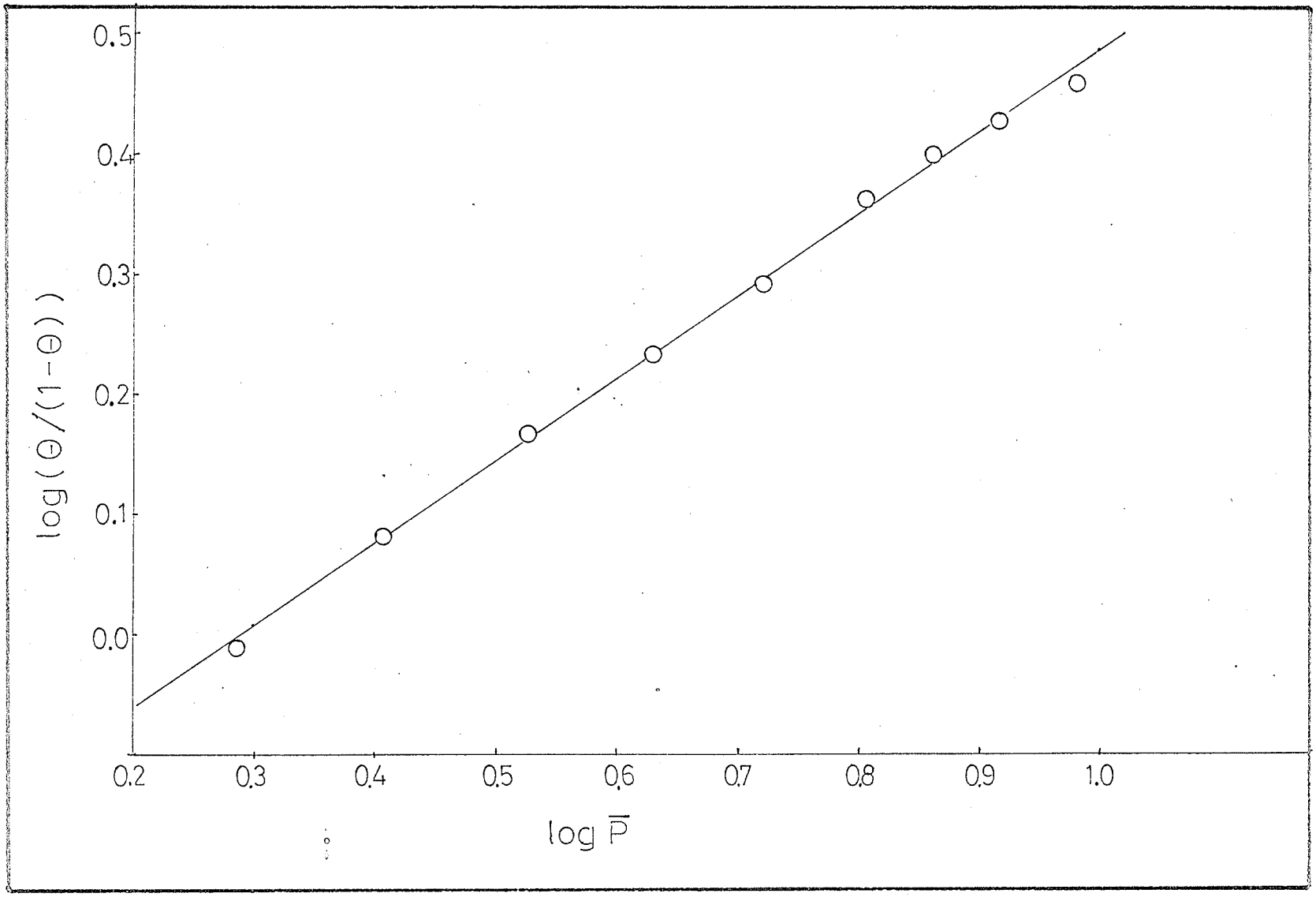
0.5
0.4
0.3
0.2
0.1
0.0
log (θ/(1-θ))
0.2
0.3
0.4
0.5
0.6
0.7
0.8
0.9
1.0
log P̄

and (3.39) for HeI, ArII, and CO_2I respectively. This relationship when written in a general form is;

$$\log\{\theta/(1 - \theta)\} = \log K + n\log\bar{P} \qquad (3.82)$$

where K and n are constants. After taking the antilog of both sides and rearranging, eqn. (3.82) becomes;

$$\theta = K\bar{P}^n/(1 + K\bar{P}^n) = g(\bar{P}) \qquad (3.83)$$

The above adsorption isotherm is neither Langmuir nor Freundlich, but is a combination of both. It has the interesting property of reducing to the Freundlich adsorption isotherm at low pressures, that is, when $K\bar{P}^n \ll 1$, then

$$\theta \simeq K\bar{P}^n \qquad (3.84)$$

and yet exhibits the characteristic Langmuir plateau at high pressures, that is, when $K\bar{P}^n \gg 1$, then

$$\theta \simeq 1 \qquad (3.85)$$

Bradley (177) has shown that a relationship of the form as that of eqn. (3.83), well describes the adsorption of carbon monoxide, argon, nitrogen, water, acetone in water, bromine in water, isoamyl alcohol in water, and benzoic acid in benzene on a number of charcoals. Sips (178) has pointed out that an equation such as (3.83) is more logical than the Freundlich equation since the former has a limiting

value of $\theta = 1$ at high pressures. In his mathematical treatment he states that n must be between -1 and +1, but for physical cases n must be greater than zero. In the limit when $n = 1$, he describes the system as follows. "This means that all the active centers have now the same adsorption energy and this gives us, as it should, the well-known Langmuir adsorption isotherm." He also points out that if n is very small the distribution curve is very flat (large spread in the adsorption energies), and the limiting case is a uniform distribution of active centers. In the case when upon adsorption, a diatomic molecule (X_2) dissociates into two equal fragments, Sips has shown that n can have a value between 0 and $\frac{1}{2}$. When $n = \frac{1}{2}$, all the sites have the same adsorption energy, and when $n << \frac{1}{2}$, the previous interpretation can be given to the system.

According to this approach, n can be expected to be less than 1 under the following conditions;

a) site energy distribution

b) dissociation upon adsorption

c) both a and b

Koble and Corrigan (179) applied eqn. (3.83) to the available adsorption data (180) of methane, ethane, propane, ethylene, and propylene on activated charcoal. The n values they obtained from these systems and their closest fractions (n') are given in Table (3.8). Considering the fractions

TABLE (3.8) THE n AND THE n' VALUES AS GIVEN BY KOBLE AND CORRIGAN (179).

Gas	n	n'
Methane	1.0	1
Ethane	0.678	2/3
Propane	0.540	1/2
Ethylene	0.632	2/3
Propylene	0.569	1/2

which best represent n, they interpreted these results in the following way.

a) Methane ($n' = 1$)

Since $n' = 1$, methane obeys Langmuir's adsorption isotherm and its adsorption may be expressed as;

$$A + \ell = A\ell \qquad (3.86)$$

where A and ℓ are respectively the gas molecule and the active center. In other words only one site is occupied by one methane molecule.

b) Propane and Propylene ($n' = \frac{1}{2}$)

Propane and propylene is interpreted by the authors to be dissociating according to the following equation;

$$A + 2\ell = R\ell + S\ell \qquad (3.87)$$

where $R\ell$ and $S\ell$ represent two different fragments adsorbed.

c) Ethane and Ethylene ($n' = 2/3$)

The equation best describing the adsorption of these two gases is given as;

$$2A + 3\ell = 3A_{2/3}\ell \qquad (3.88)$$

"This follows logically in considering that methane, the smallest molecule, occupies one site; ethane and ethylene, the next larger, occupy the equivalent of 1.5 sites per molecule, while propane and propylene occupy two sites per

molecule." (179) They pointed out that this scheme breaks down upon reaching n-butane, which once again corresponds to a single site per molecule. The deviation between the experimentally obtained n values and the nearest fraction, n', is attributed to the heterogeneity of the surface as described by Sips (178). In all cases it was found that n is equal to or is smaller than 1 and that it does not depend on the temperature.

From vacuum desorption studies, Wiig and Smith (181) have shown that the adsorption isotherm of ethyl chloride on activated carbon is described by eqn. (3.83), having an n value of less than 1.

By the least squares method the present experimental data was fitted to the following equations;

Helium

$$\log\{\theta/(1-\theta)\} = -3.345 + 2.09\log\bar{P} \qquad (3.89)$$

Argon

$$\log\{\theta/(1-\theta)\} = -1.173 + 0.873\log\bar{P} \qquad (3.90)$$

Carbon dioxide

$$\log\{\theta/(1-\theta)\} = -0.197 + 0.684\log\bar{P} \qquad (3.91)$$

The intercept for He, Ar, and CO_2 were found to correspond to 4.52×10^{-4}, 6.72×10^{-2}, and 6.36×10^{-1} respectively.

The three slopes of course, correspond to the n values. It is particulary interesting to note that in the case of helium this value is close to 2.1. According to Sips, the limiting value should be 1. In terms of adsorption mechanism, this would require for two helium atoms to occupy the same site. This interpretation is difficult to accept since, as can be seen from Fig. (3.35), the surface is essentially bare even at the highest $\bar{P}$ values. The uncertainty in n due to the experimental scatter is certainly not responsible for the difference between the logical value of $n = 1$ and that experimentally obtained. In order that n be unity, the basic V_N^* against $\bar{P}$ plot must change considerably so as to take on the general shape as that obtained for argon and carbon dioxide. Since the shape of the helium V_N^* against $\bar{P}$ plot has been found to be reproducible, the n value cannot be unity or less. The value of $n \simeq 2$ must be accepted but no meaning can be given to it at the present time.

If Sips' proposal is accepted, then the fractional value of n in the case of argon must be attributed to the surface heterogeneity. Unlike argon, the dissociation of a carbon dioxide molecule is conceivable and therefore, the fractional value of n can be attributed to stem from both dissociation and surface heterogeneity. If however, one considers the fact that a carbon dioxide sample elutes as a

single relatively narrow peak, one must dismiss the possibility of dissociation.

If one considers a sample containing two similar components (2) and (3), each of which is characterised by its net retention volume $V_N(2)$ and $V_N(3)$, then the ratio of their net retention volumes will be:

$$\frac{V_N(3)}{V_N(2)} = \frac{K_o(3)S_o\{1 - g(\bar{P})\}\exp\{\bar{P}(2B_{13} - B_{11})/RT\}}{K_o(2)S_o\{1 - g(\bar{P})\}\exp\{\bar{P}(2B_{12} - B_{11})/RT\}} \qquad (3.92)$$

Since $S_o(1 - g(\bar{P}))$ will be identical for both components, eqn. (3.92) can be reduced to;

$$V_N(3)/V_N(2) = \{K_o(3)/K_o(2)\}\exp\{2\bar{P}(B_{13} - B_{12})/RT\} \qquad (3.93)$$

It can then be expected that the ratio $V_N(3)/V_N(2)$ can increase, remain constant, or decrease with $\bar{P}$ depending whether $(B_{13} - B_{12})$ is positive, zero, or negative. A plot of $\log(V_N(3)/V_N(2))$ as a function of $\bar{P}$ should give a straight line whose slope can be used to calculate $(B_{13} - B_{12})$.

Table (3.9) contains the values of $V_N(CH_4)/V_N(CD_4)$ and $\bar{P}$ for HeII, ArIV, and CO_2IV. It can be seen that the ratio $V_N(CH_4)/V_N(CD_4)$ remains relatively constant in the helium case but decreases in the case of argon and carbon

TABLE (3.9) VALUES OF $V_N(CH_4)/V_N(CD_4)$ AND $\bar{P}$ FOR EXPERIMENTS HeII, ArIV, AND CO_2IV.

He		Ar		CO_2	
$\bar{P}$*	$\frac{V_N(CH_4)}{V_N(CD_4)}$	$\bar{P}$*	$\frac{V_N(CH_4)}{V_N(CD_4)}$	$\bar{P}$*	$\frac{V_N(CH_4)}{V_N(CD_4)}$
9.599	1.0512	9.336	1.0438	5.572	1.0326
8.404	1.0520	7.394	1.0445	4.703	1.0334
7.021	1.0517	5.695	1.0452	3.761	1.0348
5.484	1.0513	4.428	1.0461	2.958	1.0366
2.762	1.0516	2.691	1.0473	2.146	1.0393
		1.981	1.0484		

* Pressure in atmospheres.

dioxide with increasing $\bar{P}$. A plot of $V_N(CH_4)/V_N(CD_4)$ as a function of $\bar{P}$ is shown in Fig. (3.40) for all three gases. The helium plot although least interesting, is of considerable importance since it allows for the extrapolation to the $\bar{P} = 0$ region. As eqn. (3.93) indicates, $V_N(CH_4)/V_N(CD_4) \rightarrow K_o(CH_4)/K_o(CD_4)$ as $\bar{P} \rightarrow 0$. The ratio of $K_o(CH_4)/K_o(CD_4)$ obtained in this way is 1.0515. Since this ratio is independent of the carrier gas, it must be the same for all three gases, that is to say that all three curves must have the same origin.

It was found that a $\log(V_N(CH_4)/V_N(CD_4))$ against $\bar{P}$ plot was not linear for neither ArIV, nor CO_2IV. By trial and error it was found that the relationship between $V_N(CH_4)/V_N(CD_4)$ and $\bar{P}$ was as follows;

ArIV

$$\log(V_N(CH_4)/V_N(CD_4)) = 0.02134 - 0.00284\log\bar{P} \quad (3.94)$$

CO_2IV

$$V_N(CH_4)/V_N(CD_4) = 1.0285 + 0.0234/\bar{P} \quad (3.95)$$

The various constants were obtained from curve fitting by a method of least squares. The plots of $\log(V_N(CH_4)/V_N(CD_4))$ against $\log\bar{P}$ for ArIV and of $V_N(CH_4)/V_N(CD_4)$ against $1/\bar{P}$ for CO_2IV are shown in Figures (3.41) and (3.42) respectively. It is still not clear why the above relationships

FIGURE (3.40)

$V_N(CH_4)/V_N(CD_4)$ AS A FUNCTION OF $\bar{P}$

FOR HeII, ArIV, AND CO_2IV.

○ HeII

◑ ArIV

◐ CO_2IV

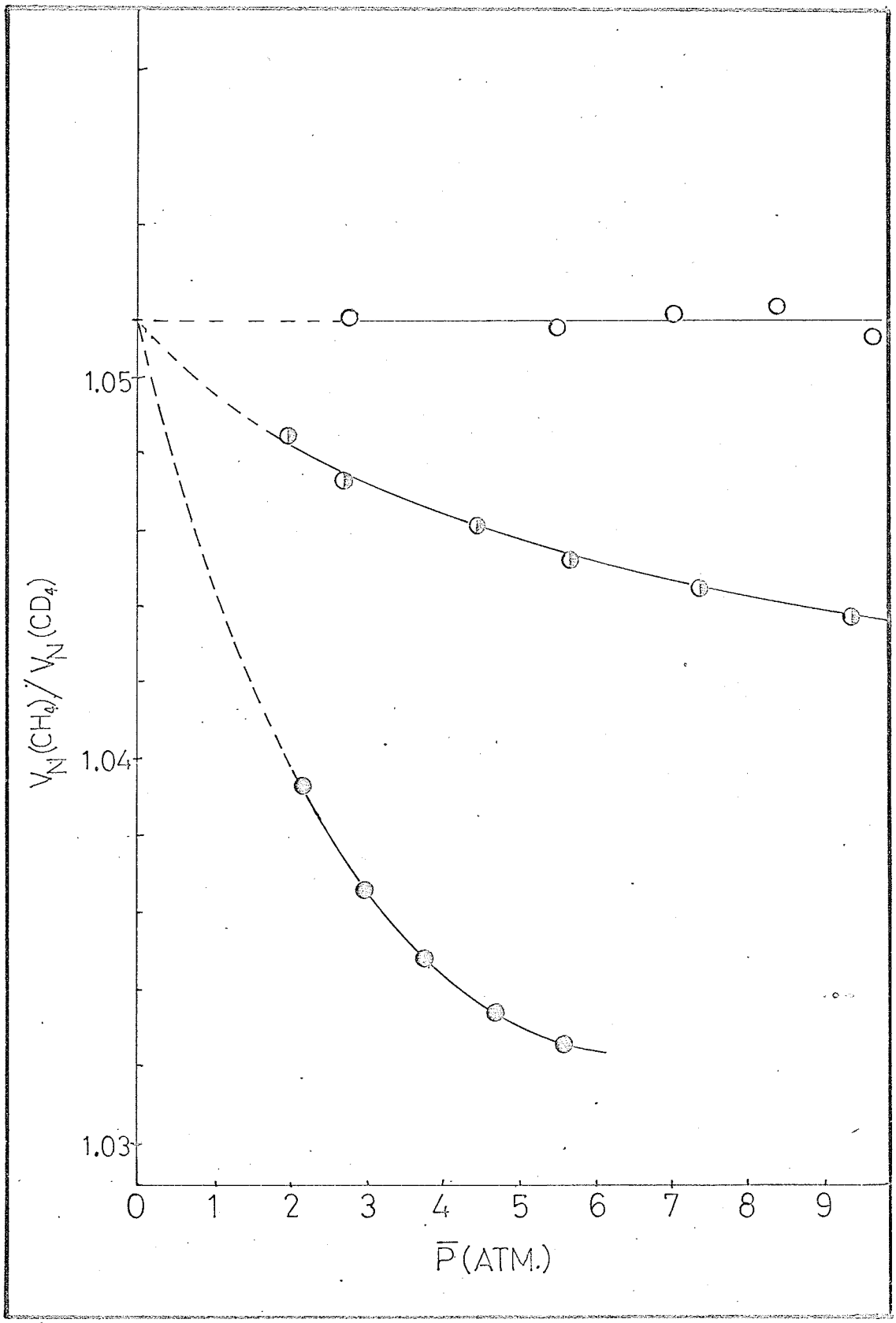
1.05
1.04
1.03
$V_{N_1}(CH_4)/V_{N_1}(CD_4)$
0
1
2
3
4
5
6
7
8
9
$\bar{P}$ (ATM.)

FIGURE (3.41)

PLOT OF $\log(V_N(CH_4)/V_N(CD_4))$ AGAINST $\log\bar{P}$ FOR ArIV.

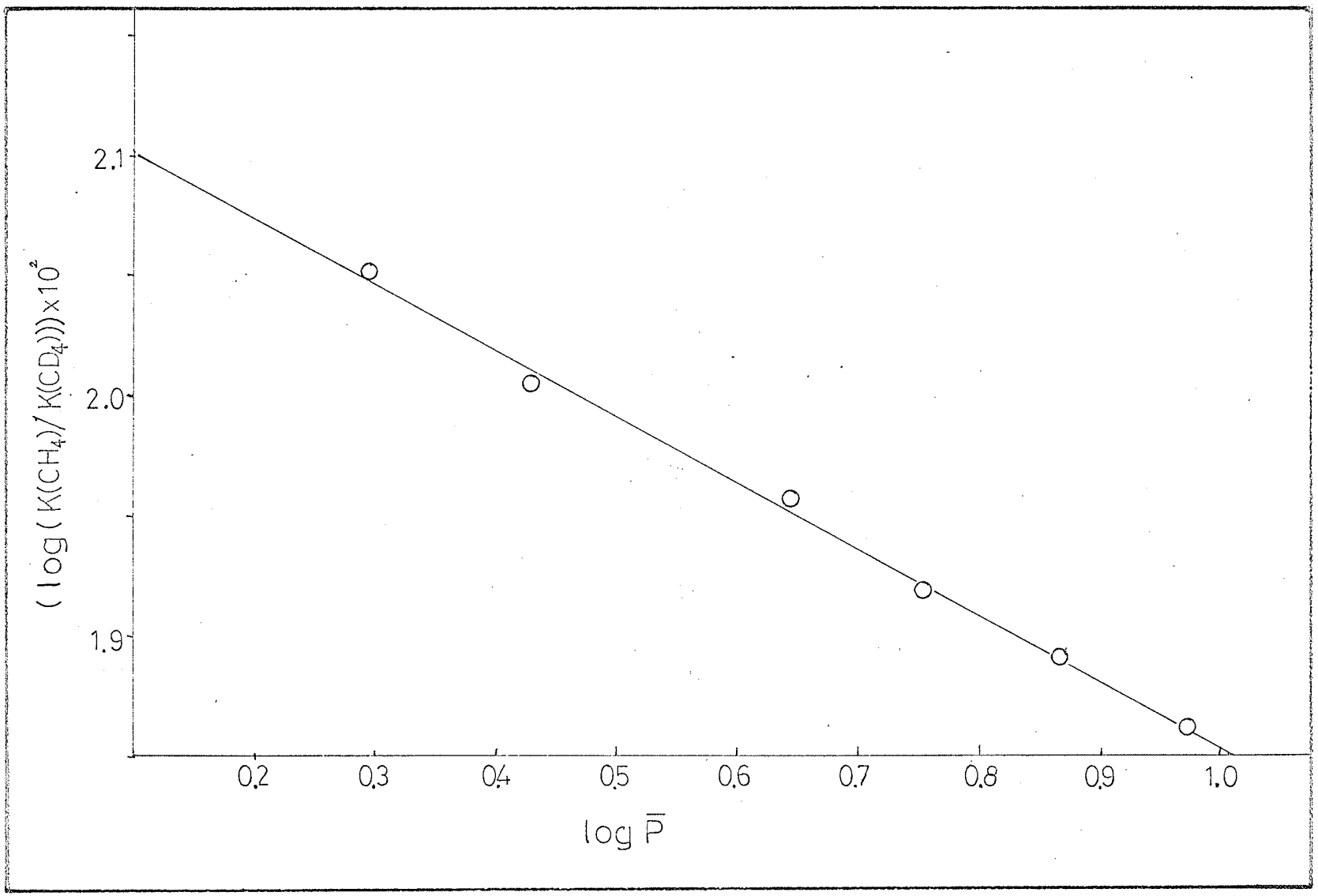
(log (K(CH4)/ K(CD4))) x 10²
2.1
2.0
1.9
0.2
0.3
0.4
0.5
0.6
0.7
0.8
0.9
1.0
log P̄

FIGURE (3.42)

PLOT OF $V_N(CH_4)/V_N(CD_4)$ AGAINST $1/\bar{P}$ FOR CO_2IV.

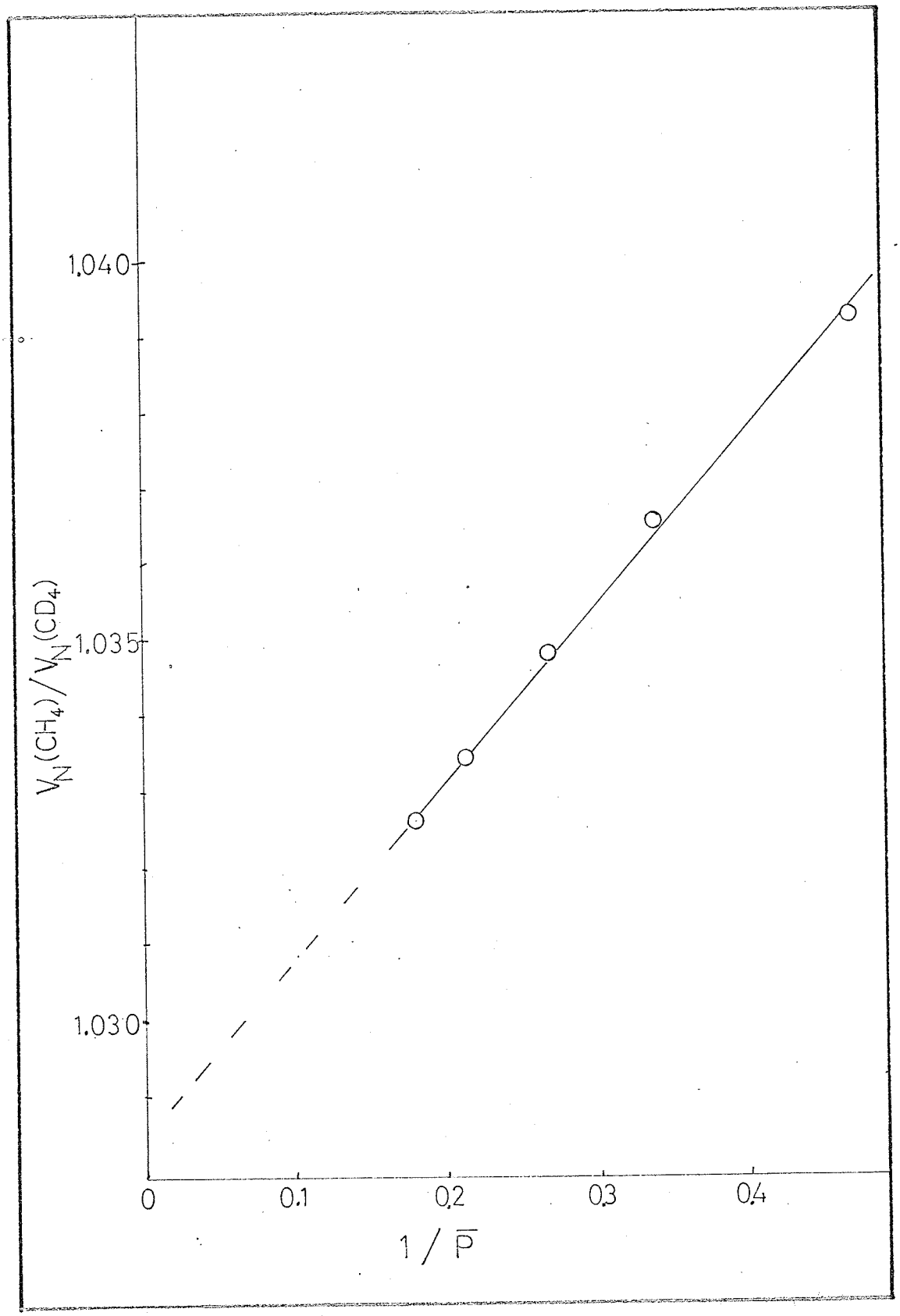
1.040
1.035
1.030
$V_N(CH_4)/V_N(CD_4)$
0
0.1
0.2
0.3
0.4
$1/\overline{P}$

exist and why they are different for the two gases.

V_N As A Function Of T

A sample (~0.45 µl.) containing approximately equal portions of H_2, N_2, O_2, Ar, CH_4, and CO_2 was subjected to a gas chromatographic process at various column temperatures. Part of the results obtained from this experiment have already been presented under the heading of 'Evaluation of V_m'. As it has already been stated;- helium was used as the carrier gas and an electron capture unit was used as a 'helium detector'.

The net retention volumes of N_2, O_2, Ar, CH_4, and CO_2 at various temperatures are presented in Table (3.10). A plot of $\log V_N$ against 1/T for N_2, O_2, and Ar is shown in Fig. (3.43). There are two points of interest associated with Fig. (3.43). One of them is the crossing of the Ar and O_2 plots at approximately $1/T = 3.2 \times 10^{-3}$ (~316°K). This indicates that it is impossible to separate Ar and O_2 at this temperature since they both have the same retention time. The other point of interest is the unusually large deviation in the N_2 plot at 273°K.

A plot of $\log V_N$ against 1/T for CH_4 and CO_2 is shown in Figures (3.44) and (3.45) respectively. The large deviation at 273°K is unmistakable in both of the figures.

The slopes and the intercepts for the linear portion

TABLE (3.10) NET RETENTION VOLUMES OF VARIOUS GASES AT DIFFERENT TEMPERATURES.

Gas	T = 351°K*	T = 335°K*	T = 320°K*	T = 306°K*	T = 273°K
H_2	8.4	9.0	9.6	10.3	12.4
N_2	19.2	22.1	25.6	29.6	46.2
Ar	24.8	28.9	33.5	39.9	62.3
O_2	26.0	30.0	34.4	38.9	56.6
CH_4	53.3	65.5	81.4	103.1	210.1
CO_2	139.9	193.0	273.8	400.1	1258.2

$V_N(CO_2)/V_N(CH_4) = 5.99$

* $\pm$ ½°

FIGURE (3.43)

PLOT OF $\log V_N$ AGAINST 1/T FOR N_2, Ar, AND O_2.

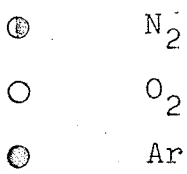

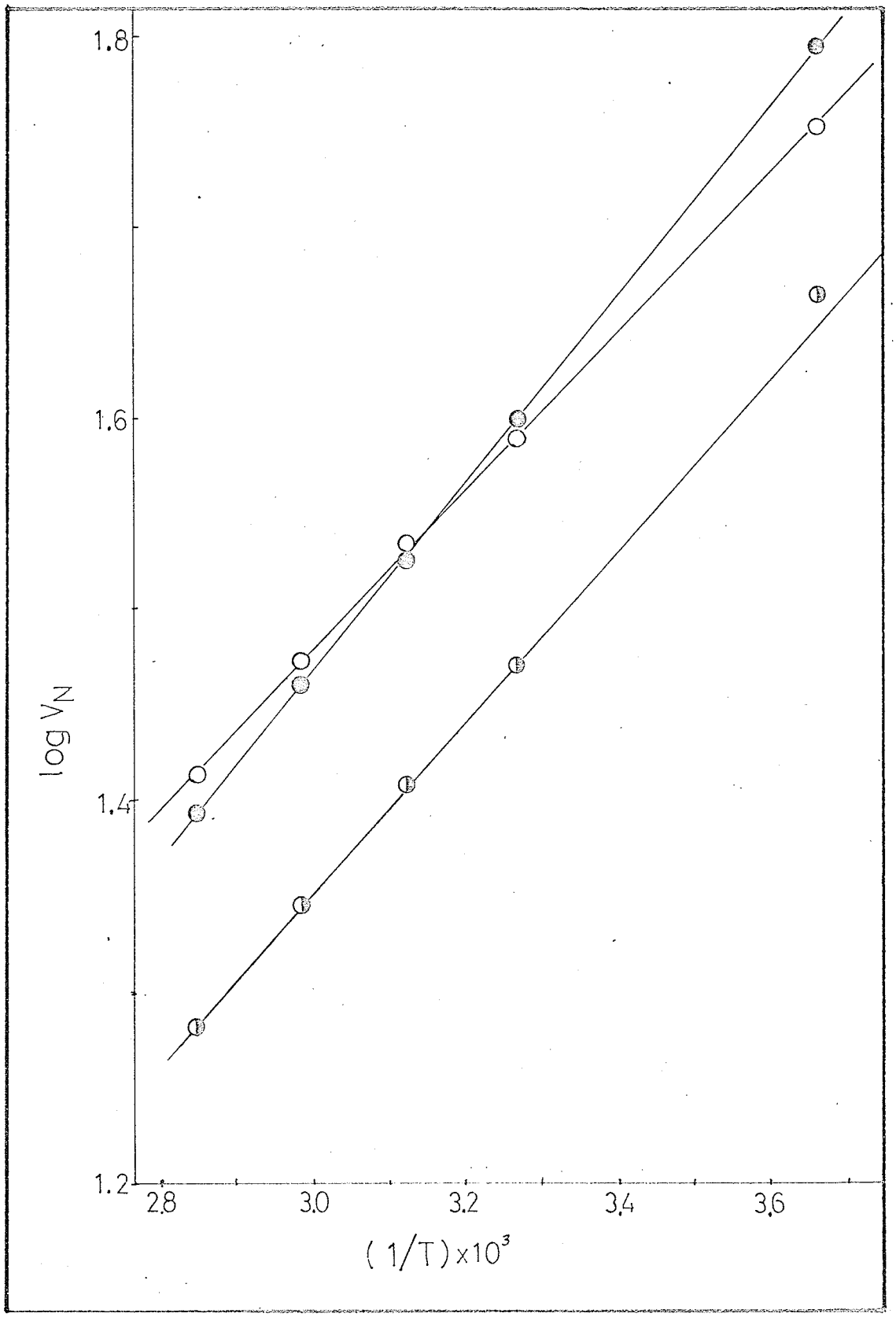
1.8
1.6
1.4
1.2
log V_N
2.8
3.0
3.2
3.4
3.6
$(1/T) \times 10^3$

FIGURE (3.44)

PLOT OF $\log V_N$ AGAINST 1/T FOR CH_4.

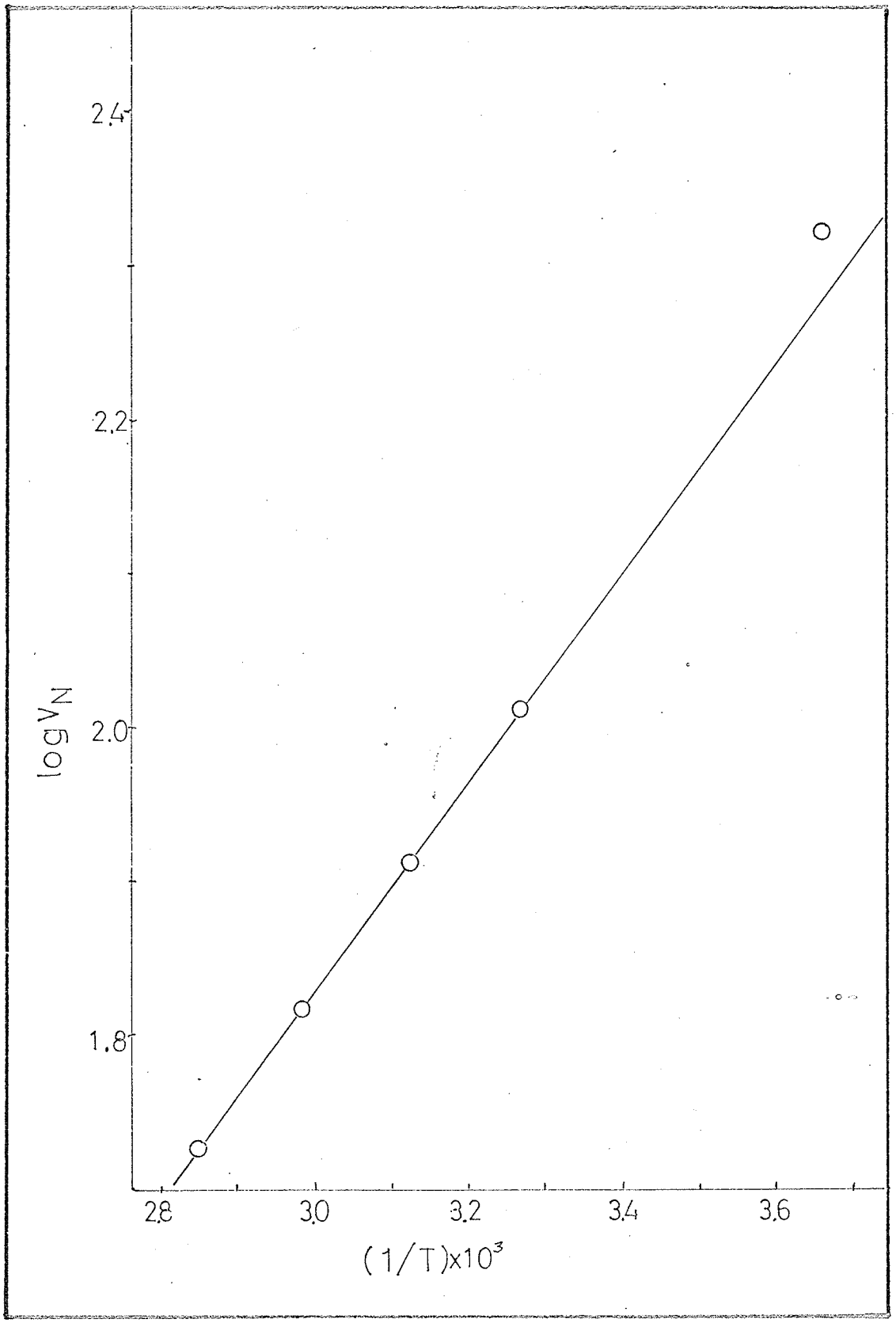
2.4
2.2
2.0
1.8
log V_N
2.8
3.0
3.2
3.4
3.6
(1/T)x10^3

FIGURE (3.45)

PLOT OF $\log V_N$ AGAINST 1/T FOR CO_2.

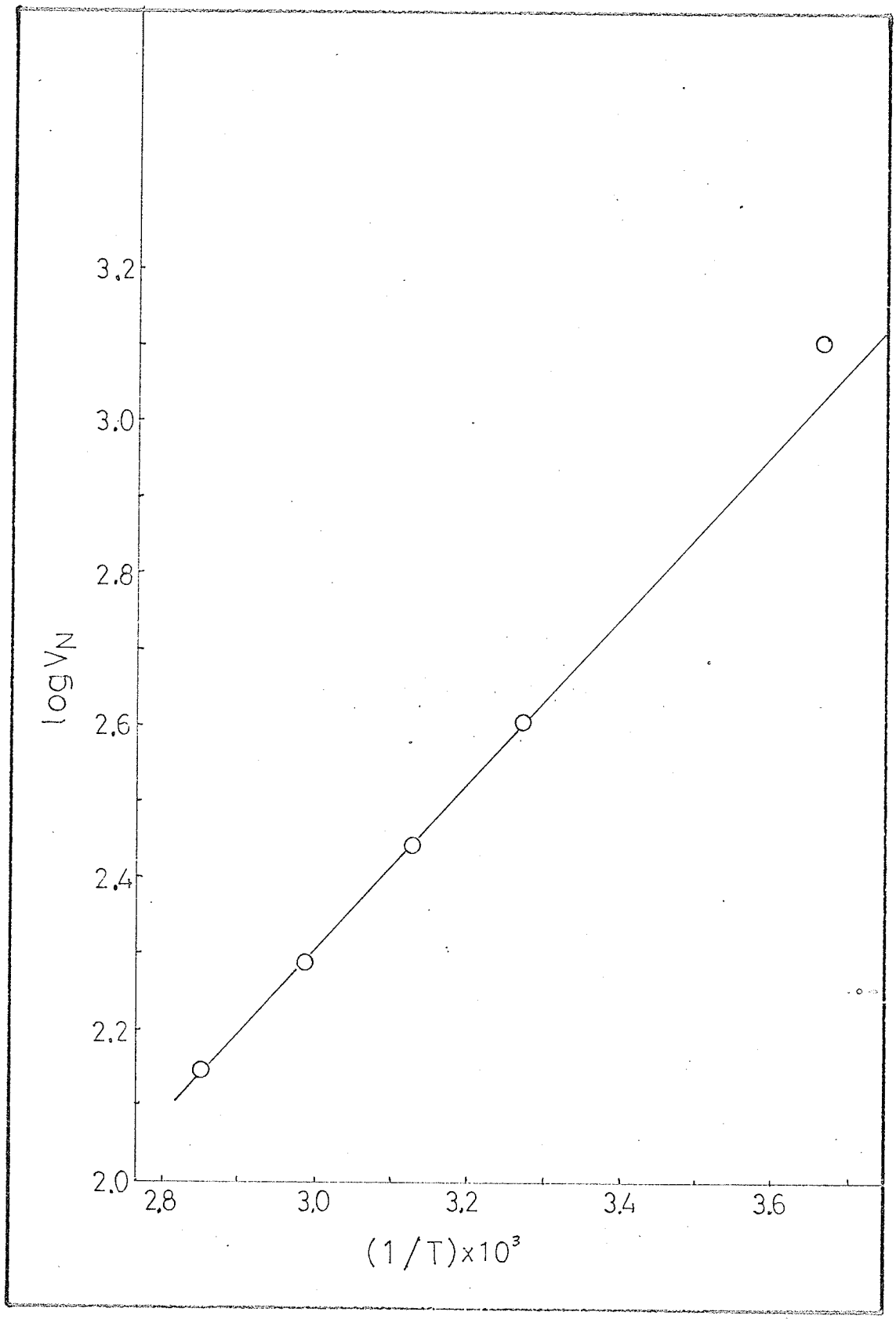
3.2
3.0
2.8
2.6
2.4
2.2
2.0
log V_N
2.8
3.0
3.2
3.4
3.6
(1/T)x10³

of the various plots were obtained by the least squares method. The ΔH° and the q values for all the gases are given in Table (3.11). The reference states will be defined later.

$K(CH_4)$ And $K(CO_2)$ As A Function Of Temperature By The Static Method

The large deviation at 273°K of the various $\log V_N$ v.s. 1/T plots was somewhat disturbing in the sense that the $V_N(CH_4)$ at 273°K obtained in this experiment was highly reproducible with that obtained in the HeI experiment. In order to confirm the authenticity of this deviation, it was required to extend the temperature range below 273°K. Considering the length of the retention time for CH_4 and CO_2 at 273°K.($\sim$1 hr. for CH_4 and $\sim$6.5 hrs. for CO_2), any lowering of the column temperature would result in extremely long experimental times.

A static method could serve a dual purpose. In the first place it could allow to extend the study into the low temperature region, and secondly it could serve as an independent method for obtaining the various thermodynamic data.

TABLE (3.11) THE ΔH° AND THE q VALUES FOR VARIOUS GAS SAMPLES USING HELIUM AS THE CARRIER GAS.

Gas	ΔH° (cal.)	q
H_2	-940	0.7858
N_2	-2063	-0.0026
Ar	-2239	-0.0009
O_2	-1917	0.5156
CH_4	-3125	-0.5087
CO_2	-4984	-2.2148

Experimental Apparatus

The apparatus which was used for this phase of work was basically that already described under the heading of 'Desorption Studies'. There are a few points that should be clarified.

a) The two stopcocks a and b of Fig (2.1), were in fact 3-way and not 2-way as Fig. (2.1) suggests. They served to connect the gas storage bulbs and the McLeod gauge directly. For convenience a block diagram of the apparatus including the connection between the McLeod gauge and the storage bulbs is shown in Fig. (3.46).

b) The thermocouple pair which served as a bucking e.m.f. for the pressure gauge was replaced by a Heathkit millivolt source which was used in its 'e.m.f. difference' mode. This unit allowed for a variable amount of e.m.f. to be bucked out and therefore, the recorder could be operated even on a 1 mv. range. In this study the thermocouple pressure gauge served only as a means of indicating as to whether equilibrium conditions have been reached or not.

c) The volume which included the sample tube, the thermocouple pressure gauge, and the interconnecting tubing including that which led to the gas buret, was calibrated by means of the gas buret. The various volumes of the gas buret were previously calibrated with mercury.

FIGURE (3.46)

THE DESORPTION APPARATUS.

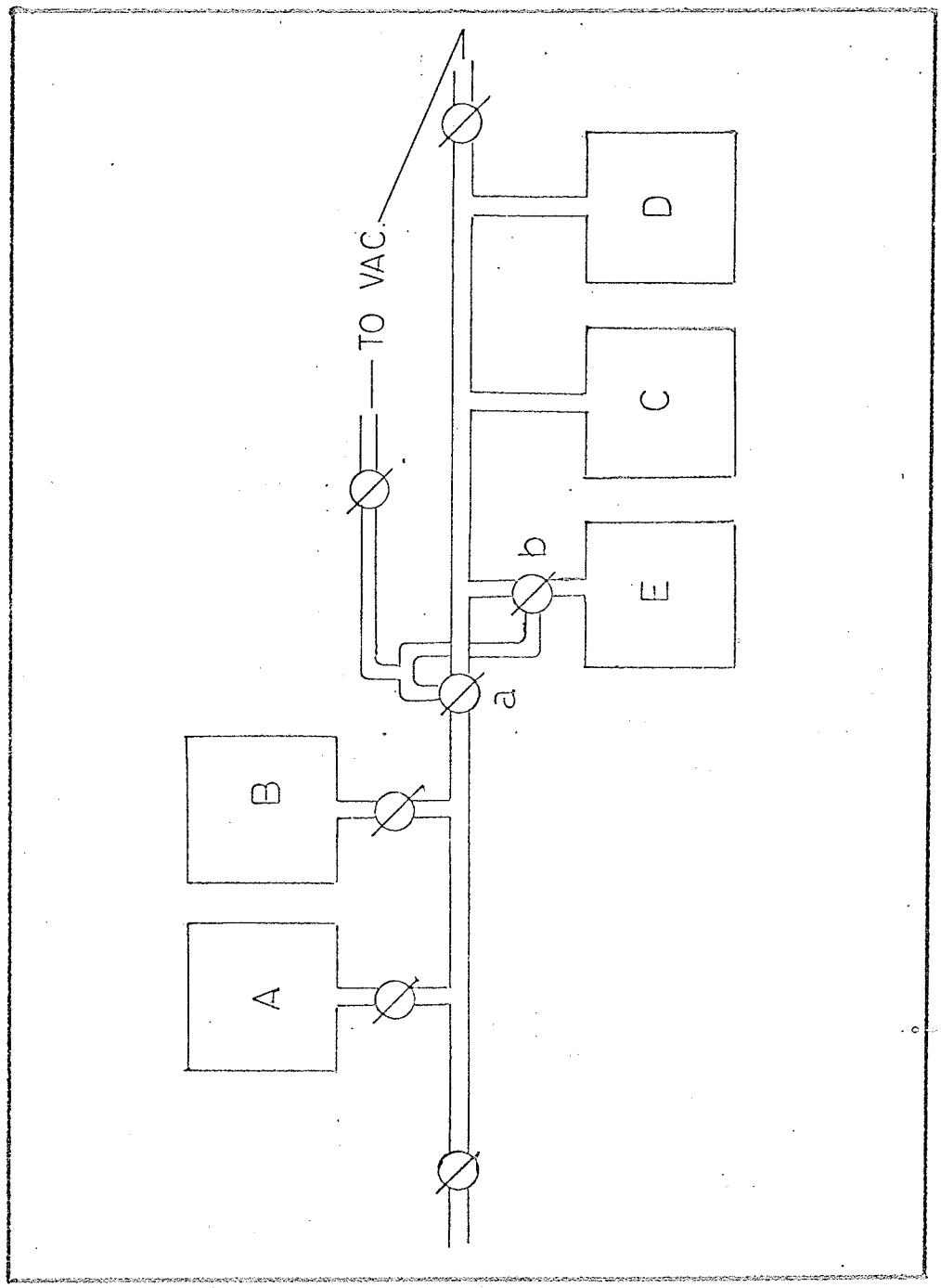
TO VAC.
A
B
C
D
E
a
b

d) From the ideal gas law relationship, the total volume of the McLeod gauge (to the mercury level in its down position) was calibrated with respect to the above defined volume. Due to the presence of mercury, the calibration was carried out at low pressures (~0.1 mm.). The McLeod gauge could now serve as a constant volume.

The methane gas was purified and introduced into the system in a manner already described.

By making appropriate connections, the purified CO_2 carrier gas could be made to enter the vacuum apparatus through the 3-way stopcock which previously served to join the gas buret to the sampling valve. After the system was purged with CO_2 for approximately 5 min., one of the storage bulbs of Fig. (3.46) was opened. After the CO_2 gas was subjected to a degassing procedure at liquid nitrogen temperature, the system was pumped down to the operating pressure range. From the experimental arrangement, the solid sample was at no time exposed to the gas.

Experimental Procedure

The solid sample (0.442 gms. of Porapak S(50 - 80 mesh), identical to the one used in the column) was heated under vacuum at 180°C. for approximately 12 hrs. before each experiment.

After the system was evacuated, the gas to be studied

was admitted into the McLeod gauge only by means of stop-cocks a and b of Fig. (3.46). After the pressure equilibrium was reached, the pressure in the storage bulb (thus in the McLeod gauge) was measured with the McLeod gauge. It should be pointed out that there are three factors which can contribute to erroneous pressure readings.

a) It was found that if the pressure was read soon after the gas was admitted to the McLeod gauge, the value obtained was somewhat lower than if a few minutes were allowed between the two events. It was found that a constant reading could be obtained after approximately 10 mins.. To be on the safe side, the pressure in the storage bulb was always measured 15 minutes after the gas was admitted into the McLeod gauge.

b) It was also found that significantly different values of pressure can be obtained if the storage bulb is cut off from the rest of the system. This can be explained in the following way. When the mercury of the McLeod gauge is raised, as it is done during pressure measurements, there is a decrease in volume with respect to the rest of the system. As the volume is decreased, the pressure in the rest of the system must increase. If the percent volume change is significant, then the pressure as measured with the McLeod gauge will always be lower than the true value. The storage bulb, due to its large volume, serves to decrease

the percent volume change.

c) It was further found that the pressure reading depended on the rate at which the mercury level was raised. If the level is raised quickly, the advancing mercury tends to compress the gas in its immediate vicinity. Since a finite time is required before the system reaches a pressure equilibrium, then the entrapped gas in the McLeod gauge is at a higher pressure than the rest of the system. The consequence of this is that the pressure readings thus obtained are always higher than the true value. In the present study great care was taken so as to raise the mercury level at a very slow rate. On the average it required approximately 10 minutes to raise the mercury to its final level. The pressure values reported are averages of 5 or 6 readings.

After the solid sample was cooled down to approximately -190°C., stopcock b was turned so as to allow the gas contained in the McLeod gauge to expand into the volume which contained the sample tube and the thermocouple pressure gauge. After the gas had frozen out (this was indicated by the thermocouple pressure gauge), the Powerstat which controlled the solid sample temperature was manually turned up by a predetermined amount. The temperature and pressure were followed by means of a potentiometer and the thermocouple pressure gauge. When the pressure had reached a constant value, the actual pressure was measured with the McLeod gauge. Due to the relatively large volume of the

system, the compressibility effect on the pressure measurements was assumed to be very small. After the pressure was determined, the temperature was raised to the next highest value. It should be pointed out that it required approximately 1.5 to 2 hrs. for the system to reach equilibrium conditions.

Calculation Of K

If one operates in the region where Henry's Law is obeyed, then the partition coefficient can be expressed in terms of concentrations, that is;

$$K = C_s/C_m \qquad (1.21)$$

Since $C_s = n_s/W_s$ and $C_m = n_m/V_m$ then eqn. (1.21) can be rewritten as follows;

$$K = n_s V_m/W_s n_m \qquad (3.96)$$

We are now dealing with the static system and the above values must be redefined.

W_s is the weight of the solid sample.

n_s is the total number of moles that are adsorbed on the surface at temperature T.

$V_m = Vx$ is the volume above the sample which is at temperature T. In order to preserve the association of V_m with the gas chromatographic column, Vx will be used to represent this volume

n_m is the total number of moles that are contained in Vx

During an experiment the temperature of the various parts of the apparatus were as follows;

a) The McLeod gauge and the interconnecting tubing were at ambient temperature.

b) The sample was at some experimental temperature T.

c) The thermocouple pressure gauge was at 273°K.

Considering this, it follows that there will be two temperature gradients present in the system. One of these will be set up along the sample containing tube since it joins directly to a part of the apparatus which is at ambient temperature. Consequently, this made it impossible to determine the value of Vx. Neither n_m nor n_s could be obtained from the pressure data since the exact value of Vx, the volume of the thermocouple pressure gauge, and the volume of the interconnecting tubing were not known. The other complicating factor was the presence of the temperature gradients. It is obvious that without the knowledge of Vx, the value of K cannot be obtained.

In order to determine the value of Vx, one must first assume that the entire apparatus, aside for the McLeod gauge, is composed of n distinct volumes V_1, V_2, V_3, ...V_n, and that each such volume is at a temperature T_1, T_2, T_3, ...T_n respectively. Let n_T represent the total number of

moles of a nonsorbing gas that is initially contained in the McLeod gauge. In terms of the ideal gas law, n_T can be expressed as;

$$n_T = P^\circ V(M)/RT_M \qquad (3.97)$$

where P°, $V(M)$, and T_M are the initial gas pressure, the volume, and the temperature of the gas in the McLeod gauge. After the gas is allowed to expand into the rest of the system, the following relationship must hold.

$$n_T = n_M + n_1 + n_2 + n_3 + \cdots\cdots + n_n \qquad (3.98)$$

where n_M, n_1, n_2, n_3, $\cdots\cdots n_n$ are the number of moles contained in the McLeod gauge, V_1, V_2, V_3, $\cdots\cdots V_n$ respectively. Since the pressure (P) will be the same in all the volumes, then in terms of eqn. (3.97) and (3.98) the following relationship can be written.

$$P^\circ V(M)/T_M = P(\ V(M)/T_M + V_1/T_1 + V_2/T_2 + V_3/T_3 + \cdots\cdots + V_n/T_n\ ) \qquad (3.99)$$

If V_1 can be assumed to represent the volume Vx which is at the temperature of the solid sample Tx, then eqn. (3.99) can be rewritten as follows;

$$P^\circ V(M)/T_M = P(\ V(M)/T_M + Vx/Tx + V_2/T_2 + V_3/T_3 + \cdots\cdots + V_n/T_n\ ) \qquad (3.100)$$

During an experiment, an increase in Tx will necessarily alter the temperature gradient associated with the sample containing tube, and therefore, will alter the relative magnitude of some of the V values. Considering that the total volume of the apparatus including the McLeod gauge is approximately 500 cc., these changes will most probably be not noticeable and for all intents and purposes it can be stated that;

$$V_2/T_2 + V_3/T_3 + \cdots\cdots + V_n/T_n = k \qquad (3.101)$$

In terms of eqn. (3.101), eqn. (3.100) can be rewritten to give;

$$\{V(M)/T_M\}\{P^o/P - 1\} = Vx/Tx + k \qquad (3.102)$$

or

$$\{V(M)/T_M\}\{P^o/P - 1\}Tx = Vx + kTx = Vxe \qquad (3.103)$$

If T_M is constant, then for a nonsorbing gas a plot of Vxe against Tx should give a straight line whose intercept will be Vx. If the k value is not constant as assumed, then the resulting plot will not be linear.

For lack of a better choice of nonsorbing gas, helium was used to determine Vx. Should helium be sorbing to any appreciable extent, the above mentioned plot will not be linear. To varify this one needs only to consider that

$K \propto 1/P$, and $\log K \propto 1/T$.

The results of this experiment are summerised in Table (3.12). A plot of Vxe as a function of Tx is shown in Fig. (3.47). As can be noticed the plot is linear. This then indicates that the assumptions made were reasonable. By a method of least squares it was found that k was 0.404 and Vx was 27.0 cc..

Having found the value of Vx and k, it now remains to relate the various measurable quantities to the partition coefficient.

For a sorbing gas, the total number of moles adsorbed on the surface at temperature Tx is;

$$n_s = n_T - n_M - n_x - n_2 - n_3 - n_4 - \cdots\cdots - n_n \qquad (3.104)$$

In terms of the ideal gas law, this can be written as;

$$\begin{aligned} n_s &= P^\circ V(M)/RT_M - PV(M)/RT_M - PVx/RTx - PV_2/RT_2 - \\ &\quad PV_3/RT_3 - \cdots\cdots - PV_n/RT_n \\ &= P^\circ V(M)/RT_M - PV(M)/RT_M - PVx/RTx - Pk/R \end{aligned} \qquad (3.105)$$

Also

$$n_x = n_m = PVx/RTx \qquad (3.106)$$

TABLE (3.12) VARIATION OF Vxe WITH Tx.

P^{o} = 25.35x2.362x10^{-3} mm. T_M = 294.5°K.

Tx(K)	P/(2.362x10^{-3})mm.	Vxe(cc.)
82	12.75	59.43
99	13.18	67.05
119	13.55	76.0
139	13.90	83.98
159	14.25	90.84
180	14.45	99.58
205	14.62	110.35

FIGURE (3.47)

Vxe AS A FUNCTION OF Tx.

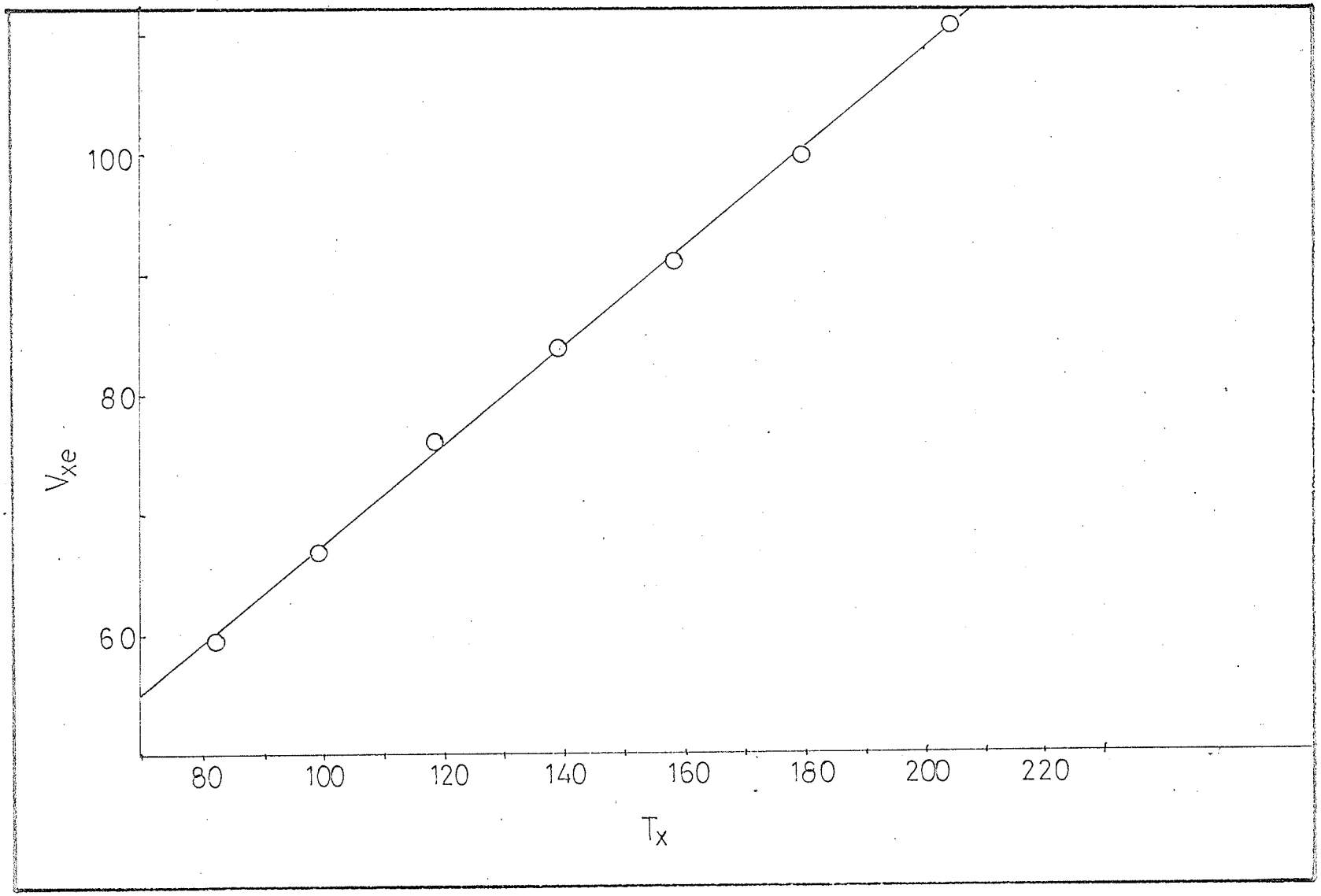
100
80
60
V_{xe}
80
100
120
140
160
180
200
220
T_x

But since

$$K = n_s Vx/W_s n_x \qquad (3.96)$$

then

$$K = (1/W_s)\{V(M)(P^\circ - P)/RT_M - PVx/RTx - Pk/R\}RTx/P \qquad (3.107)$$

and upon rearrangement

$$K = (1/W_s)\{\left(V(M)Tx/RT_M\right)(P^\circ/P - 1) - Vx - kTx\} \qquad (3.108)$$

But since

$$Vx + kTx = Vxe \qquad (3.103)$$

then eqn. (3.108) becomes;

$$K = (1/W_s)\{\left(V(M)Tx/RT_M\right)(P^\circ/P - 1) - Vxe\} \qquad (3.109)$$

Results And Discussion

The results of the experiments where $K(CH_4)$ and $K(CO_2)$ were studied as a function of temperature are summarised in Table (3.13) and (3.14) for methane and carbon dioxide respectively. Figure (3.48) shows a logK against 1/T plot for all these experiments. As can be seen the relationship is linear and the individual points show little scatter. It should be noted that for a particular gas, the choice of

TABLE (3.13) PARTITION COEFFICIENTS OF METHANE AT VARIOUS TEMPERATURES.

$P^o = 23.03 \times 10^{-3}$ mm.		$P^o = 51.49 \times 10^{-3}$ mm.		$P^o = 88.62 \times 10^{-3}$ mm.	
$T_M = 297.5$		$T_M = 294.5$		$T_M = 298$	
Tx	$Kx10^{-3}$	Tx	$Kx10^{-3}$	Tx	$Kx10^{-3}$
127.5	53.2	115.5	318	125.3	63.2
151	3.63	135	17.8	138.5	13.29
170.7	0.569	159.5	1.54	151	3.54
196	0.111	180	0.287	161	1.25
218	0.040	204	0.069	183	0.220
				205	0.617
				237.7	0.016

TABLE (3.14) PARTITION COEFFICIENTS OF CARBON DIOXIDE AT VARIOUS TEMPERATURES.

(a) T_M = 296.5		(b) T_M = 295		(c) T_M = 296.5		(d) T_M = 297.5	
Tx*	Kx10^{-3}	Tx*	Kx10^{-3}	Tx*	Kx10^{-3}	Tx*	Kx10^{-3}
155	448	161	139	157.5	229	158.5	200
168	63.7	183	18.0	168	70.8	181	16.8
180	19.8	205	1.95	179	20.3	201.5	2.15
191.5	6.00	238	0.180	192	4.87	235.5	0.207
205	1.61			204.5	1.56		
215.5	0.720			215	0.688		
241.7	0.113			242	0.130		

(a) P^o = 23.4x10^{-3}mm. (b) P^o = 54.92x10^{-3}mm. (c) P^o = 97.10x10^{-3}mm.

(d) P^o = 136.10x10^{-3}mm. * °K.

FIGURE (3.48)

PLOT OF logK AGAINST 1/T FOR CH_4 AND CO_2.

CH_4

◇ $P^o = 23.03 \times 10^{-3}$ mm.

○ $P^o = 51.49 \times 10^{-3}$ mm.

× $P^o = 88.62 \times 10^{-3}$ mm.

CO_2

⬭ $P^o = 23.40 \times 10^{-3}$ mm.

○ $P^o = 54.92 \times 10^{-3}$ mm.

× $P^o = 97.10 \times 10^{-3}$ mm.

◇ $P^o = 136.10 \times 10^{-3}$ mm.

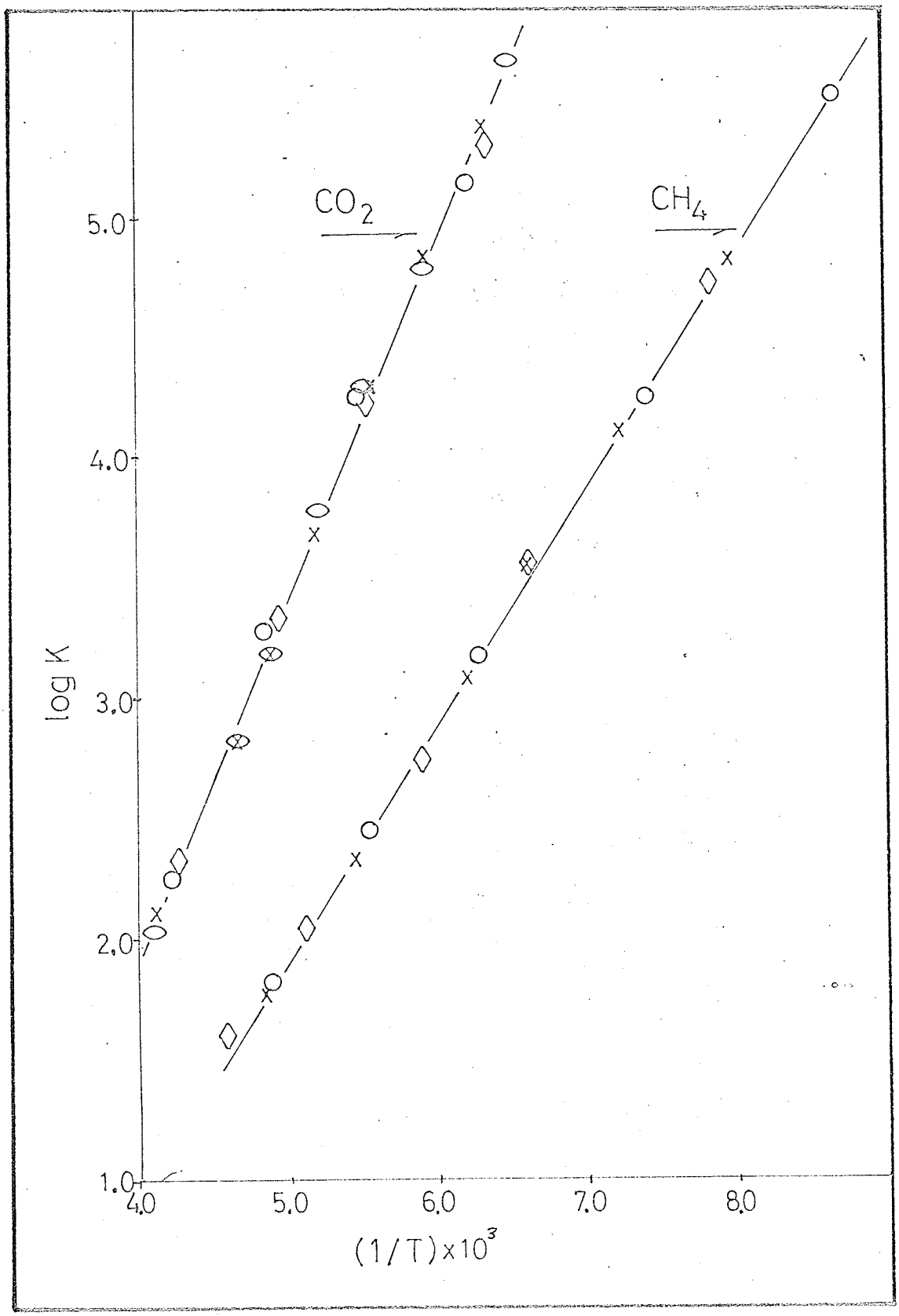
CO2
CH4
log K
5.0
4.0
3.0
2.0
1.0
4.0
5.0
6.0
7.0
8.0
(1/T)x10^3

P° has no noticeable effect on the resulting logK against 1/T plot. By the least squares method, it was found that the plots for methane and carbon dioxide are best described with the following constants.

methane

slope	975.7
intercept	-2.942

carbon dioxide

slope	1,502
intercept	-4.095

Since the slope is $-\Delta H^{\circ}/2.303R$, then the heats of adsorption are;

$\Delta H^{\circ}(CH_4)$	4.46 Kcal./mole
$\Delta H^{\circ}(CO_2)$	6.87 Kcal./mole

By extrapolation, it was found that at 273°K the partition coefficients were;

$K(CH_4)$	4.25 cc./gm.
$K(CO_2)$	25.44 cc./gm.

The ratio of $K(CO_2)/K(CH_4)$ is then 5.99. The ratio of $V_N(CO_2)/V_N(CH_4)$ was found previously to be 5.99. The two results are in excellent agreement.

From the gas chromatographic study it was found from the linear portion of the $\log V_N$ against 1/T plot that;

$\Delta H^{\circ}(CH_4)$ 3.12 Kcal./mole

$\Delta H^{\circ}(CO_2)$ 5.00 Kcal./mole

These values are somewhat lower than those obtained from the static system. Considering the fact that the $K(CO_2)/K(CH_4)$ and the $V_N(CO_2)/V_N(CH_4)$ ratios are identical, and that there is little experimental scatter, the difference between the ΔH° values cannot be attributed to experimental error. This then means that below 273°K the ΔH° values are larger than above 273°K and as the large deviations in Figures (3.44) and (3.45) suggest, there must be a change in the slope of the $\log V_N$ (or logK) against 1/T plot. This change in slope indicates that there is a change in particle properties, which in turn suggests that the particles may be undergoing a physical change.

Due to several unfortunate accidents during the column packing process, the weight of the packing in the column could not be determined directly. An indirect method which required the determination of the bulk density of the packing material had to be used. The bulk density was obtained by determining the weight of the material contained in a 10 ml. volumetric flask. Although tapping procedure was used to promote a denser packing, the final packing density could not be expected to be as high as that of the gas chromatographic column since in the former case the height of the packing material was only 4 or 5 inches where as in the

latter case the height was about 25 feet. It was found that the bulk density was 0.372 gms./cc.. Using 130.5 cc. as the calculated volume of the empty column, the weight of the material contained in the column was calculated to be 48.6 gms.. The actual weight will most probably be a little higher than this.

From the static method it was found that $K(CH_4)$ was 4.26 cc./gm. and from gas chromatography it was found that $V_N^o(CH_4)$ was 214.7 cc.. Using the relationship between V_N and K (see eqn. (1.32)), the weight of the packing material in the column was calculated to be 50.5 gms.. By comparing this to a value of 48.8 gms. and remembering that the value obtained from the indirect method is probably a little lower than the true value, it can be concluded that the results obtained from the two methods are in very good agreement and that the large deviations previously observed are genuine. This further substantiates that there is a change in the slope (ΔH^o) somewhere a little above 273°K. Although the difference between the two weights is small ($\sim$4%), the higher value was assumed to be more correct and was used to retrieve the ΔS^o values from the previously obtained q values. The thermodynamic quantities ΔS^o, and ΔG^o, are contained in Table (3.15). The K values have units of cc./gm. and the other thermodynamic quantities are defined with respect to this. Since all the work was done

TABLE (3.15) THE ΔG° AND THE ΔS° VALUES FOR VARIOUS GASES.

Gas	ΔG° (Kcal.)*	ΔS° (e.u.)
Gas Chromatography (Helium carrier gas)		
H_2	0.762	-6.23
N_2	0.048	-7.80
Ar	-0.114	-7.80
O_2	-0.062	-6.77
CH_4	-0.790	-8.80
CO_2	-1.746	-12.19
Static Method		
CH_4	-0.790	-13.46
CO_2	-1.751	-18.73

* Obtained from the various K values at 273°K. The various ΔG° values refer to an adsorption process at 273°K and are ΔG°_{273}.

using very small samples (gas chromatographic system) and very low pressures (static system), the various partial molar quantities refer to an adsorption process on a bare surface. The slight interaction of helium with the surface as noted in the experiment at 273°K, is not sufficient to warrant a change in the above definition since the ΔH°, ΔS°, and ΔG° values were obtained from experiments above 273°K where the interaction is most probably insignificant. In all cases Henry's Law was assumed.

ZONE BROADENING

In the introductory chapter it was shown that the plate height (H) is related to the carrier gas velocity (u) through the generalised form of the van Deemter equation, that is;

$$H = A + B/u + Cu \qquad (1.46)$$

where A, B, and C are constants. Although mention was made that these constants are related to the particle diameter, the gas diffusion coefficient, and the resistance to mass transfer respectively, the constants were not defined. Furthermore, due to the complexity of the gas chromatographic process, no attempt will be made to give a detailed definition to the forementioned constants. An attempt will be made however, to expand their meaning and to revise eqn.

(1.46) to the point where it can be applied to the experimental data.

The B constant

This constant is generally referred to as the longitudinal diffusion term (182, 183, 184) and can be expressed as;

$$B = 2\gamma D_g \qquad (3.110)$$

where γ and D_g are a constant and the gas diffusion coefficient respectively. The constant γ is referred to as the obstructive factor (107, 184) or the labyrinth factor (182, 184) and reflects on the tortuous and constrictive paths that a solute molecule must follow as it travels down the column.

Since the granular particles obstruct the longitudinal diffusion, γ will be less than 1. There is considerable evidence to show that $\gamma \simeq 0.6$ (107, 148, 185, 186).

The C constant

This constant is actually composed of two basic terms, C_s which is a contribution of resistance to mass transfer in the stationary phase, and C_g the resistance to mass transfer in the gaseous phase. In gas solid chromatography the C_s term is designated as C_k (187, 188, 189) and has

the form;

$$C_k = 2R(1 - R)\bar{t}_d \qquad (3.111)$$

where R as before is the fraction of the molecules in the mobile phase, and $\bar{t}_d$ is the mean desorption time of the solute molecules. van Berge and Pretorius (190A) have indicated that count must be taken of diffusion of molecules into the micropore spaces of the solid. They have shown that this contribution to mas transfer can be expressed as;

$$C_2 = \{2k(\delta/\bar{v} + \tau)d_c^2\}/\{(1 + k)^2(\delta^2 + 3\tau D_s)\} \qquad (3.112)$$

where:

- k is the mass distribution coefficient or ratio of amount of solute in the stationary phase to amount of solute in the gas phase at equilibrium.
- δ is the pore diameter (cm.).
- $\bar{v}$ is the average thermal velocity of a molecule in the gas phase.
- τ is the average residence time of an adsorbed molecule on the surface.
- d_c is the average pore length.
- D_s is the surface diffusion coefficient.

The C_g term can be expressed as (186, 187, 190B, 191);

$$C_g = \omega d_p^2/D_g \qquad (3.113)$$

where ω is another structural factor in order of unity, and d_p, as before, is the particle diameter. Giddings (190B) has shown that for porous supports the ω can be related to R by the following relationship.

$$\omega \simeq 0.82 - 0.20R \qquad (3.114)$$

The A constant

This constant can be related to the particle diameter through the following equation (182, 183);

$$A = 2\lambda d_p \qquad (3.115)$$

where λ is a geometrical constant near unity. This then means that;

$$A > d_p \qquad (3.116)$$

and according to eqn. (1.46) this contribution is carrier gas velocity independent.

It was found in many cases (147, 192-196) that the experimental data can be expressed without the A term in the plate height equation. In certain instances (193,194) the A terms were found to be slightly negative. Glueckauf (197), and Bohemen and Purnell (193) found a variation of A with flow velocity. Kieselbach (195, 198) has found that A varies with the retention volume, that is, light gases

tend to have a larger A value than the highly retained components. As Giddings and Robison (199) point out, these findings are not in agreement with eqn. (1.46) and (3.116).

Giddings (189, 200) has proposed an alternative form for the plate height equation in which the A term is coupled with the C_g term. In its simplist form this equation can be expressed as;

$$H = 1/(1/A + 1/C_g u) + B/u + C_k u \qquad (3.117)$$

This equation predicts that at low carrier gas velocity the coupling term will approach zero where as at high carrier gas velocities the term will approach A. This transition from 0 to A will have an effect on the overall H vs. u plot in that at high gas velocities there should be a levelling off effect. This levelling off has been observed on several occasions (186, 201, 202) while other data has been interpreted in terms of the coupling theory (203, 204). The observed fall off in the high velocity region cannot be totally explained by the coupling tneory since Giddings (153) and Knox (202) have shown that turbulent and coupling effects overlap one another in high-velocity packed columns. Giddings et. al. (205) have shown that as the Reynolds number is increased, the plate height of a capillary column first increases, reaches a maximum ($R_e \approx 2{,}500$), and then

very rapidly falls off to a more or less constant value. In the case of a packed sorbing column, it was observed that the maximum was much broader. The authors also point out that in the case of packed columns, turbulance is fully developed at $R_e > 100$. In conclusion they state that; "Theoretical interpretation of turbulance in packed columns is complicated by the fact that the coupling phenomenon (a consequence of flow-diffusion interactions) also reduces plate height at high velocities; both act gradually-not discontinuously as in capillaries. The two effects have not yet been unscrambled, but undoubtedly both are beneficial."

Stewart, Seager, and Giddings (206) have shown that due to the pressure drop across the column, a pressure correction must be made when the measured plate height ($\hat{H}$) is related to the carrier gas velocity. In terms of the 'classical' expression for plate height (an equation such as eqn. (1.46) but containing all the C constants), the observed plate height can be related to the carrier gas velocity by;

$$\hat{H} = (A + B/u_o P_o + C_g u_o P_o) f_2 + C_k' u_o P_o j \qquad (3.118)$$

where

$$C_k' = C_k + C_2 \qquad (3.119)$$

and

$$f_2 = (9/8)\{(a^4 - 1)(a^2 - 1)\}/(a^3 - 1)^2 \qquad (3.120)$$

a, j, and u_o are the P_i/P_o ratio, the Martin-James compressibility factor, and the carrier gas velocity at column outlet where the pressure in P_o respectively. These pressure corrections have been extended to eqn. (3.117) (194) to give the following expression for $\hat{H}$.

$$\hat{H} = \{1/(1/A + 1/C_g u_o P_o) + B/u_o P_o\} f_2 + C_k' u_o P_o j \qquad (3.121)$$

Both Giddings (188), and van Berge and Pretorius (190A) have shown that since the $\bar{t}_d$ of eqn. (3.111) is very small, the relative contribution of C_k to the plate height will be insignificant and for this reason C_k may be omitted from the plate height equation. Under these conditions equations (3.118) and (3.121) become;

$$\hat{H} = (A + B/u_o P_o + C_g u_o P_o) f_2 + C_2 u_o P_o j \qquad (3.122)$$

and

$$\hat{H} = \{1/(1/A + 1/C_g u_o P_o) + B/u_o P_o\} f_2 + C_2 u_o P_o j \qquad (3.123)$$

respectively.

Experimental

The experimental apparatus and procedure has already been described. The various D_g values were calculated from an equation proposed by Giddings el. al. (207, 208) which has the form of;

$$D_g = \frac{1.00\times10^{-3}T^{1.75}(1/M_A + 1/M_B)^{\frac{1}{2}}}{P\{(\Sigma_A v_i)^{1/3} + (\Sigma_B v_i)^{1/3}\}^2} \qquad (3.124)$$

where

M_A and M_B are the masses of the interdiffusing gases.

T is the temperature.

v_i are the atomic and structural diffusion volume increments (given in (207) and (208)).

P is the pressure.

It has been shown by the above authors that eqn. (3.124) introduces on the average an error of less than 5% where as other equations of the same class introduce errors as high as 25%.

Since the peaks were symmetrical the peak widths at half the height were determined directly without applying any corrections. All measurements were made with a travelling microscope. With the aid of the vernier scale, it was possible to measure the widths to ± 0.002 cm.. All readings

were made with respect to the center of the recorder pen trace.

Results And Discussion

It should be pointed out at the outset that this work does not represent a detailed study of zone broadening. These results are included for the following two reasons:

a) to indicate the performance of the column.

b) to add more weight to some of the previously made statements.

van Berge and Pretorius (190A) have shown that since $3\tau D_s$ of eqn. (3.112) is insignificant, the C_2 term can be reduced to;

$$C_2 = 2k(\delta/\bar{v} + \tau)d_c^2/(1 + k)^2\delta^2 \qquad (3.125)$$

Using their approximate values for the various constants, that is:

$\delta \simeq 10\times10^{-7}$

$\delta/\bar{v} \simeq 2\times10^{-11}$

$\tau \simeq 1.5\times10^{-10}$

$d_c \simeq 0.5d_p$

and for the present case;

$$k = KW_s/V_m \simeq 2.3 \qquad (3.126)$$

the value of C_2 can be estimated to be $\sim 7\times10^{-3}$.

The magnitude of C_2 term is substantial if one considers that the C_g term is in the order of $1x10^{-3}$, but its contribution to $\hat{H}/f_2$ will not be as large as that of C_g since the contribution of the former depends on u_oP_oj/f_2 where as the contribution of the latter depends on u_oP_o. The range of u_oP_oj/f_2 is $\sim$ 0 to 10 cm./sec. where as the range of u_oP_o is $\sim$ 0 to 120 cm./sec.. It must be remembered that the value of C_2 was arrived at by using the various constants given by van Berge and Pretorius for their system (silica gel). There is no evidence to show that some of these constants are applicable to the present system or whether the C_2 term is operative at all. In order to isolate the C_2 term, separate experiments must be carried out but as it was mentioned before, this is not the purpose of this study. For all intents and purposes the C_2 and the C_g terms were summed together and called C.

The various values of $\hat{H}/f_2$ which are given in this section refer to methane sample. These along with their respective u_oP_o values are tabulated in Table (3.16) for experiments HeI, Ar(II and III), and CO_2I. Plots of $\hat{H}/f_2$ against u_oP_o for the above three carrier gases are shown in Figures (3.49), (3.50), and (3.51). Aside for Fig. (3.51), the plots are of the expected hyperbolic shape. Fig. (3.51) is of particular interest since it shows a considerable levelling off at high u_oP_o values. In each case the mini-

TABLE (3.16) THE $\hat{H}/f_2$ AND THE u_oP_o VALUES FOR EXPERIMENTS HeI, Ar(II and III), AND CO_2I.

He		Ar		CO_2	
$\hat{H}/f_2$(a)	u_oP_o(b)	$\hat{H}/f_2$(a)	u_oP_o(b)	$\hat{H}/f_2$(a)	u_oP_o(b)
0.130	98.41	0.168*	75.08*	0.217	112.53
0.116	76.20	0.147	65.94	0.201	87.79
0.105	59.95	0.148*	61.74*	0.191	69.15
0.096	47.95	0.130	53.20	0.177	56.06
0.092	36.34	0.129*	50.12*	0.144	38.29
0.088	25.16	0.126	42.62	0.115	25.42
0.095	17.31	0.111*	36.01*	0.108	15.47
0.128	10.19	0.107	32.30	0.094	8.43
0.180	5.63	0.107*	28.79*	0.096	4.20
		0.103	22.14		
		0.094	14.93		
		0.090	8.52		
		0.141	2.74		

* ArIII

(a) cm. (b) cm./sec.

FIGURE (3.49)

PLOT OF $\hat{H}/f_2$ AS A FUNCTION OF $u_o P_o$ FOR HeI.

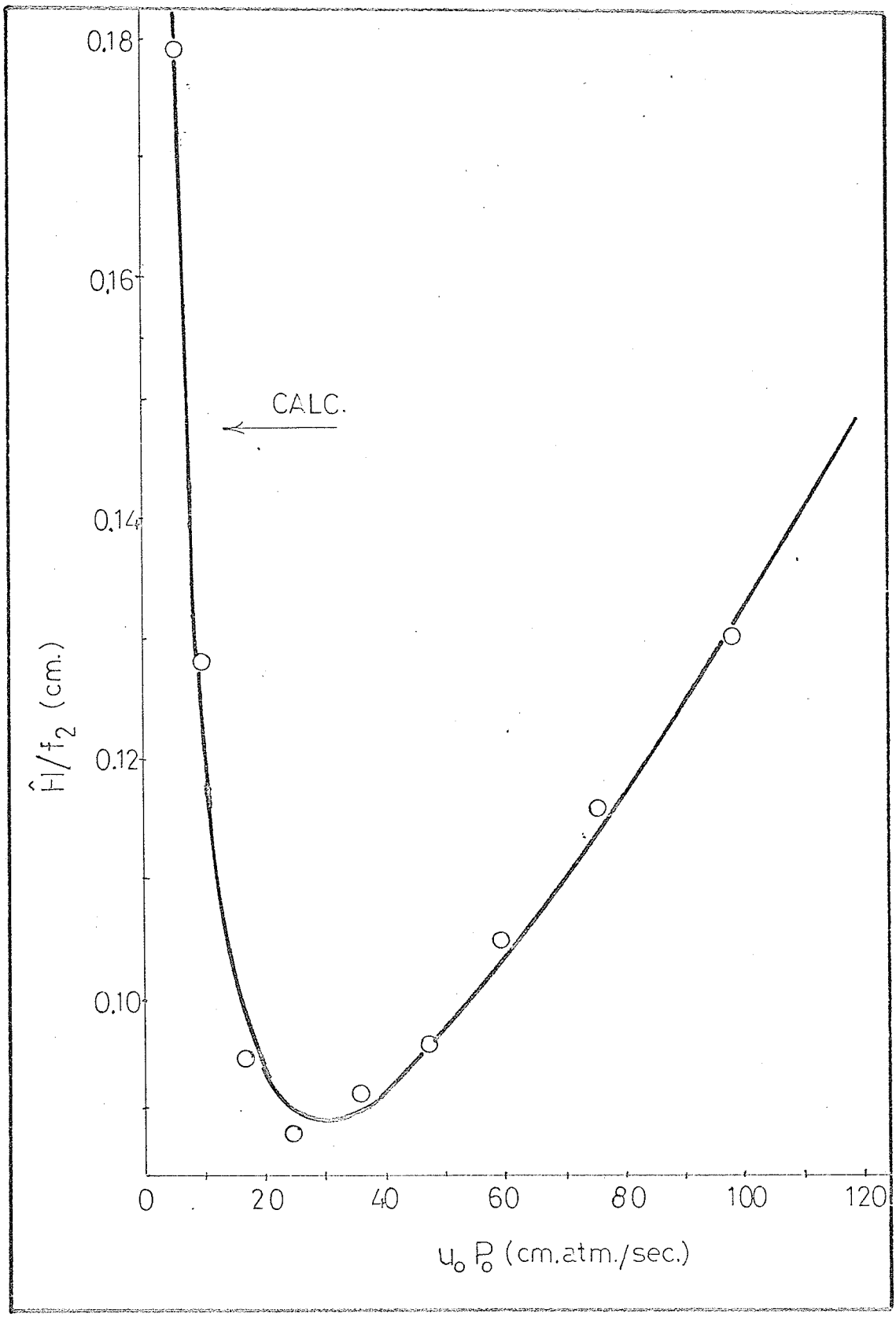
0.18
0.16
0.14
0.12
0.10
CALC.
$\hat{H}/f_2$ (cm.)
0
20
40
60
80
100
120
$u_o P_o$ (cm.atm./sec.)

FIGURE (3.50)

PLOT OF $\hat{H}/f_2$ AS A FUNCTION OF $u_o P_o$ FOR Ar(II AND III).

○ ArII

◎ ArIII

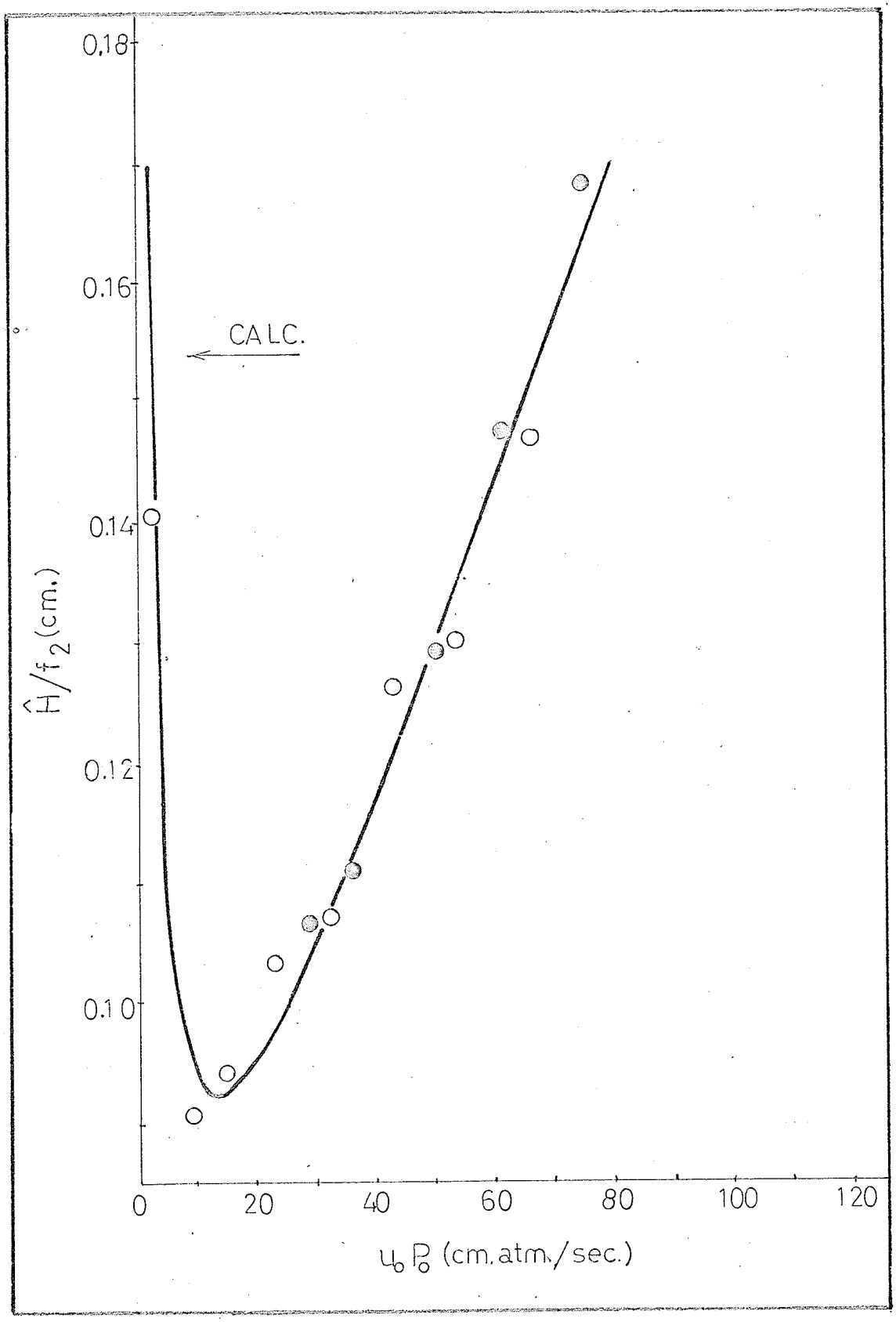
0.18
0.16
0.14
0.12
0.10
CALC.
$\hat{H}/f_2$ (cm.)
0
20
40
60
80
100
120
$u_o P_o$ (cm. atm./sec.)

FIGURE (3.51)

PLOT OF $\hat{H}/f_2$ AS A FUNCTION OF $u_o P_o$ FOR $CO_2 I$.

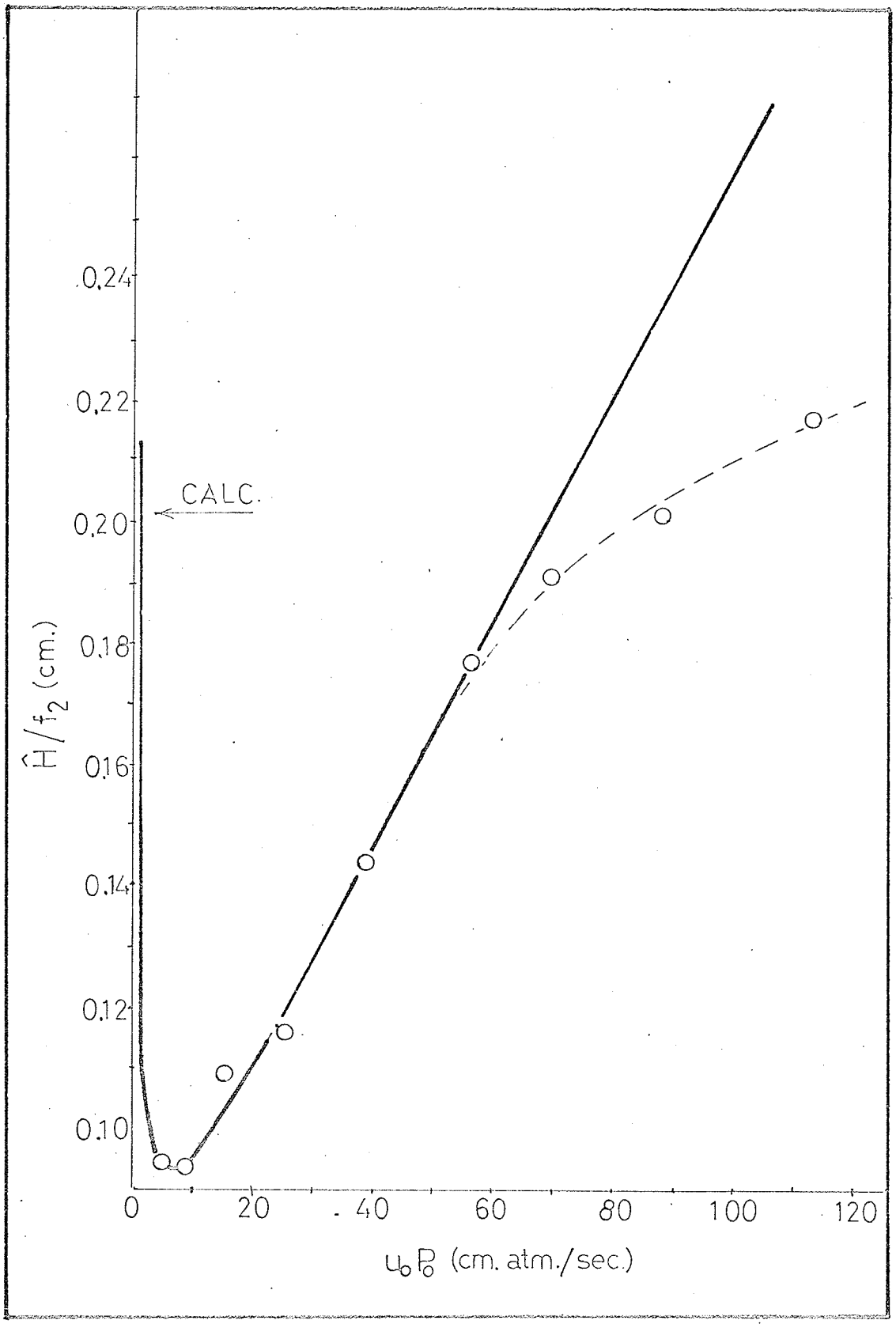
0.24
0.22
CALC.
0.20
0.18
0.16
0.14
0.12
0.10
$\hat{H}/f_2$ (cm.)
0
20
40
60
80
100
120
$u_o P_o$ (cm. atm./sec.)

mum of the curve corresponds to $\hat{H}/f_2$ of approximately 0.09 cm..

By the least squares method it was found that the experimental data for HeI and Ar(II and III) can be best expressed by the following equations;

$$\hat{H}/f_2(He) = 0.0383 + 0.776/u_oP_o + 0.000865u_oP_o \qquad (3.127)$$

$$\hat{H}/f_2(Ar) = 0.0575 + 0.217/u_oP_o + 0.00138u_oP_o \qquad (3.128)$$

A plot of these equations is included in Figures (3.49) and (3.50) and they are designated by the heavy line termed 'calc.'. As can be seen there is a very good fit between the calculated and the experimental plots. It appears that the 'classical' equation well describes the present results.

In the case of CO_2, the least squares method was applied only to the first six points corresponding to the lowest u_oP_o values. It was found that this data can be best expressed by the following equation.

$$\hat{H}/f_2(CO_2) = 0.0695 + 0.0775/u_oP_o + 0.00189u_oP_o \qquad (3.129)$$

A plot of this equation can be seen in Fig. (3.51). Again it appears that the experimental data considered is governed by the 'classical' equation.

Using eqn. (3.124) it was found that the D_g values at 273°K were as follows.

$D_g(He-CH_4)$ 0.549 $cm^2/sec.$

$D_g(Ar-CH_4)$ 0.184 $cm^2/sec.$

$D_g(CO_2-CH_4)$ 0.154 $cm^2/sec.$

Applying these along with d_p = 0.02 cm. to the A and B constants, the λ and γ values were calculated. These are given in Table (3.17). The ω values cannot be obtained from the C terms since it is not known whether these terms are C_g alone or whether they are a combination of $C_g + C_2$. If it can be assumed that the C terms are strictly C_g, then the ω values will be as those given in Table (3.17).

The λ values which should be constant for a particular column, are seen to increase as one goes from He to Ar to CO_2. This incidently is the same order as the degree of interaction between the carrier gas and the surface. Whether this is of significance it is difficult to say.

Unlike λ, γ is found to decrease with the above order of the carrier gases. The value of γ for CO_2 is somewhat low considering that in most cases this constant is close to 0.6. This discrepancy can in part be attributed to the small number of experimental points used to calculate the B constant.

The ω values follow no set pattern. An unusually high value of ω is obtained in the case of helium. According to

TABLE (3.17) THE λ, γ, AND ω VALUES AS OBTAINED FROM EXPERIMENTS HeI, Ar(II and III), AND CO_2I.

Experiment	λ	γ	ω
He	0.96	0.71	1.20
Ar	1.44	0.59	0.63
CO_2	1.74	0.25	0.73

Giddings' equation (eqn. (3.114)) the maximum value of ω should be less than 1. Perrett and Purnell (209) have reported ω values as high as 1.6. They attribute this to solvent inhomogeneities and suggest that ω is a composite of two parts, that is;

$$\omega = \omega_{fi} + \omega_{si} \qquad (3.130)$$

where ω_{fi} and ω_{si} refer to flow and solvent inhomogeneities respectively. In the present case the excessive value of ω may some how be related to the C_2 term. The fact that the ω for Ar and CO_2 are less than that for helium can stem from the dependence of the true ω on R (see eqn. (3.114)) and the C_2 constant on $k/(1 + k)^2$. Since

$$k = (1 - R)/R \qquad (3.131)$$

and

$$k = KW_s/V_m \qquad (3.126)$$

then it can be seen that both the true ω and the C_2 constant will decrease as the effective W_s becomes smaller due to carrier gas-surface interaction. This however, would probably require that the calculated ω for Ar be less than that for CO_2. The fact that this is not observed need not contradict the above reasoning if one recalls that the calculated ω was derived from a limited number of experi-

mental points and also that the C_2 term which was included in the C term when ω was calculated, depends on $u_o P_o j/f_2$ rather than $u_o P_o$. No steps were taken to prove or contradict this statement since it is of no prime importance to the present purpose.

The fall off observed in the case of CO_2 can stem from several sources. Some of the possible ones are listed below.

a) coupling effects

b) turbulence

c) decrease of true ω and C_2 with increasing pressure

d) combination of some or all of the above

Although it was found that A values of the magnitude predicted by the 'classical' equation were required to describe the present results, coupling cannot be dismissed on these grounds. The presence of the A terms can stem from extra-column contributions to $\hat{H}$ for which no correction was made.

The fall off can as equally be explained by turbulent effects. As Giddings et. al. (205) have pointed out that for packed columns turbulence can be fully developed at $R_e > 100$. If one refers to Fig. (3.23) one will observe that at the highest F_o values the Reynolds number is approximately 30 which is much higher than for the other two gases. At $R_e \simeq 30$, considerable turbulence can be expected.

The effect of pressure on true ω and C_2 has already been discussed.

The situation becomes more complicated when one considers experiments ArI, CO_2II, and CO_2III. Plots of $\hat{H}/f_2$ against u_oP_o for ArI, and Ar(II and III) are shown in Fig. (3.52), and for CO_2I, CO_2II, and CO_2III in Fig. (3.53). As can be seen there is no obvious trend in these plots. One thing is obvious though, and that is that the relationship between $\hat{H}/f_2$ and u_oP_o depends on whether the inlet pressure is changed in an increasing or decreasing direction. If as before one considers the order in which ArI, ArII, and ArIII experiments were performed and that ArII and ArIII are reproducible, a conclusion must be reached that there is a plate height hysterisis. As before, the term hysterisis refers to the fact that a different relationship is obtained if one changes the inlet pressure in an increasing or decreasing direction.

FIGURE (3.52)

PLOT OF $\hat{H}/f_2$ AS A FUNCTION OF $u_o P_o$

FOR ArI AND Ar(II AND III).

◇ ArI

○ ArII

◎ ArIII

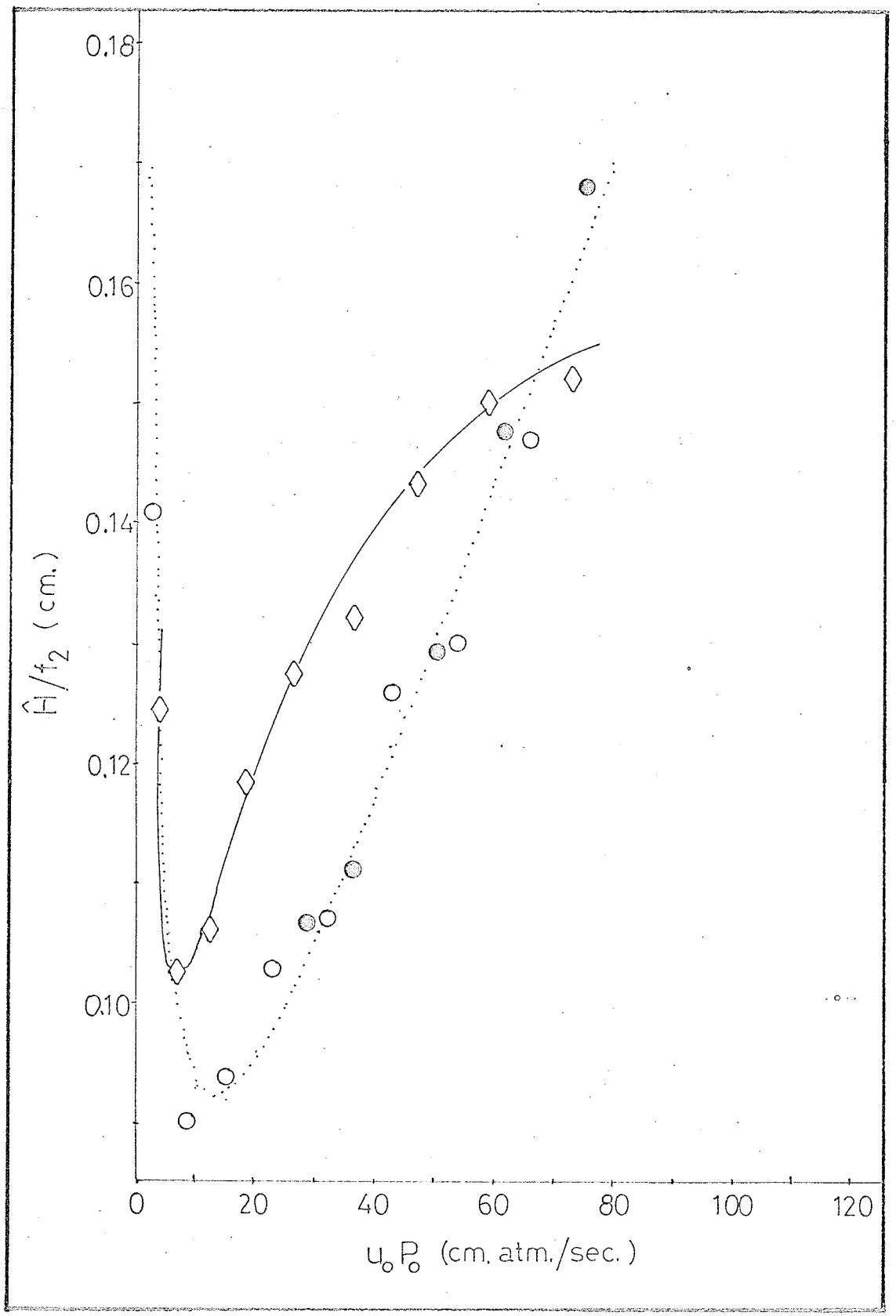
0.18
0.16
0.14
0.12
0.10
$\hat{H}/t_2$ (cm.)
0
20
40
60
80
100
120
$u_o P_o$ (cm. atm./sec.)

FIGURE (3.53)

PLOT OF $\hat{H}/f_2$ AS A FUNCTION OF $u_o P_o$

FOR CO_2I, CO_2II, AND CO_2III.

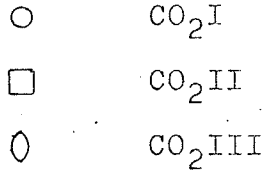

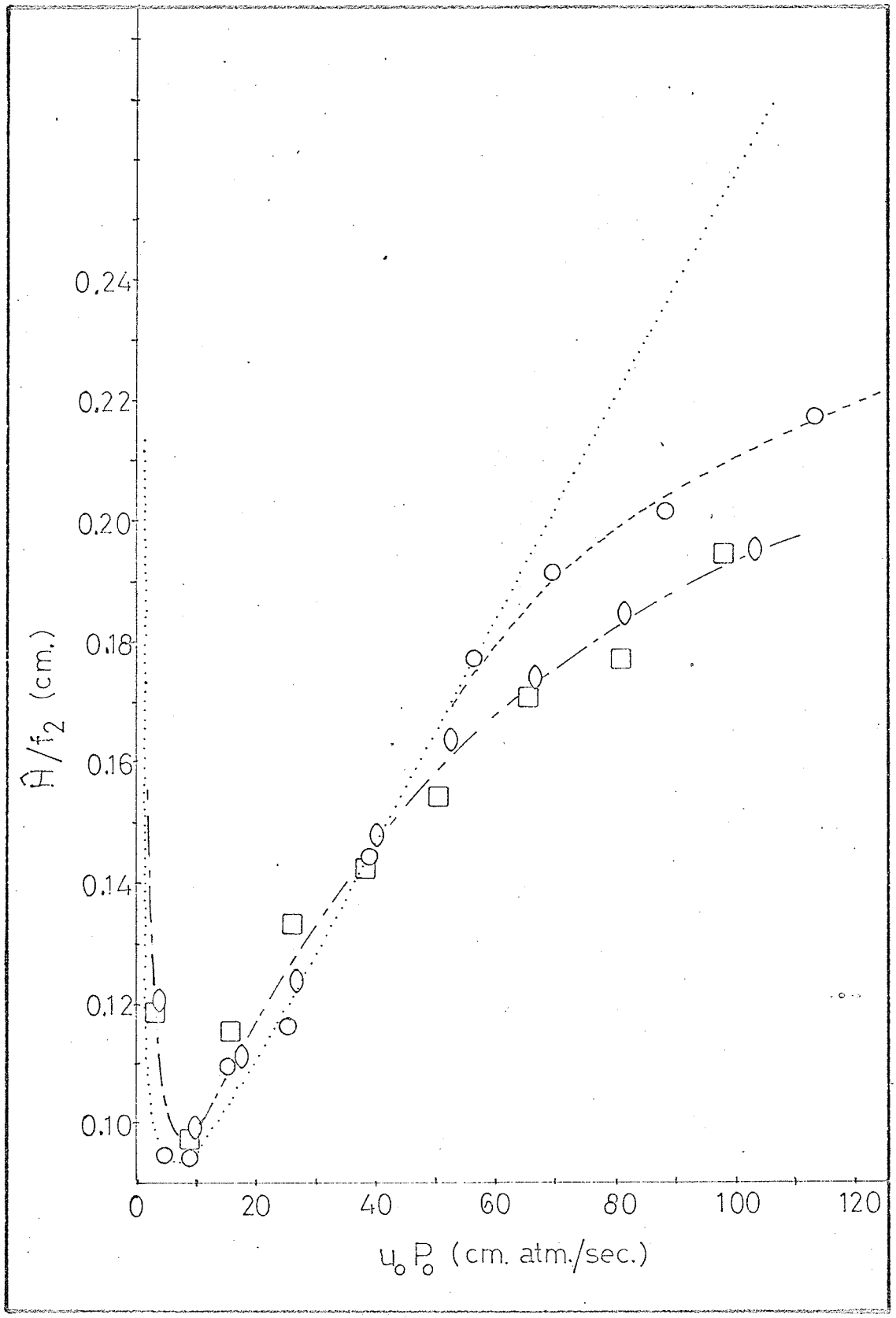
0.24
0.22
0.20
0.18
0.16
0.14
0.12
0.10
H/f2 (cm.)
0
20
40
60
80
100
120
u0 P0 (cm. atm./sec.)

CONCLUDING REMARKS

It may be said that the attempts to separate the five isotopic methanes on a conventionally packed column were on the whole unsuccessful. The results in general, however, should not be categorised by the above statement. The efforts of this study have resulted in the introduction of a conventionally packed column (having many desirable features) which is capable of quickly separating CH_4-CD_4 mixtures. Morrison (210), in his study of the thermodynamic properties of the isotopic methanes, has extended the use of this type of column to preparative work.

According to Hollis (129, 130, 132) the various porous polymer beads can be prepared from a combination of the following monomers:- ethylvinylbenzene, divinylbenzene, styrene, and t-butylstyrene. The difference between the various porous polymers stems from a different combination and/or concentration of the above monomers. This and the fact that different Porapaks were found to give a different degree of CH_4-CD_4 separation, suggests that the porous polymers can be tailored so as to enhance this selectivity. Before this can be done, it must be first determined what factor controls this selectivity. An attempt was made by the author to establish some trend within the various Porapaks but both the I.R. and the manufacturor failed to reveal

any information. Once this selectivity controlling factor is found, it should be possible by the proper choice of the many simple and substituted monomers to prepare a conventionally packed column capable of separating the five isotopic methanes.

As it was previously mentioned, the one factor which defeated the separation of the five methanes was the band broadening. One way to improve the situation is to reduce or eliminate the observed A constants in the plate height equations (equations (3.127), (3.128), and (3.129)). This can be accomplished by using other than the conventionally packed type of column. Considering that the decomposition temperature of these polymers is approximately 250°C., columns that require the glass drawing apparatus cannot be considered. Since the micropacked and the H.I.M.C. systems require a special high pressure apparatus, the best choice would probably be the porous layer capillary column prepared by the colloidal suspension method (38, 39). In the first place this type of column will completely eliminate the band broadening which is attributed to multiple streams and gas velocity inequality (the A terms). The consequence of using very small particles is a further reduction of the plate height if the C_2 term is operative ($C_2 \propto d_c \leq d_p$). The speed and efficiency of the capillary columns allows for operation at

lower column temperatures where the $K(CH_4)/K(CD_4)$ ratio is much larger. It is the author's belief that a combination of low temperature and a Porapak S coated capillary column will lead to a relatively easy analytical separation of the five methanes. This task will be undertaken immediately after the completion of the present study.

Another source of further investigation stems from the results obtained on the Saran charcoal column. From what has been observed, it appears that this material is capable of separating the CH_4-CD_4 mixtures. Its highly retentive properties indicate that a capillary column prepared from this material could be used to separate the five isotopic methanes at higher column temperatures then that of Porapak S. Unlike Porapak S, this material is not limited to the capillary column preparation by the colloidal suspension method. The possibilities of using Saran charcoal to separate the five methanes will also be investigated shortly.

With the aid of the accurate and highly reproducible flow meter, the second phase of the study has revealed some unusual properties of the column. Without repeating that which has already been said, it can be stated that there remains a number of unanswered questions. In order to answer some of these questions, many more experiments must be carried out. Some of these would require the extension of the $\bar{P}$ range. By doing this, some insight may be gained

into the nature of the 'break through'. It would also be beneficial to extend this study to hydrogen gas since it has properties somewhat similar to those of helium. Undoubtedly a temperature study would furnish additional information on both the flow properties of the column, and the nature of the n terms of the adsorption isotherms. Perhaps one of the most difficult questions to be answered is that related to the permeability and the plate height hysterisis. Without doubt this will require an extensive experimental undertaking involving a precise control of the various experimental parameters and accurate measurements.

It is the author's opinion that the anomalous effects observed in this study are worthy of further investigation.

BIBLIOGRAPHY

1. Purnell, H., "Gas Chromatography", Wiley, New York 1962, p 1.
2. James, A.T., Martin, A.J.P., Biochem. J., 50, 679 (1952).
3. Dal Nogare, S., "Gas Chromatography" L. Fowler Ed., Academic Press, New York 1963, p 2.
4. Dal Nogare, S., Juvet, R.S., Jr., "Gas-Liquid Chromatography", Interscience, New York 1962, p 2.
5. Juvet, R.S., Jr., Dal Nogare, S., Anal. Chem. 40, 33R (1968).
6. Ettre, L.S., Zlatkis, A., "The Practice Of Gas Chromatography", L.S. Ettre, A. Zlatkis Eds., New York 1967, p vii.
7. Hennis, Y., Gould, J.R., Alexander, M., Appl. Microbiol. 14, 513 (1966).
8. Silverstein, R.M., Rodin, J.O., Burkholder, W.E., Gorman, J.E., Science 157, 85 (1967).
9. Bocola, W., Bruner, F., Cartoni, G.P., Nature 209, 200 (1966).
10. Czubryt, J.J., Gesser, H.D., J. Gas Chromatog. 6, 41 (1968).
11. Purnell, J.H., "Gas Chromatography, 1966" A.B. Littlewood Ed., Elsevier, New York 1967, p 3.

12. Gil-Av, E., Charles-Sigler, R., Fishcer, G., Nurok, D., J. Gas Chromatog. 4, 51 (1966).

13. Klotz, I.M., "Chemical Thermodynamics", Benjamin, New York 1964, p 149.

14. Klotz, I.M., "Chemical Thermodynamics", Benjamin, New York 1964, p 294.

15. Klotz, I.M., "Chemical Thermodynamics", Benjamin, New York 1964, p 347.

16. James, M.R., Giddings, J.C., Keller, R.A., J. Gas Chromatog. 3, 57 (1965).

17. Golay, M.J.E., "Gas Chromatography" V.J. Coates, H.J. Noebels, I.S. Fagerson, Eds. Academic Press, New York 1958, p 1.

18. Golay, M.J.E., "Gas Chromatography, 1958" D.H. Desty Ed., Butterworths, London 1958, p 36.

19. Desty, D.H., Goldup, A., "Gas Chromatography, 1960" R.P.W. Scott Ed., Butterworths, London 1960, p 162.

20. Phillips, T.R., Owens, D.R., "Gas Chromatography, 1960" R.P.W. Scott Ed., Butterworths, London 1960, p 308.

21. Khan, M.A., "Gas Chromatography, 1962" M. van Swaay Ed., Butterworths, London 1962, p 3.

22. Adlard, E.E., Khan, M.A., Whitman, B.T., "Gas Chromatography, 1962" M. van Swaay Ed., Butterworths, London 1962, p 84.

23. Jentzsch, D., Hövermann, W., "Gas Chromatography, 1962" M. van Swaay Ed., Butterworths, London 1962, p 204.

24. Desty, D.H., Goldup, A., Swanton, W.T., "Gas Chromatography", N. Brenner, J.E. Callen, M.D. Weiss Eds., Academic Press, London 1962, p 105.

25. Dal Nogare, S., Juvet, R.S., Jr., "Gas-Liquid Chromatography", Interscience, New York 1962, p 267.

26. Kaiser, R., "Gas Phase Chromatography" Vol. 2, Butterworths, London 1963.

27. Giddings, J.C., "Advances in Analytical Chemistry And Instrumentation" Vol. 3, C.N. Reilley Ed., Interscience, New York 1964, p 354.

28. Ettre, L.S., "Open Tublar Columns", Plenum Press, New York 1965.

29. Desty, D.H., "Advances In Chromatography" Vol. 1, J.C. Giddings, R.A. Keller Eds., Arnold, London 1965, p 199.

30. Ettre, L.S., Purcell, J.E., Billeb, K., J. Chromatog. 24, 355 (1966).

31. Purnell, J.H., Nature, 184, 2,009 (1959).

32. Petitjean, D.L., Leftoult, C.F., J. Gas Chromatog. 1, 18 (1963).

33. Mohnke, M., Saffert, W., "Gas Chromatography, 1962" M. van Swaay Ed., Butterworths, London 1962, p 216.

34. Bruner, F., Cartoni, G.P., Anal. Chem. 36, 1522 (1964).

35. Desty, D.H., Haresnape, J.N., Whyman, B.H.F., Anal. Chem. 32, 302 (1960).

36. Coretti, G.C., Liberti, A., Nota, G., J. Chromatog. 34, 96 (1968).

37. Grant, D.W., J. Gas Chromatog. 6, 18 (1968).

38. Halász, I., Horváth, C., Nature 197, 71 (1963).

39. Halász, I., Horváth, C., Anal. Chem. 35, 499 (1963).

40. Kirkland, J.J., Anal. Chem. 35, 1295 (1963).

41. Schwartz, R.D., Brasseaux, D.J., Shoemake, G.R., Anal. Chem. 35, 496 (1963).

42. Schwartz, R.D., Brasseaux, D. J., Mathews, R.G., Anal. Chem. 38, 303 (1966).

43. Purcell, J.E., Nature 201, 1321 (1964).

44. Ettre, L.S., Purcell, J.E., Norem, S.D., J. Gas Chromatog. 3, 181 (1965).

45. Pope, C.G., Anal. Chem. 35, 654 (1963).

46. Ohline, R.W., Jojola, R., Anal. Chem. 36, 1681 (1964).

47. Kirkland, J.J., Anal. Chem. 37, 1458 (1965).

48. MacDonell, H.L., Anal. Chem. 40, 221 (1968).

49. Carter, H.V., Nature 197, 684 (1963).

50. Virus, N., J. Chromatog. 12, 406 (1963).

51. Wilhite, W.F., J. Gas Chromatog. 4, 47 (1966).

52. Myers, M.N., Giddings, J.C., Anal. Chem. 38, 294 (1966).

53. Halász, I., Gerlach, H.D., Anal. Chem. 38, 281 (1966).

54. Halász, I., Heine, E., Nature 194, 971 (1962).

55. Halász, I., Heine, E., Anal. Chem. 37, 495 (1965).

56. Halász, I., Heine, E., "Advances In Chromatography" Vol. 4, J.C. Giddings, R.A. Keller Eds., Marcel Dekker, New York 1967, p 207.

57. Halász, I., Heine, E., "Progress In Gas Chromatography" J.H. Purnell Ed., Interscience, New York 1968, p 187.

58. Klotz, I.M., "Chemical Thermodynamics", Benjamin, New York 1964, p 356.

59. Giddings, J.C., "Dynamics Of Chromatography" Part I, Marcel Dekker, New York 1965, p 7.

60. Martire, D.E., Locke, D.C., Anal. Chem. 37, 144 (1965).

61. Giddings, J.C., "Dynamics Of Chromatography" Part I, Marcel Dekker, New York 1965, p 95.

62. Giddings, J. C., J. Chem. Ed. 44, 704 (1967).

63. Horváth, C., "The Practice Of Gas Chromatography", L.S. Ettre and A. Zlatkis Eds., Interscience, New York 1967, p 152-162.

64. Giddings, J.C., J. Gas Chromatog. 2, 145 (1964).

65. Giddings, J.C., "Dynamics Of Chromatography" Part I, Marcel Dekker, New York 1965, p 24.

66. Jones, W.L., Anal. Chem. 33, 829 (1961).

67. van Deemter, J.J., Zuiderweg, F.J., Klinkenberg, A., Chem. Eng. Sci. 5, 271 (1956).

68. Kiselev, A.V., Nikitin, Y.S., Petrova, R.S., Shcherbakova, K.D., Yashin, Ya. I., Anal. Chem. 36, 1526 (1964).

69. Phillips, C.S.G., Scott, C.G., "Progress In Gas Chromatography", J.H. Purnell Ed., Interscience, New York 1968, p 127-129.

70. Gudzinowicz, B.J., Clark, S.J., J. Gas Chromatog. 3, 147 (1965).

71. Giddings, J.C., Anal. Chem. 35, 1999 (1963).

72. Johns, T., "Gas Chromatography", V.J. Coates, H.J. Noebels, I.S. Fagerson Eds., Academic Press, New York 1958, p 31.

73. Lipsky, S.R., Landowne, R.A., Anal. Chem. 33, 818 (1961).

74. Knight, H.S., Anal. Chem. 30, 2030 (1958).

75. Ackman, R.G., Burgher, R.D., Anal. Chem. 35, 647 (1963).

76. Sternberg, J.C., "Advances In Chromatography" Vol. 2, J.C. Giddings, R.A. Keller, Eds., Marcel Dekker, New York 1966, p 205.

77. Greene, S.A., Pust, H., J. Phys. Chem. 62, 55 (1958).

78. Petrova, R.S., Khrapova, E.V., Shcherbakova, K.D., "Gas Chromatography, 1962", M. van Swaay Ed., Butterworths, London 1962, p 18.

79. Scott, C.G., "Gas Chromatography, 1962", M. van Swaay Ed., Butterworths, London 1962, p 36.

80. Gale, R.L., Beebe, R.A., J. Phys. Chem. 68, 555 (1964).

81. King, J.Jr., Benson, S.W., Anal. Chem. 38, 261 (1966).

82. Hargrove, G.L., Sawyer, D.T., Anal. Chem. 40, 409 (1968).

83. Gregg, S.J., Stock, R. "Gas Chromatography, 1958", D.H. Desty Ed., Butterworths, London 1958, p 90.

84. Huber, J.F.K., Keulemans, A.I.M., "Gas Chromatography, 1962", van Swaay Ed., Butterworths, London 1962, p 26.

85. Owens, D.R., Hamlin, A.G., Phillips, T.R., Nature 201, 901 (1964).

86. Saint-Yrieix, A., Bull. Soc. Chim. France 1965, p 3407.

87. Cremer, E., Huber, H.F., "Gas Chromatography", N. Brenner, J.E. Callen, M.D. Weiss Eds., Academic Press, New York 1962, p 169.

88. Beebe, R.A., Evans, P.L., Kleinsteuber, T.C.W., Richards, L.W., J. Phys. Chem. 70, 1009 (1966).

89. Parcher, J.F., Urone, P., Nature 211, 628 (1966).

90. Brooks, C.S., Soil Science 99, 182 (1965).

91. Kipping, P.J., Winter, D.G., Nature 205, 1002 (1965).

92. Nelson, F., Eggertsen, F.T., Anal. Chem. 30, 1387 (1958).

93. Stock, R., Anal. Chem. 33, 966 (1961).

94. Herrington, E.F.G., "Vapour Phase Chromatography", Desty Ed., London 1956, p 5.

95. Martire, D.E., "Gas Chromatography", L. Fowler Ed., Academic Press, New York 1963, p 33.

96. Everett, D.H., Stoddart, C.T.H., Trans. Faraday Soc. 57, 746 (1961).

97. Pescar, R.E., Martin, J.J., Anal. Chem. 38, 1661 (1966).

98. Barker, P.E., Hilmi, A.K., J. Gas Chromatog. 5, 119 (1967).

99. Williams, F.W., Carhart, H.W., J. Gas Chromatog. 6, 280 (1968).

100A. Desty, D.H., Goldup, A., Luckhurst, G.R., Swanton, T.W., "Gas Chromatography, 1962", M. van Swaay Ed., Butterworths, London 1962, p 67.

100B. Everett, D.H., Trans. Faraday Soc. 61, 1637 (1965).

100C. Cruickshank, A.J.B., Windsor, M.L., Young, C.L., Proc. Roy. Soc. 295A, 259 (1966).

100D. Cruickshank, A.J.B., Windsor, M.L., Young, C.L., Proc. Roy. Soc. 295A, 271 (1966).

100E. Sie, S.T., Van Beersum, W., Rijnders, G.W.A., Separation Science 1, 459 (1966).

100F. Gainey, B.W., Young, C.L., Trans. Faraday Soc. 64, 349 (1968).

100G. Pescock, R.L., Windsor, M.L., Anal. Chem. 40, 1238 (1968).

101. Goldup, A., Luckhurst, G.,R., Swanton, W.T., Nature 193, 333 (1962).

102. Locke, D.C., Brandt, W.W., "Gas Chromatography", L. Fowler Ed., Academic Press, New York 1963, p 55.

103. Dantzler, E.M., Knobler, C.M., Windsor, M.L., J. Chromatog. 32, 433 (1968).

104. Giddings, J.C., Separation Science 1, 73 (1966).

105. McLaren, L., Myers, M.N., Giddings, J.C., Science 159, 197 (1968).

106. Cvetanović, R.J., Duncan, F.J., Falconer, W.E., Irwin, R.S., J. Am. Chem. Soc. 87, 1827 (1965).

107. Knox, J.H., McLaren, L., Anal. Chem. 36, 1477 (1964).

108. Hargrove, G.L., Sawyer, T., Anal. Chem. 39, 244 (1967).

109. Kovats, E. Sz., Strickler, H., J. Gas Chromatog. 3, 244 (1965).

110. Belyakova, L.D., Kiselev, A.V., Kovaleva, N.V., Anal. Chem. 36, 1517 (1964).

111. Conder, J.R., "Progress In Gas Chromatography", J.H. Purnell Ed., Interscience, New York 1968, p 209.

112. Kobayashi, R., Chappelear, P.S., Deans, H.A., Ind. Eng. Chem. 59 (10), 63 (1967).

113. Purnell, J.H., Endeavour 23, 142 (1964).

114. Glueckauf, E., Kitt, G.P., "Vapour Phase Chromatography", D.H. Desty Ed., Butterworths, London 1957, p 422.

115. Falconer, W.E., Cvetanović, R.J., Anal. Chem. 34, 1064 (1962).

116. Cvetanović, R.J., Duncan, F.J., Falconer, W.E., Can. J. Chem. 41, 2095 (1963).

117. Liberti, A., Cartoni, G.P., Bruner, F., J. Chromatog. 12, 8 (1963).

118. Bruner, F., Cartoni, G.P., J. Chromatog. 10, 396 (1963).

119. Cvetanović, R.J., Duncan, F.J., Falconer, W.E., Can. J. Chem. 42, 2410 (1964).

120. Akhtar, S., Smith, H.A., Chem. Rev. 64, 261 (1964).

121. Yasumori, I., Ohno, S., Bull. Chem. Soc. Japan 39, 1302 (1966).

122. Van Hook, W.A., Kelly, M.E., Anal. Chem. 37, 508 (1965).

123. Cartoni, G.P., Liberti, A., Pela, A., Anal. Chem. 39, 1618 (1967).

124. Haubach, W.J., Knobler, C.M., Katorski, A., White, D., J. Phys. Chem. 71, 1398 (1967).

125. Atkinson, J.G., Russell, A.A., Stuart, R.S., Can. J. Chem. 45, 1963 (1967).

126. Liberti, A., Cartoni, G.P., Bruner, F., "Gas Chromatography, 1964", A. Goldup Ed., The Institute Of Petroleum 1965, p 301.

127. Gant, P.L., Yang, K., J. Am. Chem. Soc. 86, 5063 (1964).

128. Bruner, F., Cartoni, G.P., J. Chromatog. 18, 390 (1965).

129. Hollis, O.L., Anal. Chem. 38, 309 (1966).

130. Hollis, O.L., Hayes, W.V., J. Gas Chromatog. 7, 235 (1966).

131. Zlatkis, A., Kaufman, H.R., J. Gas Chromatog. 7, 240 (1966).

132. Hollis, O.L., Hayes, W.V., Preprints Of Sixth International Symposium On Gas Chromatography, Rome, September 1966, Institute Of Petroleum 1966, p 1.

133. Hargrove, G.L., Sawyer, D.T., Anal. Chem. 38, 1634 (1966).

134. Root, J.W., Lee, E.K.C., Rowland, F.S., Science 143, 676 (1964).

135. Bruner, F., Cartoni, G.P., Liberti, A., Anal. Chem. 38, 298 (1966).

136. Keulemans, A.I.M., "Gas Chromatography", Second Edition, C.G. Verver, A.J.P. Martin Eds., Reinhold Publ., New York 1960, p 152.

137. Purnell, H., "Gas Chromatography", Wiley, New York 1962, p 189 and p 431.

138. Greene, S.A., Roy, H.E., Anal. Chem. 29, 569 (1957).

139. Hoffman, R.L., Evans, C.D., Anal. Chem. 38, 1309 (1966).

140. Brookman, D.J., Hargrove, G.L., Sawyer, D.T., Anal. Chem. 39, 1196 (1967).

141. Moelwyn-Hughes, E.A., "Physical Chemistry", Pargamon Press, London 1961, p 610.

142. Purnell, H., "Gas Chromatography", Wiley, New York 1963, p 254.

143. Levy, A., J. Sci. Instr. 41, 449 (1964).

144. Noble, F.W., Abel, K., Cook, D.W., Anal. Chem. 37, 1631 (1965).

145. Moore, W.J., "Physical Chemistry", Second Edition, Prentice-Hall, Englewood Cliffs 1955, p 390.

146. Giddings, J.C., "Dynamics Of Chromatography" Part I, Marcel Dekker, New York 1965, p 199.

147. Bohemen, J., Purnell, J.H., J. Chem. Soc., 360 (1961).

148. Hargrove, G.L., Sawyer, D.T., Anal. Chem. 39, 945 (1967).

149. Mottlau, A.Y., Fisher, N.E., Anal. Chem. 34, 714 (1962).

150. Innes, W.B., Anal. Chem. 28, 332 (1956).

151. Prandtl, L., "Essentials Of Fluid Dynamics", Blackie & Son, Glasgow 1954, p 102.

152. Fluid Motion Memoires "Laminar Boundry Layers", L. Rosenhead Ed., Oxford (Clarendon Press) 1963, p 121.

153. Giddings, J.C., "Dynamics Of Chromatography", Part I, Marcel Dekker, New York 1965, p 204-224.

154. Carman, P.C., "Flow Of Gases Through Porous Media", Butterworths, London 1956, p 1-33.

155. Purnell, H., "Gas Chromatography", Wiley, New York 1962, p 60-66.

156. Guiochon, G., Chromatog. Rev. 8, 1 (1966).

157. Moelwyn-Hughes, E.A., "Physical Chemistry", Pergamon Press, London 1961, p 590.

158. Dal Nogare, S., Juvet, R.S., Jr., "Gas-Liquid Chromatography", Interscience, New York 1962, p 134.

159. Bird, R.B., Stewart, W.E., Lightfoot, E.N., "Transport Phenomena", Wiley, New York 1960, p 199.

160. White, D.A., Chem. Eng. Sci. 22, 669 (1967).

161. Seely, T., J. Polymer Sci. 5, 3029 (1967).

162. McCabe, W.L., Smith, J.C., "Unit Operations Of Chemical Engineering", McGraw-Hill, New York 1967, p 161.

163. Reisch, J.C., Robinson, C.H., Wheelock, T.D., "Gas Chromatography", N. Brenner, J.E. Callen, M.D. Weiss Eds., Academic Press, New York 1962, p 91.

164. Carman, P.C., "Flow Of Gases Through Porous Media", Butterworths, London 1965, p 62.

165. Carman, P.C., "Flow Of Gases Through Porous Media", Butterworths, London 1965, p 154.

166. Guggenheim, E.A., McGlashan, M.L., Proc. Roy. Soc. A206, 448 (1951).

167. Eggers, D.F., Jr., Gregory, N.W., Halsey, G.D., Jr., Rabinovitch, B.S., "Physical Chemistry", Wiley, New York 1964, p 330.

168. Dadson, R.S., Evans, E.J., King, J.H., Proc. Phys. Soc. 92, 1115 (1967).

169. Young, D.M., Crowell, A.D., "Physical Adsorption Of Gases", Butterworths, London 1962, p 3.

170. Adlard, E.R., Khan, M.A., Whitham, B.T., "Gas Chromatography, 1960", R.P.W. Scott Ed., Butterworths, London 1960, p 251.

171. Young, D.M., Crowell, A.D., "Physical Adsorption Of Gases", Butterworths, London 1962, p 107.

172. Brunauer, S., Copeland, L.E., Kantro, D.L., "The Solid-Gas Interface" Vol. 1, E.A. Flood Ed., Marcel Dekker, New York 1967, p 77.

173. Chiche, P., J. Chim. Phys., 394 (1962).

174. Ross, S., Olivier, J.P., "On Physical Adsorption", Interscience, New York 1964, p 9.

175. Eggers, D.F., Jr., Gregory, N.W., Halsey, G.D., Jr., Rabinovitch, B.S., "Physical Chemistry", Wiley, New York 1964, p 739.

176. Ross, S., "The Solid-Gas Interface" Vol. 1, E.A. Flood Ed., Marcel Dekker, New York 1967, p 491.

177. Bradley, H., Trans. Faraday Soc. 31, 1652 (1935).

178. Sips, R., J. Chem. Phys. 16, 490 (1948).

179. Koble, R.A., Corrigan, T.E., Ind. Eng. Chem. 44, 383 (1952).

180. Ray, G.C., Box, E.O., Ind. Eng. Chem. 42, 1315 (1950).

181. Wiig, E.O., Smith, S.B., J. Phys. Chem. 55, 27 (1951).

182. Dal Nogare, S., Juvet, R.S., Jr., "Gas-Liquid Chromatography", Interscience, New York 1962, p 87-103.

183. Purnell, H., "Gas Chromatography", Wiley, New York 1962, p 117-164.

184. Giddings, J.C., "Dynamics Of Chromatography" Part I, Marcel Dekker, New York 1965, p 35.

185. Kieselbach, R., Anal. Chem. 35, 1342 (1963).

186. Sternberg, J.C., Poulson, R.E., Anal. Chem. 36, 1492 (1964).

187. Giddings, J.C., "Gas Chromatography, 1964", A. Goldup Ed., Institute Of Petroleum 1965, p 3.

188. Giddings, J.C., Anal. Chem. 36, 1170 (1964).

189. Giddings, J. C., Anal. Chem. 35, 439 (1963).

190A. van Berge, P.C., Pretorius, V., J. Gas Chromatog. 2, 235 (1964).

190B. Giddings, J.C., Anal. Chem. 34, 1186 (1962).

191. Giddings, J.C., Schettler, P.D., Anal. Chem. 36, 1483 (1964).

192. DeFord, D., Lloyd, R.J., Ayers, B.O., Anal. Chem. 35, 426 (1963).

193. Bohemen, J., Purnell, J.H., "Gas Chromatography, 1958", D.H. Desty ed., Butterworths, London 1958, p 6.

194. Giddings, J.C., Seager, S.L., Stucki, R.L., Stewart, G.H., Anal. Chem. 32, 867 (1960).

195. Kieselbach, R., Anal. Chem. 33, 806 (1961).

196. Norem, S.D., Anal. Chem. 34, 40 (1959).

197. Glueckauf, E., "Vapour Phase Chromatography", H.D. Desty Ed., Butterworths, London 1957, p 29.

198. Kieselbach, R., Anal. Chem. 33, 23 (1961).

199. Giddings, J.C., Robison, R.A., Anal. Chem. 34, 885 (1962).

200. Giddings, J.C., "Dynamics Of Chromatography" Part I, Marcel Dekker, New York 1965, p 52.

201. Myers, M.N., Giddings, J.C. Anal. Chem. 37, 1453 (1965).

202. Knox, J.H., Anal. Chem. 38, 253 (1966).

203. Giddings, J.C., Anal. Chem. 35, 1338 (1963).

204. Harper, J.M., Hammond, E.G., Anal. Chem. 37, 486 (1965).

205. Giddings, J.C., Manwaring, W.A., Myers, M.N., Science 154, 146 (1966).

206. Stewart, G.H., Seager, S.L., Giddings, J.C., Anal. Chem. 31, 1738 (1959).

207. Fuller, E.N., Schettler, P.D., Giddings, J.C., Ind. Eng. Chem. 58, 19 (1966).

208. Fuller, E.N., Giddings, J.C., J. Gas Chromatog. 3, 222 (1965).

209. Perrett, R.H., Purnell, J.H., Anal. Chem. 35, 430 (1963).

210. Norton, P.R., Private communication. (P.R. Norton is a coworker with J.A. Morrison at the National Research Council Of Canada in Ottawa.)

APPENDIX A

RAW EXPERIMANTAL DATA FOR EXPERIMENT HeI.

P_o*	P_i**	P_i***	F_o(a)	t(b)	t_R(c)	$\Delta W_{\frac{1}{2}}$(cm.)
73.90	190.0	1056	54.62	0.908	52.28	0.763
74.40	165.75	932	41.98	1.179	59.44	0.819
74.60	145.25	826	32.96	1.500	67.25	0.882
74.60	128.00	737	26.34	1.875	75.48	0.948
74.60	109.00	638	19.98	2.471	87.06	1.068
75.10	88.00	530	13.729	3.592	105.30	1.257
75.00	70.50	440	9.459	5.212	128.18	1.589
74.90	51.00	339	5.575	8.839	170.50	2.442
74.95	35.00	256	3.077	16.009	239.70	4.034

* cm.

** pressure gauge reading in p.s.i.

*** absolute pressure in cm.

(a) cc./min.

(b) time in reference to the flow meter. Approx. 6 readings.

(c) in minutes.

RAW EXPERIMANTAL DATA FOR EXPERIMENT ArI..

P_o*	P_i**	P_i***	F_o(a)	t(b)	t_R(c)	$\Delta W_{\frac{1}{2}}$(cm.)
73.70	30.50	231	2.297	21.44	274.73	3.834
74.10	44.50	304	3.984	12.365	196.45	2.515
74.90	61.50	393	6.664	7.395	144.50	1.890
75.40	77.75	478	9.825	5.018	115.93	1.609
75.30	97.00	577	14.32	3.445	93.83	1.352
74.30	117.25	681	19.97	2.471	78.67	1.156
73.65	137.50	785	26.14	1.889	68.00	1.042
73.55	156.00	880	32.55	1.519	60.36	0.946
73.35	177.50	991	40.65	1.217	53.53	0.848

RAW EXPERIMENTAL DATA FOR EXPERIMENT ArII.

P_o*	P_i**	P_i***	F_o(a)	t(b)	t_R(c)	$\Delta W_{\frac{1}{2}}$(cm.)
73.70	167.00	937	36.67	1.349	56.07	0.870
74.50	148.00	840	29.27	1.688	63.05	0.922
74.40	130.25	748	23.48	2.103	71.48	1.024
73.30	111.00	647	18.063	2.732	83.47	1.106
74.05	89.00	534	12.256	4.023	102.95	1.339
74.80	70.25	438	8.184	6.023	129.15	1.589
74.10	49.75	331	4.711	10.457	178.75	2.146
73.00	23.75	196	1.538	32.02	360.30	5.326

RAW EXPERIMENTAL DATA FOR EXPERIMENT ArIII

73.90	180.50	1007	41.64	1.188	52.47	0.872
74.10	161.00	907	34.15	1.448	58.73	0.916
74.10	143.00	814	27.72	1.782	66.28	0.964
73.95	118.00	684	19.96	2.473	79.75	1.076
73.40	103.50	609	16.077	3.069	90.18	1.192

RAW EXPERIMENTAL DATA FOR EXPERIMENT CO_2I.

P_o*	P_i**	P_i***	F_o(a)	t(b)	t_R(c)	$\Delta W_{\frac{1}{2}}$(cm.)
75.15	195.00	1084	61.37	0.808	24.20	0.457
74.70	167.00	938	48.17	1.028	27.19	0.494
74.85	144.75	823	37.87	1.306	30.71	0.543
75.30	126.50	730	30.52	1.619	34.33	0.585
75.75	99.50	590	20.72	2.383	42.40	0.650
75.00	77.75	477	13.893	3.550	53.75	0.735
75.00	57.25	371	8.453	5.831	72.28	0.924
75.20	38.75	276	4.597	10.718	106.10	1.294
75.20	24.00	199	2.291	21.50	168.60	2.052

RAW EXPERIMENTAL DATA FOR EXPERIMENT CO_2II.

74.25	19.25	174	1.654	29.78	212.00	2.856
73.70	39.00	275	4.701	10.479	104.11	1.293
74.20	59.25	381	9.117	5.407	68.82	0.936
74.85	78.75	482	14.375	3.431	52.10	0.765
74.70	99.00	587	20.87	2.365	42.18	0.646
74.55	118.00	685	27.90	1.771	36.00	0.572
74.00	138.50	790	35.78	1.382	31.58	0.526
74.00	159.25	898	44.75	1.106	28.22	0.478
74.55	179.00	1000	53.43	0.9275	25.84	0.462

RAW EXPERIMENTAL DATA FOR EXPERIMENT CO_2III.

P_o*	P_i**	P_i***	F_o(a)	t(b)	t_R(c)	$\Delta W_{\frac{1}{2}}$(cm.)
74.10	20.25	179	1.889	26.07	194.65	2.645
73.80	42.00	291	5.267	9.355	97.38	1.224
73.20	61.25	390	9.679	5.093	67.17	0.896
73.90	80.00	488	14.907	3.309	51.60	0.730
74.00	102.00	602	22.08	2.236	41.18	0.640
74.85	120.25	697	28.63	1.726	35.55	0.582
74.60	140.00	799	36.51	1.355	31.38	0.530
74.05	159.50	899	45.13	1.097	28.25	0.492
73.85	185.50	1033	57.59	0.8609	25.14	0.450

Since these are given of illustrative purposes only, the other remaining experiments will not be included.